

Caged-polyprenylated Xanthenes from the Latex and the Stem Bark of

Garcinia scortechinii

Patima Phainuphong

Master of Science Thesis in Organic Chemistry

Prince of Songkla University

2002

เลขที่	QD409	P37	2002	C. 2
Bił Key...	232594			
	7 101.8. 2547			

(1)

Thesis Title Caged-polyprenylated Xanthenes from the Latex and the Stem
 Bark of *Garcinia scortechinii*

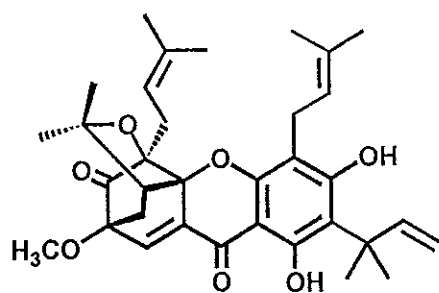
Author Miss Patima Phainuphong

Major Program Organic Chemistry

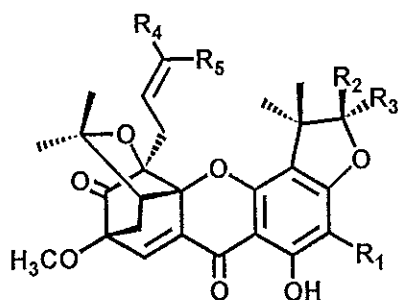
Academic Year 2002

ABSTRACT

The latex of *Garcinia scortechinii*, upon chromatographic separation, yielded seven new caged-polyprenylated xanthenes (PP1, PP3, PP4, PP5, PP6, PP8 and PP9) and one new degraded tetraprenylated xanthone (PP10) together with two known caged-tetraprenylated xanthenes [scortechinone A (PP2) and scortechinone B (PP7)]. The crude methanol extract from the stem bark of *G. scortechinii*, upon repeated chromatography, afforded five new caged-tetraprenylated xanthenes (PP13, PP14, PP15, PP16 and PP17), one known xanthone [4'',5''-dihydro-1,5-dihydroxy-6',6'-dimethylpyrano(2',3':6,7)-4'',4'',5''-trimethylfurano(2'',3'':3,4)xanthone (PP11)] and one known steroid [stigmasterol (PP12)] together with six caged-polyprenylated xanthenes (PP1, PP2, PP3, PP7, PP8 and PP9), previously isolated from the latex. The structures were elucidated by analysis of 1D and/or 2D NMR spectroscopic data and/or comparison of the NMR data with those of scortechinone A and scortechinone B. The ¹³C NMR signals were assigned from DEPT, HMQC and HMBC spectra. For known compounds, their ¹H NMR data were compared with those reported in the literature.



PP1



PP2: $R_1 = \text{isopentenyl}$; $R_2 = R_4 = R_5 = \text{CH}_3$; $R_3 = \text{H}$

PP3: $R_1 = R_3 = \text{H}$; $R_2 = R_4 = R_5 = \text{CH}_3$

PP4: $R_1 = R_2 = \text{H}$; $R_3 = R_4 = R_5 = \text{CH}_3$

PP5: $R_1 = \text{isopentenyl}$; $R_2 = \text{H}$; $R_3 = R_5 = \text{CH}_3$; $R_4 = \text{CO}_2\text{CH}_3$

PP6: $R_1 = \text{isopentenyl}$; $R_2 = \text{H}$; $R_3 = R_5 = \text{CH}_3$; $R_4 = \text{HC}=\text{O}$

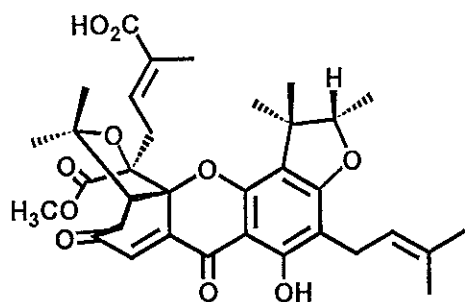
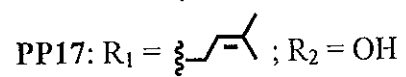
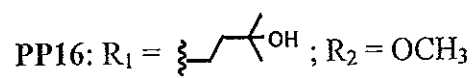
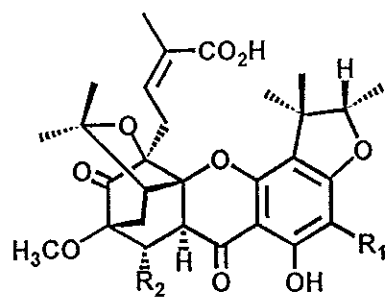
PP7: $R_1 = \text{isopentenyl}$; $R_2 = R_4 = \text{CH}_3$; $R_3 = \text{H}$; $R_5 = \text{CO}_2\text{H}$

PP9: $R_1 = \text{isopentenyl}$; $R_2 = \text{H}$; $R_3 = R_5 = \text{CH}_3$; $R_4 = \text{CO}_2\text{H}$

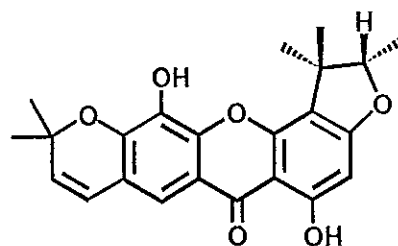
PP13: $R_1 = \text{isopentenyl}$; $R_2 = \text{H}$; $R_3 = R_4 = R_5 = \text{CH}_3$

PP14: $R_1 = \text{3-hydroxyisopentenyl}$; $R_2 = \text{H}$; $R_3 = R_4 = \text{CH}_3$; $R_5 = \text{CO}_2\text{H}$

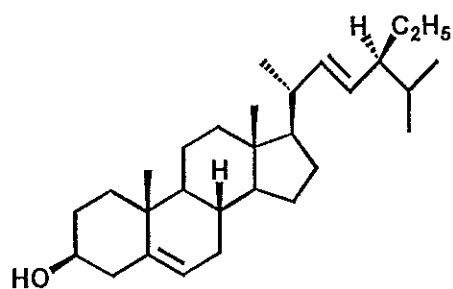
PP15: $R_1 = \text{3-hydroxyisopentenyl}$; $R_2 = \text{H}$; $R_3 = R_4 = \text{CH}_3$; $R_5 = \text{CO}_2\text{H}$



PP10



PP11

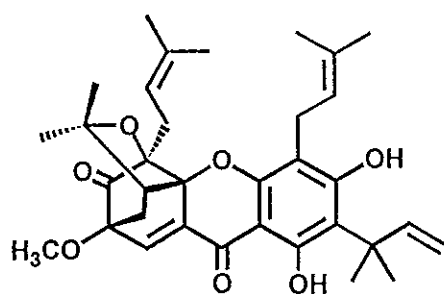


PP12

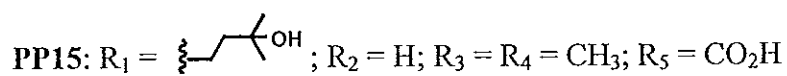
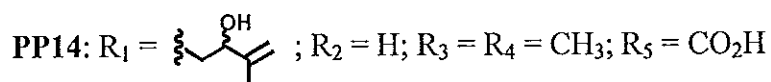
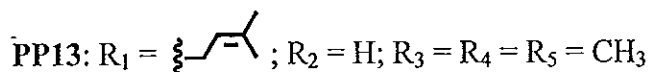
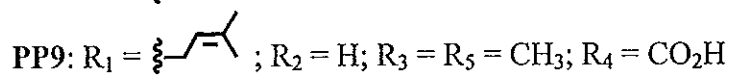
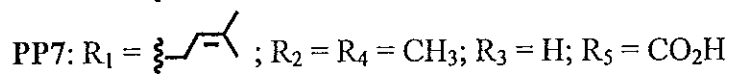
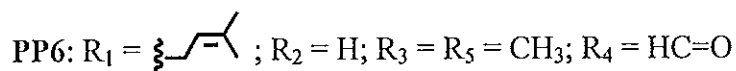
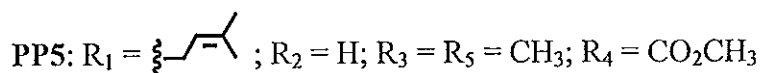
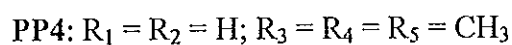
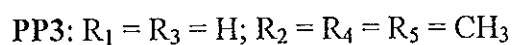
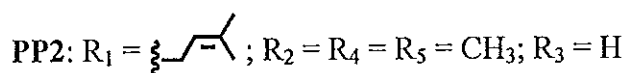
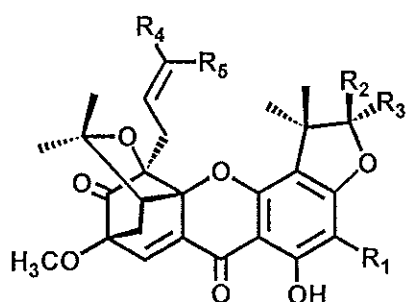
ชื่อวิทยานิพนธ์ เถงพอลิพรีนิลเตทเตนแซนโทนจากยางและเปลือกของ
Garcinia scortechinii
ผู้เขียน นางสาวปฎิมา ไพนุพงศ์
สาขาวิชา เคมีอินทรีย์
ปีการศึกษา 2545

บทคัดย่อ

นำยางของ *Garcinia scortechinii* เมื่อนำมาแยกและทำให้บริสุทธิ์ด้วยวิธีทางโครมาโทกราฟี สามารถแยกสารใหม่ได้จำนวน 8 สาร ซึ่งเป็นสารประเภท caged-polyprenylated xanthenes จำนวน 7 สาร (PP1, PP3, PP4, PP5, PP6, PP8 และ PP9) และสารประเภท degraded caged-tetraprenylated xanthone จำนวน 1 สาร (PP10) นอกจากนี้ยังแยกสารประเภท caged-tetraprenylated xanthenes ที่ทราบโครงสร้างแล้วจำนวน 2 สาร [scortechinone A (PP2) และ scortechinone B (PP7)] และจากการนำส่วนสกัดหยาบเมธานอลจากเปลือกลำต้นของ *G. scortechinii* มาแยกและทำให้บริสุทธิ์ด้วยวิธีทางโครมาโทกราฟี สามารถแยกสารใหม่ประเภท caged-tetraprenylated xanthenes จำนวน 5 สาร (PP13, PP14, PP15, PP16 และ PP17) สารประเภท xanthone จำนวน 1 สาร [4",5"-dihydro-1,5-dihydroxy-6',6'-dimethylpyrano(2',3':6,7)-4",4",5"-trimethylfurano(2",3":3,4)xanthone (PP11)] สารประเภท steroid จำนวน 1 สาร [stigmasterol (PP12)] และสารประเภท caged-polyprenylated xanthenes ซึ่งแยกได้จากส่วนยาง จำนวน 6 สาร (PP1, PP2, PP3, PP7, PP8 และ PP9) โครงสร้างทั้งหมดวิเคราะห์โดยใช้ข้อมูล 1D และ/หรือ 2D NMR สเปกโทรสโกปี และ/หรือการเปรียบเทียบข้อมูล NMR กับ scortechinone A และ scortechinone B ส่วนสัญญาณของ ¹³C สามารถวิเคราะห์โดยอาศัยข้อมูลจาก DEPT HMQC และ HMBC สเปกตรัม สำหรับสารที่มีการรายงานโครงสร้างแล้ว ได้เปรียบเทียบข้อมูล ¹H NMR สเปกตรัมกับข้อมูลที่ได้อ้างไว้



PP1



ACKNOWLEDGEMENTS

I would like to express my special gratitude and appreciation to my advisor, Associate Professor Dr. Vatcharin Rukachaisirikul, for her helpful suggestions, valuable guidance, comments and encouragement throughout my study and also her kind assistance of reading, correcting and criticizing the thesis.

My sincere thanks are extended to Assistant Professor Dr. Chatchanok Karalai, my co-advisor, for his kindness and valuable advice. In particular, I am especially grateful to Professor Dr. Walter C. Taylor, Department of Organic Chemistry, the University of Sydney, Australia, for providing 400 MHz NMR spectra and mass spectral data.

I wish to express my sincere thanks to the staff of the Department of Chemistry, Faculty of Science, Prince of Songkla University, including the officers for making this thesis possible and to Ms. Dusanee Langjae, the Scientific Equipment Center, Prince of Songkla University, for recording 500 MHz NMR spectra.

This work was made possible by a scholarship from Higher Education Development Project: Postgraduate Education and Research Program in Chemistry, funded by the Royal Thai Government. My deeply gratitude is also extended to the Graduate School, Prince of Songkla University, for partially support.

Finally, I would like to express my sincere appreciation to my family, Miss Yaowapa Sukpondma, Miss Thunwadee Ritthiwigrom and friends for their love, understanding and encouragement over the course of my study.

Patima Phainuphong

CONTENTS

	Page
Abstract (in English)	(3)
Abstract (in Thai)	(6)
Acknowledgements	(9)
Contents	(10)
List of Tables	(13)
List of Illustrations	(19)
Abbreviations and Symbols	(28)
Chapter	
1 Introduction	1
1.1 Introduction	1
1.2 Review of Literatures	2
1.2.1 Chemical constituents from the genus <i>Garcinia</i>	2
1.2.2 Chemical constituents from the twigs of <i>Garcinia</i> <i>scortechinii</i>	10
1.2.3 Biosynthesis of caged-polyprenylated xanthenes	11
1.3 The objectives	22
2 Experimental	23
2.1 Chemicals and instruments	23
2.2 Plant material	24
2.3 Chemical investigation of the latex	24

CONTENTS (Continued)

	Page
2.4 Chemical investigation of the stem bark	51
2.4.1 Extraction	51
2.4.2 Chemical investigation of the crude methanol extract of the stem bark	52
3 Results and discussion	106
3.1 Characteristic spectroscopic data of caged-polyprenylated xanthones	107
3.2 Structural determination of compounds isolated from the latex of <i>G. scortechinii</i>	109
3.2.1 Compound PP7	109
3.2.2 Compound PP9	111
3.2.3 Compound PP5	117
3.2.4 Compound PP6	120
3.2.5 Compound PP8	123
3.2.6 Compound PP10	127
3.2.7 Compound PP2	132
3.2.8 Compound PP1	134
3.2.9 Compound PP3	140
3.2.10 Compound PP4	143

CONTENTS (Continued)

	Page
3.3 Structural determination of compounds isolated from the stem	146
bark of <i>G. scortechinii</i>	
3.3.1 Compound PP13	146
3.3.2 Compound PP14	148
3.3.3 Compound PP15	154
3.3.4 Compound PP16	157
3.3.5 Compound PP17	161
3.3.6 Compound PP11	164
3.3.7 Compound PP12	167
Bibliography	303
Vitae	311

LIST OF TABLES

Table	Page
1 Compounds from <i>Garcinia mangostana</i>	3
2 Solubility of the crude material in various solvents at room temperature	24
3 Fractions obtained from GLT by column chromatography on silica gel	26
4 Subfractions obtained from fraction T2 using precoated TLC on normal phase silica gel	27
5 Subfractions obtained from fraction T4 by column chromatography on silica gel	33
6 Subfractions obtained from subfraction T4-2 by column chromatography on silica gel	34
7 Subfractions obtained from fraction T9 by column chromatography on silica gel	43
8 Subfractions obtained from T10 by column chromatography over reversed-phase C18 silica gel	48
9 Subfractions obtained from T11 by column chromatography over reversed-phase C18 silica gel	50
10 Solubility of the crude methanol extract in various solvents at room temperature	52
11 Fractions obtained from GSBC by column chromatography on silica gel	53
12 Subfractions obtained from fraction B1 by column chromatography on silica gel	54

LIST OF TABLES (Continued)

Table	Page
13 Subfractions obtained from subfraction B1-2 by column chromatography on silica gel	55
14 Subfractions obtained from fraction B3 by flash column chromatography on silica gel	56
15 Subfractions obtained from subfraction B3-2 by flash column chromatography on silica gel	57
16 Subfractions obtained from fraction B4 by column chromatography on silica gel	61
17 Subfractions obtained from subfraction B4-3 by flash column chromatography on silica gel	62
18 Subfractions obtained from subfraction B4-3-2 by flash column chromatography on silica gel	63
19 Subfractions obtained from subfraction B4-4 by flash column chromatography on silica gel	66
20 Subfractions obtained from subfraction B4-5 by flash column chromatography on silica gel	69
21 Subfractions obtained from subfraction B4-6 by flash column chromatography on silica gel	71
22 Subfractions obtained from subfraction B4-7 by column chromatography on silica gel	73

LIST OF TABLES (Continued)

Table	Page
23 Subfractions obtained from subfraction B4-7-2 by flash column chromatography on silica gel	73
24 Subfractions obtained from fraction B7 by column chromatography on silica gel	76
25 Subfractions obtained from subfraction B7-4 by column chromatography on silica gel	77
26 Subfractions obtained from subfraction B7-4-3 by column chromatography on silica gel	78
27 Subfractions obtained from subfraction B7-5 by column chromatography on silica gel	79
28 Subfractions obtained from subfraction B7-5-2 by flash column chromatography on silica gel	80
29 Subfractions obtained from B7-6 by column chromatography over reversed-phase C18 silica gel	82
30 Subfractions obtained from B7-8 by column chromatography over reverse-phase C18 silica gel	86
31 Subfractions obtained from subfraction B7-8-2 by flash column chromatography on silica gel	87
32 Subfractions obtained from fraction B8 by column chromatography over reversed-phase C18 silica gel	89

LIST OF TABLES (Continued)

Table	Page
33 Subfractions obtained from subfraction B8-5 by flash column chromatography on silica gel	90
34 Subfractions obtained from subfraction B8-5-2 by column chromatography on silica gel	91
35 Subfractions obtained from subfraction B8-6 by column chromatography on silica gel	92
36 Subfractions obtained from subfraction B8-6-3 by column chromatography on silica gel	93
37 Subfractions obtained from subfraction B8-7 by column chromatography on silica gel	95
38 Subfractions obtained from subfraction B8-8 by column chromatography on silica gel	96
39 Subfractions obtained from subfraction B8-8-2 by flash column chromatography on silica gel	97
40 Subfractions obtained from subfraction B8-8-3 by flash column chromatography on silica gel	99
41 Subfractions obtained from subfraction B8-10 by column chromatography on silica gel	101
42 Subfractions obtained from subfraction B8-10-5 by flash column chromatography on silica gel	103

LIST OF TABLES (Continued)

Table	Page
43 The ^1H NMR data of scortechinone B and PP7	110
44 The ^1H NMR data of scortechinone B and PP9	113
45 The ^{13}C NMR data of scortechinone B and PP9	114
46 The HMBC correlations of scortechinone B and PP9	116
47 The NMR data of compound PP5	118
48 The NMR data of compound PP6	122
49 The NMR data of compound PP8	126
50 The NMR data of compound PP10	130
51 The ^1H NMR data of scortechinone A and PP2	133
52 The ^1H NMR data of scortechinone A and PP1	135
53 The ^{13}C NMR data of scortechinone A and PP1	137
54 The HMBC correlations of scortechinone A and PP1	138
55 The NMR data of compound PP3	142
56 The NMR data of compound PP4	144
57 The ^1H NMR data of PP13 and GF3	147
58 The ^1H NMR data of scortechinone C and PP14	150
59 The ^{13}C NMR data of scortechinone C and PP14	151
60 The HMBC correlations of scortechinone C and PP14	153
61 The NMR data of compound PP15	156
62 The NMR data of compound PP16	159

LIST OF TABLES (Continued)

Table	Page
63 The NMR data of compound PP17	136
64 The NMR data of PP11 and 4",5"-dihydro-1,5-dihydroxy-6',6'-dimethylpyrano(2',3':6,7)-4",4",5"-trimethylfurano(2",3":3,4)-xanthone	166

LIST OF ILLUSTRATIONS

Figure	Page
1 <i>Garcinia scortechinii</i>	1
2 UV (MeOH) spectrum of PP7	169
3 FT-IR (neat) spectrum of PP7	169
4 ¹ H NMR (500 MHz) (CDCl ₃) spectrum of PP7	170
5 Mass spectrum of PP9	171
6 UV (MeOH) spectrum of PP9	172
7 FT-IR (neat) spectrum of PP9	172
8 ¹ H NMR (500 MHz) (CDCl ₃) spectrum of PP9	173
9 ¹³ C NMR (125 MHz) (CDCl ₃) spectrum of PP9	174
10 DEPT spectrum of PP9	175
11 NOEDIFF spectrum of PP9 after irradiation at δ_{H} 6.41	176
12 NOEDIFF spectrum of PP9 after irradiation at δ_{H} 4.54	177
13 NOEDIFF spectrum of PP9 after irradiation at δ_{H} 1.46	178
14 2D HMQC spectrum of PP9	179
15 2D HMBC spectrum of PP9	180
16 Mass spectrum of PP5	181
17 UV (MeOH) spectrum of PP5	182
18 FT-IR (neat) spectrum of PP5	182
19 ¹ H NMR (500 MHz) (CDCl ₃) spectrum of PP5	183
20 ¹³ C NMR (125 MHz) (CDCl ₃) spectrum of PP5	184

LIST OF ILLUSTRATIONS (Continued)

Figure	Page
21 DEPT spectrum of PP5	185
22 NOEDIFF spectrum of PP5 after irradiation at δ_{H} 6.20	186
23 NOEDIFF spectrum of PP5 after irradiation at δ_{H} 4.55	187
24 NOEDIFF spectrum of PP5 after irradiation at δ_{H} 1.47	188
25 2D HMQC spectrum of PP5	189
26 2D HMBC spectrum of PP5	190
27 Mass spectrum of PP6	191
28 UV (MeOH) spectrum of PP6	192
29 FT-IR (neat) spectrum of PP6	192
30 ^1H NMR (500 MHz) (CDCl_3) spectrum of PP6	193
31 ^{13}C NMR (125 MHz) (CDCl_3) spectrum of PP6	194
32 DEPT spectrum of PP6	195
33 NOEDIFF spectrum of PP6 after irradiation at δ_{H} 6.23	196
34 NOEDIFF spectrum of PP6 after irradiation at δ_{H} 4.56	197
35 NOEDIFF spectrum of PP6 after irradiation at δ_{H} 1.45	198
36 2D HMQC spectrum of PP6	199
37 2D HMBC spectrum of PP6	200
38 Mass spectrum of PP8	201
39 UV (MeOH) spectrum of PP8	202
40 FT-IR (neat) spectrum of PP8	202

LIST OF ILLUSTRATIONS (Continued)

Figure	Page
41 ^1H NMR (400 MHz) (CDCl_3) spectrum of PP8	203
42 ^{13}C NMR (100 MHz) (CDCl_3) spectrum of PP8	204
43 DEPT spectrum of PP8	205
44 NOEDIFF spectrum of PP8 after irradiation at δ_{H} 4.40	206
45 NOEDIFF spectrum of PP8 after irradiation at δ_{H} 3.16	207
46 NOEDIFF spectrum of PP8 after irradiation at δ_{H} 1.98	208
47 NOEDIFF spectrum of PP8 after irradiation at δ_{H} 1.63	209
48 NOEDIFF spectrum of PP8 after irradiation at δ_{H} 1.10	210
49 2D HMQC spectrum of PP8	211
50 2D HMBC spectrum of PP8	212
51 Mass spectrum of PP10	213
52 UV (MeOH) spectrum of PP10	214
53 FT-IR (neat) spectrum of PP10	214
54 ^1H NMR (500 MHz) (CDCl_3) spectrum of PP10	215
55 ^{13}C NMR (125 MHz) (CDCl_3) spectrum of PP10	216
56 DEPT spectrum of PP10	217
57 NOEDIFF spectrum of PP10 after irradiation at δ_{H} 6.67	218
58 NOEDIFF spectrum of PP10 after irradiation at δ_{H} 4.37	219
59 NOEDIFF spectrum of PP10 after irradiation at δ_{H} 1.27	220
60 2D HMQC spectrum of PP10	221

LIST OF ILLUSTRATIONS (Continued)

Figure	Page
61 2D HMBC spectrum of PP10	222
62 UV (MeOH) spectrum of PP2	223
63 FT-IR (neat) spectrum of PP2	223
64 ^1H NMR (500 MHz) (CDCl_3) spectrum of PP2	224
65 Mass spectrum of PP1	225
66 UV (MeOH) spectrum of PP1	226
67 FT-IR (neat) spectrum of PP1	226
68 ^1H NMR (500 MHz) (CDCl_3) spectrum of PP1	227
69 ^{13}C NMR (125 MHz) (CDCl_3) spectrum of PP1	228
70 DEPT spectrum of PP1	229
71 NOEDIFF spectrum of PP1 after irradiation at δ_{H} 6.43	230
72 2D HMQC spectrum of PP1	231
73 2D HMBC spectrum of PP1	232
74 Mass spectrum of PP3	233
75 UV (MeOH) spectrum of PP3	234
76 FT-IR (neat) spectrum of PP3	234
77 ^1H NMR (500 MHz) (CDCl_3) spectrum of PP3	235
78 ^{13}C NMR (125 MHz) (CDCl_3) spectrum of PP3	236
79 DEPT spectrum of PP3	237
80 NOEDIFF spectrum of PP3 after irradiation at δ_{H} 1.59	238

LIST OF ILLUSTRATIONS (Continued)

Figure	Page
81 2D HMQC spectrum of PP3	239
82 2D HMBC spectrum of PP3	240
83 Mass spectrum of PP4	241
84 UV (MeOH) spectrum of PP4	242
85 FT-IR (neat) spectrum of PP4	242
86 ¹ H NMR (500 MHz) (CDCl ₃) spectrum of PP4	243
87 ¹³ C NMR (125 MHz) (CDCl ₃) spectrum of PP4	244
88 DEPT spectrum of PP4	245
89 NOEDIFF spectrum of PP4 after irradiation at δ_{H} 4.55	246
90 NOEDIFF spectrum of PP4 after irradiation at δ_{H} 1.49	247
91 2D HMQC spectrum of PP4	248
92 2D HMBC spectrum of PP4	249
93 UV (MeOH) spectrum of PP13	250
94 FT-IR (neat) spectrum of PP13	250
95 ¹ H NMR (500 MHz) (CDCl ₃) spectrum of PP13	251
96 Mass spectrum of PP14	252
97 UV (MeOH) spectrum of PP14	253
98 FT-IR (neat) spectrum of PP14	253
99 ¹ H NMR (400 MHz) (CDCl ₃) spectrum of PP14	254
100 ¹³ C NMR (100 MHz) (CDCl ₃) spectrum of PP14	255

LIST OF ILLUSTRATIONS (Continued)

Figure	Page
101 DEPT spectrum of PP14	256
102 NOEDIFF spectrum of PP14 after irradiation at δ_{H} 5.43	257
103 NOEDIFF spectrum of PP14 after irradiation at δ_{H} 4.55	258
104 NOEDIFF spectrum of PP14 after irradiation at δ_{H} 1.84	259
105 NOEDIFF spectrum of PP14 after irradiation at δ_{H} 1.46	260
106 2D HMQC spectrum of PP14	261
107 2D HMBC spectrum of PP14	262
108 Mass spectrum of PP15	263
109 UV (MeOH) spectrum of PP15	264
110 FT-IR (neat) spectrum of PP15	264
111 ^1H NMR (400 MHz) (CDCl_3) spectrum of PP15	265
112 ^{13}C NMR (100 MHz) (CDCl_3) spectrum of PP15	266
113 DEPT spectrum of PP15	267
114 NOEDIFF spectrum of PP15 after irradiation at δ_{H} 5.20	268
115 NOEDIFF spectrum of PP15 after irradiation at δ_{H} 1.52	269
116 NOEDIFF spectrum of PP15 after irradiation at δ_{H} 1.42	270
117 2D HMQC spectrum of PP15	271
118 2D HMBC spectrum of PP15	272
119 UV (MeOH) spectrum of PP16	273
120 FT-IR (neat) spectrum of PP16	273

LIST OF ILLUSTRATIONS (Continued)

Figure	Page
121 ^1H NMR (500 MHz) (CDCl_3) spectrum of PP16	274
122 ^{13}C NMR (125 MHz) (CDCl_3) spectrum of PP16	275
123 DEPT spectrum of PP16	276
124 NOEDIFF spectrum of PP16 after irradiation at δ_{H} 6.60	277
125 NOEDIFF spectrum of PP16 after irradiation at δ_{H} 4.40	278
126 NOEDIFF spectrum of PP16 after irradiation at δ_{H} 1.65	279
127 NOEDIFF spectrum of PP16 after irradiation at δ_{H} 1.11	280
128 2D HMQC spectrum of PP16	281
129 2D HMBC spectrum of PP16	282
130 UV (MeOH) spectrum of PP17	283
131 FT-IR (neat) spectrum of PP17	283
132 ^1H NMR (500 MHz) (CDCl_3) spectrum of PP17	284
133 ^{13}C NMR (125 MHz) (CDCl_3) spectrum of PP17	285
134 DEPT spectrum of PP17	286
135 NOEDIFF spectrum of PP17 after irradiation at δ_{H} 6.64	287
136 NOEDIFF spectrum of PP17 after irradiation at δ_{H} 1.57	288
137 NOEDIFF spectrum of PP17 after irradiation at δ_{H} 1.34	289
138 NOEDIFF spectrum of PP17 after irradiation at δ_{H} 1.10	290
139 2D HMQC spectrum of PP17	291
140 2D HMBC spectrum of PP17	292

LIST OF ILLUSTRATIONS (Continued)

Figure	Page
141 UV (MeOH) spectrum of PP11	293
142 FT-IR (neat) spectrum of PP11	293
143 ¹ H NMR (500 MHz) (CDCl ₃) spectrum of PP11	294
144 ¹³ C NMR (125 MHz) (CDCl ₃) spectrum of PP11	295
145 DEPT spectrum of PP11	296
146 NOEDIFF spectrum of PP11 after irradiation at δ_{H} 6.45	297
147 NOEDIFF spectrum of PP11 after irradiation at δ_{H} 4.55	298
148 2D HMQC spectrum of PP11	299
149 2D HMBC spectrum of PP11	300
150 FT-IR (KBr) spectrum of PP12	301
151 ¹ H NMR (500 MHz) (CDCl ₃) spectrum of PP12	302
Scheme	Page
1 Biosynthetic pathway of morellin (8)	12
2 Biosynthesis of gambogic acid (15)	13
3 Biosynthesis of the morellins	14
4 Biosynthesis of the morellins (8-13)	16
5 Biosynthetic formation of the heterocyclic bicyclo[2,2,2]octenone system	17
6 Biosynthetic pathway of the morellins	18

LIST OF ILLUSTRATIONS (Continued)

Scheme	Page
7 Biosynthesis of bractatin (16) and its derivatives	19
8 Biosynthetic route of gaudispirolactone (29)	20

ABBREVIATIONS AND SYMBOLS

<i>s</i>	=	<i>singlet</i>
<i>d</i>	=	<i>doublet</i>
<i>t</i>	=	<i>triplet</i>
<i>q</i>	=	<i>quartet</i>
<i>h</i>	=	<i>heptet</i>
<i>m</i>	=	<i>multiplet</i>
<i>br</i>	=	<i>broad</i>
<i>brs</i>	=	<i>broad singlet</i>
<i>brt</i>	=	<i>broad triplet</i>
<i>brq</i>	=	<i>broad quartet</i>
<i>brdd</i>	=	<i>broad doublet of doublet</i>
<i>dd</i>	=	<i>doublet of doublet</i>
<i>qt</i>	=	<i>quartet of triplet</i>
<i>ht</i>	=	<i>heptet of triplet</i>
<i>md</i>	=	<i>multiple of doublet</i>
<i>mt</i>	=	<i>multiple of triplet</i>
<i>ddd</i>	=	<i>doublet of doublet of doublet</i>
<i>qdd</i>	=	<i>quartet of doublet of doublet</i>
<i>mdd</i>	=	<i>multiple of doublet of doublet</i>
δ	=	chemical shift relative to TMS
<i>J</i>	=	coupling constant

ABBREVIATIONS AND SYMBOLS (Continued)

m/z	=	a value of mass divided by charge
$^{\circ}\text{C}$	=	degree celcius
R_f	=	retention factor
g	=	gram
mg	=	milligram
mL	=	milliliter
cm^{-1}	=	reciprocal centimeter
nm	=	nanometer
λ_{max}	=	maximum wavelength
ν	=	absorption frequencies
ϵ	=	Molar extinction coefficient
Hz	=	hertz
MHz	=	megahertz
ppm	=	part per million
rel. int.	=	relative intensity
$[\alpha]_D$	=	specific rotation
c	=	concentration
H-n	=	position of protons
C-n	=	position of carbons
UV	=	Ultraviolet
IR	=	Infrared

ABBREVIATIONS AND SYMBOLS (Continued)

NMR	=	Nuclear Magnetic Resonance
1D NMR	=	One Dimensional Nuclear Magnetic Resonance
2D NMR	=	Two Dimensional Nuclear Magnetic Resonance
MS	=	Mass Spectroscopy
HMQC	=	Heteronuclear Multiple Quantum Coherence
HMBC	=	Heteronuclear Multiple Bond Correlation
DEPT	=	Distortionless Enhancement by Polarization transfer
NOE	=	Nuclear Overhauser Effect
NOEDIFF	=	NOE Difference Spectroscopy
TLC	=	Thin-Layer Chromatography
TMS	=	tetramethylsilane
DMSO	=	dimethylsulphoxide
CHCl ₃	=	chloroform
EtOAc	=	ethyl acetate
MeOH	=	methanol

ABBREVIATIONS AND SYMBOLS (Continued)

CDCl_3	=	deuteriochloroform
ASA	=	anisaldehyde-sulphuric acid in acetic acid solution

CHAPTER 1

INTRODUCTION

1.1 Introduction

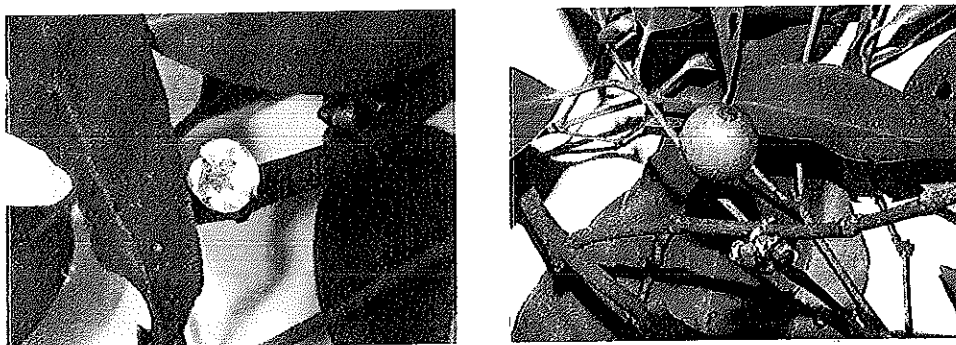


Figure 1 *Garcinia scortechinii*

Garcinia scortechinii, a plant belonging to the Guttiferae family (Clusiaceae), is a treelet of 4 m or a small slender tree, occasionally reaching 15 m tall, 75 cm girth. Inner bark contains copious, opaque, yellow to orange-yellow exudate. Leaves are occasionally grey-green. Flowers and fruits are very similar to *Garcinia domosa*. Commonly, this plant is scattered through Malaya, plains, low undulating country, ridges to 700 m and primary and secondary forest (Whitmore, 1973).

1.2 Review of Literatures

1.2.1 Chemical constituents from the genus *Garcinia*

The genus *Garcinia* (family Guttiferae) has been extensively investigated from phytochemical and pharmacological points of view. Various compounds have been isolated from this genus, such as xanthenes (Huang, 2001; Ito, 2001; Xu, 2001; Nilar, 2002; Suksamrarn, 2002), caged-polyprenylated xanthonoids (Rukachaisirikul, 2000a; Cao, 1998a, b; Asano, 1996; Kartha, 1963), benzophenones (Cuesta Rudio, 2001; Huang, 2001; Ali, 2000; Iinuma, 1996d; Spino, 1995; Fukuyama, 1993; Gustafson, 1992; Nyemba, 1990), benzophenone-xanthone dimers (Kosela, 2000, 1999; Iinuma, 1996a, b), biflavonoids (Thoisson, 2000; Spino, 1995; Fukuyama, 1993; Goh, 1992; Gunatilaka, 1983) and triterpenes (Nguyen, 2000; Rukachaisirikul, 2000a, b; Thoisson, 2000). Some of these compounds exhibit a wide range of biological and pharmacological activities, e.g. healing of skin infections and wounds (Ilyas, 1994), antioxidant (Peres, 2000; Kosela, 2000; Iinuma, 1996c; Minami, 1996), antibacterial (Permana, 2001; Peres, 2000; Rukachaisirikul, 2000a; Ito, 1997; Iinuma, 1996a, d; Parveen, 1991), antifungal (Kosela, 2000; Gopalakrishnan, 1997), anti-HIV (Kosela, 2000; Lin, 1997; Gustafson, 1992), antiinflammatory (Peres, 2000; Chairungrilerd, 1996; Ilyas, 1994; Parveen, 1991), antiimmunosuppressive (Ilyas, 1994; Parveen, 1991), antimalarial (Kosela, 2000; Likhiwitayawuid, 1998a, b), antiprotozoal (Parveen, 1991), antitumor (Ito, 1998) and cytotoxic (Permana, 2001; Kosela, 2000; Thoisson, 2000; Xu, 2000; Cao, 1998a, b) activities.

According to information from NAPRALERT database, developed by University of Illinois at Chicago and Chemical Abstracts in the year 2001, chemical constituents isolated from 62 species of the genus *Garcinia* were summarized (Ritthiwigrom, 2002). The continuing search on SciFinder database and <http://www.sciencedirect.com> revealed that only additional chemical constituents isolated from *G. mangostana* as shown in Table 1 were reported in the year 2002.

Table 1 Compounds from *Garcinia mangostana*

Investigation part	Compound	Structure	Bibliography
green fruit	mangostenol	2a	Suksamrarn, <i>et al.</i> , 2002
hulls	mangostenone A	2g	
	mangostenone B	2h	
	trapezifolixanthone	2i	
	tovophyllin B	2j	
	α -mangostin	2e	
	β -mangostin	2f	
	garcinone B	2k	
	mangostinone	2l	
	mangostanol	2m	
	epicatechin	1a	
heartwood	β -mangostin	2f	Nilar, <i>et al.</i> , 2002

Table 1 (Continued)

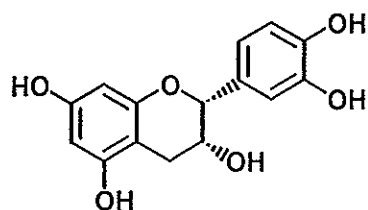
Investigation part	Compound	Structure	Bibliography
heartwood	garciniafuran	2n	Nilar, <i>et al.</i> , 2002
	1-hydroxy-8-(2-hydroxy-3-methylbut-3-enyl)-3,6,7-trimethoxy-2-(3-methylbut-2-enyl)xanthone	2r	
	1,6-dihydroxy-8-(2-hydroxy-3-methylbut-3-enyl)-3,7-dimethoxy-2-(3-methylbut-2-enyl)xanthone	2s	
	mangostanin	2o	
	6- <i>O</i> -methylmangostanin	2p	
	1,6-dihydroxy-2-(2-hydroxy-3-methylbut-3-enyl)-3,7-dimethoxy-8-(3-methylbut-2-enyl)xanthone	2b	
	1-hydroxy-2-(2-hydroxy-3-methylbut-3-enyl)-3,6,7-trimethoxy-8-(3-methylbut-2-enyl)xanthone	2c	

Table 1 (Continued)

Investigation part	Compound	Structure	Bibliography
heartwood	1,3-dihydroxy-2-(2-hydroxy-3-methylbut-3-enyl)-6,7-dimethoxy-8-(3-methylbut-2-enyl)xanthone	2d	Nilar, <i>et al.</i> , 2002
	(16 <i>E</i>)-1,6-dihydroxy-8-(3-hydroxy-3-methylbut-1-enyl)-3,7-dimethoxy-2-(3-methylbut-2-enyl)xanthone	2t	
	(16 <i>E</i>)-1-hydroxy-8-(3-hydroxy-3-methylbut-1-enyl)-3,6,7-trimethoxy-2-(3-methylbut-2-enyl)xanthone	2u	
	1,6-dihydroxy-3,7-dimethoxy-2-(3-methylbut-2-enyl)xanthone	2q	
	1,6-dihydroxy-3,7-dimethoxy-2-(3-methylbut-2-enyl)-8-(2-oxo-3-methylbut-3-enyl)xanthone	2v	

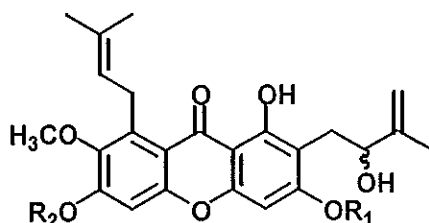
Structures of compounds in Table 1

1. Flavonoid



1a: epicatechin

2. Xanthenes

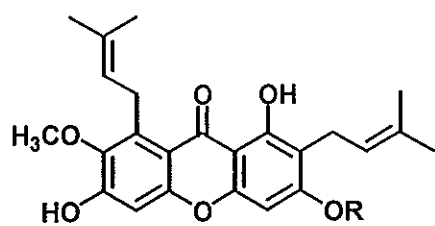
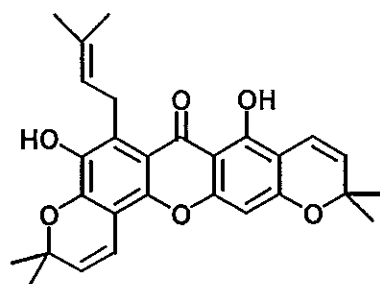


2a: $R_1 = H$; $R_2 = H$: mangostenol

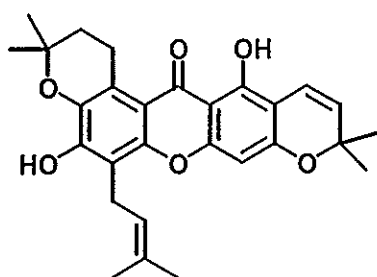
2b: $R_1 = CH_3$; $R_2 = H$: 1,6-dihydroxy-2-(2-hydroxy-3-methylbut-3-enyl)-3,7-dimethoxy-8-(3-methylbut-2-enyl)xanthone

2c: $R_1 = R_2 = CH_3$: 1-hydroxy-2-(2-hydroxy-3-methylbut-3-enyl)-3,6,7-trimethoxy-8-(3-methylbut-2-enyl)xanthone

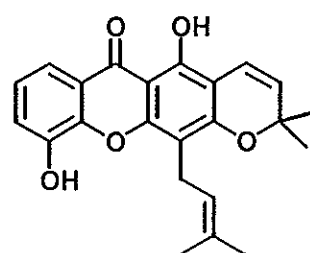
2d: $R_1 = H$; $R_2 = CH_3$: 1,3-dihydroxy-2-(2-hydroxy-3-methylbut-3-enyl)-6,7-dimethoxy-8-(3-methylbut-2-enyl)xanthone

2c: R = H : α -mangostin2f: R = CH₃ : β -mangostin

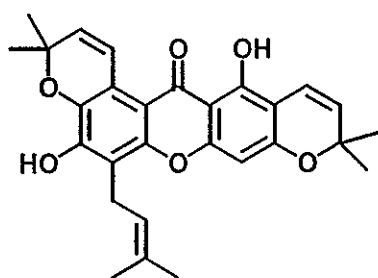
2g: mangostenone A



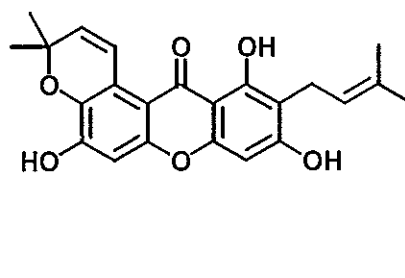
2h: mangostenone B



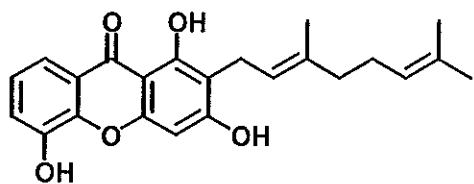
2i: trapezifolixanthone



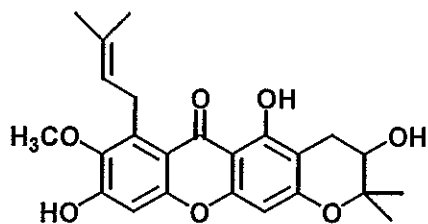
2j: tovophyllin



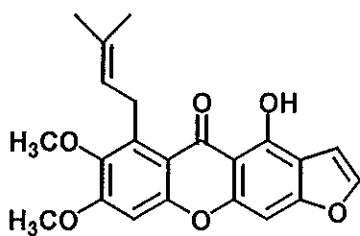
2k: garcinone B



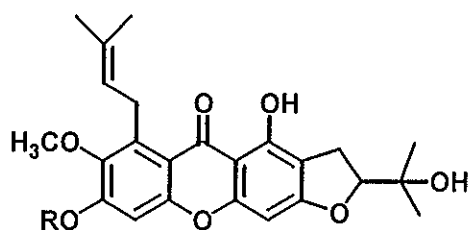
2l: mangostinone



2m: mangostanol

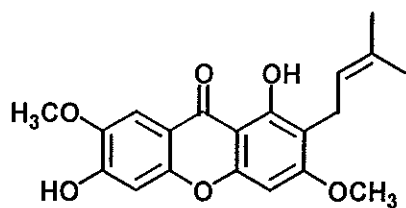


2n: garciniafuran

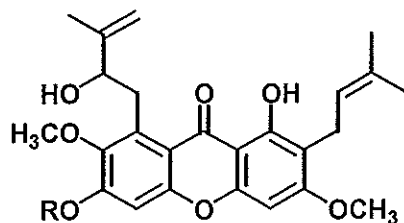


2o: R = H : mangostanin

2p: R = Me : 6-O-methylmangostanin

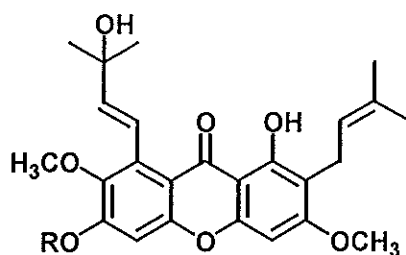


2q: 1,6-dihydroxy-3,7-dimethoxy-2-(3-methylbut-2-enyl)xanthone



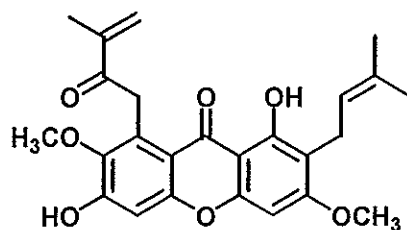
2r: R = CH₃ : 1-hydroxy-8-(2-hydroxy-3-methylbut-3-enyl)-3,6,7-trimethoxy-2-(3-methylbut-2-enyl)xanthone

2s: R = H : 1,6-dihydroxy-8-(2-hydroxy-3-methylbut-3-enyl)-3,7-dimethoxy-2-(3-methylbut-2-enyl)xanthone



2t: R = H : (16*E*)-1,6-dihydroxy-8-(3-hydroxy-3-methylbut-1-enyl)-3,7-dimethoxy-2-(3-methylbut-2-enyl)xanthone

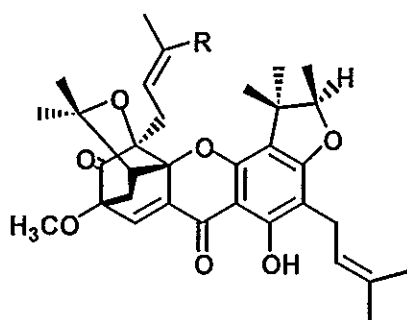
2u: R = CH₃ : (16*E*)-1-hydroxy-8-(3-hydroxy-3-methylbut-1-enyl)-3,6,7-trimethoxy-2-(3-methylbut-2-enyl)xanthone



2v: 1,6-dihydroxy-3,7-dimethoxy-2-(3-methylbut-2-enyl)-8-(2-oxo-3-methylbut-3-enyl)xanthone

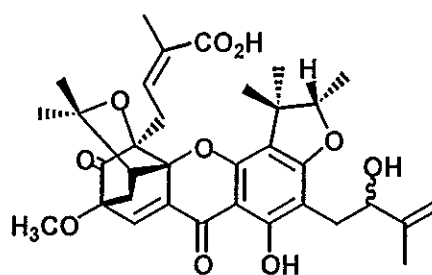
1.2.2 Chemical constituents from the twigs of *Garcinia scortechnii*

The chemical investigation of *Garcinia scortechnii* was first reported in the year 2000 by Rukachaisirikul. From the methanol extract from the twigs of *Garcinia scortechnii*, three new caged-tetraprenylated xanthenes [scortechinone A-C (3-5)] together with two known compounds [friedelin (6) and stigmasterol (7)] were isolated. The antibacterial activity of scortechinone A-C (3-5) against methicillin-resistant *Staphylococcus aureus* (MRSA) was also examined (Rukachaisirikul, 2000a).

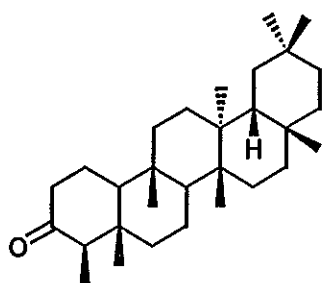


3: R = CH₃

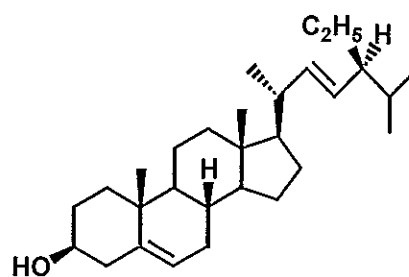
4: R = CO₂H



5



6

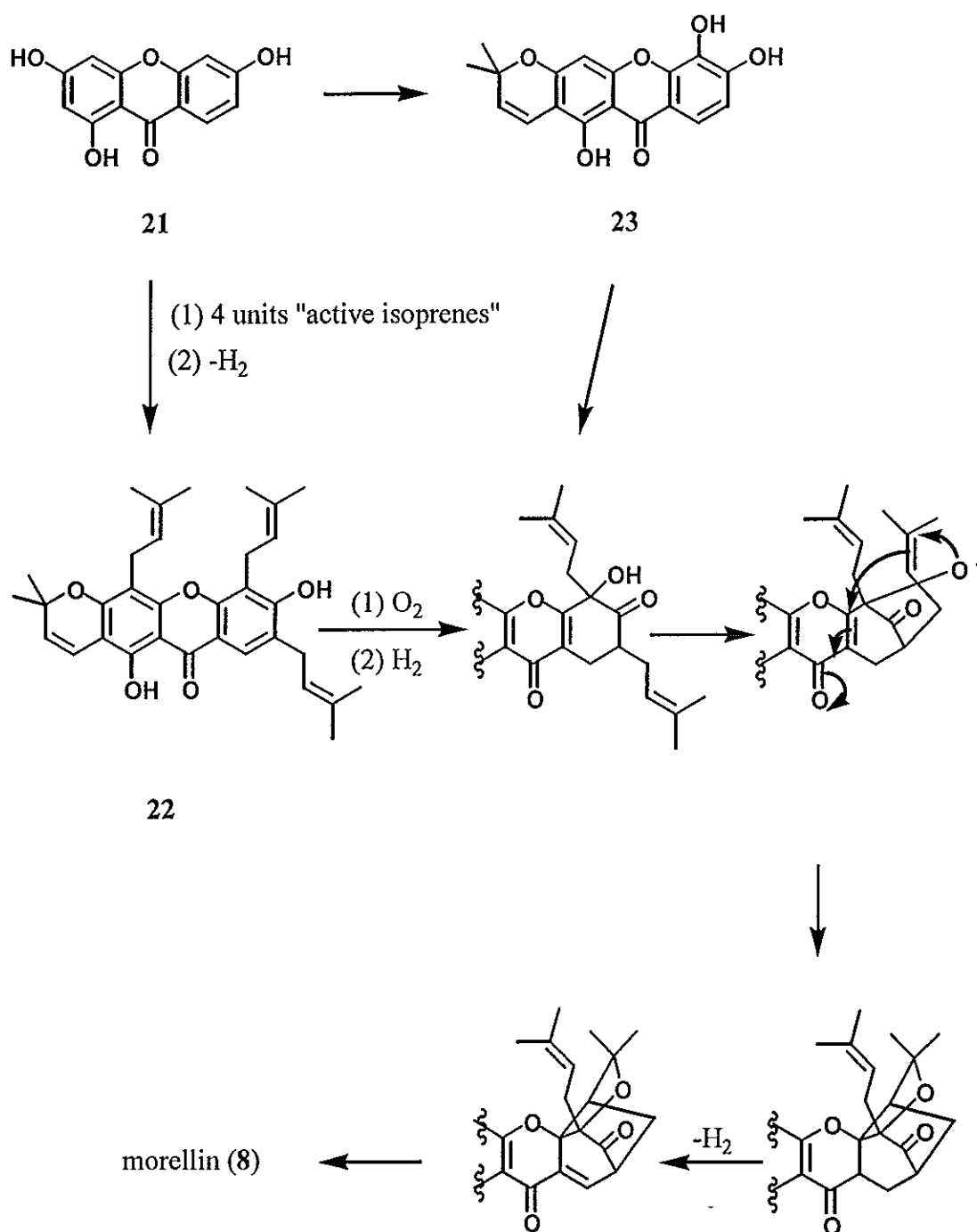


7

1.2.3 Biosynthesis of caged-polyprenylated xanthenes

Caged-polyprenylated xanthenes are exclusively found in several plants which belong to the genus *Garcinia*, e.g. *G. morella* (Kartha, 1963; Yates, 1963; Ollis, 1965; Karanjgaonkar, 1966), *G. hanburyi* (Asano, 1996), *G. gaudichaudii* (Cao, 1998a, b) and *G. scortechinii* (Rukachaisirikul, 2000a). Their biosynthesis has already been hypothesized. Although there are no experimental data on the biosynthesis, the polyisoprenylated xanthonoids can be considered to be formed by polyisoprenylation of xanthone precursor. Herein, the proposed biosyntheses for caged-polyprenylated xanthenes were summarized.

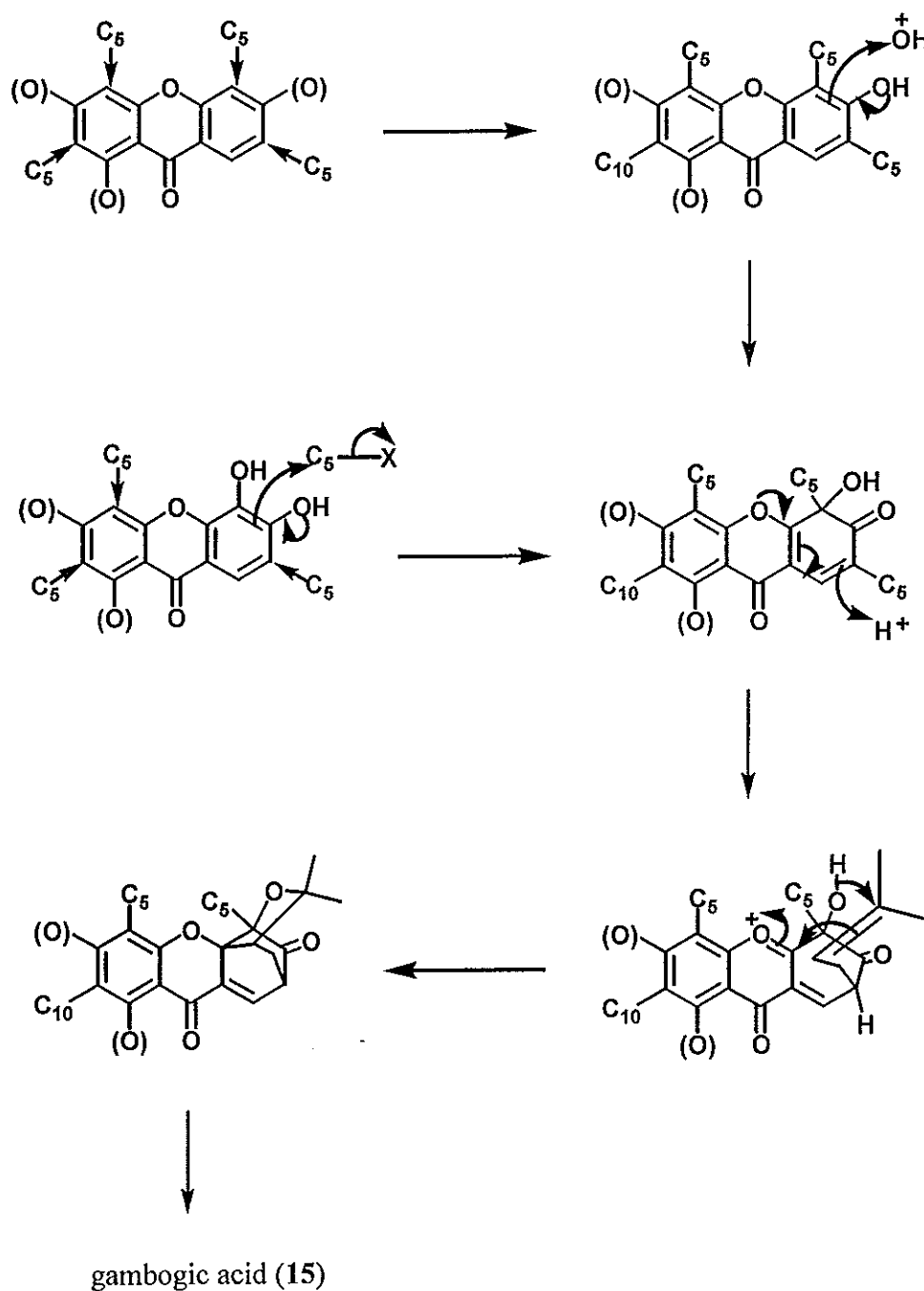
The first biosynthesis of caged-polyprenylated xanthenes was reported in the year 1963. Kartha *et al.* proposed that morellin (**8**) can be derived biogenetically from 1,3,7-trihydroxyxanthone (**21**) and four units of "active isoprene", as outlined in **Scheme 1**. A phenol (presumably derived from acetate or acetate-malonate units) could be transformed to a bicyclo-octenone by the cyclization of an isoprenoid side chain. Since there was no evidence for the reaction sequence proposed in **Scheme 1**, a mechanism might or might not involve hydrogenation and dehydrogenation after the formation of chromene **22**. On the other hand, morellin (**8**), might be derived from jacareubin (**23**) of which a dimethylallyl group has cyclized with an adjacent phenolic hydroxyl to form a 2,2-dimethylchromene.



Scheme 1 Biosynthetic pathway of morellin (8)

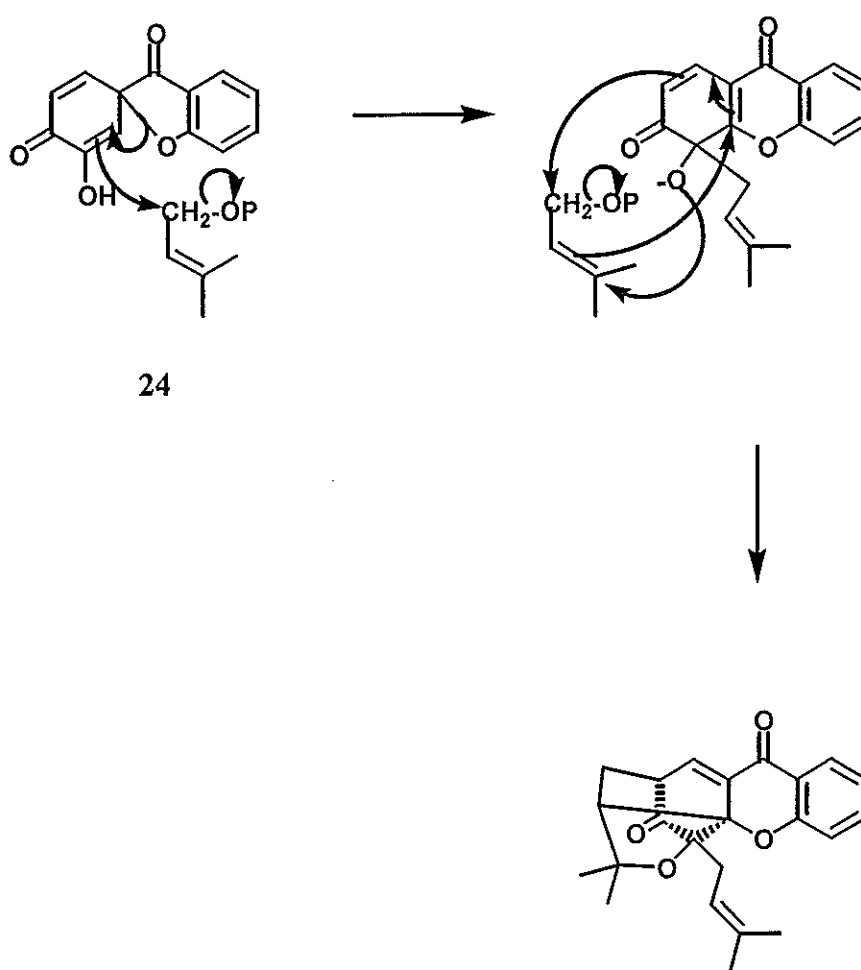
Based on the biosynthesis of morellin (8) (Kantha, 1963), Ollis *et al.* suggested the biosynthesis of gambogic acid (15) which is simpler and obviates the necessity to

have a sequence of reduction and oxidation reactions, as shown in **Scheme 2**. In addition, the xanthonoid precursor could either be of jacareubin oxygenation pattern (see 23) or a quinol intermediate (Ollis, 1965).



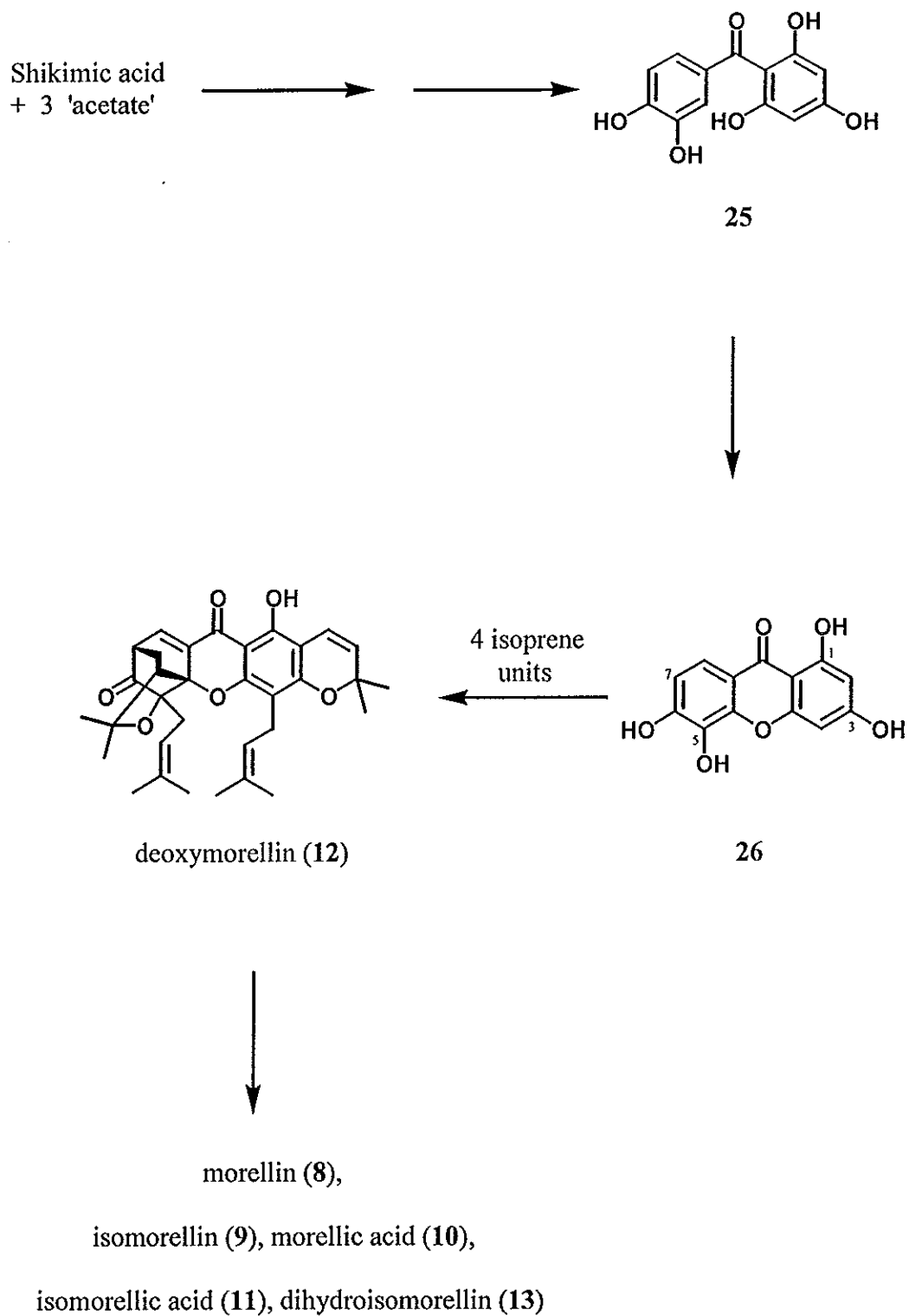
Scheme 2 Biosynthesis of gambogic acid (15)

In the year 1968, Gottlieb proposed the xanthone biosynthesis which involves a dienone intermediate (24). The pyrone oxygen played a major role in the construction of bicyclic system. This allows the formation of the morellins to be rationalized through isoprenylation reaction as shown in **Scheme 3**.

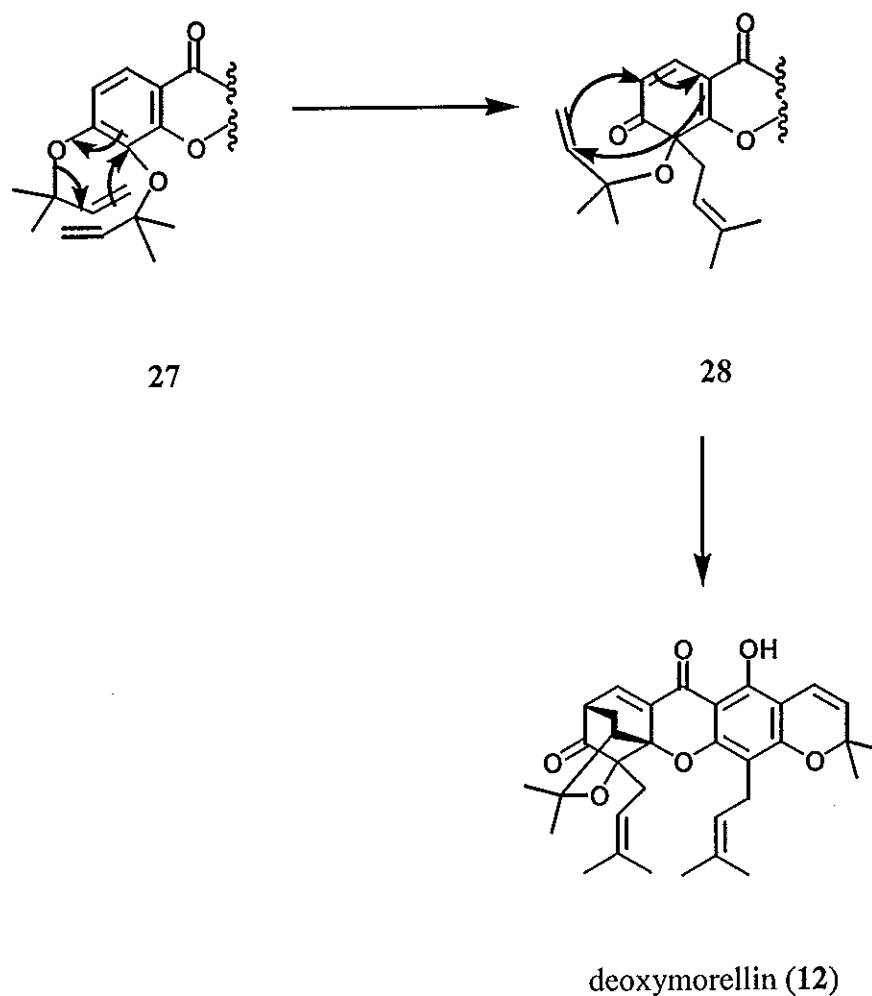


Scheme 3 Biosynthesis of the morellins

In contrast to previous biogenetic suggestions, Quillin *et al.*, in the year 1971, proposed that the morellins (8-13) and gambogic acid (15) might be derived directly from 1,3,5,6-tetrahydroxyxanthone (26) which can be formed by oxidative coupling of benzophenone such as maclurin (25). Isoprenylation of the xanthone (26) with four isoprene units can lead to deoxymorellin (12) and related metabolites (Scheme 4). They postulate that isoprenylation occurs at C-7 in the shikimate derived ring, such as 26, is unattractive since 7-isoprenylxanthenes are not yet known. An alternative route to the heterocyclic bicyclo[2, 2, 2]octenone system involves a Claisen rearrangement on the 5,6-diallyl ether (27) followed by a Diels-Alder reaction on the intermediate dienone (28) as shown in Scheme 5. Quillin *et al.* also showed that 1-hydroxy-5,6-diallyloxyxanthone and jacareubin 5,6-diallyl ether formed bicyclo[2, 2, 2]octenone functionality after boiling in decalin for 14 hours. Therefore, it is suggested that this synthetic pathway may be involved in the biosynthesis of morellins and gambogic acid.

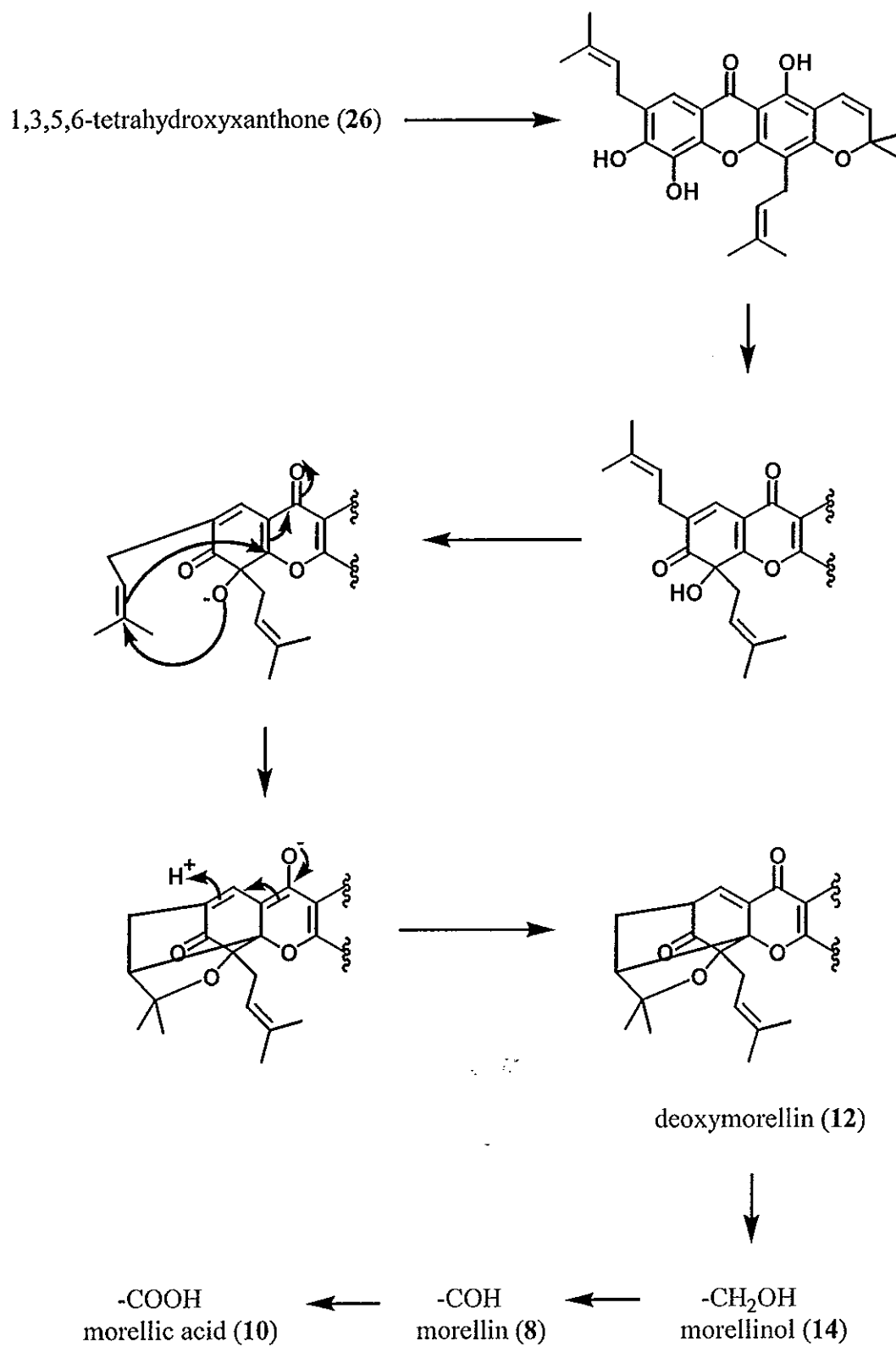


Scheme 4 Biosynthesis of the morellins (8-13)



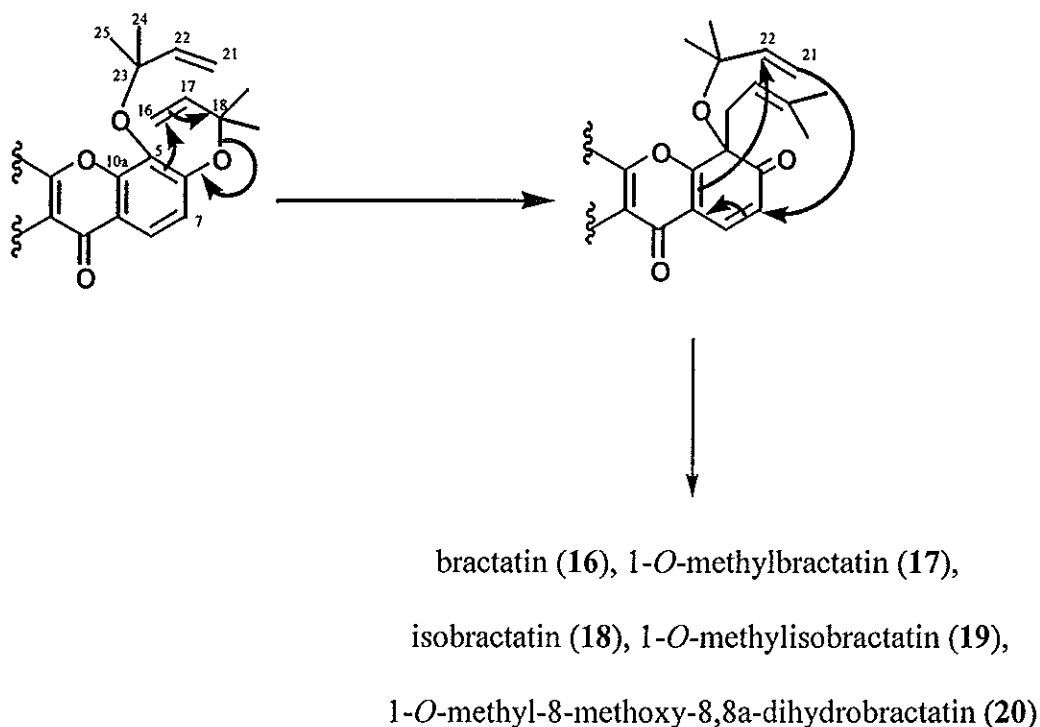
Scheme 5 Biosynthetic formation of the heterocyclic bicyclo[2,2,2]octenone system

Venkataraman, in the year 1974, proposed a modified biosynthesis pathway which the pyrone carbonyl group (see Scheme 1), not the pyrone oxygen (see Scheme 2), played an important role in the concerted series of reactions as shown in Scheme 6. Deoxymorellin (12) is the first pigment formed in the biosynthesis and the progressive oxidation of a methyl group then leads to morellinol (14), morellin (8), and morellic acid (10) (Sultanbawa, 1980).



Scheme 6 Biosynthetic pathway of the morellins

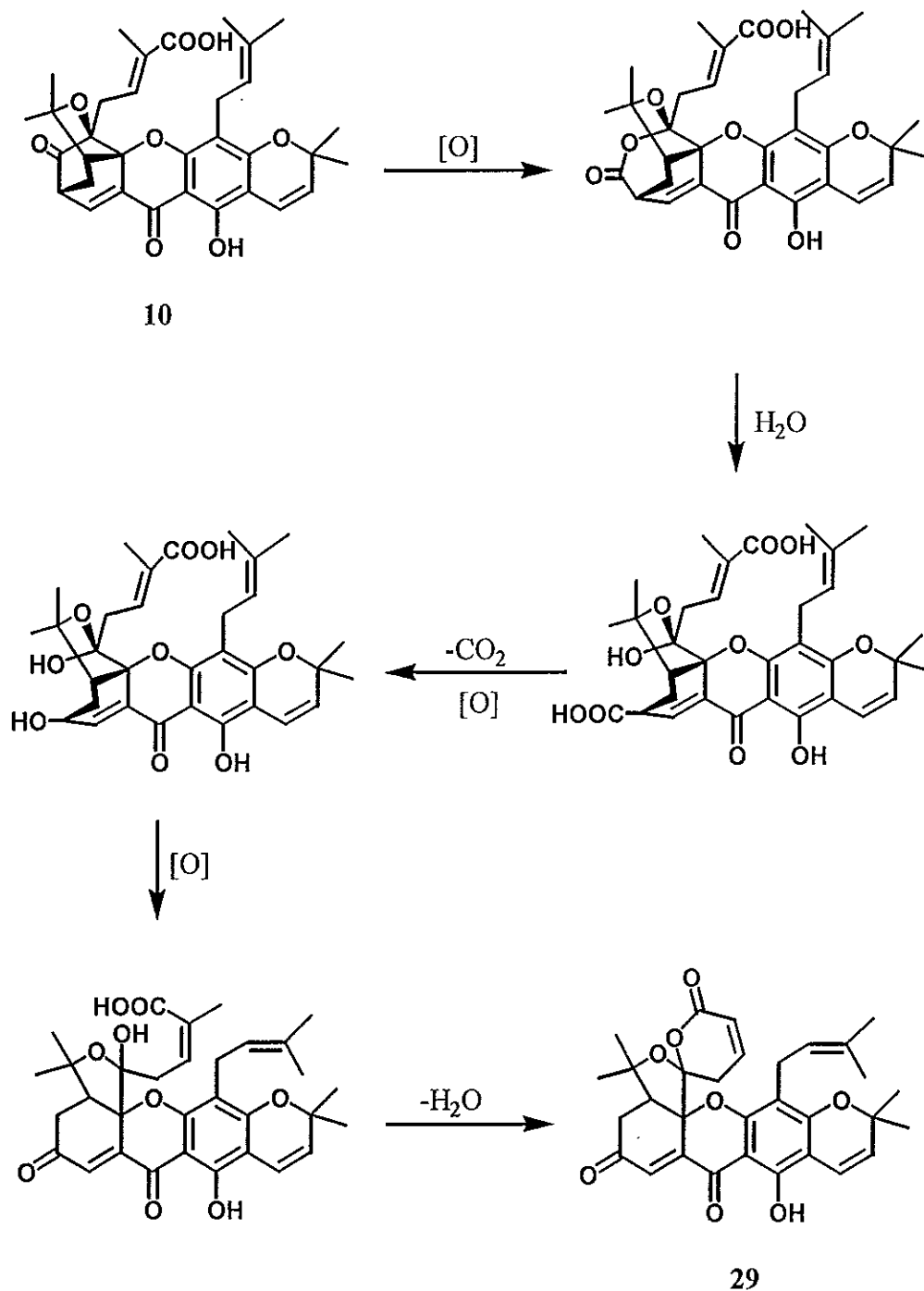
In the year 2000, Thoison *et al.* proposed the biosynthesis for bractatin (**16**), 1-*O*-methylbractatin (**17**), isobractatin (**18**), 1-*O*-methylisobractatin (**19**), 1-*O*-methyl-8-methoxy-8,8a-dihydrobractatin (**20**) based on the biosynthesis proposed by Quillin *et al.* (Quillin, 1971). The Claisen rearrangement involving migration of the allyloxy group at C-6 to the ortho position leads to an intermediate that undergoes a Diels-Alder cyclization of the double bond C-22 - C-21 on C-10a and C-7, respectively, as shown in **Scheme 7**.



Scheme 7 Biosynthesis of bractatin (16) and its derivatives

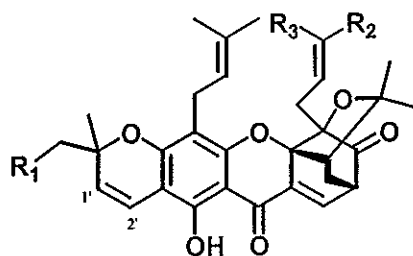
Lastly, a plausible biosynthetic route of gaudispirolactone (**29**), a degraded derivative of a caged-polyprenylated xanthone, starting from morellic acid (**10**), was shown in **Scheme 8** (Wu, 2001). Oxidation of the ketone (**10**), followed by hydrolysis

of an ester functionality, gave the cleaved product which underwent a series of reactions: decarboxylation, oxidation and dehydration to afford the spiro lactone (29).

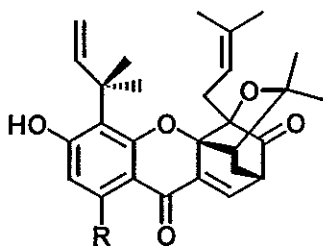


Scheme 8 Biosynthetic route of gaudispirolactone (29)

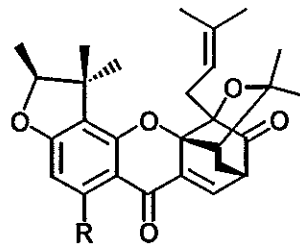
Structures of caged-polyprenylated xanthenes related the biosynthesis above



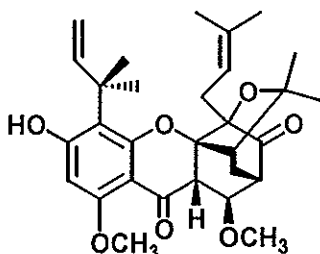
	R ₁	R ₂	R ₃
8:	H	CHO	Me : morellin
9:	H	Me	CHO : isomorellin
10:	H	Me	CO ₂ H : morellic acid
11:	H	CO ₂ H	Me : isomorellic acid
12:	H	Me	Me : deoxymorellin
13:	H	CHO	Me : dihydroisomorellin
			(single bond at C-1' and C-2')
14:	H	CH ₂ OH	Me : morellinol
15:	Me ₂ C=CH-CH ₂	Me	CO ₂ H : gambogic acid



16: R = OH : bractatin



18: R = OH : isobractatin

17: R = OMe : 1-*O*-methylbractatin19: R = OMe : 1-*O*-methylisobractatin20: 1-*O*-methyl-8-methoxy-8,8a-dihydrobractatin

1.3 The objectives

Based on the literature search, phytochemical studies on the twigs of *Garcinia scortechinii* have shown that caged-polyprenylated xanthenes, the major components, exhibited antibacterial activity against methicillin-resistant *Staphylococcus aureus* (MRSA). Therefore, we are interested in investigating other parts of this plant with the hope that additional new caged-polyprenylated xanthenes with better antibacterial activity against MRSA will be isolated. This research involved isolation, purification and structure elucidation of the chemical constituents isolated from the latex and the stem bark of *G. scortechinii* which were collected at the Ton Nga Chang Wildlife Sanctuary.

CHAPTER 2

EXPERIMENTAL

2.1 Chemicals and instruments

Melting points are determined on an electrothermal melting point apparatus (Electrothermal 9100) and reported without correction. Infrared spectra (IR) were obtained on a FTS165 FT-IR spectrometer and Perkin Elmer Spectrum GX FT-IR system and recorded on wavenumber (cm^{-1}). ^1H and ^{13}C -Nuclear magnetic resonance (^1H and ^{13}C NMR) spectra were recorded on a FTNMR, Varian UNITY INOVA 500 MHz or Bruker AMX 400 using a solution in deuteriochloroform with tetramethylsilane (TMS) as an internal standard. Spectra were recorded as chemical shift parameter (δ) value in ppm down field from TMS (δ 0.00). Ultraviolet spectra (UV) were measured with specord S100 spectrophotometer (Analytik Jena Ag). Principle bands (λ_{max}) were recorded as wavelengths (nm) and $\log \varepsilon$ in methanol solution. Optical rotations were measured in methanol solution with sodium D line (589 nm) on an AUTOPOL[®]II automatic polarimeter. Thin-layer chromatography (TLC) and precoated thin-layer chromatography were performed on silica gel 60 GF₂₅₄ (Merck) or reversed-phase C-18. Column chromatography was performed on silica gel (Merck) type 100 (70-230 Mesh ASTM) or reversed-phase C-18. The solvents for extraction and chromatography were distilled at their boiling point ranges

prior to use except for petroleum ether (bp. 40-60°C) and ethyl acetate which were analytical grade reagent.

2.2 Plant material

The latex and the stem bark of *Garcinia scortechinii* were collected at the Ton Nga Chang Wildlife Sanctuary, Hat Yai, Songkla, Thailand in June 2000. The plant was identified by Ajarn Prakart Sawangchote, Department of Biology, Faculty of Science, Prince of Songkla University, Hat Yai Songkla, where a voucher specimen has been deposited.

2.3 Chemical investigation of the latex

The latex was primarily tested for its solubility in various solvents at room temperature. The results were demonstrated in **Table 2**.

Table 2 Solubility of the crude material in various solvents at room temperature

solvent	solubility at room temperature
Petroleum ether	-
Chloroform	+ (yellow solution with brown solid)
Ethyl acetate	+ (yellow solution with brown solid)
Methanol	++ (yellow solution)

Table 2 (Continued)

solvent	solubility at room temperature
Water	-
10% HCl	-
10% NaOH	++ (red-brown solution)

Symbol meaning : - insoluble, + partailly soluble, ++ well soluble

It was shown that the crude material was slightly soluble in both chloroform and ethyl acetate but it was soluble well in methanol and 10% aqueous NaOH, indicating that it contained moderately polar and acidic compounds.

The crude material (8.36 g) was separated into two parts by dissolving with chloroform. **GLT**, the chloroform soluble part, was a yellow solid (8.18 g) while **GLM**, the methanol soluble part, was a brown gum (0.1797 g). The chromatogram on normal phase TLC of **GLM** showed no definite spot. Thus, it was not further investigated. Further separation of **GLT** (8.18 g) was carried out by column chromatography on silica gel. Elution was conducted initially with pure chloroform and gradually increased the polarity until pure methanol. Fractions with the similar chromatogram were combined and evaporated under reduced pressure to dryness to afford eleven fractions, as shown in **Table 3**.

Table 3 Fractions obtained from GLT by column chromatography on silica gel

fraction	Weight (g)	Physical appearance
T1	0.1299	Yellow gum
T2	0.1881	Yellow gum
T3	0.0179	Yellow gum
T4	1.0964	Yellow solid with yellow gum
T5	1.8644	Yellow solid with yellow gum
T6	0.3211	Yellow solid with yellow gum
T7	0.0513	Yellow gum
T8	3.7317	Yellow solid with yellow gum
T9	0.5568	Yellow gum
T10	0.3268	Brown gum
T11	0.3075	Brown gum

Fraction T1 The chromatogram on normal phase TLC (80% CHCl₃/Petrol) showed many UV-active spots without any major spots. Therefore, it was not further investigated.

Fraction T2 The chromatogram on normal phase TLC (10% EtOAc/Petrol, 2 times) showed four major yellow spots with the R_f values of 0.41, 0.37, 0.31 and 0.25. Further separation on precoated TLC using 20% EtOAc/Petrol as a mobile phase (2 times) afforded six subfractions, as shown in **Table 4**.

Table 4 Subfractions obtained from fraction T2 using precoated TLC on normal phase silica gel

fraction	Weight (g)	Physical appearance
P1	0.0056	Yellow gum
P2	0.0291	Yellow solid with yellow gum
P3	0.0186	Yellow solid with yellow gum
P4	0.0283	Yellow solid
P5	0.0346	Yellow solid with yellow gum
P6	0.0326	Yellow gum

Subfraction P1 The chromatogram on normal phase TLC (10% EtOAc/Petrol, 2 times) showed four UV-active spots with the R_f values of 0.60, 0.28, 0.23 and 0.08. Because it was obtained in low quantity, it was not further investigated.

Subfraction P2 The chromatogram on normal phase TLC (10% EtOAc/Petrol, 2 times) showed two spots; one yellow spot with the R_f value of 0.45 and a pale yellow spot with the R_f value of 0.41. Further purification was performed by precoated TLC, using 5% EtOAc/Petrol as a mobile phase (20 times), to afford two bands.

Band P2-1 (PP1) It was obtained as a yellow gum (0.0106 g). The chromatogram on normal phase TLC (5% EtOAc/Petrol, 12 times) showed only one yellow spot with the R_f value of 0.59.

$[\alpha]_D^{29} = -200^\circ$ ($c = 1.5 \times 10^{-2} \text{ g/100 cm}^3$, MeOH)	
UV λ_{max} nm (MeOH) ($\log \epsilon$)	361 (3.81)
IR (neat) $\nu_{\text{cm}^{-1}}$	3397 (O-H stretching), 2968, 2927, 2858 (C-H stretching), 1746, 1634 (C=O stretching)
$^1\text{H NMR}$ (CDCl_3) (δ ppm) (500 MHz)	13.62 (<i>s</i> , 1H), 7.70 (<i>s</i> , 1H), 7.48 (<i>d</i> , $J = 1.0$ Hz, 1H), 6.43 (<i>dd</i> , $J = 17.5$ and 10.5 Hz, 1H), 5.46 (<i>d</i> , $J = 17.5$ Hz, 1H), 5.37 (<i>dd</i> , $J = 10.5$ and 1.0 Hz, 1H), 5.14 (<i>mt</i> , $J = 6.5$ Hz, 1H), 4.43 (<i>mdd</i> , $J = 10.0$ and 5.0 Hz, 1H), 3.63 (<i>s</i> , 3H), 3.30 (<i>d</i> , $J = 6.5$ Hz, 2H), 2.62-2.56 (<i>m</i> , 1H), 2.54 (<i>d</i> , $J = 10.0$ Hz, 1H), 2.50 (<i>d</i> , $J = 10.0$ Hz, 1H), 2.33 (<i>d</i> , $J = 13.0$ Hz, 1H), 1.70 (<i>s</i> , 3H), 1.66 (<i>d</i> , $J = 1.0$ Hz, 3H), 1.65 (<i>s</i> , 3H), 1.61 (<i>dd</i> , $J = 13.0$ and 10.0 Hz, 1H), 1.60 (<i>s</i> , 3H), 1.59 (<i>s</i> , 3H), 1.37 (<i>s</i> , 3H), 1.28 (<i>s</i> , 3H), 1.01 (<i>s</i> , 3H)
$^{13}\text{C NMR}$ (CDCl_3) (δ ppm) (125 MHz)	201.96, 179.09, 163.32, 162.86, 156.27, 149.53, 135.27, 134.02, 132.35, 132.31, 122.36, 117.54, 113.69, 111.62, 108.18, 100.95, 88.68, 84.81, 83.53, 53.95, 49.71, 40.96, 30.24, 30.07, 29.01, 28.82, 27.16, 26.90, 25.66, 25.54, 22.16, 18.07, 16.69
DEPT (135°) (CDCl_3)	CH 149.53, 134.02, 122.36, 117.54, 49.71 CH ₂ 113.69, 30.24, 28.82, 22.16 CH ₃ 53.95, 30.07, 29.01, 27.16, 26.90, 25.66, 25.54,

	18.07, 16.69
EIMS (m/z) (% rel. int.)	534 (100), 465 (45), 437 (38), 247 (46), 203 (12), 149 (40), 69 (44)

Band P2-2 It was obtained as a yellow gum (0.0070 g). The chromatogram on normal phase TLC (5% EtOAc/Petrol, 12 times) showed two yellow spots with the R_f values of 0.59 and 0.53. Because it was obtained in low quantity, it was not further investigated.

Subfraction P3 The chromatogram on normal phase TLC (10% EtOAc/Petrol, 2 times) showed three yellow spots with the R_f values of 0.45, 0.41 and 0.30 and one UV-active spot with the R_f value of 0.12. Because it was obtained in low quantity, it was not further investigated.

Subfraction P4 (PP2) The chromatogram on normal phase TLC (10% EtOAc/Petrol, 2 times) showed only one spot with the same R_f value as scortechinone A, obtained from its twigs. It melted at 152.6-154.8°C.

$[\alpha]_D^{29} = +18^\circ$ ($c = 2.8 \times 10^{-2}$ g/100 cm ³ , MeOH)	
UV λ_{\max} nm (MeOH) ($\log \epsilon$)	362 (3.88)
IR (neat) $\nu_{\text{cm}^{-1}}$	3454 (O-H stretching), 2927, 2856 (C-H stretching), 1745, 1634 (C=O stretching)
¹ H NMR (CDCl ₃) (δ ppm) (500 MHz)	13.19 (<i>s</i> , 1H), 7.51 (<i>d</i> , $J = 1.5$ Hz, 1H), 5.22 (<i>ht</i> , $J = 7.0$ and 1.5 Hz, 1H), 4.41-4.36 (<i>m</i> , 1H), 4.38 (<i>q</i> , $J = 7.0$ Hz, 1H), 3.63 (<i>s</i> , 3H), 3.27-3.17 (<i>m</i> , 2H), 2.69 (<i>md</i> , $J = 14.5$ Hz, 1H), 2.56 (<i>dd</i> , J

= 14.5 and 10.0 Hz, 1H), 2.56 (*d*, $J = 9.5$ Hz, 1H), 2.33 (*brd*, $J = 13.0$ Hz, 1H), 1.75 (*brs*, 3H), 1.71 (*s*, 3H), 1.68 (*brs*, 3H), 1.65 (*dd*, $J = 13.0$ and 9.5 Hz, 1H), 1.58 (*s*, 3H), 1.41 (*d*, $J = 7.0$ Hz, 3H), 1.36 (*brs*, 3H), 1.29 (*s*, 3H), 1.16 (*s*, 3H), 1.06 (*s*, 3H)

Subfraction P5 The chromatogram on normal phase TLC (10% EtOAc/Petrol, 2 times) showed two yellow spots with the R_f values of 0.25 and 0.23. Further purification was performed by precoated TLC, using 8% EtOAc/Petrol as a mobile phase (36 times), to afford two bands.

Band P5-1 (PP3) It was obtained as a yellow solid (0.0071 g), melting at 176.8-177.9 °C. The chromatogram on normal phase TLC (8% EtOAc/Petrol, 7 times) showed only one yellow spot with the R_f value of 0.57.

$[\alpha]_D^{29} = +222^\circ$ ($c = 1.8 \times 10^{-2}$ g/100 cm³, MeOH)

UV λ_{\max} nm (MeOH) ($\log \epsilon$) 333 (3.94), 360 (4.01)

IR (neat) $\nu_{\text{cm}^{-1}}$ 3461 (O-H stretching), 2967, 2929 (C-H stretching), 1744, 1640 (C=O stretching)

¹H NMR (CDCl₃) (δ ppm) 13.03 (*s*, 1H), 7.52 (*d*, $J = 1.5$ Hz, 1H), 6.04 (*s*, 1H), 4.40 (*q*, $J = 6.5$ Hz, 1H), 4.38 (*md*, $J = 10.5$ Hz, 1H), 3.64 (*s*, 3H), 2.71 (*md*, $J = 14.5$ Hz, 1H), 2.59 (*d*, $J = 9.5$ Hz, 1H), 2.58 (*dd*, $J = 14.5$ and 10.5 Hz, 1H), 2.36 (*d*, $J = 13.0$ Hz,

	1H), 1.72 (<i>s</i> , 3H), 1.66 (<i>dd</i> , $J = 13.0$ and 9.5 Hz, 1H), 1.59 (<i>s</i> , 3H), 1.41 (<i>d</i> , $J = 6.5$ Hz, 1H), 1.38 (<i>brs</i> , 3H), 1.30 (<i>s</i> , 3H), 1.17 (<i>s</i> , 3H), 1.09 (<i>brs</i> , 3H)
^{13}C NMR (CDCl_3) (δ ppm) (125 MHz)	202.07, 178.25, 168.68, 166.22, 155.82, 135.69, 134.37, 132.02, 117.31, 113.68, 101.42, 92.75, 91.05, 89.54, 84.92, 84.23, 83.29, 53.99, 49.93, 43.16, 30.80, 30.79, 29.01, 28.99, 25.55, 23.87, 21.04, 16.90, 13.48
DEPT (135°) (CDCl_3)	CH 134.37, 117.31, 92.75, 91.05, 49.93 CH ₂ 30.80, 28.99 CH ₃ 53.99, 30.79, 29.01, 25.55, 23.87, 21.04, 16.90, 13.48
FABMS (m/z) (% rel. int.)	495 (60), 467 (100), 399 (19), 223 (17), 195 (21), 127 (29), 113 (71), 97 (>100), 85 (>100)

Band P5-2 (PP4) It was obtained as a yellow solid (0.0117 g), melting at 188.9-190.0 °C. The chromatogram on normal phase TLC (8% EtOAc/Petrol, 7 times) showed only one yellow spot with the R_f value of 0.54.

$[\alpha]_D^{29} = -240^\circ$ ($c = 2.5 \times 10^{-2}$ g/100 cm³, MeOH)

UV λ_{max} nm (MeOH) ($\log \epsilon$) 333 (3.93), 361 (4.02)

IR (neat) $\nu_{\text{cm}^{-1}}$ 3461 (O-H stretching), 2983, 2930 (C-H stretching), 1742, 1635 (C=O stretching)

^1H NMR (CDCl_3) (δ ppm) (500 MHz)	13.09 (<i>s</i> , 1H), 7.52 (<i>d</i> , $J = 1.0$ Hz, 1H), 6.03 (<i>s</i> , 1H), 4.55 (<i>q</i> , $J = 6.5$ Hz, 1H), 4.36 (<i>md</i> , $J = 11.0$ Hz, 1H), 3.64 (<i>s</i> , 3H), 2.68 (<i>md</i> , $J = 14.5$ Hz, 1H), 2.61 (<i>d</i> , $J = 9.5$ Hz, 1H), 2.55 (<i>dd</i> , $J = 14.5$ and 11.0 Hz, 1H), 2.36 (<i>dd</i> , $J = 13.0$, 1.0 Hz, 1H), 1.72 (<i>s</i> , 3H), 1.67 (<i>dd</i> , $J = 13.0$ and 9.5 Hz, 1H), 1.49 (<i>s</i> , 3H), 1.42 (<i>s</i> , 3H), 1.38 (<i>brs</i> , 3H), 1.30 (<i>d</i> , $J = 6.5$ Hz, 3H), 1.29 (<i>s</i> , 3H), 1.07 (<i>brs</i> , 3H)
^{13}C NMR (CDCl_3) (δ ppm) (125 MHz)	202.07, 178.12, 168.47, 166.37, 156.34, 135.56, 134.36, 132.07, 117.32, 112.58, 101.39, 92.80, 91.69, 89.60, 84.91, 84.42, 83.22, 53.95, 49.99, 43.39, 30.99, 30.69, 29.01, 28.98, 28.16, 25.52, 20.04, 16.76, 16.30
DEPT (135°) (CDCl_3)	CH 134.36, 117.32, 92.80, 91.69, 49.99 CH ₂ 30.69, 28.98 CH ₃ 53.95, 30.99, 29.01, 28.16, 25.52, 20.04, 16.76, 16.30
FABMS (m/z) (% rel. int.)	495 (70), 467 (100), 399 (29), 247 (23), 223 (38), 209 (26), 195 (45), 179 (36), 169 (57), 155 (74), 141 (76), 127 (>100), 113 (>100), 97 (>100), 85 (>100)

Subfraction P6 The chromatogram on normal phase TLC (20% EtOAc/Petrol, 2 times) showed many spots without any major spots. Because it was obtained in low quantity, it was not further investigated.

Fraction T3 The chromatogram on normal phase TLC (20% EtOAc/Petrol, 2 times) showed many spots without any major spots. Because it was obtained in low quantity, it was not further investigated.

Fraction T4 The chromatogram on normal phase TLC (30% EtOAc/Petrol, 2 times) showed three UV-active spots with the R_f values of 0.67, 0.58 and 0.46 and two yellow spots with the R_f values of 0.53 and 0.37. It was further separated by column chromatography on silica gel. Elution was conducted initially with pure chloroform and gradually increased the polarity until pure methanol. Fractions with the similar chromatogram were combined and evaporated under reduced pressure to dryness to afford four subfractions, as shown in **Table 5**.

Table 5 Subfractions obtained from fraction T4 by column chromatography on silica gel

fraction	Weight (g)	Physical appearance
T4-1	0.0063	Yellow gum
T4-2	0.1112	Yellow gum
T4-3	0.0270	Yellow gum
T4-4	0.9219	Yellow solid with yellow gum

Subfraction T4-1 The chromatogram on normal phase TLC (15% EtOAc/Petrol, 3 times) showed many spots. Because it was obtained in low quantity, it was not further investigated.

Subfraction T4-2 The chromatogram on normal phase TLC (15% EtOAc/Petrol, 3 times) showed four UV-active spots with the R_f values of 0.49, 0.40, 0.33 and 0.11 and three yellow spots with the R_f values of 0.27, 0.22 and 0.04. It was further separated by column chromatography on silica gel. Elution was conducted initially with 15% EtOAc/Petrol and gradually increased the polarity until pure methanol. Fractions with the similar chromatogram were combined and evaporated under reduced pressure to dryness to afford five subfractions, as shown in Table 6.

Table 6 Subfractions obtained from subfraction T4-2 by column chromatography on silica gel

fraction	Weight (g)	Physical appearance
T4-2-1	0.0128	Yellow gum
T4-2-2	0.0192	Yellow gum
T4-2-3	0.0079	Yellow gum
T4-2-4	0.0727	Yellow gum
T4-2-5	0.0078	Yellow gum

Subfraction T4-2-1 The chromatogram on normal phase TLC (20% EtOAc/Petrol, 2 times) showed three UV-active spots with the R_f values of 0.62, 0.55

and 0.18 and four yellow spots with the R_f values of 0.48, 0.46, 0.40 and 0.36. Because it was obtained in low quantity, it was not further investigated.

Subfraction T4-2-2 The chromatogram on normal phase TLC (20% EtOAc/Petrol, 2 times) showed one UV-active spot with the R_f value of 0.46 and two yellow spots with the R_f values of 0.40 and 0.36. It was further separated by precoated TLC, using 10% EtOAc/Petrol as a mobile phase (21 times), to afford two bands.

Band T4-2-2-1 It was obtained as a yellow gum (0.0053 g). The chromatogram on normal phase TLC (10% EtOAc/Petrol, 10 times) showed one major yellow spot with the R_f value of 0.57. Further purification was performed on precoated TLC, using 8% EtOAc/Petrol as a mobile phase (22 times), to give a yellow gum (0.0016 g). The chromatogram on normal phase TLC (10% EtOAc/Petrol, 10 times) showed only one yellow spot with the R_f value of 0.57. It became a dark yellow spot after dipping the TLC plate in ASA reagent and subsequently heating. Because it was obtained in low quantity, it was not further investigated.

Band T4-2-2-2 It was obtained as a yellow gum (0.0062 g). The chromatogram on normal phase TLC (10% EtOAc/Petrol, 10 times) showed one major yellow spot with the R_f value of 0.52. Further purification was performed on precoated TLC, using 8% EtOAc/Petrol as a mobile phase (22 times), to give **PP5** as a yellow gum (0.0039 g). The chromatogram on normal phase TLC (10% EtOAc/Petrol, 10 times) showed only one yellow spot with the R_f value of 0.52. It became a dark yellow spot after dipping the TLC plate in ASA reagent and subsequently heating.

$[\alpha]_D^{29} = -95^\circ$ ($c = 2.1 \times 10^{-2}$ g/100 cm ³ , MeOH)	
UV λ_{\max} nm (MeOH) ($\log \epsilon$)	364 (3.90)
IR (neat) $\nu_{\text{cm}^{-1}}$	3461 (O-H stretching), 2974, 2927, 2857 (C-H stretching), 1742, 1718, 1634 (C=O stretching)
¹ H NMR (CDCl ₃) (δ ppm) (500 MHz)	13.13 (<i>s</i> , 1H), 7.58 (<i>s</i> , 1H), 6.20 (<i>mdd</i> , $J = 10.0$ and 6.0 Hz, 1H), 5.22 (<i>mt</i> , $J = 7.0$ Hz, 1H), 4.55 (<i>q</i> , $J = 6.5$ Hz, 1H), 3.64 (<i>s</i> , 3H), 3.63 (<i>s</i> , 3H), 3.21 (<i>d</i> , $J = 7.0$ Hz, 2H), 2.83 (<i>dd</i> , $J = 15.5$ and 6.0 Hz, 1H), 2.61 (<i>d</i> , $J = 9.5$ Hz, 1H), 2.56 (<i>dd</i> , $J = 15.5$ and 10.0 Hz, 1H), 2.35 (<i>d</i> , $J = 13.0$ Hz, 1H), 1.75 (<i>s</i> , 3H), 1.73 (<i>s</i> , 3H), 1.69 (<i>s</i> , 3H), 1.69 (<i>dd</i> , $J = 13.0$ and 9.5 Hz, 1H), 1.47 (<i>s</i> , 3H), 1.41 (<i>s</i> , 3H), 1.38 (<i>s</i> , 3H), 1.30 (<i>d</i> , $J = 6.5$ Hz, 3H), 1.30 (<i>s</i> , 3H)
¹³ C NMR (CDCl ₃) (δ ppm) (125 MHz)	201.80, 177.64, 167.53, 166.85, 163.48, 154.00, 135.32, 133.32, 132.08, 130.22, 121.59, 112.04, 106.10, 101.36, 91.28, 89.43, 84.90, 83.64, 83.55, 53.99, 51.82, 49.85, 43.70, 30.88, 30.77, 29.13, 28.95, 28.18, 25.72, 21.40, 20.31, 17.79, 16.35, 11.79
DEPT (135°) (CDCl ₃)	CH 135.32, 133.32, 121.59, 91.28, 49.85 CH ₂ 30.77, 29.13, 21.40 CH ₃ 53.99, 51.82, 30.88, 28.95, 28.18, 25.72, 20.31, 17.79, 16.35, 11.79

FABMS (*m/z*) (% rel. int.) 607 (76), 579 (44), 553 (29), 525 (25), 467
(97), 439 (22), 391 (100)

Subfraction T4-2-3 The chromatogram on normal phase TLC (20% EtOAc/Petrol, 2 times) showed one UV-active spot with the R_f value of 0.46 and three yellow spots with the R_f values of 0.40, 0.36 and 0.31. Because it was obtained in low quantity, it was not further investigated.

Subfraction T4-2-4 The chromatogram on normal phase TLC (30% EtOAc/Petrol, 2 times) showed four yellow spots with the R_f values of 0.55, 0.52, 0.21 and 0.17 and one UV-active spot with the R_f value of 0.37. It was further separated by precoated TLC, using 15% EtOAc/Petrol as a mobile phase (14 times), to afford two bands.

Band T4-2-4-1 It was obtained as a yellow gum (0.0276 g). The chromatogram on normal phase TLC (30% EtOAc/Petrol) showed four yellow spots with the R_f values of 0.34, 0.32, 0.11 and 0.09. Further purification was performed on precoated TLC, using 8% EtOAc/Petrol as a mobile phase (26 times), to give **PP6** as a yellow gum (0.0031 g). The chromatogram on normal phase TLC (30% EtOAc/Petrol) showed only one yellow spot with the R_f value of 0.32.

$[\alpha]_D^{29} = -120^\circ$ ($c = 2.5 \times 10^{-2}$ g/100 cm³, MeOH)

UV λ_{\max} nm (MeOH) ($\log \epsilon$) 360 (3.96)

IR (neat) $\nu_{\text{cm}^{-1}}$ 3469 (O-H stretching), 2959, 2927, 2856 (C-H stretching), 1743, 1690, 1634 (C=O stretching)

¹H NMR (CDCl₃) (δ ppm) 13.08 (*s*, 1H), 9.23 (*s*, 1H), 7.60 (*s*, 1H), 6.23

(500 MHz)	(<i>mdd</i> , $J = 8.0$ and 5.5 Hz, 1H), 5.21 (<i>t</i> , $J = 6.5$ Hz, 1H), 4.56 (<i>q</i> , $J = 6.5$ Hz, 1H), 3.63 (<i>s</i> , 3H), 3.20 (<i>d</i> , $J = 6.5$ Hz, 2H), 2.89 (<i>dd</i> , $J = 15.5$ and 5.5 Hz, 1H), 2.66 (<i>d</i> , $J = 9.5$ Hz, 1H), 2.62 (<i>dd</i> , $J = 15.5, 8.0$ Hz, 1H), 2.38 (<i>d</i> , $J = 13.0$ Hz, 1H), 1.75 (<i>s</i> , 3H), 1.74 (<i>s</i> , 3H), 1.69 (<i>dd</i> , $J = 13.0$ and 9.5 Hz, 1H), 1.69 (<i>s</i> , 3H), 1.45 (<i>s</i> , 3H), 1.42 (<i>s</i> , 3H), 1.36 (<i>s</i> , 3H), 1.31 (<i>s</i> , 3H), 1.30 (<i>d</i> , $J = 6.5$ Hz, 3H)
^{13}C NMR (CDCl_3) (δ ppm) (125 MHz)	202.05, 194.45, 177.43, 167.28, 163.63, 154.06, 145.53, 140.86, 135.90, 132.37, 132.12, 121.42, 112.17, 106.37, 101.30, 91.41, 89.57, 84.92, 84.03, 83.15, 54.00, 49.82, 43.73, 30.96, 30.64, 29.38, 28.93, 28.15, 25.80, 21.44, 20.50, 17.84, 16.34, 8.75
DEPT (135°) (CDCl_3)	CH 194.45, 145.53, 135.90, 121.42, 91.41, 49.82 CH ₂ 30.64, 29.38, 21.44 CH ₃ 54.00, 30.96, 28.93, 28.15, 25.80, 20.50, 17.84, 16.34, 8.75
FABMS (m/z) (% rel. int.)	577 (13), 549 (38), 437 (35), 391 (52), 381 (82), 367 (23), 351 (29), 339 (49), 323 (26), 309 (22), 297 (23), 279 (>100), 259 (100), 245 (42), 233 (>100), 217 (88), 203 (83), 191

(>100), 167 (>100), 149 (>100), 123 (>100),
111 (>100), 97 (>100), 83 (>100)

Band T4-2-4-2 It was obtained as a yellow gum (0.0017 g). The chromatogram on normal phase TLC (30% EtOAc/Petrol) showed one yellow spot with the R_f value of 0.11. Because it was obtained in low quantity, it was not further investigated.

Subfraction T4-2-5 The chromatogram on normal phase TLC (70% EtOAc/Petrol, 3 times) showed no definite spot. Thus, it was not further investigated.

Subfraction T4-3 The chromatogram on normal phase TLC (20% EtOAc/Petrol, 3 times) showed many spots without any major spots. Because it was obtained in low quantity, it was not further investigated.

Subfraction T4-4 The chromatogram on normal phase TLC (40% EtOAc/Petrol) showed one major spot with the R_f value of 0.36 and two minor UV-active spots with the R_f values of 0.53 and 0.45. Its was shown by TLC comparison with **PP7** that the major spot was **PP7**, obtained from fraction **T6**.

Fraction T5 The chromatogram on normal phase TLC (30% EtOAc/Petrol, 2 times) showed one major yellow spot with the same R_f value as **PP7** (R_f 0.37), obtained from fraction **T6**.

Fraction T6 Upon standing at room temperature, a yellow solid (0.1715 g) (**PP7**) precipitated. It melting at 161.8-163.2°C. Its chromatogram on normal phase TLC (40% EtOAc/Petrol) showed only one yellow spot with the same R_f value as scortechinone B, obtained from its twigs. The filtrate became a yellow gum (0.0492 g) after evaporation to dryness under reduced pressure. The chromatogram on normal

phase TLC (50% EtOAc/Petrol) showed one major yellow spot with the same R_f value as **PP7** together with three minor UV-active spots with the R_f values of 0.56, 0.53 and 0.35.

$$[\alpha]_D^{29} = -158^\circ \text{ (c = } 9.5 \times 10^{-2} \text{ g/100cm}^3 \text{, MeOH)}$$

UV λ_{\max} (nm) (MeOH) ($\log \epsilon$)	366 (3.76)
IR (neat) $\nu_{\text{cm}^{-1}}$	3600-2500 (O-H stretching), 2925, 2851 (C-H stretching), 1745, 1690, 1636 (C=O stretching)
$^1\text{H NMR}$ (CDCl_3) (δ ppm) (500 MHz)	13.10 (<i>s</i> , 1H), 7.58 (<i>d</i> , $J = 1.5$ Hz, 1H), 5.68 (<i>ddq</i> , $J = 10.0, 4.5$ and 1.5 Hz, 1H), 5.21 (<i>ht</i> , $J = 7.5$ and 1.5 Hz, 1H), 4.46 (<i>q</i> , $J = 6.5$ Hz, 1H), 3.63 (<i>s</i> , 3H), 3.28 (<i>brdd</i> , $J = 16.0$ and 10.0 Hz, 1H), 3.18 (<i>mdd</i> , $J = 15.0$ and 7.5 Hz, 1H), 3.12 (<i>mdd</i> , $J = 15.0$ and 7.5 Hz, 1H), 2.85 (<i>ddq</i> , $J = 16.0$ and 4.5 and 2.0 Hz, 1H), 2.60 (<i>d</i> , $J = 9.5$ Hz, 1H), 2.34 (<i>brd</i> , $J = 13.0$ Hz, 1H), 1.72 (<i>s</i> , 9H), 1.69 (<i>dd</i> , $J = 13.0$ and 9.5 Hz, 1H), 1.66 (<i>d</i> , $J = 1.5$ Hz, 3H), 1.38 (<i>s</i> , 3H), 1.37 (<i>s</i> , 3H), 1.29 (<i>s</i> , 3H), 1.22 (<i>d</i> , $J = 6.5$ Hz, 3H)

Fraction T7 The chromatogram on normal phase TLC (50% EtOAc/Petrol) showed two UV-active spots with the R_f values of 0.53 and 0.35 and two yellow spots with the R_f values of 0.47 and 0.29. It was further separated on precoated TLC, using 4% MeOH/ CHCl_3 as a mobile phase (3 times), to afford two bands.

	CH ₂ 28.56, 23.98, 21.42
	CH ₃ 57.38, 52.38, 30.49, 27.16, 26.08, 25.76, 22.06, 20.72, 17.71, 13.82
FABMS (<i>m/z</i>) (% rel. int.)	625 (100), 607 (33), 289 (35), 233 (47), 153 (81), 135 (91)

Band T7-2 It was obtained as a yellow gum (0.0176 g). The chromatogram on normal phase TLC (5% MeOH/CHCl₃) showed two spots; one UV-active spot with the same R_f value as PP8 and pale yellow spot with the R_f value of 0.35.

Fraction T8 The chromatogram on normal phase TLC (50% EtOAc/Petrol) showed two major spots which were PP7 and PP8 together with two minor UV-active spots with the R_f values of 0.53 and 0.10.

Fraction T9 The chromatogram on normal phase TLC (50% EtOAc/Petrol) showed three yellow spots with the R_f values of 0.47, 0.32 and 0.25 and one UV-active spot with the R_f value of 0.11. It was further separated by column chromatography on silica gel. Elution was conducted initially with pure chloroform and gradually increased the polarity until pure methanol. Fractions with the similar chromatogram were combined and evaporated under reduced pressure to dryness to afford nine fractions, as shown in **Table 7**.

Table 7 Subfractions obtained from fraction T9 by column chromatography on silica gel

fraction	Weight (g)	Physical appearance
T9-1	0.0071	Yellow gum
T9-2	0.0049	Yellow gum
T9-3	0.0028	Yellow gum
T9-4	0.0048	Yellow gum
T9-5	0.0119	Yellow gum
T9-6	0.0976	Yellow gum
T9-7	0.1430	Orange-yellow gum
T9-8	0.0383	Orange-yellow gum
T9-9	0.0828	Orange gum

Subfraction T9-1 The chromatogram on normal phase TLC (3% MeOH/CHCl₃) showed one major UV-active spot with the R_f value of 0.52. It was further separated by precoated TLC, using 2% MeOH/CHCl₃ as a mobile phase (2 times), to afford a yellow gum (0.0017 g). The chromatogram on normal phase TLC (2% MeOH/CHCl₃) showed one UV-active-spot with the R_f value of 0.37. Because it was obtained in low quantity, it was not further investigated.

Subfraction T9-2 The chromatogram on normal phase TLC (3% MeOH/CHCl₃) showed no definite spot. Thus, it was not further investigated.

	stretching)
^1H NMR (CDCl_3) (δ ppm)	13.10 (<i>s</i> , 1H), 7.61 (<i>d</i> , $J = 1.0$ Hz, 1H), 6.41
(500 MHz)	(<i>ddq</i> , $J = 10.0, 5.5$ and 1.5 Hz, 1H), 5.22 (<i>mt</i> , $J = 7.0$ Hz, 1H), 4.54 (<i>q</i> , $J = 6.5$ Hz, 1H), 3.63 (<i>s</i> , 3H), 3.20 (<i>d</i> , $J = 7.0$ Hz, 2H), 2.79 (<i>mdd</i> , $J = 15.0$ and 5.5 Hz, 1H), 2.61 (<i>d</i> , $J = 9.5$ Hz, 1H), 2.56 (<i>dd</i> , $J = 15.0$ and 10.0 Hz, 1H), 2.33 (<i>d</i> , $J = 13.0$ Hz, 1H), 1.74 (<i>s</i> , 3H), 1.72 (<i>s</i> , 3H), 1.69 (<i>dd</i> , $J = 13.0$ and 9.5 Hz, 1H), 1.67 (<i>s</i> , 3H), 1.46 (<i>s</i> , 3H), 1.41 (<i>s</i> , 3H), 1.38 (<i>s</i> , 3H), 1.30 (<i>d</i> , $J = 6.5$ Hz, 3H), 1.29 (<i>s</i> , 3H)
^{13}C NMR (CDCl_3) (δ ppm)	202.01, 177.50, 171.00, 166.86, 163.49,
(125 MHz)	154.00, 135.86, 135.40, 132.13, 132.03, 129.34, 121.52, 111.99, 106.19, 101.34, 91.28, 89.41, 84.96, 83.70, 83.30, 54.10, 49.78, 43.70, 30.92, 30.87, 29.28, 28.87, 28.15, 25.70, 21.39, 20.32, 17.77, 16.33, 11.44
DEPT (135°) (CDCl_3)	CH 135.86, 135.40, 121.52, 91.28, 49.78
	CH ₂ 30.92, 29.28, 21.39
	CH ₃ 54.10, 30.87, 28.87, 28.15, 25.70, 20.32, 17.77, 16.33, 11.44
EIMS (m/z) (% rel. int.)	592 (10), 564 (100), 495 (21), 437 (50), 381 (51), 289 (30), 277 (32)

Band T9-7-3 It was obtained as a yellow gum (0.0051 g). The chromatogram on normal phase TLC (5% MeOH/CHCl₃) showed one major yellow spot with the R_f value of 0.44. Further purification was performed by precoated TLC, using 50% EtOAc/Petrol as a mobile phase (3 times), to give **PP10** as a yellow gum (0.0028 g). The chromatogram on normal phase TLC (50% EtOAc/Petrol, 2 times) showed only one yellow spot with the R_f value of 0.27.

$[\alpha]_D^{29} = +48^\circ$ ($c = 2.1 \times 10^{-2}$ g/100 cm³, MeOH)

UV λ_{\max} nm (MeOH) (log ϵ) 368 (4.11)

IR (neat) $\nu_{\text{cm}^{-1}}$ 3600-2500 (O-H stretching), 2958, 2926, 2851
(C-H stretching), 1753, 1690, 1640 (C=O
stretching)

¹H NMR (CDCl₃) (δ ppm) 12.69 (*s*, 1H), 6.77 (*mt*, $J = 7.5$ and 1.5 Hz,
(500 MHz) 1H), 6.62 (*s*, 1H), 5.21 (*mt*, $J = 7.5$ and 1.5 Hz,
1H), 4.37 (*q*, $J = 6.5$ Hz, 1H), 3.63 (*s*, 3H), 3.22
(*d*, $J = 7.5$ Hz, 2H), 3.17 (*dd*, $J = 13.0$ and 7.0
Hz, 1H), 2.94 (*dd*, $J = 16.5$ and 13.0 Hz, 1H),
2.79 (*dd*, $J = 15.0$ and 7.5 Hz, 1H), 2.69 (*dd*, J
 $= 15.0$ and 7.5 Hz, 1H), 2.62 (*dd*, $J = 16.5$ and
7.0 Hz, 1H), 1.76 (*s*, 3H), 1.75 (*s*, 3H), 1.69 (*s*,
3H), 1.67 (*s*, 3H), 1.45 (*s*, 3H), 1.42 (*s*, 3H),
1.41 (*d*, $J = 6.5$ Hz, 3H), 1.27 (*s*, 3H)

¹³C NMR (CDCl₃) (δ ppm) 197.00, 182.07, 171.31, 170.60, 167.95,
(125 MHz) 162.94, 152.92, 145.85, 137.11, 132.37, 130.32,

		128.55, 121.32, 112.66, 106.44, 102.83, 93.81, 90.64, 90.62, 85.12, 55.88, 52.29, 43.46, 38.27, 35.89, 31.21, 25.78, 25.43, 24.40, 21.45, 21.06, 17.74, 13.72, 12.46
DEPT (135°) (CDCl ₃)	CH	137.11, 128.55, 121.32, 90.64, 55.88
	CH ₂	38.27, 35.89, 21.45
	CH ₃	52.29, 31.21, 25.78, 25.43, 24.40, 21.06, 17.74, 13.72, 12.46
EIMS (<i>m/z</i>) (% rel. int.)		608 (100), 553 (36), 509 (62), 422 (69), 407 (32), 379 (68), 367 (90), 249 (21), 178 (26), 69 (40), 57 (52)

Subfraction T9-8 The chromatogram on normal phase TLC (5% MeOH/CHCl₃) showed no definite spot. Thus, it was not further investigated.

Subfraction T9-9 The chromatogram on normal phase TLC (15% MeOH/CHCl₃) showed one major yellow spot with the R_f value of 0.27. It was further separated by flash column chromatography. Elution was conducted initially with 15% MeOH/CHCl₃ and gradually increased the polarity until pure methanol. Fractions with the similar chromatogram were combined and evaporated under reduced pressure to dryness to afford six subfractions of which chromatograms showed many spots without any major spots. No further investigation was performed.

Fraction T10 The chromatogram on normal phase TLC (pure EtOAc) showed four yellow spots with the R_f values of 0.58, 0.50, 0.08 and 0.04 and two UV-active spots with the R_f values of 0.63 and 0.43. It was further separated by column

chromatography over reversed-phase C18 silica gel. Elution was conducted initially with 80% MeOH/H₂O and gradually decreased the polarity until pure methanol. Fractions with the similar chromatogram were combined and evaporated under reduced pressure to dryness to afford four subfractions, as shown in **Table 8**.

Table 8 Subfractions obtained from **T10** by column chromatography over reversed-phase C18 silica gel

fraction	Weight (g)	Physical appearance
T10-1	0.0265	Brown gum
T10-2	0.0162	Yellow gum
T10-3	0.0455	Yellow gum
T10-4	0.0289	Yellow gum

Subfraction T10-1 The chromatogram on normal phase TLC (10% MeOH/CHCl₃) showed many spots without any major spots. Thus, it was not further investigated.

Subfraction T10-2 The chromatogram on normal phase TLC (10% MeOH/CHCl₃) showed three yellow spots with the R_f values of 0.24, 0.14 and 0.09. It was further separated by precoated TLC, using 10% MeOH/CHCl₃ as a mobile phase (6 times), to afford two bands, both as a yellow gum in 0.0019 g and 0.0042 g. Their chromatograms on normal phase TLC (10% MeOH/CHCl₃) showed at least two components. Because they were obtained in low quantity, they were not further investigated.

Subfraction T10-3 The chromatogram on normal phase TLC (10% MeOH/CHCl₃) showed two yellow spots with the R_f values of 0.54 and 0.09 together with two UV-active spots with the R_f values of 0.14 and 0.03. It was further separated by precoated TLC, using 10% MeOH/CHCl₃ as a mobile phase (7 times), to afford two bands, both as a yellow gum in 0.0037 g and 0.0103 g. Their chromatograms on normal phase TLC (10% MeOH/CHCl₃) showed one major yellow spot but, on reversed-phase TLC (80% MeOH/H₂O), it possessed at least two yellow spots. Therefore, they were not further investigated.

Subfraction T10-4 The chromatogram on normal phase TLC (10% MeOH/CHCl₃) showed many UV-active spots without any major spots. Thus, it was not further investigated.

Fraction T11 The chromatogram on reversed-phase C18 TLC (50% MeOH/H₂O) showed two yellow major spots with the R_f values of 0.14 and 0.06. It was further separated by column chromatography over reversed-phase C18 silica gel. Elution was conducted initially with 50% MeOH/H₂O and gradually decreased the polarity until pure methanol. Fractions with the similar chromatogram were combined and evaporated under reduced pressure to dryness to afford four subfractions, as shown in **Table 9**.

Table 9 Subfractions obtained from T11 by column chromatography over reversed-phase C18 silica gel

fraction	Weight (g)	Physical appearance
T11-1	0.0894	Brown-yellow gum
T11-2	0.0435	Orange-yellow gum
T11-3	0.0604	Orange-yellow gum
T11-4	0.0382	Orange-yellow gum

Subfraction T11-1 The chromatogram on normal phase TLC (25% MeOH/CHCl₃) showed no definite spot. Thus, it was not further investigated.

Subfraction T11-2 The chromatogram on normal phase TLC (25% MeOH/CHCl₃) showed two yellow spots with the R_f values of 0.34 and 0.07 and one UV-active spot with the R_f value of 0.22. It was partitioned between ethyl acetate (20 ml) and 0.1M *di*-sodium tetraborate (45 ml) to give a yellow gum (0.0053 g) from the organic phase. The chromatogram on normal phase TLC (25% MeOH/CHCl₃) showed many UV-active spots. Thus, it was not further investigated. The borate layer was acidified with 10% HCl and extracted with ethyl acetate (4x30 ml) to afford an orange-yellow gum (0.0386 g). The chromatogram on normal phase TLC (20% MeOH/CHCl₃) showed two yellow spots with the R_f values of 0.29 and 0.10 together with two UV-active spots with the R_f values of 0.24 and 0.14. Further separation by flash column chromatography was performed. Elution was conducted initially with 15% MeOH/CHCl₃ and gradually increased the polarity until pure methanol. Fractions with the similar chromatogram were combined and evaporated under

reduced pressure to dryness to afford two subfractions, both as a yellow gum in 0.0196 g and 0.0349 g. Attempted purification of both subfractions by repeated chromatography was unsuccessful.

Subfraction T11-3 The chromatogram on normal phase TLC (10% MeOH/CHCl₃) showed many UV-active spots without any major spots. Thus, it was not further investigated.

Subfraction T11-4 The chromatogram on normal phase TLC (10% MeOH/CHCl₃) showed three UV-active spots with the R_f values of 0.91, 0.88 and 0.76. It was further separated by column chromatography over reversed-phase C18 silica gel. Elution was conducted initially with 60% MeOH/H₂O and gradually decreased the polarity until pure methanol. Fractions with the similar chromatogram were combined and evaporated under reduced pressure to dryness to afford two subfractions, both as a yellow gum in 0.0079 g and 0.0114 g. Attempted purification by repeated chromatography was unsuccessful.

2.4 Chemical investigation of the stem bark

2.4.1 Extraction

The stem bark (2,290 g) of *G. scortechinii*, cut into small segments, was extracted with MeOH (5.5 L) over the period of 7 days at room temperature for three times. After filtration, the filtrate was evaporated to dryness under reduced pressure to give a crude methanol extract as a dark brown gum in 114.14 g.

2.4.2 Chemical investigation of the crude methanol extract of the stem bark

The crude methanol extract was primarily tested for its solubility in various solvents at room temperature. The results were demonstrated in **Table 10**.

Table 10 Solubility of the crude methanol extract in various solvents at room temperature

solvent	solubility at room temperature
Petroleum ether	+ (yellow solution with brown solid)
Chloroform	+ (yellow solution with brown solid)
Ethyl acetate	+ (yellow solution with brown solid)
Methanol	++ (brown solution)
Water	+ (orange-yellow solution with brown solid)
10% HCl	+ (orange-yellow solution with brown solid)
10% NaOH	++ (brown solution)

Symbol meaning: + partailly soluble, ++ well soluble

It was shown that the crude methanol extract was slightly soluble in petroleum ether, chloroform, ethyl acetate, water and 10% aqueous HCl but it was soluble well in methanol and 10% aqueous NaOH, indicating that it contained less to moderately polar and acidic compounds.

The crude methanol extract (111.14 g) was separated into two parts by dissolving with chloroform. **GSBC**, the chloroform soluble part, was a brown-yellow gum (14.92 g) while **GSBM**, the methanol soluble part, was a brown solid (84.46 g). The chromatogram on normal phase TLC of **GSBM** showed no definite spot. Further separation of **GSBC** (14.92 g) was carried out by column chromatography on silica gel. Elution was conducted initially with pure chloroform and gradually increased the polarity until pure methanol. Fractions with the similar chromatogram were combined and evaporated under reduced pressure to dryness to afford nine fractions, as shown in **Table 11**.

Table 11 Fractions obtained from **GSBC** by column chromatography on silica gel

fraction	Weight (g)	Physical appearance
B1	0.8608	Pale yellow gum
B2	0.2891	Red-purple gum
B3	0.1706	Yellow gum
B4	0.9207	Yellow gum with white solid
B5	6.7742	Brown-yellow gum
B6	0.9634	Yellow gum
B7	1.3801	Yellow gum
B8	1.8484	Brown-yellow gum
B9	2.4984	Brown gum

Fraction B1 The chromatogram on normal phase TLC (1% EtOAc/Petrol) showed three UV-active spots with the R_f values of 0.32, 0.16 and 0.07. Many additional spots were observed after dipping the TLC plate in ASA reagent and subsequently heating. It was further separated by column chromatography on silica gel. Elution was conducted initially with 0.5% EtOAc/Hexane and gradually increased the polarity until pure ethyl acetate. Fractions with the similar chromatogram were combined and evaporated under reduced pressure to dryness to afford four subfractions, as shown in **Table 12**.

Table 12 Subfractions obtained from fraction **B1** by column chromatography on silica gel

fraction	Weight (g)	Physical appearance
B1-1	0.0301	White gum
B1-2	0.3179	Pale yellow gum
B1-3	0.2269	Pale yellow gum
B1-4	0.1330	Brown gum

Subfraction B1-1 The chromatogram on normal phase TLC (0.5% EtOAc/Petrol) showed one oval UV-active spot with the R_f value of 0.43. Many additional spots were observed after dipping the TLC plate in ASA reagent and subsequently heating. Thus, it was not further investigated.

Subfraction B1-2 The chromatogram on normal phase TLC (3% EtOAc/Petrol) showed two UV-active spots with the R_f values of 0.54 and 0.47. Both

of them became dark blue spots and one additional purple spot with the R_f value of 0.36 was observed after dipping the TLC plate in ASA reagent and subsequently heating. Further separation was performed by column chromatography on silica gel. Elution was conducted with 2% EtOAc/Petrol. Fractions with the similar chromatogram were combined and evaporated under reduced pressure to dryness to afford two subfractions, as shown in Table 13.

Table 13 Subfractions obtained from subfraction B1-2 by column chromatography on silica gel

fraction	Weight (g)	Physical appearance
B1-2-1	0.0037	White solid
B1-2-2	0.3255	Pale yellow gum

Subfraction B1-2-1 The chromatogram on normal phase TLC (3% EtOAc/Petrol) showed two UV-active spots with the R_f values of 0.54 and 0.47. Both of them became dark blue spots after dipping the TLC plate in ASA reagent and subsequently heating. Because it was obtained in low quantity, it was not further investigated.

Subfraction B1-2-2 The chromatogram on normal phase TLC (3% EtOAc/Petrol) showed two UV-active spots with the R_f values of 0.48 and 0.47. Both of them became dark blue spots and three additional purple spots with the R_f values of 0.36, 0.27 and 0.24 were observed after dipping the TLC plate in ASA reagent and

subsequently heating. Attempted purification by column chromatography on silica gel was unsuccessful.

Subfraction B1-3 The chromatogram on normal phase TLC (3% EtOAc/Petrol) showed many spots without any major spots after dipping the TLC plate in ASA reagent and subsequently heating. Therefore, it was not further investigated.

Subfraction B1-4 The chromatogram on normal phase TLC (3% EtOAc/Petrol) showed no definite spot. Thus, it was not further investigated.

Fraction B2 The chromatogram on normal phase TLC (10% EtOAc/Petrol) showed many spots without any major spots. Thus, it was not further investigated.

Fraction B3 The chromatogram on normal phase TLC (10% EtOAc/Petrol) showed three major UV-active spots with the R_f values of 0.35, 0.27 and 0.17. It was further separated by flash column chromatography. Elution was conducted initially with 5% EtOAc/Petrol and gradually increased the polarity until pure ethyl acetate. Fractions with the similar chromatogram were combined and evaporated under reduced pressure to dryness to afford four subfractions, as shown in **Table 14**.

Table 14 Subfractions obtained from fraction **B3** by flash column chromatography on silica gel

fraction	Weight (g)	Physical appearance
B3-1	0.1164	Yellow gum
B3-2	0.0306	Yellow gum

Table 14 (Continued)

fraction	Weight (g)	Physical appearance
B3-3	0.0011	Yellow gum
B3-4	0.0169	Yellow gum

Subfraction B3-1 The chromatogram on normal phase TLC (3% EtOAc/Petrol) showed many spots without any major spots. Therefore, it was not further investigated.

Subfraction B3-2 The chromatogram on normal phase TLC (8% EtOAc/Petrol) showed three UV-active spots with the R_f values of 0.41, 0.35 and 0.28. It was further separated by flash column chromatography. Elution was conducted initially with 5% EtOAc/Petrol and gradually increased the polarity until 10% EtOAc/Petrol. Fractions with the similar chromatogram were combined and evaporated under reduced pressure to dryness to afford three subfractions, as shown in **Table 15**.

Table 15 Subfractions obtained from subfraction **B3-2** by flash column chromatography on silica gel

fraction	Weight (g)	Physical appearance
B3-2-1	0.0027	Yellow gum
B3-2-2	0.0020	Yellow gum
B3-2-3	0.0262	Yellow gum

Subfraction B3-2-1 The chromatogram on normal phase TLC (8% EtOAc/Petrol) showed two UV-active spots with the R_f values of 0.32 and 0.25. Because it was obtained in low quantity, it was not further investigated.

Subfraction B3-2-2 The chromatogram on normal phase TLC (8% EtOAc/Petrol) showed two UV-active spots with the R_f values of 0.25 and 0.18. Because it was obtained in low quantity, it was not further investigated.

Subfraction B3-2-3 The chromatogram on normal phase TLC (8% EtOAc/Petrol) showed one UV-active spot with the R_f values of 0.18 and one additional dark blue spot was observed after dipping the TLC plate in ASA reagent and subsequently heating. Further purification was performed on precoated TLC, using 8% EtOAc/Petrol as a mobile phase (18 times), to afford two bands.

Band B3-2-3-1 It was obtained as a yellow solid (0.0157 g). The chromatogram on normal phase TLC (10% EtOAc/Petrol, 2 times) showed two UV-active spots with the R_f values of 0.26 and 0.22. Further purification was performed on precoated TLC, using 10% EtOAc/Petrol as a mobile phase (10 times), to give **PP11** as a yellow solid (0.0118 g), melting at 173.2-174.9°C. The chromatogram on normal phase TLC (10% EtOAc/Petrol, 2 times) showed only one UV-active spot with the R_f value of 0.22.

$[\alpha]_D^{29} = +83^\circ$ ($c = 1.2 \times 10^{-2}$ g/100 cm³, MeOH)

UV λ_{\max} nm (MeOH) ($\log \epsilon$) 273 (4.72), 331 (4.20), 373 (3.97)

IR (neat) $\nu_{\text{cm}^{-1}}$ 3380 (O-H stretching), 2967, 2923, 2856 (C-H stretching), 1639 (C=O stretching)

¹H NMR (CDCl₃) (δ ppm) 13.28 (*s*, 1H), 7.49 (*s*, 1H), 6.45 (*d*, $J = 10.5$)

(500 MHz)	Hz, 1H), 6.24 (<i>s</i> , 1H), 5.73 (<i>d</i> , $J = 10.5$ Hz, 1H), 5.49 (<i>brs</i> , 1H), 4.55 (<i>q</i> , $J = 7.0$ Hz, 1H), 1.60 (<i>s</i> , 3H), 1.53 (<i>s</i> , 3H), 1.52 (<i>s</i> , 3H), 1.42 (<i>d</i> , $J = 7.0$ Hz, 3H), 1.32 (<i>s</i> , 3H)
^{13}C NMR (CDCl_3) (δ ppm)	180.10, 165.89, 164.16, 152.61, 144.82, 144.53,
(125 MHz)	132.30, 130.77, 121.44, 117.52, 114.75, 113.45, 113.00, 103.36, 93.81, 90.88, 78.87, 43.75, 28.46, 25.55, 21.25, 14.28
DEPT (135°) (CDCl_3)	CH 130.77, 121.44, 113.45, 93.81, 90.88 CH ₃ 28.46, 25.55, 21.25, 14.28

Band B3-2-3-2 (PP12) It was obtained as a white solid (0.0037 g), melting at 154.3-156.1°C. The chromatogram on normal phase TLC (10% EtOAc/Petrol, 2 times) showed only one dark blue spot with the same R_f value as stigmasterol after dipping the TLC plate in ASA reagent and subsequently heating.

$[\alpha]_{\text{D}}^{29} = -31^\circ$ ($c = 1.6 \times 10^{-2}$ g/100 cm³, MeOH)

IR (KBr) $\nu_{\text{cm}^{-1}}$ 3341 (O-H stretching), 2958, 2936, 2868 (C-H stretching)

^1H NMR (CDCl_3) (δ ppm)
(500 MHz) 5.36-5.33 (*m*, 1H), 5.15 (*dd*, $J = 15.0$ and 9.0 Hz, 1H), 5.01 (*dd*, $J = 15.0$ and 9.0 Hz, 1H), 3.56-3.48 (*m*, 1H), 2.29 (*ddd*, $J = 13.0, 5.0$ and 2.0 Hz, 1H), 2.24 (*qd*, $J = 11.5$ and 2.0 Hz, 1H), 2.09-1.93 (*m*, 3H), 1.88-1.80 (*m*, 2H), 1.75-1.66

(*m*, 1H), 1.60-1.39 (*m*, 11H), 1.30-1.04 (*m*, 5H),
1.05 (*d*, $J = 6.5$ Hz, 3H), 1.01 (*s*, 3H), 0.97-0.90
(*m*, 2H), 0.84 (*d*, $J = 6.5$ Hz, 3H), 0.80 (*t*, $J =$
7.5 Hz, 3H), 0.79 (*d*, $J = 6.5$ Hz, 3H), 0.69 (*s*,
3H)

Subfraction B3-3 The chromatogram on normal phase TLC (15% EtOAc/Petrol) showed three UV-active spots with the R_f values of 0.41, 0.36 and 0.32. Because it was obtained in low quantity, it was not further investigated.

Subfraction B3-4 The chromatogram on normal phase TLC (15% EtOAc/Petrol) showed three major UV-active spots with the R_f values of 0.29, 0.23 and 0.21. Further purification was performed on precoated TLC, using 10% EtOAc/Petrol as a mobile phase (17 times), to afford four bands, as a yellow gum in 0.0013 g, 0.0031 g, 0.0019 and 0.0018 g. Their chromatograms on normal phase TLC (15% EtOAc/Petrol) showed at least two components. Because they were obtained in low quantity, they were not further investigated.

Fraction B4 Upon standing at room temperature, a white solid (0.1032 g) precipitated. Its chromatogram on normal phase TLC (10% EtOAc/Petrol) showed only one dark blue spot with the same R_f value as **PP12** after dipping the TLC plate in ASA reagent and subsequently heating. The filtrate became a yellow gum (0.8175 g) after evaporation to dryness under reduced pressure. The chromatogram on normal phase TLC (20% EtOAc/Petrol) showed five UV-active spots with the R_f values of 0.52, 0.46, 0.37, 0.23 and 0.21 and one oval yellow spot with the R_f value of 0.10 together with a dark blue spot with the same R_f value as **PP12** after dipping the TLC

plate in ASA reagent and subsequently heating. Further separation was performed by column chromatography on silica gel. Elution was conducted initially with 15% EtOAc/Petrol and gradually increased the polarity until 20% EtOAc/Petrol. Fractions with the similar chromatogram were combined and evaporated under reduced pressure to dryness to afford nine subfractions, as shown in Table 16.

Table 16 Subfractions obtained from fraction B4 by column chromatography on silica gel

fraction	Weight (g)	Physical appearance
B4-1	0.0249	Yellow gum
B4-2	0.0263	Yellow gum
B4-3	0.0860	Orange-yellow gum
B4-4	0.0828	Yellow gum with white solid
B4-5	0.1428	Yellow gum with white solid
B4-6	0.1842	Yellow gum
B4-7	0.0728	Yellow gum
B4-8	0.0717	Brown-yellow gum
B4-9	0.0976	Brown-yellow gum

Subfraction B4-1 The chromatogram on normal phase TLC (8% EtOAc/Petrol, 2 times) showed no definite spot. Thus, it was not further investigated.

Subfraction B4-2 The chromatogram on normal phase TLC (8% EtOAc/Petrol, 2 times) showed one major UV-active spot with the R_f value of 0.29.

Further purification was performed on precoated TLC, using 5% EtOAc/Petrol as a mobile phase (8 times), to give a pale yellow gum (0.0029 g). The chromatogram on normal phase TLC (5% EtOAc/Petrol) showed only one UV-active spot with the R_f value of 0.15. However, its ^1H NMR spectrum indicated that it was not pure. Because it was obtained in low quantity, it was not further investigated.

Subfraction B4-3 The chromatogram on normal phase TLC (8% EtOAc/Petrol, 2 times) showed two yellow spots with the R_f values of 0.28 and 0.12 and one UV-active spot with the R_f value of 0.25. It was further separated by flash column chromatography. Elution was conducted initially with 5% EtOAc/Petrol and gradually increased the polarity until 50% EtOAc/Petrol. Fractions with the similar chromatogram were combined and evaporated under reduced pressure to dryness to afford three subfractions, as shown in **Table 17**.

Table 17 Subfractions obtained from subfraction **B4-3** by flash column chromatography on silica gel

fraction	Weight (g)	Physical appearance
B4-3-1	0.0012	Pale yellow gum
B4-3-2	0.0612	Yellow gum
B4-3-3	0.0160	Yellow gum

Subfraction B4-3-1 The chromatogram on normal phase TLC (8% EtOAc/Petrol, 3 times) showed no definite spot. Thus, it was not further investigated.

Subfraction B4-3-2 The chromatogram on normal phase TLC (8% EtOAc/Petrol, 3 times) showed one UV-active spot with the R_f value of 0.48 and two yellow spots with the R_f values of 0.46 and 0.42. It was further separated by flash column chromatography. Elution was conducted initially with 2% EtOAc/Petrol and gradually increased the polarity until 50% EtOAc/Petrol. Fractions with the similar chromatogram were combined and evaporated under reduced pressure to dryness to afford five subfractions, as shown in **Table 18**.

Table 18 Subfractions obtained from subfraction **B4-3-2** by flash column chromatography on silica gel

fraction	Weight (g)	Physical appearance
B4-3-2-1	0.0274	Yellow gum
B4-3-2-2	0.0047	Yellow gum
B4-3-2-3	0.0050	Yellow gum
B4-3-2-4	0.0122	Yellow gum
B4-3-2-5	0.0159	Yellow gum

Subfraction B4-3-2-1 The chromatogram on normal phase TLC (8% EtOAc/Petrol, 4 times) showed two UV-active spots with the R_f values of 0.54 and 0.47 and three yellow spots with the R_f values of 0.42, 0.40 and 0.36. Further purification was performed on precoated TLC, using 8% EtOAc/Petrol as a mobile phase (11 times), to afford four bands.

Band B4-3-2-1-1 It was obtained as a pale yellow gum (0.0042 g). The chromatogram on normal phase TLC (8% EtOAc/Petrol, 3 times) showed one UV-active spot with the R_f value of 0.48. However, its ^1H NMR spectrum indicated that it was not pure.

Band B4-3-2-1-2 It was obtained as a pale yellow gum (0.0014 g). The chromatogram on normal phase TLC (8% EtOAc/Petrol, 3 times) showed one UV-active spot with the R_f value of 0.37. Because it was obtained in low quantity, it was not further investigated.

Band B4-3-2-1-3 It was obtained as a yellow gum (0.0106 g). The chromatogram on normal phase TLC (8% EtOAc/Petrol, 3 times) showed one yellow spot with the same R_f value as **PP1**, obtained from the latex.

Band B4-3-2-1-4 It was obtained as a pale yellow gum (0.0043 g). The chromatogram on normal phase TLC (8% EtOAc/Petrol, 3 times) showed one yellow spot with the R_f value of 0.34. However, its ^1H NMR spectrum indicated that it was not pure.

Subfraction B4-3-2-2 The chromatogram on normal phase TLC (8% EtOAc/Petrol, 4 times) showed one major yellow spot with the same R_f value as **PP1**, obtained from the latex, and under this spot, there was one minor yellow spot with the R_f value of 0.40. Because it was obtained in low quantity, it was not further investigated.

Subfraction B4-3-2-3 The chromatogram on normal phase TLC (8% EtOAc/Petrol, 4 times) showed two yellow spots with the R_f values of 0.40 and 0.32 and one UV-active spot with the R_f value of 0.36. Further purification was performed on precoated TLC, using 8% EtOAc/Petrol as a mobile phase (11 times), to afford two

bands, both as a yellow gum in 0.0018 g and 0.0010 g. Each chromatogram on normal phase TLC (8% EtOAc/Petrol, 3 times) showed only one yellow spot with the R_f values of 0.33 and 0.30, respectively. Because they were obtained in low quantity, they were not further investigated.

Subfraction B4-3-2-4 The chromatogram on normal phase TLC (8% EtOAc/Petrol, 4 times) showed three yellow spots with the R_f values of 0.40, 0.32 and 0.30 and one UV-active spot with the R_f value of 0.36. Further purification was performed on precoated TLC, using 8% EtOAc/Petrol as a mobile phase (11 times), to afford three bands

Band B4-3-2-4-1 It was obtained as a pale yellow gum (0.0011 g). The chromatogram on normal phase TLC (8% EtOAc/Petrol, 3 times) showed one UV-active spot with the R_f value of 0.32. Because it was obtained in low quantity, it was not further investigated.

Band B4-3-2-4-2 It was obtained as a yellow gum (0.0016 g). The chromatogram on normal phase TLC (8% EtOAc/Petrol, 3 times) showed one UV-active spot with the R_f value of 0.32 and one yellow spot with the R_f value of 0.29. Because it was obtained in low quantity, it was not further investigated.

Band B4-3-2-4-3 It was obtained as a yellow gum (0.0044 g). The chromatogram on normal phase TLC (8% EtOAc/Petrol, 3 times) showed one yellow spot with the R_f value of 0.27. However, its ^1H NMR spectrum indicated that it was not pure.

Subfraction B4-3-2-5 The chromatogram on normal phase TLC (8% EtOAc/Petrol, 4 times) showed no definite spot. Thus, it was not further investigated.

Subfraction B4-3-3 The chromatogram on normal phase TLC (8% EtOAc/Petrol, 3 times) showed many spots without any major spots. Thus, it was not further investigated.

Subfraction B4-4 The chromatogram on normal phase TLC (10% EtOAc/Petrol, 2 times) showed one UV-active spot with the R_f value of 0.50 and two yellow spots with the R_f values of 0.46 and 0.42. It was further separated by flash column chromatography. Elution was conducted initially with 2% EtOAc/Petrol and gradually increased the polarity until 50% EtOAc/Petrol. Fractions with the similar chromatogram were combined and evaporated under reduced pressure to dryness to afford five subfractions, as shown in **Table 19**.

Table 19 Subfractions obtained from subfraction B4-4 by flash column chromatography on silica gel

fraction	Weight (g)	Physical appearance
B4-4-1	0.0061	Yellow gum
B4-4-2	0.0076	Yellow gum
B4-4-3	0.0046	Yellow gum
B4-4-4	0.0110	Yellow gum
B4-4-5	0.0522	Yellow gum

Subfraction B4-4-1 The chromatogram on normal phase TLC (8% EtOAc/Petrol, 5 times) showed many spots without any major spots. Thus, it was not further investigated.

Subfraction B4-4-2 The chromatogram on normal phase TLC (8% EtOAc/Petrol, 5 times) showed one major UV-active spot with the R_f value of 0.36 and one minor yellow spot with the R_f value of 0.34. Further purification was performed on precoated TLC, using 8% EtOAc/Petrol as a mobile phase (3 times), to afford two bands.

Band B4-4-2-1 It was obtained as a yellow solid (0.0026 g). The chromatogram on normal phase TLC (8% EtOAc/Petrol, 5 times) showed one UV-active spot with the same R_f value as **PP11**.

Band B4-4-2-2 It was obtained as a yellow solid (0.0010 g). The chromatogram on normal phase TLC (8% EtOAc/Petrol, 5 times) showed one yellow spot with the same R_f value as **PP2**.

Subfraction B4-4-3 The chromatogram on normal phase TLC (8% EtOAc/Petrol, 5 times) showed one UV-active spot with the R_f value of 0.36 and two yellow spots with the R_f values of 0.34 and 0.32. Because it was obtained in low quantity, it was not further investigated.

Subfraction B4-4-4 The chromatogram on normal phase TLC (8% EtOAc/Petrol, 5 times) showed two yellow spots with the R_f values of 0.34 and 0.32. Further purification was performed on precoated TLC, using 8% EtOAc/Petrol as a mobile phase (22-times), to afford two bands.

Band B4-4-4-1 It was obtained as a yellow solid (0.0022 g). The chromatogram on normal phase TLC (8% EtOAc/Petrol, 5 times) showed one yellow spot with the same R_f value as **PP2**.

Band B4-4-4-2 (PP13) It was obtained as a yellow gum (0.0024 g).

The chromatogram on normal phase TLC (8% EtOAc/Petrol, 5 times) showed one yellow spot with the R_f value of 0.32.

$[\alpha]_D^{29} = -176^\circ$ ($c = 1.7 \times 10^{-2} \text{ g/100 cm}^3$, MeOH)

UV λ_{max} nm (MeOH) ($\log \epsilon$) 363 (4.03)

IR (neat) $\nu_{\text{cm}^{-1}}$ 3461 (O-H stretching), 2959, 2926, 2849 (C-H stretching), 1745, 1634 (C=O stretching)

$^1\text{H NMR}$ (CDCl_3) (δ ppm) 13.24 (*s*, 1H), 7.51 (*d*, $J = 1.0$ Hz, 1H), 5.22
(500 MHz) (*mt*, $J = 7.0$ Hz, 1H), 4.54 (*q*, $J = 7.0$ Hz, 1H),
4.36 (*md*, $J = 10.5$ Hz, 1H), 3.64 (*s*, 3H), 3.22
(*d*, $J = 7.0$ Hz, 2H), 2.67 (*md*, $J = 14.5$ Hz, 1H),
2.58 (*d*, $J = 9.5$ Hz, 1H), 2.54 (*dd*, $J = 14.5$ and
10.5 Hz, 1H), 2.34 (*d*, $J = 13.0$ Hz, 1H), 1.75
(*s*, 3H), 1.72 (*s*, 3H), 1.68 (*brs*, 3H), 1.66 (*dd*,
 $J = 13.0$ and 9.5 Hz, 1H), 1.49 (*s*, 3H), 1.41 (*s*,
3H), 1.36 (*brs*, 3H), 1.30 (*d*, $J = 7.0$ Hz, 3H),
1.29 (*s*, 3H), 1.02 (*s*, 3H)

Subfraction B4-4-5 The chromatogram on normal phase TLC (8% EtOAc/Petrol, 5 times) showed no definite spot. Thus, it was not further investigated.

Subfraction B4-5 The chromatogram on normal phase TLC (10% EtOAc/Petrol, 2 times) showed one UV-active spot with the R_f value of 0.50 and three yellow spots with the R_f values of 0.46, 0.42 and 0.35. One additional dark blue spot

with the same R_f value as **PP12** was observed after dipping the TLC plate in ASA reagent and subsequently heating. Further separation was performed by flash column chromatography. Elution was conducted initially with 2% EtOAc/Petrol and gradually increased the polarity until 20% EtOAc/Petrol. Fractions with the similar chromatogram were combined and evaporated under reduced pressure to dryness to afford four subfractions, as shown in **Table 20**.

Table 20 Subfractions obtained from subfraction **B4-5** by flash column chromatography on silica gel

fraction	Weight (g)	Physical appearance
B4-5-1	0.0041	Yellow gum
B4-5-2	0.0460	Yellow gum with white solid
B4-5-3	0.0077	Yellow gum
B4-5-4	0.0500	Yellow gum

Subfraction B4-5-1 The chromatogram on normal phase TLC (8% EtOAc/Petrol) showed many UV-active spots without any major spots. Thus, it was not further investigated.

Subfraction B4-5-2 The chromatogram on normal phase TLC (8% EtOAc/Petrol) showed one UV-active spot with the R_f value of 0.20 and one yellow spot with the R_f value of 0.16. One additional dark-blue spot with the R_f value of 0.17 (**PP12**), the major spot, was observed after dipping the TLC plate in ASA reagent and subsequently heating.

Subfraction B4-5-3 The chromatogram on normal phase TLC (8% EtOAc/Petrol) showed one UV-active spot with the R_f value of 0.20 and two yellow spots with the R_f values of 0.16 and 0.14. Further purification was performed on precoated TLC, using 8% EtOAc/Petrol as a mobile phase (7 times), to afford three bands.

Band B4-5-3-1 It was obtained as a pale yellow gum (0.0001 g). The chromatogram on normal phase TLC (8% EtOAc/Petrol, 5 times) showed one UV-active spot with the R_f value of 0.35. Because it was obtained in low quantity, it was not further investigated.

Band B4-5-3-2 It was obtained as a yellow gum (0.0006 g). The chromatogram on normal phase TLC (8% EtOAc/Petrol, 5 times) showed one yellow spot with the R_f value of 0.33. Because it was obtained in low quantity, it was not further investigated.

Band B4-5-3-3 It was obtained as a yellow solid (0.0025 g). The chromatogram on normal phase TLC (8% EtOAc/Petrol, 5 times) showed one yellow spot with the same R_f value as **PP3**.

Subfraction B4-5-4 The chromatogram on normal phase TLC (8% EtOAc/Petrol) showed many UV-active spots without any major spots. Thus, it was not further investigated.

Subfraction B4-6 The chromatogram on normal phase TLC (10% EtOAc/Petrol, 2 times) showed one yellow spot with the R_f value of 0.35 and one UV-active spot with the R_f value of 0.27. One additional dark blue spot with the same R_f value as **PP12** was observed after dipping the TLC plate in ASA reagent and subsequently heating. Further separation was performed by flash column

chromatography. Elution was conducted initially with 2% EtOAc/Petrol and gradually increased the polarity until 20% EtOAc/Petrol. Fractions with the similar chromatogram were combined and evaporated under reduced pressure to dryness to afford five subfractions, as shown in Table 21.

Table 21 Subfractions obtained from subfraction B4-6 by flash column chromatography on silica gel

fraction	Weight (g)	Physical appearance
B4-6-1	0.0586	Yellow gum
B4-6-2	0.0191	Yellow gum
B4-6-3	0.0026	Yellow gum
B4-6-4	0.0237	Yellow gum
B4-6-5	0.0668	Yellow gum

Subfraction B4-6-1 The chromatogram on normal phase TLC (10% EtOAc/Petrol, 3 times) showed two yellow spots with the R_f values of 0.33 and 0.31 and one UV-active spot with the R_f value of 0.32. One additional dark blue spot with the R_f value of 0.17 (**PP12**), the major spot, was observed after dipping the TLC plate in ASA reagent and subsequently heating.

Subfraction B4-6-2 The chromatogram on normal phase TLC (10% EtOAc/Petrol, 3 times) showed one major yellow spot with the R_f value of 0.31 and two yellow minor spots with the R_f values of 0.33 and 0.29. The major spot had the same R_f value as **PP3**.

Subfraction B4-6-3 The chromatogram on normal phase TLC (10% EtOAc/Petrol, 3 times) showed two pale spots; one yellow spot with the R_f value of 0.29 and one UV-active spot with the R_f value of 0.27. Because it was obtained in low quantity, it was not further investigated.

Subfraction B4-6-4 The chromatogram on normal phase TLC (10% EtOAc/Petrol, 3 times) showed one major UV-active spot with the R_f value of 0.27. Further purification was performed on precoated TLC, using 5% MeOH/CHCl₃ as a mobile phase, to afford a white solid (0.0051 g). The chromatogram on normal phase TLC (10% EtOAc/Petrol) showed two UV-active spots with the R_f values of 0.13 and 0.07. Attempted purification by repeated chromatography was unsuccessful.

Subfraction B4-6-5 The chromatogram on normal phase TLC (10% EtOAc/Petrol, 3 times) showed no definite spot. Thus, it was not further investigated.

Subfraction B4-7 The chromatogram on normal phase TLC (15% EtOAc/Petrol) showed three UV-active spots with the R_f values of 0.30, 0.27 and 0.22. Further separation was performed by column chromatography. Elution was conducted initially with 10% EtOAc/Petrol and gradually increased the polarity until 50% EtOAc/Petrol. Fractions with the similar chromatogram were combined and evaporated under reduced pressure to dryness to afford two subfractions, as shown in **Table 22**.

Table 22 Subfractions obtained from subfraction B4-7 by column chromatography on silica gel

fraction	Weight (g)	Physical appearance
B4-7-1	0.0248	Yellow gum
B4-7-2	0.0556	Yellow gum

Subfraction B4-7-1 The chromatogram on normal phase TLC (0.5% MeOH/CHCl₃) showed many UV-active spots without any major spots. Thus, it was not further investigated.

Subfraction B4-7-2 The chromatogram on normal phase TLC (0.5% MeOH/CHCl₃) showed three UV-active spots with the R_f values of 0.50, 0.44 and 0.39. Further separation was performed by flash column chromatography. Elution was conducted with 0.1% MeOH/CHCl₃. Fractions with the similar chromatogram were combined and evaporated under reduced pressure to dryness to afford three subfractions, as shown in Table 23.

Table 23 Subfractions obtained from subfraction B4-7-2 by flash column chromatography on silica gel

fraction	Weight (g)	Physical appearance
B4-7-2-1	0.0103	Yellow gum
B4-7-2-2	0.0194	Yellow gum

Table 23 (Continued)

fraction	Weight (g)	Physical appearance
B4-7-2-3	0.0155	Yellow gum

Subfraction B4-7-2-1 The chromatogram on normal phase TLC (0.1% MeOH/CHCl₃, 3 times) showed many UV-active spots without any major spots. Thus, it was not further investigated.

Subfraction B4-7-2-2 The chromatogram on normal phase TLC (0.1% MeOH/CHCl₃, 3 times) showed three UV-active spots with the R_f values of 0.42, 0.37 and 0.34. Further purification was performed on precoated TLC, using 0.1% MeOH/CHCl₃ as a mobile phase (11 times), to afford four bands.

Band B4-7-2-2-1 It was obtained as a pale yellow gum (0.0015 g). The chromatogram on normal phase TLC (0.1% MeOH/CHCl₃, 3 times) showed one UV-active spot with the R_f value of 0.42. Because it was obtained in low quantity, it was not further investigated.

Band B4-7-2-2-2 It was obtained as a pale yellow gum (0.0020 g). The chromatogram on normal phase TLC (0.1% MeOH/CHCl₃, 3 times) showed two UV-active spots with the R_f values of 0.37 and 0.34. Because it was obtained in low quantity, it was not further investigated.

Band B4-7-2-2-3 It was obtained as a pale yellow gum (0.0018 g). The chromatogram on normal phase TLC (0.1% MeOH/CHCl₃, 3 times) showed one UV-active spot with the R_f value of 0.34. Because it was obtained in low quantity, it was not further investigated.

Band B4-7-2-2-4 It was obtained as a pale yellow gum (0.0020 g). The chromatogram on normal phase TLC (0.1% MeOH/CHCl₃, 3 times) showed two UV-active spots with the R_f value of 0.41 and 0.34. Because it was obtained in low quantity, it was not further investigated.

Subfraction B4-7-2-3 The chromatogram on normal phase TLC (0.1% MeOH/CHCl₃, 3 times) showed no definite spot. Thus, it was not further investigated.

Subfraction B4-8 The chromatogram on normal phase TLC (15% EtOAc/Petrol) showed three UV-active spots with the R_f values of 0.22, 0.20 and 0.15. Further separation was performed by column chromatography. Elution was conducted initially with 0.1% EtOAc/CHCl₃ and gradually increased the polarity until 0.5% EtOAc/CHCl₃. Fractions with the similar chromatogram were combined and evaporated under reduced pressure to dryness to afford eight subfractions. Each subfraction was obtained in low quantity and their chromatograms on normal phase TLC (0.1% MeOH/CHCl₃, 3 times) showed many spots. Therefore, they were not further investigated.

Subfraction B4-9 The chromatogram on normal phase TLC (15% EtOAc/Petrol) showed no definite spot. Thus, it was not further investigated.

Fraction B5 The chromatogram on normal phase TLC (50% EtOAc/Petrol) showed one major yellow spot with the same R_f value as **PP7**.

Fraction B6 The chromatogram on normal phase TLC (50% EtOAc/Petrol) showed two major spots which were **PP7** and **PP8**.

Fraction B7 The chromatogram on normal phase TLC (50% EtOAc/Petrol) showed two major spots which were **PP7** and **PP8** together with one yellow spot with

the R_f value of 0.26. Further separation was performed by column chromatography. Elution was conducted initially with 30% EtOAc/Petrol and gradually increased the polarity until pure methanol. Fractions with the similar chromatogram were combined and evaporated under reduced pressure to dryness to afford nine subfractions, as shown in **Table 24**.

Table 24 Subfractions obtained from fraction B7 by column chromatography on silica gel

fraction	Weight (g)	Physical appearance
B7-1	0.0096	Yellow gum
B7-2	0.1059	Orange-yellow gum
B7-3	0.3287	Orange-yellow gum
B7-4	0.2949	Orange-yellow gum
B7-5	0.2341	Orange-yellow gum
B7-6	0.1101	Orange-yellow gum
B7-7	0.0443	Brown-yellow gum
B7-8	0.2048	Brown-yellow gum
B7-9	0.0912	Brown-yellow gum

Subfraction B7-1 The chromatogram on normal phase TLC (40% EtOAc/Petrol) showed no definite spot. Thus, it was not further investigated.

Subfraction B7-2 The chromatogram on normal phase TLC (40% EtOAc/Petrol) showed one yellow spot with the same R_f value as PP7.

Subfraction B7-3 The chromatogram on normal phase TLC (40% EtOAc/Petrol) showed two major spots which were **PP7** and **PP8**.

Subfraction B7-4 The chromatogram on normal phase TLC (40% EtOAc/Petrol) showed two major spots which were **PP7** and **PP8** together with one UV-active spot with the R_f value of 0.29. Further separation was performed by column chromatography. Elution was conducted initially with pure chloroform and gradually increased the polarity with methanol until 70%MeOH/CHCl₃. Fractions with the similar chromatogram were combined and evaporated under reduced pressure to dryness to afford four subfractions, as shown in **Table 25**.

Table 25 Subfractions obtained from subfraction B7-4 by column chromatography on silica gel

fraction	Weight (g)	Physical appearance
B7-4-1	0.0055	Yellow gum
B7-4-2	0.0019	Yellow gum
B7-4-3	0.2172	Yellow gum
B7-4-4	0.0279	Yellow gum

Subfraction B7-4-1 The chromatogram on normal phase TLC (30% EtOAc/Petrol) showed no definite spot. Thus, it was not further investigated.

Subfraction B7-4-2 The chromatogram on normal phase TLC (30% EtOAc/Petrol) showed two major spots which were **PP7** and **PP8**.

Subfraction B7-4-3 The chromatogram on normal phase TLC (30% EtOAc/Petrol) showed two major spots which were **PP7** and **PP8** together with one UV-active spot with the R_f value of 0.21. Further separation was performed by column chromatography. Elution was conducted initially with 10% EtOAc/Petrol and gradually increased the polarity until pure ethyl acetate. Fractions with the similar chromatogram were combined and evaporated under reduced pressure to dryness to afford four subfractions, as shown in **Table 26**.

Table 26 Subfractions obtained from subfraction **B7-4-3** by column chromatography on silica gel

fraction	Weight (g)	Physical appearance
B7-4-3-1	0.0050	Yellow gum
B7-4-3-2	0.0469	Orange-yellow gum
B7-4-3-3	0.1178	Orange-yellow gum
B7-4-3-4	0.0184	Brown-yellow gum

Subfraction B7-4-3-1 The chromatogram on normal phase TLC (30% EtOAc/Petrol, 2 times) showed no definite spot. Thus, it was not further investigated.

Subfraction B7-4-3-2 The chromatogram on normal phase TLC (30% EtOAc/Petrol, 2 times) showed two major spots which were **PP7** and **PP8**.

Subfraction B7-4-3-3 The chromatogram on normal phase TLC (30% EtOAc/Petrol, 2 times) showed one major UV-active spot which was **PP8**

together with one UV-active spot with the R_f value of 0.21. Attempted purification by flash column chromatography on silica gel was unsuccessful.

Subfraction B7-4-3-4 The chromatogram on normal phase TLC (30% EtOAc/Petrol, 2 times) showed no definite spot. Thus, it was not further investigated.

Subfraction B7-5 The chromatogram on normal phase TLC (40% EtOAc/Petrol) showed two major spots which were **PP7** and **PP8** together with four minor UV-active spots with the R_f values of 0.29, 0.24, 0.22 and 0.16. Further separation was performed by column chromatography on silica gel. Elution was conducted initially with 30% EtOAc/Petrol and gradually increased the polarity until pure ethyl acetate. Fractions with the similar chromatogram were combined and evaporated under reduced pressure to dryness to afford five subfractions, as shown in **Table 27**.

Table 27 Subfractions obtained from subfraction **B7-5** by column chromatography on silica gel

fraction	Weight (g)	Physical appearance
B7-5-1	0.0029	Yellow gum
B7-5-2	0.1333	Yellow gum
B7-5-3	0.0383	Yellow gum
B7-5-4	0.0381	Yellow gum
B7-5-5	0.0117	Yellow gum

Subfraction B7-5-1 The chromatogram on normal phase TLC (2% MeOH/CHCl₃, 2 times) showed no definite spot. Thus, it was not further investigated.

Subfraction B7-5-2 The chromatogram on normal phase TLC (2% MeOH/CHCl₃, 2 times) showed one major spot which was **PP8** together with three minor UV-active spots with the R_f values of 0.30, 0.26 and 0.22. Further separation was performed by flash column chromatography on silica gel. Elution was conducted initially with 2% MeOH/CHCl₃ and gradually increased the polarity until 5% MeOH/CHCl₃. Fractions with the similar chromatogram were combined and evaporated under reduced pressure to dryness to afford two subfractions, as shown in **Table 28**.

Table 28 Subfractions obtained from subfraction **B7-5-2** by flash column chromatography on silica gel

fraction	Weight (g)	Physical appearance
B7-5-2-1	0.0186	Yellow gum
B7-5-2-2	0.1269	Yellow gum

Subfraction B7-5-2-1 The chromatogram on normal phase TLC (30% EtOAc/Petrol, 2 times) showed three UV-active spots with the R_f values of 0.34, 0.20 and 0.14. It was further separated by precoated TLC, using 30% EtOAc/Petrol as a mobile phase (5 times), to afford two bands, as pale yellow gum in 0.0015 g and 0.0017 g. Their chromatograms on normal phase TLC (30% EtOAc/Petrol, 5 times)

showed it possessed at least two yellow spots. Therefore, they were not further investigated.

Subfraction B7-5-2-2 The chromatogram on normal phase TLC (30% EtOAc/Petrol, 2 times) showed one major UV-active spot which was **PP8**.

Subfraction B7-5-3 The chromatogram on normal phase TLC (2% MeOH/CHCl₃, 2 times) showed two major spots which were **PP8** and **PP9**.

Subfraction B7-5-4 The chromatogram on normal phase TLC (2% MeOH/CHCl₃, 2 times) showed one major yellow spot which was **PP9**.

Subfraction B7-5-5 The chromatogram on normal phase TLC (2% MeOH/CHCl₃, 2 times) showed no definite spot. Therefore, it was not further investigated.

Subfraction B7-6 The chromatogram on normal phase TLC (50% EtOAc/Petrol) showed three yellow spots with the R_f values of 0.49, 0.43 and 0.36 and one UV-active spot with the R_f value of 0.23. It was further separated by column chromatography over reversed-phase C18 silica gel. Elution was conducted initially with 50% MeOH/H₂O and gradually decreased the polarity until pure methanol. Fractions with the similar chromatogram were combined and evaporated under reduced pressure to dryness to afford five subfractions, as shown in **Table 29**.

Table 29 Subfractions obtained from B7-6 by column chromatography over reversed-phase C18 silica gel

fraction	Weight (g)	Physical appearance
B7-6-1	0.0076	Yellow gum
B7-6-2	0.0537	Yellow gum
B7-6-3	0.0016	Yellow gum
B7-6-4	0.0027	Yellow gum
B7-6-5	0.0580	Yellow gum

Subfraction B7-6-1 The chromatogram on normal phase TLC (40% EtOAc/Petrol, 3 times) showed no definite spot. Thus, it was not further investigated.

Subfraction B7-6-2 The chromatogram on normal phase TLC (40% EtOAc/Petrol, 3 times) showed two major yellow spots with the R_f values of 0.52 and 0.42. It was further separated by precoated TLC, using 40% EtOAc/Petrol as a mobile phase (4 times), to afford two bands.

Band B7-6-2-1 (PP14) It was obtained as a yellow gum (0.0040 g). The chromatogram on normal phase TLC (40% EtOAc/Petrol, 3 times) showed one yellow spot with the R_f value of 0.52.

$[\alpha]_D^{29} = -353^\circ$ ($c = 1.7 \times 10^{-2}$ g/100 cm³, MeOH)

UV λ_{\max} nm (MeOH) ($\log \epsilon$) 366 (4.23)

IR (neat) $\nu_{\text{cm}^{-1}}$ 3600-2500 (O-H stretching), 2952, 2927, 2849
(C-H stretching), 1745, 1694, 1634 (C=O)

	stretching)
¹ H NMR (CDCl ₃) (δ ppm) (400 MHz)	7.52 (<i>d</i> , <i>J</i> = 1.3 Hz, 1H), 5.43 (<i>md</i> , <i>J</i> = 10.4 Hz, 1H), 5.03 (<i>brs</i> , 1H), 4.88 (<i>brs</i> , 1H), 4.55 (<i>q</i> , <i>J</i> = 6.6 Hz, 1H), 4.50 (<i>dd</i> , <i>J</i> = 10.8 and 3.0 Hz, 1H), 3.63 (<i>s</i> , 3H), 3.51 (<i>dd</i> , <i>J</i> = 15.6 and 10.4 Hz, 1H), 2.92 (<i>dd</i> , <i>J</i> = 14.3 and 10.8 Hz, 1H), 2.75 (<i>md</i> , <i>J</i> = 15.6 Hz, 1H), 2.68 (<i>dd</i> , <i>J</i> = 14.3 and 3.0 Hz, 1H), 2.63 (<i>d</i> , <i>J</i> = 9.5 Hz, 1H), 2.32 (<i>d</i> , <i>J</i> = 13.6 Hz, 1H), 1.84 (<i>s</i> , 3H), 1.72 (<i>dd</i> , <i>J</i> = 13.6 and 9.5 Hz, 1H), 1.72 (<i>s</i> , 3H), 1.67 (<i>brs</i> , 3H), 1.46 (<i>s</i> , 3H), 1.39 (<i>s</i> , 3H), 1.37 (<i>d</i> , <i>J</i> = 6.6 Hz, 3H), 1.28 (<i>s</i> , 3H)
¹³ C NMR (CDCl ₃) (δ ppm) (100 MHz)	203.08, 177.82, 167.90, 167.68, 164.12, 155.00, 147.13, 135.81, 134.80, 132.50, 129.45, 112.72, 110.58, 102.36, 101.32, 92.07, 89.18, 85.10, 84.08, 83.56, 74.88, 53.84, 49.69, 43.49, 30.91, 30.44, 29.00, 28.69, 28.50, 27.98, 21.09, 19.68, 18.25, 16.19
DEPT (135°) (CDCl ₃)	CH 135.81, 134.80, 92.07, 74.88, 49.69 CH ₂ 110.58, 30.44, 29.00, 28.50 CH ₃ 53.84, 30.91, 28.69, 27.98, 21.09, 19.68, 18.25, 16.19
EIMS (<i>m/z</i>) (% rel. int.)	608 (13), 580 (77), 537 (66), 509 (100), 383 (24), 277 (30), 233 (31)

Band B7-6-2-2 (PP15) It was obtained as a yellow gum (0.0185 g).

The chromatogram on normal phase TLC (40% EtOAc/Petrol, 3 times) showed one yellow spot with the R_f value of 0.42.

$[\alpha]_D^{29} = -263^\circ$ ($c = 1.9 \times 10^{-2}$ g/100 cm³, MeOH)

UV λ_{\max} nm (MeOH) ($\log \epsilon$) 367 (4.16)

IR (neat) $\nu_{\text{cm}^{-1}}$ 3600-2500 (O-H stretching), 2967, 2929 (C-H stretching), 1745, 1690, 1634 (C=O stretching)

¹H NMR (CDCl₃) (δ ppm) 7.52 (*d*, $J = 2.4$ Hz, 1H), 5.20 (*md*, $J = 12.0$ Hz, 1H), 4.60 (*q*, $J = 6.8$ Hz, 1H), 3.79 (*dd*, $J = 16.2$ and 12.0 Hz, 1H), 3.64 (*s*, 3H), 2.72 (*ddd*, $J = 14.7$, 7.2 and 3.2 Hz, 1H), 2.71 (*md*, $J = 16.2$ Hz, 1H), 2.62 (*d*, $J = 9.6$ Hz, 1H), 2.61 (*dd*, $J = 14.7$ and 3.2 Hz, 1H), 2.35 (*d*, $J = 13.5$ Hz, 1H), 2.05 (*ddd*, $J = 13.5$, 7.2 and 3.2 Hz, 1H), 1.73-1.66 (*m*, 1H), 1.70 (*s*, 3H), 1.69 (*dd*, $J = 13.5$ and 9.6 Hz, 1H), 1.63 (*dd*, $J = 2.3$ and 1.4 Hz, 3H), 1.52 (*s*, 3H), 1.42 (*d*, $J = 6.8$ Hz, 3H), 1.40 (*s*, 3H), 1.38 (*s*, 3H), 1.28 (*s*, 3H), 1.24 (*s*, 3H)

¹³C NMR (CDCl₃) (δ ppm) 202.90, 178.09, 167.67, 165.86, 163.73, 154.31, 135.38, 134.68, 132.48, 129.88, 112.24, 105.98, 101.46, 92.12, 89.09, 85.09, 84.32, 83.41, 73.18, 53.79, 49.78, 43.74, 39.42, 30.83, 30.35, 30.04, 29.10, 28.89, 28.77, 27.60, 21.01, 19.38,

	17.27, 16.83
DEPT (135°) (CDCl ₃)	CH 135.38, 134.68, 92.12, 49.78
	CH ₂ 39.42, 30.35, 29.10, 17.27
	CH ₃ 53.79, 30.83, 30.04, 28.89, 28.77, 27.60, 21.01, 19.38, 16.83
EIMS (<i>m/z</i>) (% rel. int.)	610 (6), 582 (78), 564 (71), 508 (63), 456 (20), 438 (29), 381 (100), 275 (26), 233 (29), 191 (20), 177 (37), 161 (22), 149 (30), 135 (34), 123 (32), 109 (28), 97 (33), 81 (36), 69 (69)

Subfraction B7-7 The chromatogram on normal phase TLC (50% EtOAc/Petrol) showed many spots without any major spots. Thus, it was not further investigated.

Subfraction B7-8 The chromatogram on normal phase TLC (50% EtOAc/Petrol) showed four yellow spots with the R_f value of 0.49, 0.43, 0.36 and 0.27. It was further separated by column chromatography over reversed-phase C18 silica gel. Elution was conducted initially with 50% MeOH/H₂O and gradually decreased the polarity until pure methanol. Fractions with the similar chromatogram were combined and evaporated under reduced pressure to dryness to afford five subfractions, as shown in Table 30.

Table 30 Subfractions obtained from **B7-8** by column chromatography over reverse-phase C18 silica gel

fraction	Weight (g)	Physical appearance
B7-8-1	0.0294	Yellow gum
B7-8-2	0.0732	Yellow gum
B7-8-3	0.0126	Yellow gum
B7-8-4	0.0234	Yellow gum
B7-8-5	0.0667	Yellow gum

Subfraction B7-8-1 The chromatogram on normal phase TLC (40% EtOAc/Petrol, 3 times) showed no definite spot. Thus, it was not further investigated.

Subfraction B7-8-2 The chromatogram on normal phase TLC (40% EtOAc/Petrol, 3 times) showed two major yellow spots with the R_f values of 0.45 and 0.36. It was further separated by flash column chromatography on silica gel. Elution was conducted initially with 30% EtOAc/Petrol and gradually increased the polarity until pure ethyl acetate. Fractions with the similar chromatogram were combined and evaporated under reduced pressure to dryness to afford three subfractions, as shown in **Table 31**.

Table 31 Subfractions obtained from subfraction B7-8-2 by flash column chromatography on silica gel

fraction	Weight (g)	Physical appearance
B7-8-2-1	0.0020	Yellow gum
B7-8-2-2	0.0339	Yellow gum
B7-8-2-3	0.0378	Yellow gum

Subfraction B7-8-2-1 The chromatogram on normal phase TLC (40% EtOAc/Petrol) showed no definite spot. Therefore, it was not further investigated.

Subfraction B7-8-2-2 The chromatogram on normal phase TLC (40% EtOAc/Petrol) showed three yellow spots with the R_f values of 0.29, 0.27 and 0.23. It was further separated by precoated TLC, using 40% EtOAc/Petrol as a mobile phase (3 times), to afford three bands.

Band B7-8-2-2-1 It was obtained as a yellow gum (0.0014 g). The chromatogram on normal phase TLC (40% EtOAc/Petrol) showed two yellow spots with the R_f values of 0.29 and 0.19. Because it was obtained in low quantity, it was not further investigated.

Band B7-8-2-2-2 It was obtained as a yellow gum (0.0023 g). The chromatogram on normal phase TLC (40% EtOAc/Petrol) showed one yellow spot with the same R_f value as **PP14**.

Band B7-8-2-2-3 It was obtained as a yellow gum (0.0228 g). The chromatogram on normal phase TLC (40% EtOAc/Petrol) showed one yellow spot with the same R_f value as **PP15**.

Subfraction B7-8-3 The chromatogram on normal phase TLC (40% EtOAc/Petrol, 2 times) showed many spots without any major spots. Thus, it was not further investigated.

Subfraction B7-8-4 The chromatogram on normal phase TLC (40% EtOAc/Petrol, 2 times) showed one major yellow spot with the same R_f value as **PP9**.

Subfraction B7-8-5 The chromatogram on normal phase TLC (40% EtOAc/Petrol, 2 times) showed no definite spot. Therefore, it was not further investigated.

Subfraction B7-9 The chromatogram on normal phase TLC (50% EtOAc/Petrol) showed no definite spot. Thus, it was not further investigated.

Fraction B8 The chromatogram on normal phase TLC (70% EtOAc/Petrol) showed three UV-active spots with the R_f values of 0.57, 0.49 and 0.37. It was further separated by column chromatography over reversed-phase C18 silica gel. Elution was conducted initially with 15% MeOH/H₂O and gradually decreased the polarity until pure methanol. Fractions with the similar chromatogram were combined and evaporated under reduced pressure to dryness to afford twelve subfractions, as shown in **Table 32**.

Table 32 Subfractions obtained from fraction **B8** by column chromatography over reversed-phase C18 silica gel

fraction	Weight (g)	Physical appearance
B8-1	0.0045	Brown gum
B8-2	0.0044	Brown gum
B8-3	0.0457	Brown gum
B8-4	0.0909	Yellow gum
B8-5	0.0597	Yellow gum
B8-6	0.1217	Yellow gum
B8-7	0.0427	Yellow gum
B8-8	0.1447	Yellow gum
B8-9	0.0882	Yellow gum
B8-10	0.3036	Yellow gum
B8-11	0.0927	Yellow gum
B8-12	0.4361	Brown gum

Subfraction B8-1 The chromatogram on normal phase TLC (5% MeOH/CHCl₃) showed no definite spot. Thus, it was not further investigated.

Subfraction B8-2 The chromatogram on normal phase TLC (5% MeOH/CHCl₃) showed one UV-active spot with the R_f value of 0.21. However, its ¹H NMR spectrum indicated that it was not pure. Because it was obtained in low quantity, it was not further purified.

Subfraction B8-3 The chromatogram on normal phase TLC (5% MeOH/CHCl₃) showed two UV-active spots with the R_f values of 0.29 and 0.21. Attempted purification by flash column chromatography on silica gel was unsuccessful.

Subfraction B8-4 The chromatogram on normal phase TLC (5% MeOH/CHCl₃) showed many spots without any major spots. Thus, it was not further investigated.

Subfraction B8-5 The chromatogram on normal phase TLC (5% MeOH/CHCl₃) showed four yellow spots with the R_f values of 0.41, 0.38, 0.32 and 0.27 and two UV-active spots with the R_f values of 0.22 and 0.18. Further separation was performed by flash column chromatography on silica gel. Elution was conducted initially with 2% MeOH/CHCl₃ and gradually increased the polarity until 20% MeOH/CHCl₃. Fractions with the similar chromatogram were combined and evaporated under reduced pressure to dryness to afford three subfractions, as shown in **Table 33**.

Table 33 Subfractions obtained from subfraction **B8-5** by flash column chromatography on silica gel

fraction	Weight (g)	Physical appearance
B8-5-1	0.0052	Yellow gum
B8-5-2	0.0311	Yellow gum
B8-5-3	0.0200	Yellow gum

Subfraction B8-5-1 The chromatogram on normal phase TLC (5% MeOH/CHCl₃) showed no definite spot. Thus, it was not further investigated.

Subfraction B8-5-2 The chromatogram on normal phase TLC (5% MeOH/CHCl₃) showed two major yellow spots with the R_f values of 0.32 and 0.27. It was further separated by column chromatography on silica gel. Elution was conducted initially with 2% MeOH/CHCl₃ and gradually increased the polarity until 20% MeOH/CHCl₃. Fractions with the similar chromatogram were combined and evaporated under reduced pressure to dryness to afford two subfractions, as shown in **Table 34**.

Table 34 Subfractions obtained from subfraction B8-5-2 by column chromatography on silica gel

fraction	Weight (g)	Physical appearance
B8-5-2-1	0.0062	Yellow gum
B8-5-2-2	0.0230	Yellow gum

Subfraction B8-5-2-1 The chromatogram on normal phase TLC (5% MeOH/CHCl₃) showed many spots. Because it was obtained in low quantity, it was not further investigated.

Subfraction B8-5-2-2 The chromatogram on normal phase TLC (5% MeOH/CHCl₃) showed two major yellow spots with the R_f values of 0.32 and 0.27. It was further separated on precoated TLC, using 4% MeOH/CHCl₃ as a mobile phase (7 times), to give a yellow gum (0.0025 g). The chromatogram on normal phase TLC

(4% MeOH/CHCl₃) showed only one yellow spot with the R_f value of 0.21. However, its ¹H NMR spectrum indicated that it was not pure. Because it was obtained in low quantity, it was not further investigated.

Subfraction B8-5-3 The chromatogram on normal phase TLC (5% MeOH/CHCl₃) showed no definite spot. Thus, it was not further investigated.

Subfraction B8-6 The chromatogram on normal phase TLC (5% MeOH/CHCl₃) showed four yellow spots with the R_f values of 0.51, 0.48, 0.44 and 0.38 and three UV-active spots with the R_f values of 0.34, 0.22 and 0.16. It was further separated by column chromatography on silica gel. Elution was conducted initially with 3% MeOH/CHCl₃ and gradually increased the polarity until 50% MeOH/CHCl₃. Fractions with the similar chromatogram were combined and evaporated under reduced pressure to dryness to afford four subfractions, as shown in **Table 35**.

Table 35 Subfractions obtained from subfraction B8-6 by column chromatography on silica gel

fraction	Weight (g)	Physical appearance
B8-6-1	0.0477	Yellow gum
B8-6-2	0.0251	Yellow gum
B8-6-3	0.0229	Yellow gum
B8-6-4	0.0173	Yellow gum

Subfraction B8-6-1 The chromatogram on normal phase TLC (4% MeOH/CHCl₃) showed many spots. Thus, it was not further investigated.

Subfraction B8-6-2 The chromatogram on normal phase TLC (4% MeOH/CHCl₃) showed two major UV-active spots with the R_f values of 0.19 and 0.11. It was further separated on precoated TLC, using 4% MeOH/CHCl₃ as a mobile phase (7 times), to afford two bands, both as a yellow gum in 0.0013 g and 0.0018 g. Their chromatograms on normal phase TLC (4% MeOH/CHCl₃) showed at least two components. Because they were obtained in low quantity, they were not further investigated.

Subfraction B8-6-3 The chromatogram on normal phase TLC (4% MeOH/CHCl₃) showed two yellow spots with the R_f values of 0.22 and 0.15 and two UV-active spots with the R_f values of 0.19 and 0.07. It was further separated by column chromatography on silica gel. Elution was conducted initially with 3% MeOH/CHCl₃ and gradually increased the polarity until 10% MeOH/CHCl₃. Fractions with the similar chromatogram were combined and evaporated under reduced pressure to dryness to afford two subfractions, as shown in **Table 36**.

Table 36 Subfractions obtained from subfraction B8-6-3 by column chromatography on silica gel

fraction	Weight (g)	Physical appearance
B8-6-3-1	0.0179	Yellow gum
B8-6-3-2	0.0017	Yellow gum

Subfraction B8-6-3-1 The chromatogram on normal phase TLC (4% MeOH/CHCl₃) showed one major UV-active spots with the R_f values of 0.07. It was further separated on precoated TLC, using 4% MeOH/CHCl₃ as a mobile phase (7 times), to give a yellow gum (0.0021 g). The chromatogram on normal phase TLC (4% MeOH/CHCl₃) showed only one UV-active spot with the R_f value of 0.07. However, its ¹H NMR spectrum indicated that it was not pure. Because it was obtained in low quantity, it was not further purified.

Subfraction B8-6-3-2 The chromatogram on normal phase TLC (4% MeOH/CHCl₃) showed one yellow spot with the R_f value of 0.15 and two UV-active spots with the R_f values of 0.07 and 0.06. Because it was obtained in low quantity, it was not further investigated.

Subfraction B8-6-4 The chromatogram on normal phase TLC (4% MeOH/CHCl₃) showed no definite spot. Thus, it was not further investigated.

Subfraction B8-7 The chromatogram on normal phase TLC (2% MeOH/CHCl₃) showed four yellow spots with the R_f values of 0.33, 0.28, 0.23 and 0.16 and one UV-active spot with the R_f value of 0.12. It was further separated by column chromatography on silica gel. Elution was conducted initially with 2% MeOH/CHCl₃ and gradually increased the polarity until 50% MeOH/CHCl₃. Fractions with the similar chromatogram were combined and evaporated under reduced pressure to dryness to afford three subfractions, as shown in **Table 37**.

Table 37 Subfractions obtained from subfraction B8-7 by column chromatography on silica gel

fraction	Weight (g)	Physical appearance
B8-7-1	0.0187	Yellow gum
B8-7-2	0.0095	Yellow gum
B8-7-3	0.0095	Yellow gum

Subfraction B8-7-1 The chromatogram on normal phase TLC (5% MeOH/CHCl₃, 2 times) showed many spots without any major spots. Thus, it was not further investigated.

Subfraction B8-7-2 The chromatogram on normal phase TLC (5% MeOH/CHCl₃, 2 times) showed one major UV-active spot with the R_f value of 0.47 together with three minor yellow spots with the R_f values of 0.58, 0.54 and 0.50. It was further separated on precoated TLC, using 5% MeOH/CHCl₃ as a mobile phase (6 times), to give a pale yellow gum (0.0019 g). The chromatogram on normal phase TLC (4% MeOH/CHCl₃) showed only one UV-active spot with the R_f value of 0.15. Because it was obtained in low quantity, it was not further investigated.

Subfraction B8-7-3 The chromatogram on normal phase TLC (5% MeOH/CHCl₃, 2 times) showed many spots without any major spots. Thus, it was not further investigated.

Subfraction B8-8 The chromatogram on normal phase TLC (2% MeOH/CHCl₃) showed five yellow spots with the R_f values of 0.36, 0.30, 0.23, 0.15 and 0.10 and one UV-active spot with the R_f value of 0.19. It was further separated by

column chromatography on silica gel. Elution was conducted initially with 2% MeOH/CHCl₃ and gradually increased the polarity until 50% MeOH/CHCl₃. Fractions with the similar chromatogram were combined and evaporated under reduced pressure to dryness to afford four subfractions, as shown in **Table 38**.

Table 38 Subfractions obtained from subfraction **B8-8** by column chromatography on silica gel

fraction	Weight (g)	Physical appearance
B8-8-1	0.0042	Yellow gum
B8-8-2	0.0562	Yellow gum
B8-8-3	0.0566	Yellow gum
B8-8-4	0.0171	Yellow gum

Subfraction B8-8-1 The chromatogram on normal phase TLC (4% MeOH/CHCl₃) showed two UV-active spots with the R_f values of 0.80 and 0.74 and one yellow spot with the R_f value of 0.60. Because it was obtained in low quantity, it was not further investigated.

Subfraction B8-8-2 The chromatogram on normal phase TLC (4% MeOH/CHCl₃) showed three yellow spots with the R_f values of 0.60, 0.48 and 0.40 and one UV-active spot with the R_f value of 0.30. Further separation was performed by flash column chromatography on silica gel. Elution was conducted initially with 1% MeOH/CHCl₃ and gradually increased the polarity until 20% MeOH/CHCl₃.

Fractions with the similar chromatogram were combined and evaporated under reduced pressure to dryness to afford three subfractions, as shown in Table 39.

Table 39 Subfractions obtained from subfraction B8-8-2 by flash column chromatography on silica gel

fraction	Weight (g)	Physical appearance
B8-8-2-1	0.0027	Yellow gum
B8-8-2-2	0.0339	Yellow gum
B8-8-2-3	0.0063	Yellow gum

Subfraction B8-8-2-1 The chromatogram on normal phase TLC (4% MeOH/CHCl₃, 2 times) showed four UV-active spots with the R_f values of 0.49, 0.45, 0.42 and 0.38. Because it was obtained in low quantity, it was not further investigated.

Subfraction B8-8-2-2 The chromatogram on normal phase TLC (4% MeOH/CHCl₃, 2 times) showed four yellow spots with the R_f values of 0.68, 0.57, 0.46 and 0.40. It was further separated by precoated TLC, using 4% MeOH/CHCl₃ as a mobile phase (3 times), to afford four bands.

Band B8-8-2-2-1 It was obtained as a yellow gum (0.0013 g). The chromatogram on normal phase TLC (4% MeOH/CHCl₃, 2 times) showed one yellow spot with the R_f value of 0.68. Because it was obtained in low quantity, it was not further investigated.

Band B8-8-2-2-2 It was obtained as a yellow gum (0.0025 g). The chromatogram on normal phase TLC (4% MeOH/CHCl₃, 2 times) showed one yellow spot with the same R_f value as **PP14**.

Band B8-8-2-2-3 It was obtained as a yellow gum (0.0154 g). The chromatogram on normal phase TLC (4% MeOH/CHCl₃, 2 times) showed one yellow spot with the same R_f value as **PP15**.

Band B8-8-2-2-4 It was obtained as a yellow gum (0.0021 g). The chromatogram on normal phase TLC (4% MeOH/CHCl₃, 2 times) showed only one yellow spot with the R_f value of 0.40. However, its ¹H NMR spectrum indicated that it was not pure. Because it was obtained in low quantity, it was not further purified.

Subfraction B8-8-2-3 The chromatogram on normal phase TLC (4% MeOH/CHCl₃, 2 times) showed many yellow and UV-active spots. Because it was obtained in low quantity, it was not further investigated.

Subfraction B8-8-3 The chromatogram on normal phase TLC (4% MeOH/CHCl₃) showed one yellow spot with the R_f value of 0.38 and four UV-active spots with the R_f values of 0.30, 0.21, 0.17 and 0.14. Further separation was performed by flash column chromatography on silica gel. Elution was conducted initially with 1% MeOH/CHCl₃ and gradually increased the polarity until 30% MeOH/CHCl₃. Fractions with the similar chromatogram were combined and evaporated under reduced pressure to dryness to afford three subfractions, as shown in **Table 40**.

Table 40 Subfractions obtained from subfraction B8-8-3 by flash column chromatography on silica gel

fraction	Weight (g)	Physical appearance
B8-8-3-1	0.0070	Yellow gum
B8-8-3-2	0.0091	Yellow gum
B8-8-3-3	0.0249	Yellow gum

Subfraction B8-8-3-1 The chromatogram on normal phase TLC (4% MeOH/CHCl₃, 2 times) showed many spots. Because it was obtained in low quantity, it was not further investigated.

Subfraction B8-8-3-2 The chromatogram on normal phase TLC (4% MeOH/CHCl₃, 3 times) showed one major yellow spot with the same R_f value as PP15.

Subfraction B8-8-3-3 The chromatogram on normal phase TLC (4% MeOH/CHCl₃, 3 times) showed one major UV-active spot with the R_f value of 0.47 together with three minor yellow spots with the R_f values of 0.67, 0.65 and 0.59. It was further separated on precoated TLC, using 4% MeOH/CHCl₃ as a mobile phase (5 times), to give a pale yellow gum (0.0130 g). The chromatogram on normal phase TLC (6% MeOH/CHCl₃) showed one major UV-active spot with the R_f value of 0.44 together with one minor yellow spot with the R_f value of 0.54. Three additional dark-blue spots with the R_f values of 0.50, 0.34 and 0.28 were observed after dipping the TLC plate in ASA reagent and subsequently heating. Further purification was performed on precoated TLC, using 6% MeOH/CHCl₃ as a mobile phase, to give

PP16 as a pale yellow gum (0.0065 g). The chromatogram on normal phase TLC (4% MeOH/CHCl₃) showed only one UV-active spot with the R_f value of 0.30.

$[\alpha]_D^{29} = +77^\circ$ ($c = 1.3 \times 10^{-2}$ g/100 cm³, MeOH)

UV λ_{\max} nm (MeOH) ($\log \epsilon$)	304 (4.24)
IR (neat) $\nu_{\text{cm}^{-1}}$	3690-2350 (O-H stretching), 2971, 2930 (C-H stretching), 1751, 1692, 1633 (C=O stretching)
¹ H NMR (CDCl ₃) (δ ppm) (500 MHz)	12.11 (<i>s</i> , 1H), 6.60 (<i>mt</i> , $J = 7.0$ Hz, 1H), 4.47 (<i>d</i> , $J = 1.0$ Hz, 1H), 4.40 (<i>q</i> , $J = 6.5$ Hz, 1H), 3.51 (<i>s</i> , 3H), 3.38 (<i>s</i> , 3H), 3.21 (<i>mdd</i> , $J = 17.0$ and 7.0 Hz, 1H), 3.18 (<i>brs</i> , 1H), 3.12 (<i>mdd</i> , $J = 17.0$ and 7.0 Hz, 1H), 2.70 (<i>d</i> , $J = 8.5$ Hz, 1H), 2.63-2.59 (<i>m</i> , 2H), 2.02 (<i>d</i> , $J = 14.0$ Hz, 1H), 1.97 (<i>d</i> , $J = 1.0$ Hz, 3H), 1.72-1.68 (<i>m</i> , 2H), 1.65 (<i>dd</i> , $J = 14.0$ and 8.5 Hz, 1H), 1.44 (<i>s</i> , 3H), 1.43 (<i>s</i> , 3H), 1.35 (<i>d</i> , $J = 6.5$ Hz, 3H), 1.29 (<i>s</i> , 3H), 1.28 (<i>s</i> , 3H), 1.21 (<i>s</i> , 3H), 1.11 (<i>s</i> , 3H)
¹³ C NMR (CDCl ₃) (δ ppm) (125 MHz)	205.50, 192.09, 170.87, 166.64, 161.50, 152.17, 137.77, 128.14, 113.75, 106.10, 102.37, 90.31, 87.03, 86.42, 82.68, 81.40, 75.10, 71.03, 57.41, 52.39, 48.90, 45.24, 43.93, 42.18, 30.46, 29.09, 29.06, 28.42, 27.19, 26.08, 23.92, 22.11, 20.88, 17.18, 13.87
DEPT (135°) (CDCl ₃)	CH 137.77, 90.31, 75.10, 48.90, 45.24

CH₂ 42.18, 28.42, 23.92, 17.18

CH₃ 57.41, 52.39, 30.46, 29.09, 29.06, 27.19, 26.08,
22.11, 20.88, 13.87

Subfraction B8-8-4 The chromatogram on normal phase TLC (4% MeOH/CHCl₃) showed many spots without any major spots. Thus, it was not further investigated.

Subfraction B8-9 The chromatogram on normal phase TLC (2% MeOH/CHCl₃) showed no definite spot. Thus, it was not further investigated.

Subfraction B8-10 The chromatogram on normal phase TLC (2% MeOH/CHCl₃) showed three major spots; two yellow spots with the same R_f values as PP7 and PP9 and one UV-active spot with the R_f value of 0.09. It was further separated by column chromatography on silica gel. Elution was conducted initially with 2% MeOH/CHCl₃ and gradually increased the polarity until 70% MeOH/CHCl₃. Fractions with the similar chromatogram were combined and evaporated under reduced pressure to dryness to afford six subfractions, as shown in Table 41.

Table 41 Subfractions obtained from subfraction B8-10 by column chromatography on silica gel

fraction	Weight (g)	Physical appearance
B8-10-1	0.0044	Yellow gum
B8-10-2	0.1131	Yellow gum

Table 41 (Continued)

fraction	Weight (g)	Physical appearance
B8-10-3	0.1174	Yellow gum with white solid
B8-10-4	0.0366	Yellow gum
B8-10-5	0.0795	Yellow gum
B8-10-6	0.0344	Brown gum

Subfraction B8-10-1 The chromatogram on normal phase TLC (4% MeOH/CHCl₃) showed many spots. Because it was obtained in low quantity, it was not further investigate

Subfraction B8-10-2 The chromatogram on normal phase TLC (4% MeOH/CHCl₃) showed two major yellow spots with the same R_f value as PP7 and PP9.

Subfraction B8-10-3 Upon standing at room temperature, a white solid (0.0409 g) precipitated. Its chromatogram on normal phase TLC (4% MeOH/CHCl₃) showed two green spots with the R_f value of 0.27 and 0.23. Attempted purification by repeated chromatography was unsuccessful. The filtrate became a yellow gum (0.0679 g) after evaporation to dryness under reduced pressure. The chromatogram on normal phase TLC (4% MeOH/CHCl₃) showed many spots. Thus, it was not further investigated.

Subfraction B8-10-4 The chromatogram on normal phase TLC (6% MeOH/CHCl₃, 2 times) showed one major UV-active spot with the R_f value of 0.48 together with four minor spots; three UV-active spots with the R_f values of 0.65, 0.43

and 0.39 and one yellow spot with the R_f value of 0.55. Its was shown by TLC comparison with **PP17** that the major spot was **PP17**, obtained from fraction **B8-10-5-2**.

Subfraction B8-10-5 The chromatogram on normal phase TLC (6% MeOH/CHCl₃, 2 times) showed one major UV-active spot with the R_f value of 0.48 together with three minor spots; two yellow spots with the R_f values of 0.78 and 0.55 and one UV-active spot with the R_f value of 0.26. Further separation was performed by flash column chromatography on silica gel. Elution was conducted initially with 2% MeOH/CHCl₃ and gradually increased the polarity until 40% MeOH/CHCl₃. Fractions with the similar chromatogram were combined and evaporated under reduced pressure to dryness to afford two subfractions, as shown in **Table 42**.

Table 42 Subfractions obtained from subfraction **B8-10-5** by flash column chromatography on silica gel

fraction	Weight (g)	Physical appearance
B8-10-5-1	0.0086	Yellow gum
B8-10-5-2	0.0372	Pale yellow gum

Subfraction B8-10-5-1 The chromatogram on normal phase TLC (6% MeOH/CHCl₃) showed one yellow spot with the R_f value of 0.61 and two UV-active spots with the R_f values of 0.38 and 0.33. Because it was obtained in low quantity, it was not further investigated.

Subfraction B8-10-5-2 The chromatogram on normal phase TLC (6% MeOH/CHCl₃) showed one major UV-active spot with the R_f value of 0.38 and

one minor UV-active spot with the R_f value of 0.33. It was further separated on precoated TLC, using 5% MeOH/CHCl₃ as a mobile phase (7 times), to give **PP17** as a pale yellow gum (0.0211 g). The chromatogram on normal phase TLC (6% MeOH/CHCl₃) showed only one UV-active spot with the R_f value of 0.38.

$[\alpha]_D^{29} = +83^\circ$ ($c = 1.2 \times 10^{-2}$ g/100 cm³, MeOH)

UV λ_{\max} nm (MeOH) ($\log \epsilon$) 304 (4.31)

IR (neat) $\nu_{\text{cm}^{-1}}$ 3650-2360 (O-H stretching), 2967, 2929 (C-H stretching), 1750, 1690, 1633 (C=O stretching)

¹H NMR (CDCl₃) (δ ppm) 12.08 (*s*, 1H), 6.64 (*mt*, $J = 7.0$ Hz, 1H), 5.23
(500 MHz) (*mt*, $J = 7.0$ Hz, 1H), 4.82 (*d*, $J = 1.0$ Hz, 1H),
4.40 (*q*, $J = 6.5$ Hz, 1H), 3.48 (*s*, 3H), 3.26-3.13
(*m*, 2H), 3.24-3.17 (*m*, 2H), 3.19 (*s*, 1H), 2.72
(*d*, $J = 8.5$ Hz, 1H), 2.08 (*d*, $J = 14.0$ Hz, 1H),
1.97 (*d*, $J = 1.0$ Hz, 3H), 1.76 (*s*, 3H), 1.69 (*s*,
3H), 1.57 (*dd*, $J = 14.0$ and 8.5 Hz, 1H), 1.43
(*s*, 3H), 1.42 (*s*, 3H), 1.34 (*d*, $J = 6.5$ Hz, 3H),
1.22 (*s*, 3H), 1.10 (*s*, 3H)

¹³C NMR (CDCl₃) (δ ppm) 206.43, 191.72, 171.77, 166.85, 161.65, 152.10,
(125 MHz) 138.66, 132.16, 127.65, 121.59, 113.62, 105.34,
102.41, 90.18, 86.97, 86.35, 82.54, 81.97,
67.24, 52.05, 49.70, 45.44, 43.94, 30.47, 28.33,
27.31, 26.09, 25.79, 22.59, 22.12, 21.43, 20.76,
17.74, 13.83

DEPT (135°) (CDCl ₃)	CH	138.66, 121.59, 90.18, 67.24, 49.70, 45.44
	CH ₂	28.33, 22.59, 21.43
	CH ₃	52.05, 30.47, 27.31, 26.09, 25.79, 22.12, 20.76, 17.74, 13.83

Subfraction B8-10-6 The chromatogram on normal phase TLC (6% MeOH/CHCl₃, 2 times) showed no definite spot. Thus, it was not further investigated.

Subfraction B8-11 The chromatogram on normal phase TLC (2% MeOH/CHCl₃) showed two major yellow spots with the same R_f value as **PP7** and **PP9**.

Subfraction B8-12 The chromatograms on normal phase TLC (2% MeOH/CHCl₃) and reversed-phase C18 TLC (60% MeOH/H₂O) showed no definite spot. Thus, it was not further investigated.

Fraction B9 The chromatograms on normal phase TLC (70% EtOAc/Petrol) and reversed-phase C18 TLC (60% MeOH/H₂O) showed no definite spot. Thus, it was not further investigated.

CHAPTER 3

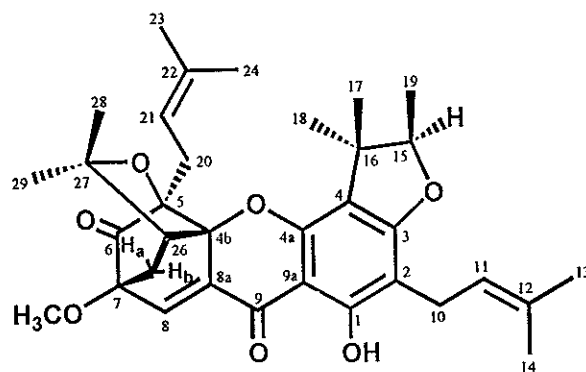
RESULTS AND DISCUSSION

Chemical investigation of *Garcinia scortechinii* involved isolation, purification and structural elucidation of compounds isolated from its latex and stem bark. The latex was separated into two parts by dissolving with chloroform. The chloroform soluble part, upon repeated chromatography, afforded two known caged-tetraprenylated xanthenes (PP2 and PP7), seven new caged-polyprenylated xanthenes (PP1, PP3, PP4, PP5, PP6, PP8 and PP9) and one new degraded tetraprenylated xanthone (PP10). The stem bark was extracted with methanol. The crude methanol extract was separated into two parts by dissolving with chloroform. Upon chromatographic separation, the chloroform soluble part yielded six caged-polyprenylated xanthenes (PP1, PP2, PP3, PP7, PP8 and PP9), previously isolated from the latex, and seven additional compounds: five new caged-tetraprenylated xanthenes (PP13, PP14, PP15, PP16 and PP17), one known xanthone (PP11) and one known steroid (PP12). The structures of caged-polyprenylated xanthenes were elucidated by analysis of 1D and/or 2D NMR spectroscopic data and/or comparison of the NMR data with those of scortechinone A and scortechinone B. The ^{13}C NMR signals were assigned from DEPT, HMQC and HMBC spectra. For other known compounds, their ^1H NMR data were compared with those reported in the literature.

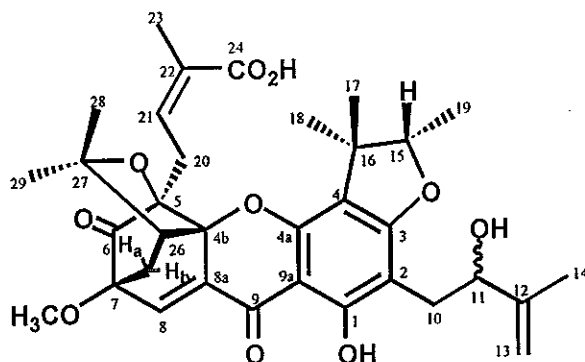
3.1 Characteristic spectroscopic data of caged-polyprenylated xanthenes

Most of compounds isolated from the latex and the stem bark of *G. scortechinii* were caged-polyprenylated xanthenes. Their UV spectrum showed an absorption band in the range of 360-368 nm due to a conjugated carbonyl chromophore. The IR spectrum exhibited absorption bands of a hydroxyl group (in the range of 3600-2500 cm^{-1}), an unconjugated carbonyl group (approximately at 1746 cm^{-1}) and a chelated *ortho*-hydroxyl carbonyl group (approximately at 1636 cm^{-1}). Compounds of this type showed signals for a chelated hydroxy proton (δ_{H} 13.00, 1-OH), an olefinic proton of an α,β -unsaturated carbonyl moiety at δ 7.58 (H-8) and characteristic signals for -OC(Me)₂-CHCH₂-C- unit of a caged-prenylated moiety at δ_{H} 2.55 (*d*, $J=9.6$ Hz, 1H, H-26), 2.33 (*dd*, $J=12.8, 1.4$ Hz, 1H, H_a-25), 1.66 (*dd*, $J=12.8, 9.6$ Hz, 1H, H_b-25), 1.71 (*s*, 3H, Me-28) and 1.29 (*s*, 3H, Me-29) in the ¹H NMR spectrum [see scortechinone A (1) (Rukachaisirikul, 2000a)]. This moiety was assigned to be located on C-4b, C-5 and C-7 due to the HMBC correlations of the olefinic proton, H-8, with C-25, the methylene protons, H_a-25 and H_b-25, with C-4b, C-6, C-7 and C-8 and the methine proton, H-26, with C-4b, C-5 and C-7. The chemical-shift values of Me-28 and Me-29 were assigned by the NOEDIFF data observed between Me-28 and H-26 and between Me-29 and H_a-25 as well as the methoxy protons (7-OCH₃). Furthermore, the ¹H NMR spectrum of most of caged-polyprenylated xanthenes, isolated from the latex and the stem bark of *G. scortechinii*, also showed characteristic signals for a 2,3,3-trimethylhydrofuran unit: the *quartet* signal of the methine proton (δ_{H} 4.37, H-15) coupled to the *doublet* signal of the methyl protons (δ_{H} 1.41, H-19) with a *J*-coupling constant value of 6.6 Hz

together with two methyl protons [δ_{H} 1.16 (Me-17) and 1.58 (Me-18)]. This unit was fused to the aromatic ring by linkage of its *gem*-dimethyl carbon and ring oxygen atom with C-4 and C-3, respectively, according to the HMBC correlations of Me-17 and Me-18 with C-4 together with the chemical-shift values of C-3 (δ_{C} 166.87) and C-4 (δ_{C} 113.03). Caged-polyprenylated xanthenes, which had the 2,3,3-trimethylhydrofuran ring, were divided into two types by the consideration of the relative stereochemistry of H-15, the α - and β -position. In the case of scortechinone A, Me-18 gave enhancement with H-15 and the methylene proton (H_a-20) and Me-24 of a C-5 prenyl group in the NOEDIFF spectrum. These indicated that Me-18, H-15 and the C-5 prenyl group were located on the same side of the molecule, the α -side. For scortechinone C (2) (Rukachaisirikul, 2000a), H-15 was assigned to be located on the β -position since irradiation of Me-17 and Me-18 enhanced the signals of H-15 of the hydrofuran unit and H_a-20 of the C-5 α,β -unsaturated carboxylic acid unit, respectively. In the case of caged-polyprenylated xanthenes which had a 3-methylbut-2-enyl group [see (1)], the chemical-shift values of Me-13 and Me-23 were assigned by the NOE enhancement observed between Me-13 and H-11 and between Me-23 and H-21.



1: scortechinone A

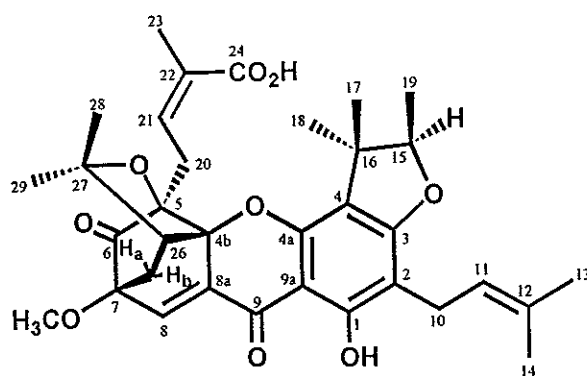


2: scortechinone C

3.2 Structural determination of compounds isolated from the latex of *G. scortechinii*

3.2.1 Compound PP7

Compound PP7 was isolated as a yellow solid, melting at 161.8-163.2°C. The IR spectrum (Figure 3) exhibited absorption bands at 3600-2500 (a hydroxyl group of a carboxylic acid), 1745 (an unconjugated carbonyl group), 1690 (an α,β -unsaturated carboxyl group) and 1636 cm^{-1} (a chelated *ortho*-hydroxyl carbonyl group). Its UV spectrum (Figure 2) showed an absorption band due to a conjugated carbonyl chromophore at λ_{max} 366 nm. Compound PP7 was identified as scortechinone B (3), which was previously isolated from the twigs of *G. scortechinii* (Rukachaisirikul, 2000a) by comparison of its ^1H NMR data (Figure 4) (Table 43) and co-chromatography with scortechinone B (3).



3

Table 43 The ^1H NMR data of scortechinone B and PP7

Position	Scortechinone B (δ_{H})	PP7 (δ_{H})
1-OH	13.10 (<i>s</i> , 1H)	13.10 (<i>s</i> , 1H)
7-OCH ₃	3.52 (<i>s</i> , 3H)	3.63 (<i>s</i> , 3H)
H-8	7.56 (<i>d</i> , $J=1.2$ Hz, 1H)	7.58 (<i>d</i> , $J=1.5$ Hz, 1H)
H _a -10	3.17 (<i>mdd</i> , $J=14.4, 7.2$ Hz, 1H)	3.18 (<i>mdd</i> , $J=15.0, 7.5$ Hz, 1H)
H _b -10	3.11 (<i>mdd</i> , $J=14.4, 7.2$ Hz, 1H)	3.12 (<i>mdd</i> , $J=15.0, 7.5$ Hz, 1H)
H-11	5.20 (<i>ht</i> , $J=7.2, 1.5$ Hz, 1H)	5.21 (<i>ht</i> , $J=7.5, 1.5$ Hz, 1H)
Me-13	1.65 (<i>q</i> , $J=1.5$ Hz, 3H)	1.66 (<i>d</i> , $J=1.5$ Hz, 3H)
Me-14	1.72 (<i>brs</i> , 3H)	1.72 (<i>s</i> , 3H)
H-15	4.46 (<i>q</i> , $J=6.6$ Hz, 1H)	4.46 (<i>q</i> , $J=6.5$ Hz, 1H)
Me-17	1.37 (<i>s</i> , 3H)	1.38* (<i>s</i> , 3H)
Me-18	1.37 (<i>s</i> , 3H)	1.37* (<i>s</i> , 3H)
Me-19	1.23 (<i>d</i> , $J=6.6$ Hz, 3H)	1.22 (<i>d</i> , $J=6.5$ Hz, 3H)
H _a -20	3.27 (<i>brdd</i> , $J=16.0, 9.6$ Hz, 1H)	3.28 (<i>brdd</i> , $J=16.0, 10.0$ Hz, 1H)
H _b -20	2.83 (<i>ddq</i> , $J=16.0, 4.5, 2.0$ Hz, 1H)	2.85 (<i>ddq</i> , $J=16.0, 4.5, 2.0$ Hz, 1H)
H-21	5.67 (<i>ddq</i> , $J=9.6, 4.5, 1.5$ Hz, 1H)	5.68 (<i>ddq</i> , $J=10.0, 4.5, 1.5$ Hz, 1H)
Me-23	1.72 (<i>s</i> , 3H)	1.72 (<i>s</i> , 3H)

Table 43 (Continued)

Position	Scortechinone B (δ_H)	PP7 (δ_H)
H _a -25	2.33 (<i>dd</i> , $J=13.2, 1.2$ Hz, 1H)	2.34 (<i>brd</i> , $J=13.0$ Hz, 1H)
H _b -25	1.68 (<i>dd</i> , $J=13.2, 9.2$ Hz, 1H)	1.69 (<i>dd</i> , $J=13.0, 9.5$ Hz, 1H)
H-26	2.60 (<i>d</i> , $J=9.2$ Hz, 1H)	2.60 (<i>d</i> , $J=9.5$ Hz, 1H)
Me-28	1.72 (<i>s</i> , 3H)	1.72 (<i>s</i> , 3H)
Me-29	1.28 (<i>s</i> , 3H)	1.29 (<i>s</i> , 3H)

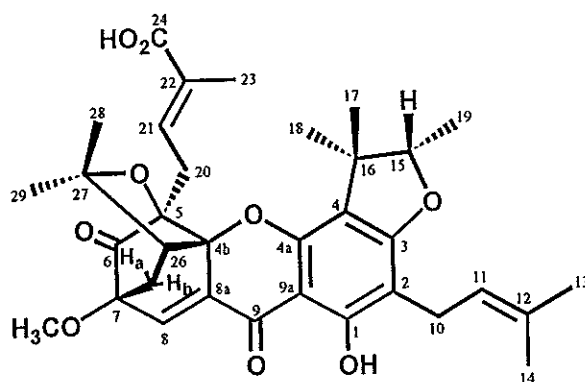
* interchangeable

3.2.2 Compound PP9

Compound PP9, a yellow gum, was found to have a molecular formula of C₃₄H₄₂O₇ by EIMS (m/z 592) (Figure 5). The IR spectrum (Figure 7) exhibited almost identical absorption bands to scortechinone B at 3500-2500 (a hydroxyl group of a carboxylic acid), 1746 (an unconjugated carbonyl group), 1691 (an α,β -unsaturated carboxyl group) and 1635 cm⁻¹ (a chelated *ortho*-hydroxyl carbonyl group). The presence of three carbonyl groups was confirmed by the signals at δ 202.01, 177.50 and 171.00 in the ¹³C NMR spectrum (Figure 9) (Table 45). The UV absorption band at λ_{max} 362 nm (Figure 6) was similar to that of scortechinone B. These results suggested that PP9 had a caged-polyprenylated xanthone moiety. Its ¹H NMR signals (Figure 8) (Table 44) were similar to those of scortechinone B. It consisted of signals for one chelated hydroxy proton (δ_H 13.10, *s*, 1-OH), one olefinic proton (δ_H 7.61, *d*, $J=1.0$ Hz, H-8), one methoxyl group (δ_H 3.63, *s*), one unit of a 3-methylbut-2-enyl group [δ_H 5.22 (*mt*, $J=7.0$ Hz, 1H, H-11), 3.20 (*d*, $J=7.0$ Hz, 2H, H-

10), 1.74 (*s*, 3H, Me-13) and 1.67 (*s*, 3H, Me-14)], one unit of -OC(Me)₂-CHCH₂-C- [δ_{H} 2.61 (*d*, *J*=9.5 Hz, 1H, H-26), 2.33 (*d*, *J*=13.0 Hz, 1H, H_a-25), 1.72 (*s*, 3H, Me-28), 1.69 (*dd*, *J*=13.0, 9.5 Hz, 1H, H_b-25) and 1.29 (*s*, 3H, Me-29)], one unit of a 2,3,3-trimethylhydrofuran ring [δ_{H} 4.54 (*q*, *J*=6.5 Hz, H-15), 1.46 (*s*, 3H, Me-18), 1.41 (*s*, 3H, Me-17) and 1.30 (*d*, *J*=6.5 Hz, 3H, Me-19)] and one unit of a 3-carboxybut-2-enyl group [δ_{H} 6.41 (*qdd*, *J*=10.0, 5.5, 1.5 Hz, 1H, H-21), 2.79 (*mdd*, *J*=15.0, 5.5, 1.5 Hz, 1H, H_a-20), 2.56 (*dd*, *J*=15.0, 10.0 Hz, 1H, H_b-20) and 1.38 (*s*, 3H, Me-23)]. The ¹³C NMR, DEPT (Figure 10) and HMQC (Figure 14) spectra showed resonances for 17 quaternary carbons, 5 methine carbons, 3 methylene carbons and 9 methyl carbons. The HMBC data (Figure 15) (Table 46) established the attachment of all substituents to be identical to that of scortechinone B. However, the olefinic proton (H-21) of the C-5 substituent was shifted to lower field than that of scortechinone B (Table 44), suggesting that H-21 lied in the deshielding zone of the carboxyl group. These indicated that PP9 differed from scortechinone B in the configuration of a double bond of the C-5 side chain. The configuration at the double bond was found to be *E* since irradiation of H-21 (Figure 11) enhanced the signal of methylene proton (H_a-20), not the methyl protons (Me-23) in the NOEDIFF experiment. The relative stereochemistry was also provided by NOEDIFF results. When the oxymethine proton (H-15) of the hydrofuran ring was irradiated (Figure 12), a *singlet* signal of the methyl protons at δ_{H} 1.41 (Me-17) and a *doublet* signal of the methyl protons at δ_{H} 1.30 (Me-19) were enhanced. The NOEDIFF data observed between the methyl protons (Me-18) and H-21 as well as the methylene protons (H_a-20 and H_b-20) of the C-5 3-carboxybut-2-enyl group (Figure 13) indicated that the C-5 substituent was *cis* to Me-18. These results suggested that H-15 was on β -

position. Thus, PP9 had the structure 4, a new naturally occurring caged-tetraprenylated xanthone of which the structure differed from scortechinone B in the stereochemistry of C-15 and the configuration of the double bond of the C-5 substituent.



4

Table 44 The ^1H NMR data of scortechinone B and PP9

Position	Scortechinone B (δ_{H})	PP9 (δ_{H})
1-OH	13.10 (<i>s</i> , 1H)	13.10 (<i>s</i> , 1H)
7-OCH ₃	3.52 (<i>s</i> , 3H)	3.63 (<i>s</i> , 3H)
H-8	7.56 (<i>d</i> , $J=1.2$ Hz, 1H)	7.61 (<i>d</i> , $J=1.0$ Hz, 1H)
H _a -10	3.17 (<i>mdd</i> , $J=14.4, 7.2$ Hz, 1H)	3.20 (<i>d</i> , $J=7.0$ Hz, 2H)
H _b -10	3.11 (<i>mdd</i> , $J=14.4, 7.2$ Hz, 1H)	
H-11	5.20 (<i>ht</i> , $J=7.2, 1.5$ Hz, 1H)	5.22 (<i>mt</i> , $J=7.0$ Hz, 1H)
Me-13	1.65 (<i>q</i> , $J=1.5$ Hz, 3H)	1.67 (<i>s</i> , 3H)
Me-14	1.72 (<i>brs</i> , 3H)	1.74 (<i>s</i> , 3H)
H-15	4.46 (<i>q</i> , $J=6.6$ Hz, 1H)	4.54 (<i>q</i> , $J=6.5$ Hz, 1H)
Me-17	1.37 (<i>s</i> , 3H)	1.41 (<i>s</i> , 3H)
Me-18	1.37 (<i>s</i> , 3H)	1.46 (<i>s</i> , 3H)

Table 44 (Continued)

Position	Scortechinone B (δ_H)	PP9 (δ_H)
Me-19	1.23 (<i>d</i> , $J=6.6$ Hz, 3H)	1.30 (<i>d</i> , $J=6.5$ Hz, 3H)
H _a -20	3.27 (<i>brdd</i> , $J=16.0, 9.6$ Hz, 1H)	2.79 (<i>mdd</i> , $J=15.0, 5.5$ Hz, 1H)
H _b -20	2.83 (<i>ddq</i> , $J=16.0, 4.5, 2.0$ Hz, 1H)	2.56 (<i>dd</i> , $J=15.0, 10.0$ Hz, 1H)
H-21	5.67 (<i>ddq</i> , $J=9.6, 4.5, 1.5$ Hz, 1H)	6.41 (<i>ddq</i> , $J=10.0, 5.5, 1.5$ Hz, 1H)
Me-23	1.72 (<i>s</i> , 3H)	1.38 (<i>s</i> , 3H)
H _a -25	2.33 (<i>dd</i> , $J=13.2, 1.2$ Hz, 1H)	2.33 (<i>d</i> , $J=13.0$ Hz, 1H)
H _b -25	1.68 (<i>dd</i> , $J=13.2, 9.2$ Hz, 1H)	1.69 (<i>dd</i> , $J=13.0, 9.5$ Hz, 1H)
H-26	2.60 (<i>d</i> , $J=9.2$ Hz, 1H)	2.61 (<i>d</i> , $J=9.5$ Hz, 1H)
Me-28	1.72 (<i>s</i> , 3H)	1.72 (<i>s</i> , 3H)
Me-29	1.28 (<i>s</i> , 3H)	1.29 (<i>s</i> , 3H)

Table 45 The ^{13}C NMR data of scortechinone B and PP9

Position	C-type	Scortechinone B (δ_C)	PP9 (δ_C)
1-OH	C	163.46	163.49
2	C	105.81	106.19
3	C	167.08	166.86
4	C	112.30	111.99
4a	C	154.07	154.00
4b	C	89.37	89.41
5	C	83.77	83.30
6	C=O	202.30	202.01
7	C	84.93	84.96
7-OCH ₃	CH ₃	53.88	54.10

Table 45 (Continued)

Position	C-type	Scortechinone B (δ_c)	PP9 (δ_c)
8	CH	135.09	135.40
8a	C	132.38	132.13
9	C=O	177.60	177.50
9a	C	101.27	101.34
10	CH ₂	21.35	21.39
11	CH	121.69	121.52
12	C	132.05	132.03
13	CH ₃	25.66	25.70
14	CH ₃	17.72	17.77
15	CH	91.40	91.28
16	C	43.50	43.70
17	CH ₃	19.95*	28.15
18	CH ₃	28.09*	20.32
19	CH ₃	15.81	16.33
20	CH ₂	29.91	29.28
21	CH	136.99	135.86
22	C	128.68	129.34
23	CH ₃	20.57	11.44
24	C=O	170.67	171.00
25	CH ₂	30.54	30.92
26	CH	49.75	49.78
27	C	83.71	83.70
28	CH ₃	30.93	30.87
29	CH ₃	28.79	28.87

* interchangeable

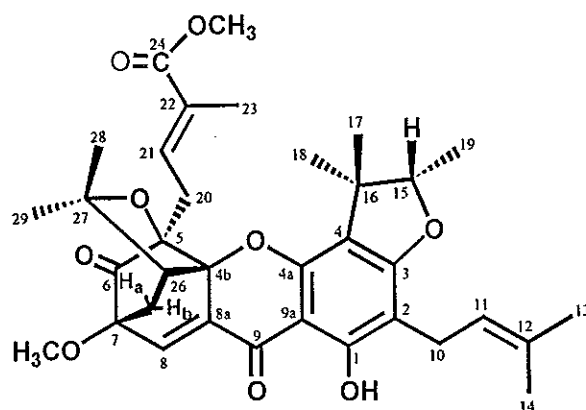
Table 46 The HMBC correlations of scortechinone B and PP9

Proton	Scortechinone B (Carbon)	PP9 (Carbon)
1-OH	C-1, C-2, C-3, C-9, C-9a	C-1, C-2, C-3, C-9a
7-OCH ₃	C-7	C-7
H-8	C-4b, C-6, C-7, C-8a, C-9, C-25	C-4b, C-6, C-8a, C-9
H-10	C-1, C-2, C-3, C-11, C-12	C-1, C-2, C-3, C-11, C-12
H-11	C-10, C-13, C-14	C-10, C-13, C-14
Me-13	C-11, C-12, C-14	C-11, C-12, C-14
Me-14	C-11, C-12, C-13	C-11, C-12, C-13
H-15	C-3, C-4, C-16, C-17, C-18, C-19	C-3, C-4, C-17, C-18
Me-17	C-4, C-15, C-16, C-18	C-4, C-15, C-16, C-18
Me-18	C-4, C-15, C-16, C-17	C-4, C-15, C-16, C-17
Me-19	C-15, C-16	C-15, C-16
H _a -20	C-4b, C-5, C-6, C-21, C-22	C-4b, C-5, C-6, C-21, C-22
H _b -20	C-4b, C-5, C-6, C-21, C-22	C-5, C-6, C-21, C-22
H-21	C-22, C-23	C-24
Me-23	C-21, C-22, C-24	C-21, C-22, C-24
H _a -25	C-4b, C-6, C-7, C-8, C-26, C-27	C-4b, C-7, C-8, C-26, C-27
H _b -25	C-6, C-7, C-8, C-27	C-6, C-7, C-8, C-26, C-27
H-26	C-4b, C-5, C-7, C-27, C-28	C-4b, C-5, C-7, C-28
Me-28	C-26, C-27, C-29	C-26, C-27, C-29
Me-29	C-26, C-27, C-28	C-26, C-27, C-28

3.2.3 Compound PP5

Compound **PP5** with a molecular formula of $C_{35}H_{42}O_9$ determined by FABMS (m/z 607, $[M+H]^+$) (**Figure 16**) was isolated as a yellow gum. The IR spectrum (**Figure 18**) with absorption bands at 3461 (a hydroxyl group), 1742 (an unconjugated carbonyl group), 1718 (an α,β -unsaturated carbonyl for ester group) and 1634 cm^{-1} (a chelated *ortho*-hydroxyl carbonyl group) and UV absorption band at λ_{max} 364 nm (**Figure 17**) suggested that **PP5** was a caged-polyprenylated xanthone. Its ^1H NMR spectrum (**Figure 19**) (**Table 47**) was similar to that of **PP9** except for one additional *singlet* of a methoxyl group. The presence of the methoxyl group was confirmed by a signal of an oxymethyl carbon at δ_{C} 51.82 in the ^{13}C NMR spectrum (**Figure 20**) (**Table 47**). The HMBC data (**Figure 26**) (**Table 47**) between the methoxy protons (δ_{H} 3.64, 24-OCH₃) and C-24 (δ_{C} 167.53) established the attachment of the methoxyl group at C-24, suggesting that the C-5 substituent was α,β -unsaturated methyl ester, not α,β -unsaturated carboxylic acid. The configuration at C-21/C-22 double bond was found to be the same as that of **PP9** by NOEDIFF experiment since irradiation of the olefinic proton (δ_{H} 6.20, H-21) (**Figure 22**) gave enhancement with the methylene proton (δ_{H} 2.83, H_a-20), not the methyl protons (δ_{H} 1.38, Me-23). The attachment of other substituents were identical to that of **PP9**, according to the HMBC data. Irradiation of the oxymethine proton (δ_{H} 4.55, H-15) (**Figure 23**) enhanced a *singlet* signal of the methyl protons (δ_{H} 1.41, Me-17) and a *doublet* signal of the methyl protons (δ_{H} 1.30, Me-19) whereas irradiation of the methyl protons (δ_{H} 1.47, Me-18) (**Figure 24**) enhanced signals of one of the methylene protons (δ_{H} 2.56, H_b-20) of the

C-5 unsaturated ester unit and the methyl protons (Me-19). These suggested that the relative configurations at C-5 and C-15 in **PP5** were the same as those of **PP9**. Therefore, the structure of **PP5** was assigned as **5**, a new naturally occurring caged-tetraprenylated xanthone with the C-5 methyl 2-butenyl-3-carboxylate unit.



5

Table 47 The NMR data of compound **PP5**

Position	δ_{H} (<i>mult.</i> , J_{Hz})	δ_{C} (C-type)	HMBC correlation
1-OH	13.13 (<i>s</i>)	163.48 (C)	C-1, C-2, C-9a
2		106.10 (C)	
3		166.85 (C)	
4		112.04 (C)	
4a		154.00 (C)	
4b		89.43 (C)	
5		83.55 (C)	
6		201.80 (C=O)	
7		84.90 (C)	

Table 47 (Continued)

Position	δ_{H} (mult., J_{Hz})	δ_{C} (C-type)	HMBC correlation
7-OCH ₃	3.63 (<i>s</i>)	53.99 (CH ₃)	C-7
8	7.58 (<i>s</i>)	135.32 (CH)	C-4b, C-5, C-6, C-8a, C-9
8a		132.08 (C)	
9		177.64 (C=O)	
9a		101.36 (C)	
10	3.21 (<i>d</i> , 7.0)	21.40 (CH ₂)	C-1, C-2, C-3, C-11, C-12
11	5.22 (<i>mt</i> , 7.0)	121.59 (CH)	C-10, C-13, C-14
12		132.08 (C)	
13	1.69 (<i>s</i>)	25.70 (CH ₃)	C-11, C-12, C-14
14	1.75 (<i>s</i>)	17.79 (CH ₃)	C-11, C-12, C-13
15	4.55 (<i>q</i> , 6.5)	91.28 (CH)	C-3, C-4, C-17
16		43.70 (C)	
17	1.41 (<i>s</i>)	28.18 (CH ₃)	C-4, C-15, C-16, C-18
18	1.47 (<i>s</i>)	20.31 (CH ₃)	C-4, C-15, C-16, C-17
19	1.30 (<i>d</i> , 6.5)	16.35 (CH ₃)	C-15, C-16
20	H _a : 2.83 (<i>dd</i> , 15.5 and 6.0) H _b : 2.56 (<i>dd</i> , 15.5 and 10.0)	29.13 (CH ₂)	C-4b, C-5, C-6, C-21, C-22 C-5, C-6, C-21, C-22
21	6.20 (<i>mdd</i> , 10.0 and 6.0)	133.32 (CH)	C-24
22		130.22 (C)	
23	1.38 (<i>s</i>)	11.79 (CH ₃)	C-21, C-22, C-24
24		167.53 (C=O)	
24-OCH ₃	3.64 (<i>s</i>)	51.82 (CH ₃)	C-24
25	H _a : 2.35 (<i>d</i> , 13.0) H _b : 1.69 (<i>dd</i> , 13.0 and 9.5)	30.77 (CH ₂)	C-4b, C-7, C-8, C-26, C-27 C-6, C-8, C-26, C-27
26	2.61 (<i>d</i> , 9.5)	49.85 (CH)	C-4b, C-5, C-7

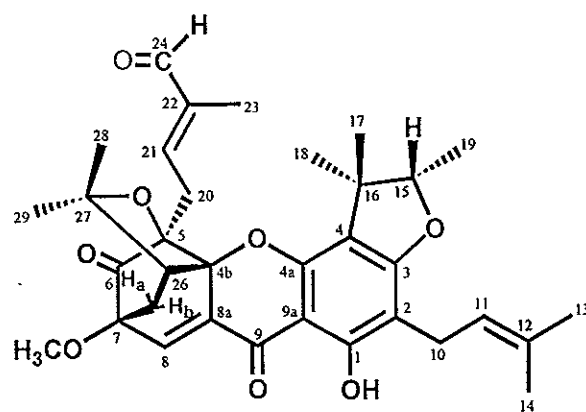
Table 47 (Continued)

Position	δ_{H} (mult., J_{Hz})	δ_{C} (C-type)	HMBC correlation
27		83.64 (C)	
28	1.73 (s)	30.88 (CH ₃)	C-26, C-27, C-29
29	1.30 (s)	28.95 (CH ₃)	C-26, C-27, C-28

3.2.4 Compound PP6

Compound PP6, a yellow gum, was found to have a molecular formula of C₃₄H₄₀O₈ by FABMS (m/z 577, [M+H]⁺) (Figure 27). The IR spectrum (Figure 29) exhibited absorption bands at 3469 (a hydroxyl group), 1743 (an unconjugated carbonyl group), 1690 (an α,β -unsaturated carbonyl group) and 1634 cm⁻¹ (a chelated *ortho*-hydroxyl group). The presence of these carbonyl functionalities was confirmed by the carbon signals in the ¹³C NMR spectrum (Figure 31) (Table 48) at δ 202.05, 194.45 and 177.43. Furthermore, the DEPT spectrum (Figure 32) revealed that the carbon signal at δ 194.45 was an aldehyde carbonyl carbon. The UV absorption band at λ_{max} 360 nm (Figure 28) was similar to that of PP9. These results suggested that PP6 had a caged-polyprenylated xanthone moiety. Its ¹H NMR spectrum (Figure 30) (Table 48) was similar to that of PP9 except for an additional signal of an aldehyde proton at δ 9.23. The formyl group was assigned to be at C-24 due to HMBC data (Figure 37) (Table 48) between the aldehyde proton (δ_{H} 9.23, H-24) and C-21 (δ_{C} 145.53), C-22 (δ_{C} 140.86) and C-23 (δ_{C} 8.75). These suggested the replacement at C-5 of the 3-carboxybut-2-enyl substituent in PP9 with a 2-butenyl-3-carboxaldehyde

unit. Irradiation of the olefinic proton (δ_{H} 6.23, H-21) (**Figure 33**) caused an NOE enhancement of the aldehyde proton (H-24), suggesting that the configuration at the C-21/C-22 double bond was *E*. The attachment of other substituents was identical to that of **PP9**, according to the HMBC data. Irradiation of the methine proton (δ_{H} 4.56, H-15) (**Figure 34**) enhanced signals of the methyl protons at δ_{H} 1.42 (Me-17) and δ_{H} 1.30 (Me-19) whereas irradiation of the methyl protons (δ_{H} 1.45, Me-18) (**Figure 35**) enhanced signals of Me-19 and the methylene protons [δ_{H} 2.89 (H_a-20) and 2.62 (H_b-20)] of the C-5 unsaturated aldehyde unit, indicating that the relative configuration at C-5 and C-15 in **PP6** was the same as **PP9** (H-15 and the C-5 substituent were on β - and α -face, respectively). Thus, the structure of **PP6** was assigned as **6**, a new naturally occurring caged-tetraprenylated xanthone with the C-5 2-butenyl-3-carboxaldehyde unit.



6

Table 48 The NMR data of compound PP6

Position	δ_{H} (<i>mult.</i> , J_{Hz})	δ_{C} (C-type)	HMBC correlation
1-OH	13.08 (<i>s</i>)	163.63 (C)	C-1, C-2, C-3, C-9a
2		106.37 (C)	
3		167.28 (C)	
4		112.17 (C)	
4a		154.06 (C)	
4b		89.57 (C)	
5		83.15 (C)	
6		202.05 (C=O)	
7		84.92 (C)	
7-OCH ₃	3.63 (<i>s</i>)	54.00 (CH ₃)	C-7
8	7.60 (<i>s</i>)	135.90 (CH)	C-4b, C-6, C-9
8a		132.37 (C)	
9		177.43 (C=O)	
9a		101.30 (C)	
10	3.20 (<i>d</i> , 6.5)	21.44 (CH ₂)	C-1, C-2, C-3, C-11, C-12
11	5.21 (<i>t</i> , 6.5)	121.42 (CH)	C-10, C-13, C-14
12		132.12 (C)	
13	1.69 (<i>s</i>)	25.80 (CH ₃)	C-11, C-12, C-14
14	1.75 (<i>s</i>)	17.84 (CH ₃)	C-11, C-12, C-13
15	4.56 (<i>q</i> , 6.5)	91.41 (CH)	C-3, C-4, C-17
16		43.73 (C)	
17	1.42 (<i>s</i>)	28.15 (CH ₃)	C-4, C-15, C-16, C-18
18	1.45 (<i>s</i>)	20.50 (CH ₃)	C-4, C-15, C-16, C-17
19	1.30 (<i>d</i> , 6.5)	16.34 (CH ₃)	C-15, C-16
20	H _a : 2.89 (<i>dd</i> , 15.5 and 5.5)	29.38 (CH ₂)	C-4b, C-5, C-6, C-21, C-22

Table 48 (Continued)

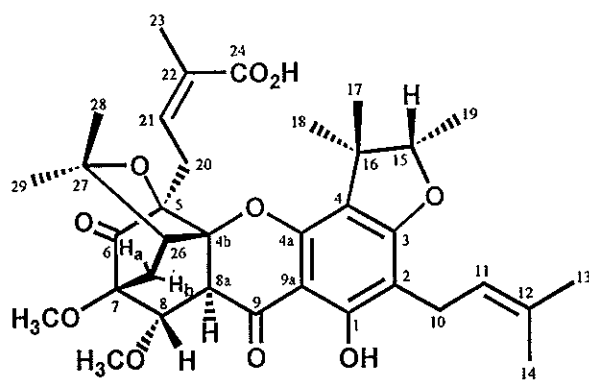
Position	δ_{H} (mult., J_{Hz})	δ_{C} (C-type)	HMBC correlation
	H _b : 2.62 (<i>dd</i> , 15.5 and 8.0)		C-5, C-6, C-21, C-22
21	6.23 (<i>mdd</i> , 8.0 and 5.5)	145.53 (CH)	C-23, C-24
22		140.86 (C)	
23	1.36 (<i>s</i>)	8.75 (CH ₃)	C-21, C-22, C-24
24	9.23 (<i>s</i>)	194.45 (HC=O)	C-21, C-22, C-23
25	H _a : 2.38 (<i>d</i> , 13.0)	30.64 (CH ₂)	C-4b, C-8, C-26, C-27
	H _b : 1.69 (<i>dd</i> , 13.0 and 9.5)		C-6, C-27
26	2.66 (<i>d</i> , 9.5)	49.82 (CH)	C-4b, C-7, C-28
27		84.03 (C)	
28	1.74 (<i>s</i>)	30.96 (CH ₃)	C-26, C-27, C-29
29	1.31 (<i>s</i>)	28.93 (CH ₃)	C-26, C-27, C-28

3.2.5 Compound PP8

Compound PP8 was obtained as a pale yellow gum with a molecular formula of C₃₅H₄₄O₁₀ determined by FABMS (m/z 625, [M+H]⁺) (Figure 38). The IR spectrum (Figure 40) exhibited absorption bands at 3600-2500 (a hydroxyl group of carboxylic acid), 1751 (an unconjugated carbonyl group), 1687 (an α,β -unsaturated carboxyl group) and 1634 cm⁻¹ (a chelated *ortho*-hydroxyl carbonyl group), indicating that PP8 had three carbonyl groups. The carbon signals at δ 205.70, 195.02 and 177.26 in the ¹³C NMR spectrum (Figure 42) (Table 49) confirmed the presence of three carbonyl groups. Although, its UV spectrum (Figure 39) showed an absorption band at lower wavelength (λ_{max} 304 nm) but the ¹H NMR spectrum (Figure 41) (Table 49) showed

characteristic signals of a caged-prenylated moiety, $-\text{OC}(\text{Me})_2\text{-CHCH}_2\text{-C-}$ [δ_{H} 2.70 (*d*, $J=8.8$ Hz, 1H, H-26), 2.02 (*d*, $J=14.2$ Hz, 1H, H_a-25), 1.63 (*dd*, $J=14.2, 8.8$ Hz, 1H, H_b-25), 1.41 (*s*, 3H, Me-28) and 1.20 (*s*, 3H, Me-29)]. Comparison of its ^1H NMR data with those of **PP9** revealed the similar results except for the absence of the olefinic proton signal at the lowest field (δ_{H} 7.61, H-8 in **PP9**), suggesting that **PP8** did not have C-8 double bond. In addition, two additional methine-proton signals [δ_{H} 4.46 (*s*, 1H, H-8) and 3.16 (*s*, 1H, H-8a)] and one additional methoxy-proton signal (δ_{H} 3.36, 3H, 8-OCH₃) were present. The methoxyl group was assigned to be at C-8 due to a HMBC correlation (**Figure 50**) (**Table 49**) between the methoxy protons (8-OCH₃) and C-8 (δ_{C} 75.18), suggesting the 1,4-addition of methanol to the α,β -unsaturated ketone functionality. These corresponded to the ^{13}C NMR and DEPT (**Figure 43**) spectra which showed 16 quaternary carbons, 6 methine carbons, 3 methylene carbons and 10 methyl carbons. The attachment of other substituents was also identical to that of **PP9**, according to the HMBC data. The relative stereochemistry was provided by NOEDIFF experiments. When the oxymethine proton (δ_{H} 4.40, H-15) of the hydrofuran ring was irradiated (**Figure 44**), the *singlet* signal of the methyl protons (δ_{H} 1.43, Me-17) and the *doublet* signal of the methyl protons (δ_{H} 1.34, Me-19) were enhanced, indicating that H-15 was *cis* to Me-17. Irradiation of the methyl protons (δ_{H} 1.10, Me-18) (**Figure 48**) enhanced signals of Me-19, Me-17, the methylene protons (δ_{H} 3.29-3.17, H-20), the olefinic proton (δ_{H} 6.62, H-21) and the methyl protons (δ_{H} 1.98, Me-23) of the C-5 α,β -unsaturated carboxylic acid unit. These indicated that Me-18, Me-19 and the C-5 α,β -unsaturated carboxylic acid unit were located on the same side of the molecule, the α -position.

Therefore, H-15 was on β -position. The configuration at C-21/C-22 double bond was assigned to be *Z* by enhancement of H-21 after irradiation of Me-23 (**Figure 46**). Irradiation of the methylene proton (δ_{H} 1.63, H_b-25) (**Figure 47**) enhanced signals of the methine proton (δ_{H} 2.70, H-26), the methylene proton (δ_{H} 2.02, H_a-25) and the oxymethine proton (δ_{H} 4.46, H-8) but did not affect the signals of the methoxy protons (δ_{H} 3.36, 8-OCH₃) and the methine proton (δ_{H} 3.16, H-8a). In addition, irradiation of H-8a (**Figure 45**) enhanced signals of H-8, 8-OCH₃ and H-21 of the C-5 3-carboxybut-2-enyl substituent. These results indicated that H-8 and H-8a were *trans* and located on β - and α -position, respectively. Therefore, **PP8** had the structure **7**, a new caged-tetraprenylated xanthone. Compound **PP8** might be derived from **PP9** by addition of methanol to C-8 double bond. The lack of this α,β -unsaturated carbonyl functional group might affect the absorption maximum in the UV spectrum.



7

Table 49 The NMR data of compound PP8

Position	δ_{H} (<i>mult.</i> , J_{Hz})	δ_{C} (C-type)	HMBC correlation
1-OH	12.08 (<i>s</i>)	161.59 (C)	C-1, C-2, C-3, C-9a
2		105.35 (C)	
3		166.84 (C)	
4		113.67 (C)	
4a		152.17 (C)	
4b		86.33 (C)	
5		87.06 (C)	
6		205.70 (C=O)	
7		81.37 (C)	
7-OCH ₃	3.50 (<i>s</i>)	52.38 (CH ₃)	C-7
8	4.46 (<i>s</i>)	75.19 (CH)	C-5, C-6, C-7, 8-OCH ₃ , C-8a, C-9, C-25
8-OCH ₃	3.36 (<i>s</i>)	57.38 (CH ₃)	C-8
8a	3.16 (<i>s</i>)	48.84 (CH)	C-5, C-7, C-8, C-9, C-26
9		195.02 (C=O)	
9a		102.40 (C)	
10	3.26-3.17 (<i>m</i>)	21.42 (CH ₂)	C-1, C-2, C-3, C-11, C-12
11	5.25 (<i>mt</i> , 7.0)	121.56 (CH)	C-10, C-13, C-14
12		132.14 (C)	
13	1.69 (<i>s</i>)	25.76 (CH ₃)	C-2, C-11, C-12, C-14
14	1.76 (<i>s</i>)	17.71 (CH ₃)	C-2, C-11, C-12, C-13
15	4.40 (<i>q</i> , 6.8)	90.18 (CH)	C-3, C-4, C-16, C-17, C-18
16		43.92 (C)	
17	1.43 (<i>s</i>)	26.08 (CH ₃)	C-4, C-15, C-16, C-18
18	1.10 (<i>s</i>)	22.06 (CH ₃)	C-15, C-16, C-17
19	1.34 (<i>d</i> , 6.8)	13.82 (CH ₃)	C-15, C-16

Table 49 (Continued)

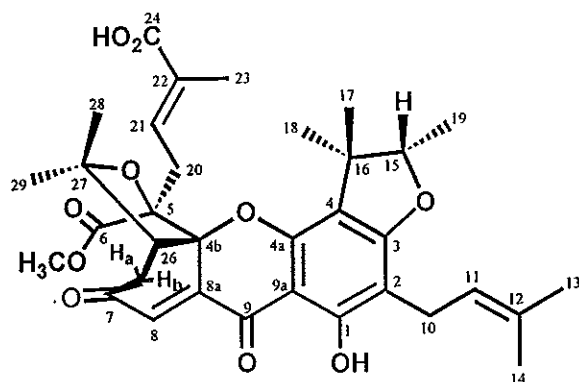
Position	δ_{H} (mult., J_{Hz})	δ_{C} (C-type)	HMBC correlation
20	3.29-3.17 (<i>m</i>)	28.56 (CH ₂)	C-4b, C-5, C-6, C-21, C-22, C-24
21	6.62 (<i>qt</i> , 6.8 and 1.5)	139.31 (CH)	C-5, C-6, C-23, C-24
22		127.36 (C)	
23	1.98 (<i>d</i> , 1.5)	20.72 (CH ₃)	C-21, C-22, C-24
24		172.26 (C=O)	
25	H _a : 2.02 (<i>d</i> , 14.2)	23.98 (CH ₂)	C-5, C-7, C-8, C-26, C-27
	H _b : 1.63 (<i>dd</i> , 14.2 and 8.8)		C-7, C-8, C-26, C-27
26	2.70 (<i>d</i> , 8.8)	45.26 (CH)	C-4b, C-5, C-7, C-25, C-28
27		82.35 (C)	
28	1.41 (<i>s</i>)	30.49 (CH ₃)	C-26, C-27, C-29
29	1.20 (<i>s</i>)	27.16 (CH ₃)	C-25, C-26, C-27, C-28

3.2.6 Compound PP10

Compound PP10, a yellow gum, was found to have a molecular formula of C₃₄H₄₀O₁₀ by EIMS (m/z 608) (Figure 51). The IR spectrum (Figure 53) exhibited absorption bands at 3600-3500 (a hydroxyl group of a carboxylic acid), 1753 (a carbonyl of ester group), 1690 (α,β -unsaturated carbonyl groups) and 1640 cm⁻¹ (a chelated *ortho*-hydroxyl carbonyl group). The presence of four carbonyl functionalities was confirmed by the signals at δ 197.00, 182.07, 171.31 and 170.60 in the ¹³C NMR spectrum (Figure 55) (Table 50). Compound PP10 had one carbonyl group more than PP9. Its UV absorption band at λ_{max} 368 nm (Figure 52) was due to a conjugated carbonyl chromophore. The ¹H NMR spectrum (Figure 54) (Table 50)

showed signals of one chelated hydroxy proton (δ_{H} 12.69, *s*, 1-OH), one olefinic proton (δ_{H} 6.62, *s*, H-8), one methoxyl group (δ_{H} 3.63, *s*, 6-OCH₃), one unit of a 3-methylbut-2-enyl group [δ_{H} 5.21 (*mt*, $J=7.5$ Hz, 1H, H-11), 3.22 (*d*, $J=7.5$ Hz, 2H, H-10), 1.75 (*s*, 3H, Me-14) and 1.69 (*s*, 3H, Me-13)], one unit of a 3-carboxybut-2-enyl group [δ_{H} 6.67 (*mt*, $J=7.5$ Hz, 1H, H-21), 2.79 (*dd*, $J=15.0, 7.5$ Hz, 1H, H_a-20), 2.69 (*dd*, $J=15.0, 7.5$ Hz, 1H, H_b-20) and 1.67 (*s*, 3H, Me-23)], one unit of a 2,3,3-trimethylhydrofuran ring [δ_{H} 4.37 (*q*, $J=6.5$ Hz, 1H, H-15), 1.42 (*s*, 3H, Me-17), 1.41 (*d*, $J=6.5$ Hz, 1H, Me-19) and 1.27 (*s*, 3H, Me-18)] and one unit of -OC(Me)₂-CHCH₂-C- [δ_{H} 3.17 (*dd*, $J=13.0, 7.0$ Hz, 1H, H-26), 2.94 (*dd*, $J=16.5, 13.0$ Hz, 1H, H_a-25), 2.62 (*dd*, $J=16.5, 7.0$ Hz, 1H, H_b-25), 1.76 (*s*, 3H, Me-28) and 1.45 (*s*, 3H, Me-29)]. The ¹³C NMR, DEPT (Figure 56) and HMQC (Figure 60) spectra showed resonances for 17 quaternary carbons, 5 methine carbons, 3 methylene carbons and 9 methyl carbons. The 3-methylbut-2-enyl group was assigned to be located on C-2 (δ_{C} 106.44) since its methylene protons (H-10) showed the correlations with C-1 (δ_{C} 162.94), C-2 and C-3 (δ_{C} 167.95) in the HMBC spectrum (Figure 61) (Table 50). Both Me-17 and Me-18 of the 2,3,3-trimethylhydrofuran ring showed the HMBC correlations with C-4 (δ_{C} 112.66) and C-4a (δ_{C} 152.92), suggesting the attachment of its *gem*-dimethyl carbon and ring oxygen atom on C-4 and C-3, respectively. The chemical-shift values of C-3 and C-4 in the ¹³C NMR spectrum supported these conclusions. The methoxyl group was connected to the carbonyl carbon at δ 171.31 (C-6) based on a correlation between the methoxy protons and C-6, indicating the presence of the methyl ester group. Both the methyl ester group and the 3-carboxybut-2-enyl group were attached on the same oxyquaternary carbon (δ 93.81, C-5) due to

the HMBC correlations of the methylene proton (H_b -20) of the side chain with C-5 and C-6. The HMBC correlation of the methylene protons (H-25) with the carbonyl carbon at δ 197.00 revealed that C-7 was a carbonyl carbon. One of these methylene protons (H_b -25) also showed a 3J correlation only with an oxyquaternary carbon (δ_C 90.62, C-4b) but did not correlate with C-6. These suggested bond cleavage between C-6 and C-7 in the structure of **PP9**. Both C-6 and C-7 in **PP9** became a carbonyl carbon in **PP10**. The remaining olefinic proton (δ_H 6.62), which was directly attached to C-8 (δ_C 128.55) in the HMQC spectrum, was attributed to H-8 according to its 3J HMBC correlations with a quaternary carbon (C-4b) and a carbonyl carbon (δ_C 182.07, C-9). The relative stereochemistry was provided by NOEDIFF results. The NOE enhancement between the oxymethine proton (H-15) and Me-17 and Me-19 of the 2,3,3-trimethylhydrofuran ring (**Figure 58**) and between Me-18 and Me-19 and the methylene proton (H_b -20) of the C-5 3-carboxybut-2-enyl unit (**Figure 59**) suggested that H-15 and the C-5 side chain were at β - and α -position, respectively, the same as **PP9**. The configuration of C-21/C-22 double bond of the C-5 substituent was found to be *E* since irradiation of the olefinic proton (H-21) (**Figure 57**) did not show the NOE enhancement with the methyl protons (Me-23). Thus, **PP10** had cleavaged structure **8**, a new degraded tetraprenylated xanthone.



8

Table 50 The NMR data of compound PP10

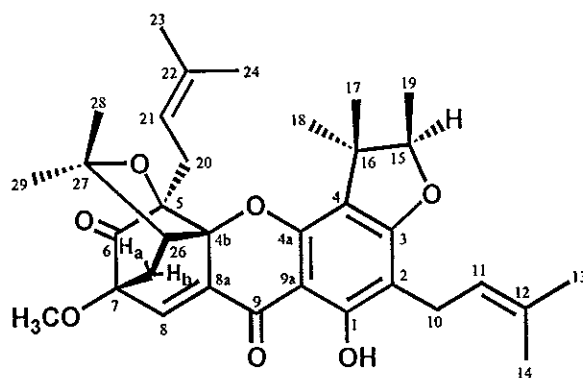
Position	δ_{H} (<i>mult.</i> , J_{Hz})	δ_{C} (C-type)	HMBC correlation
1-OH	12.69 (<i>s</i>)	162.94 (C)	C-1, C-2, C-9a
2		106.44 (C)	
3		167.95 (C)	
4		112.66 (C)	
4a		152.92 (C)	
4b		90.62 (C)	
5		93.81 (C)	
6		171.31 (C=O)	
6-OCH ₃	3.63 (<i>s</i>)	52.29 (CH ₃)	C-6
7		197.00 (C=O)	
8	6.62 (<i>s</i>)	128.55 (CH)	C-4b, C-9
8a		145.85 (C)	
9		182.07 (C=O)	
9a		102.83 (C)	
10	3.22 (<i>d</i> , 7.5)	21.45 (CH ₂)	C-1, C-2, C-3, C-11, C-12

Table 50 (Continued)

Position	δ_{H} (<i>mult.</i> , J_{Hz})	δ_{C} (C-type)	HMBC correlation
11	5.21 (<i>mt</i> , 7.5)	121.32 (CH)	C-13, C-14
12		132.37 (C)	
13	1.69 (<i>s</i>)	25.78 (CH ₃)	C-11, C-12, C-14
14	1.75 (<i>s</i>)	17.74 (CH ₃)	C-11, C-12, C-13
15	4.37 (<i>q</i> , 6.5)	90.64 (CH)	C-17, C-18
16		43.46 (C)	
17	1.42 (<i>s</i>)	24.40 (CH ₃)	C-4, C-4a, C-15, C-16, C-18
18	1.27 (<i>s</i>)	21.06 (CH ₃)	C-4, C-4a, C-15, C-16, C-17
19	1.41 (<i>d</i> , 6.5)	13.72 (CH ₃)	C-4, C-15, C-16, C-18
20	H _a : 2.79 (<i>dd</i> , 15.0 and 7.5) H _b : 2.69 (<i>dd</i> , 15.0 and 7.5)	35.89 (CH ₂)	C-5, C-21, C-22 C-5, C-6, C-21, C-22
21	6.67 (<i>mt</i> , 7.5)	137.11 (CH)	C-23, C-24
22		130.32 (C)	
23	1.67 (<i>s</i>)	12.46 (CH ₃)	C-21, C-22, C-24
24		170.60 (C=O)	
25	H _a : 2.94 (<i>dd</i> , 16.5 and 13.0) H _b : 2.62 (<i>dd</i> , 16.5 and 7.0)	38.27 (CH ₂)	C-7, C-26, C-27 C-4b, C-7, C-26
26	3.17 (<i>dd</i> , 13.0 and 7.0)	55.88 (CH)	C-4b, C-5, C-28
27		85.12 (C)	
28	1.76 (<i>s</i>)	31.21 (CH ₃)	C-26, C-27, C-29
29	1.45 (<i>s</i>)	25.43 (CH ₃)	C-26, C-27, C-28

3.2.7 Compound PP2

Compound **PP2** was obtained as a yellow solid, melting at 152.6-154.8°C. The IR spectrum (**Figure 63**) exhibited absorption bands at 3454 (a hydroxyl group), 1745 (an unconjugated carbonyl group) and 1634 cm^{-1} (a chelated *ortho*-hydroxyl carbonyl group), indicating that **PP2** had two carbonyl groups. Its UV spectrum (**Figure 62**) showed an absorption band at λ_{max} 362 nm due to a conjugated carbonyl chromophore. Compound **PP2** was identified as scortechinone A (**1**), which was previously isolated from the twigs of *G. scortechinii* (Rukachaisirikul, 2000a), by comparison of its ^1H NMR data (**Figure 64**) (**Table 51**) and co-chromatography with scortechinone A (**1**).



1

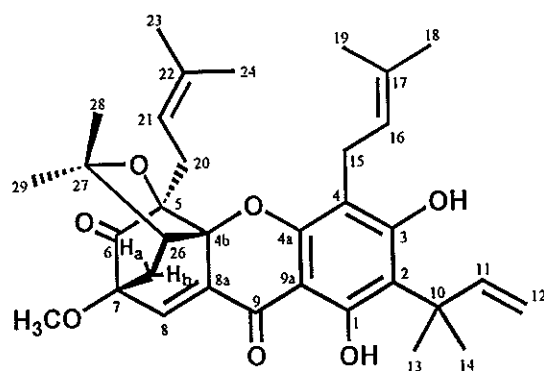
Table 51 The ^1H NMR data of scortechinone A and PP2

Position	Scortechinone A (δ_{H})	PP2 (δ_{H})
1-OH	13.15 (<i>s</i> , 1H)	13.19 (<i>s</i> , 1H)
7-OCH ₃	3.62 (<i>s</i> , 3H)	3.63 (<i>s</i> , 3H)
H-8	7.49 (<i>d</i> , $J=1.4$ Hz, 1H)	7.51 (<i>d</i> , $J=1.5$ Hz, 1H)
H-10	3.22 (<i>d</i> , $J=7.2$ Hz, 2H)	3.27-3.17 (<i>m</i> , 2H)
H-11	5.22 (<i>ht</i> , $J=7.2, 1.4$ Hz, 1H)	5.22 (<i>ht</i> , $J=7.0, 1.5$ Hz, 1H)
Me-13	1.68 (<i>brq</i> , $J=1.2$ Hz, 3H)	1.68 (<i>brs</i> , 3H)
Me-14	1.75 (<i>brq</i> , $J=1.2$ Hz, 3H)	1.75 (<i>brs</i> , 3H)
H-15	4.37 (<i>q</i> , $J=6.4$ Hz, 1H)	4.38 (<i>q</i> , $J=7.0$ Hz, 1H)
Me-17	1.16 (<i>s</i> , 3H)	1.16 (<i>s</i> , 3H)
Me-18	1.58 (<i>s</i> , 3H)	1.58 (<i>s</i> , 3H)
Me-19	1.41 (<i>d</i> , $J=6.4$ Hz, 3H)	1.41 (<i>d</i> , $J=7.0$ Hz, 3H)
H _a -20	2.79 (<i>ddh</i> , $J=14.4, 4.5, 1.5$ Hz, 1H)	2.69 (<i>md</i> , $J=14.5$ Hz, 1H)
H _b -20	2.55 (<i>dd</i> , $J=14.4, 10.5$ Hz, 1H)	2.56 (<i>dd</i> , $J=14.5, 10.0$ Hz, 1H)
H-21	4.41-4.37 (<i>m</i> , 1H)	4.41-4.36 (<i>m</i> , 1H)
Me-23	1.36 (<i>bri</i> , $J=1.5$ Hz, 3H)	1.36 (<i>brs</i> , 3H)
Me-24	1.07 (<i>bri</i> , $J=1.4$ Hz, 3H)	1.06 (<i>brs</i> , 3H)
H _a -25	2.33 (<i>dd</i> , $J=12.8, 1.4$ Hz, 1H)	2.33 (<i>brd</i> , $J=13.0$ Hz, 1H)
H _b -25	1.65 (<i>dd</i> , $J=12.8, 9.6$ Hz, 1H)	1.65 (<i>dd</i> , $J=13.0, 9.5$ Hz, 1H)
H-26	2.55 (<i>d</i> , $J=9.6$ Hz, 1H)	2.56 (<i>d</i> , $J=9.5$ Hz, 1H)
Me-28	1.71 (<i>s</i> , 3H)	1.71 (<i>s</i> , 3H)
Me-29	1.29 (<i>s</i> , 3H)	1.29 (<i>s</i> , 3H)

3.2.8 Compound PP1

Compound **PP1**, a yellow gum, was found to have a molecular formula of $C_{34}H_{42}O_7$ determined by EIMS spectrum (Figure 65) which showed a molecular ion at m/z 534 for $[M-28]^+$. The IR spectrum (Figure 67) exhibited absorption bands at 3397 (a hydroxyl group), 1746 (an unconjugated carbonyl group) and 1634 cm^{-1} (a chelated *ortho*-hydroxyl carbonyl group), indicating that **PP1** had two carbonyl groups, the same as scortechinone A. The presence of these carbonyl functionalities was confirmed by the signals at δ 201.96 and 179.09 in the ^{13}C NMR spectrum (Figure 69) (Table 53). The UV absorption band at λ_{max} 361 nm (Figure 66) was similar to that of scortechinone A. These results suggested that **PP1** had a caged-polyprenylated xanthone moiety. Comparison of its 1H NMR spectrum (Figure 68) (Table 52) with that of scortechinone A revealed the similar results (a caged-polyprenylated xanthone with two isoprene groups) except for the absence of an oxymethine proton and a secondary methyl group of a hydrofuran ring. Additional signals were observed: a *singlet* signal at δ 7.70 of a hydroxyl group and characteristic signals of a 1,1-dimethylallyl group [δ_H 6.43 (*dd*, $J=17.5, 10.5$ Hz, 1H, H-11), 5.46 (*d*, $J=17.5$ Hz, 1H, H_a-12), 5.37 (*dd*, $J=10.5, 1.0$ Hz, 1H, H_b-12), 1.60 (*s*, 3H, Me-13) and 1.59 (*s*, 3H, Me-14)]. The additional hydroxyl group was assigned to be at C-3 (δ_C 163.32) by its HMBC correlations (Figure 73) (Table 54) with C-2 (δ_C 111.62), C-3, C-4 (δ_C 108.18) and C-4a (δ_C 156.27). Both methyl-proton signals (Me-13 and Me-14) of the 1,1-dimethylallyl group showed a HMBC correlation with C-2, suggesting the attachment of this group at C-2. Irradiation of the olefinic proton (H-11) of the 1,1-dimethylallyl group (Figure 71) caused an NOE enhancement of the olefinic proton at

δ_{H} 5.37 (H_b-12), indicating that H-11 was *cis* to H_b-12. One of two isoprenyl groups [δ_{H} 5.14 (*mt*, $J=6.5$ Hz, 1H, H-16), 3.30 (*d*, $J=6.5$ Hz, 2H, H-15), 1.70 (*s*, 3H, Me-19) and 1.66 (*d*, $J=1.0$ Hz, 3H, Me-18)] was assigned to be at C-4 by the HMBC correlations of its methylene proton (H-15) with C-3, C-4 and C-4a. Furthermore, the HMBC data established the identical attachment of remaining substituents (the C-5 isoprenyl group and 7-OCH₃) to that of scortechinone A. Thus, PP1 had the structure **9**, a new caged-tetraprenylated xanthone with the uncyclized isoprenyl unit at C-4.



9

Table 52 The ¹H NMR data of scortechinone A and PP1

Position	Scortechinone A (δ_{H})	PP1 (δ_{H})
1-OH	13.15 (<i>s</i> , 1H)	13.62 (<i>s</i> , 1H)
3-OH	-	7.70 (<i>s</i> , 1H)
7-OCH ₃	3.62 (<i>s</i> , 3H)	3.63 (<i>s</i> , 3H)
H-8	7.49 (<i>d</i> , $J=1.4$ Hz, 1H)	7.48 (<i>d</i> , $J=1.0$ Hz, 1H)
H-10	3.22 (<i>d</i> , $J=7.2$ Hz, 2H)	-
H-11	5.22 (<i>ht</i> , $J=7.2, 1.4$ Hz, 1H)	6.43 (<i>dd</i> , $J=17.5, 10.5$ Hz, 1H)

Table 52 (Continued)

Position	Scortechinone A (δ_{H})	PP1 (δ_{H})
H _a -12	-	5.46 (<i>d</i> , $J=17.5$ Hz, 1H)
H _b -12	-	5.37 (<i>dd</i> , $J=10.5, 1.0$ Hz, 1H)
Me-13	1.68 (<i>brq</i> , $J=1.2$ Hz, 3H)	1.60 (<i>s</i> , 3H)
Me-14	1.75 (<i>brq</i> , $J=1.2$ Hz, 3H)	1.59 (<i>s</i> , 3H)
H-15	4.37 (<i>q</i> , $J=6.4$ Hz, 1H)	3.30 (<i>d</i> , $J=6.5$ Hz, 2H)
H-16	-	5.14 (<i>mt</i> , $J=6.5$ Hz, 1H)
Me-17	1.16 (<i>s</i> , 3H)	-
Me-18	1.58 (<i>s</i> , 3H)	1.66 (<i>d</i> , $J=1.0$ Hz, 3H)
Me-19	1.41 (<i>d</i> , $J=6.4$ Hz, 3H)	1.70 (<i>s</i> , 3H)
H _a -20	2.79 (<i>ddh</i> , $J=14.4, 4.5, 1.5$ Hz, 1H)	2.62-2.56 (<i>m</i> , 1H)
H _b -20	2.55 (<i>dd</i> , $J=14.4, 10.5$ Hz, 1H)	2.54 (<i>d</i> , $J=10.0$ Hz, 1H)
H-21	4.41-4.37 (<i>m</i> , 1H)	4.43 (<i>mdd</i> , $J=10.0, 5.5$ Hz, 1H)
Me-23	1.36 (<i>brt</i> , $J=1.5$ Hz, 3H)	1.37 (<i>s</i> , 3H)
Me-24	1.07 (<i>brt</i> , $J=1.4$ Hz, 3H)	1.01 (<i>s</i> , 3H)
H _a -25	2.33 (<i>dd</i> , $J=12.8, 1.4$ Hz, 1H)	2.33 (<i>d</i> , $J=13.0$ Hz, 1H)
H _b -25	1.65 (<i>dd</i> , $J=12.8, 9.6$ Hz, 1H)	1.61 (<i>dd</i> , $J=13.0, 10.0$ Hz, 1H)
H-26	2.55 (<i>d</i> , $J=9.6$ Hz, 1H)	2.50 (<i>d</i> , $J=10.0$ Hz, 1H)
Me-28	1.71 (<i>s</i> , 3H)	1.65 (<i>s</i> , 3H)
Me-29	1.29 (<i>s</i> , 3H)	1.28 (<i>s</i> , 3H)

Table 53 The ^{13}C NMR data of scortechinone A and PP1

Position	C-type	Scortechinone A (δ_{C})	PP1 (δ_{C})
1-OH	C	163.26	162.86
2	C	105.77	111.62
3	C	166.87	163.32
4	C	113.03	108.18
4a	C	153.82	156.27
4b	C	89.30	88.68
5	C	84.19	84.20
6	C=O	202.26	201.96
7	C	84.90	84.81
7-OCH ₃	CH ₃	54.94	53.95
8	CH	133.96	134.02
8a	C	132.38	132.35
9	C=O	178.23	179.09
9a	C	101.39	100.95
10	CH ₂	21.42	-
	C	-	40.96
11	CH	121.75	149.53
12	C	131.98	-
	CH ₂	-	113.69
13	CH ₃	25.70	27.16*
14	CH ₃	17.73	26.90*
15	CH	90.61	-
	CH ₂	-	22.16
16	C	43.47	-
	CH	-	122.36

Table 53 (Continued)

Position	C-type	Scortechinone A (δ_c)	PP1 (δ_c)
17	CH ₃	21.07	-
	C	-	132.31
18	CH ₃	24.06	25.66
19	CH ₃	13.57	18.07
20	CH ₂	28.93	28.82
21	CH	117.17	117.54
22	C	135.59	135.27
23	CH ₃	25.47	25.54
24	CH ₃	16.87	16.69
25	CH ₂	30.85	30.24
26	CH	49.94	49.71
27	C	83.23	83.53
28	CH ₃	30.78	30.07
29	CH ₃	28.97	29.01

* interchangeable

Table 54 The HMBC correlations of scortechinone A and PP1

Proton	Scortechinone A (Carbon)	PP1 (Carbon)
1-OH	C-1, C-2, C-3, C-9, C-9a	C-1, C-2, C-9a
3-OH	-	C-2, C-3, C-4, C-4a
7-OCH ₃	C-7	C-7
H-8	C-4b, C-6, C-7, C-8a, C-9, C-25	C-4b, C-6, C-8a, C-9
H-10	C-1, C-2, C-3, C-11, C-12	-

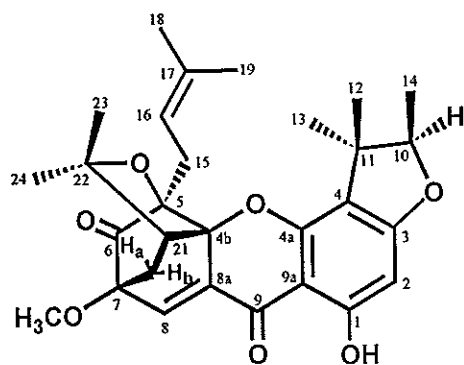
Table 54 (Continued)

Proton	Scortechinone A (Carbon)	PP1 (Carbon)
H-11	C-10, C-13, C-14	C-10, C-14
H _a -12	-	C-10, C-11
H _b -12	-	C-10
Me-13	C-11, C-12, C-14	C-2, C-10, C-14
Me-14	C-11, C-12, C-13	C-2, C-10
H-15	C-3, C-4, C-16, C-17, C-18, C-19	C-3, C-4, C-4a, C-16, C-17
H-16	-	C-15, C-18, C-19
Me-17	C-4, C-15, C-16, C-18	-
Me-18	C-4, C-15, C-16, C-17	C-16, C-17, C-19
Me-19	C-15, C-16	C-16, C-17, C-18
H _a -20	C-4b, C-5, C-6, C-21, C-22	C-4b, C-5, C-6, C-22
H _b -20	C-4b, C-5, C-6, C-21, C-22	C-4b, C-5, C-6, C-22
H-21	C-22, C-23, C-24	-
Me-23	C-21, C-22, C-24	C-21, C-22, C-24
Me-24	C-21, C-22, C-23	C-21, C-22, C-23
H _a -25	C-4b, C-6, C-7, C-8, C-26, C-27	C-4b, C-7, C-8, C-26, C-27
H _b -25	C-6, C-7, C-8, C-27	C-7, C-26
H-26	C-4b, C-5, C-7, C-28	C-4b, C-28
Me-28	C-26, C-27, C-29	C-26, C-29
Me-29	C-26, C-27, C-28	C-26, C-27

3.2.9 Compound PP3

Compound **PP3** with a molecular formula of $C_{29}H_{34}O_7$ by FABMS (m/z 495, $[M+H]^+$) (**Figure 74**), was isolated as a yellow solid, melting at 176.8-177.9°C. The IR spectrum (**Figure 76**) showed the absorption bands at 1744 (an unconjugated carbonyl group) and 1640 cm^{-1} (a chelated *ortho*-hydroxyl carbonyl group). Carbon signals at δ 202.07 and 178.25 in the ^{13}C NMR spectrum (**Figure 78**) (**Table 55**) supported IR spectral data. An absorption band of a hydroxyl group was also observed at 3461 cm^{-1} . Its UV spectrum (**Figure 75**) showed two absorption bands at λ_{max} 333 and 360 nm. The caged structure was evident by characteristic signals of $-OC(Me)_2-CHCH_2-C-$ unit [δ_H 2.59 (*d*, $J=9.5$ Hz, 1H, H-21), 2.36 (*d*, $J=13.0$ Hz, 1H, H_a-20), 1.72 (*s*, 3H, Me-23), 1.66 (*dd*, $J=13.0, 9.5$ Hz, 1H, H_b-20) and 1.30 (*s*, 3H, Me-24)] in the 1H NMR spectrum (**Figure 77**) (**Table 55**). Furthermore, the 1H NMR spectrum showed signals of one chelated hydroxy proton (δ_H 13.03, *s*, 1-OH), two olefinic protons [δ_H 7.52 (*d*, $J=1.5$ Hz, 1H, H-8) and 6.04 (*s*, 1H, H-2)], one methoxyl group (δ_H 3.64, *s*, 7-OCH₃), one unit of a 3-methylbut-2-enyl group [δ_H 4.38 (*md*, $J=10.5$ Hz, 1H, H-16), 2.71 (*md*, $J=14.5$ Hz, 1H, H_a-15), 2.58 (*dd*, $J=14.5, 10.5$ Hz, 1H, H_b-15), 1.38 (*brs*, 3H, Me-18) and 1.09 (*brs*, 3H, Me-19)] and one unit of a 2,3,3-trimethylhydrofuran ring [δ_H 4.40 (*q*, $J=6.5$ Hz, 1H, H-10), 1.59 (*s*, 3H, Me-13), 1.41 (*d*, $J=6.5$ Hz, 3H, Me-14) and 1.17 (*s*, 3H, Me-12)]. The ^{13}C NMR, DEPT (**Figure 79**) and HMQC (**Figure 81**) spectra showed resonances for 14 quaternary carbons, 5 methine carbons, 2 methylene carbons and 8 methyl carbons. In the HMBC spectrum (**Figure 82**) (**Table 55**), the chelated hydroxy proton (δ_H 13.03, 1-OH) showed a

correlation with a methine aromatic carbon at δ 92.75 (C-2) which correlated to the aromatic proton (δ_{H} 6.04, H-2) in the HMQC spectrum. In addition, H-2 showed cross peaks with C-1 (δ_{C} 166.22), C-3 (δ_{C} 168.68) and C-4 (δ_{C} 113.68). Two methyl-proton signals (Me-12 and Me-13) of the 2,3,3-trimethylhydrofuran ring showed the HMBC correlation with C-4, suggesting the attachment of this group at C-3 and C-4. The chemical-shift values of C-3 and C-4 confirmed that the hydrofuran ring was fused to the aromatic ring by linkage of its *gem*-dimethyl carbon and ring oxygen atom with C-4 and C-3, respectively. The olefinic proton at δ 7.52, which correlated to an olefinic carbon at δ 134.37 in the HMQC spectrum, showed the HMBC correlations with C-4b (δ_{C} 89.54), C-6 (δ_{C} 202.08) and C-9 (δ_{C} 178.25). These data established its location at C-8. The methoxyl group (δ_{H} 3.64) was placed at C-7 (δ_{C} 84.92) according to a correlation between its protons with C-7. The HMBC correlations of the methylene protons [δ_{H} 2.71 (H_a-15) and 2.58 (H_b-15)] of the 3-methylbut-2-enyl group with C-4b, C-5 (δ_{C} 84.23) and C-6 established the attachment of this prenyl group at C-5. The relative stereochemistry of **PP3** was established by NOEDIFF results. The methyl protons (Me-13) of the hydrofuran ring gave NOE enhancement with the methine proton (H-10), the methylene proton (H_b-15) and the methyl protons (Me-19) (**Figure 80**). These results indicated that the C-5 prenyl group was located on the same side, the α side of the molecule, as Me-13 and H-10. Thus, **PP3** had the structure **10**, a new caged-triprenylated xanthone without a C-2 isoprenyl substituent.



10

Table 55 The NMR data of compound PP3

Position	δ_{H} (<i>mult.</i> , J_{Hz})	δ_{C} (C-type)	HMBC correlation
1-OH	13.03 (<i>s</i>)	166.22 (C)	C-1, C-2, C-3, C-9a
2	6.04 (<i>s</i>)	92.75 (CH)	C-1, C-3, C-4, C-9a
3		168.68 (C)	
4		113.68 (C)	
4a		155.82 (C)	
4b		89.54 (C)	
5		84.23 (C)	
6		202.08 (C=O)	
7		84.92 (C)	
7-OCH ₃	3.64 (<i>s</i>)	53.99 (CH ₃)	C-7
8	7.52 (<i>d</i> , 1.5)	134.37 (CH)	C-4b, C-5, C-6, C-8a, C-9, C-21
8a		132.02 (C)	
9		178.25 (C=O)	
9a		101.42 (C)	
10	4.40 (<i>q</i> , 6.5)	91.05 (CH)	C-11, C-12, C-13
11		43.16 (C)	

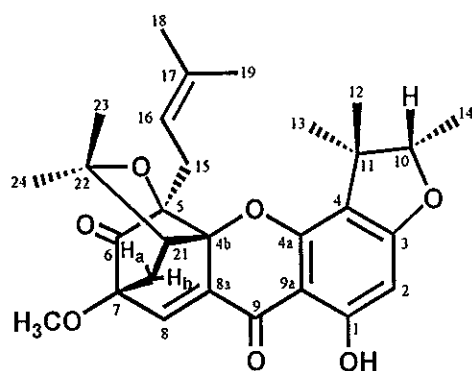
Table 55 (Continued)

Position	δ_{H} (<i>mult.</i> , J_{Hz})	δ_{C} (C-type)	HMBC correlation
12	1.17 (<i>s</i>)	21.04 (CH ₃)	C-4, C-10, C-11, C-13, C-14
13	1.59 (<i>s</i>)	23.87 (CH ₃)	C-4, C-10, C-11, C-12
14	1.41 (<i>d</i> , 6.5)	13.48 (CH ₃)	C-10, C-11
15	H _a : 2.71 (<i>md</i> , 14.5) H _b : 2.58 (<i>dd</i> , 14.5 and 10.5)	28.99 (CH ₂)	C-4b, C-5, C-16, C-17 C-4b, C-5, C-6, C-16, C-17
16	4.38 (<i>md</i> , 10.5)	117.31 (CH)	
17		135.69 (C)	
18	1.38 (<i>brs</i>)	25.55 (CH ₃)	C-16, C-17, C-19
19	1.09 (<i>brs</i>)	16.90 (CH ₃)	C-16, C-17, C-18
20	H _a : 2.36 (<i>d</i> , 13.0) H _b : 1.66 (<i>dd</i> , 13.0 and 9.5)	30.80 (CH ₂)	C-4b, C-7, C-8, C-21, C-22 C-6, C-7, C-8, C-21, C-22
21	2.59 (<i>d</i> , 9.5)	49.93 (CH)	C-4b, C-5, C-6, C-20, C-23
22		83.29 (C)	
23	1.72 (<i>s</i>)	30.79 (CH ₃)	C-21, C-22
24	1.30 (<i>s</i>)	29.01 (CH ₃)	C-20, C-21, C-22, C-23

3.2.10 Compound PP4

Compound PP4 was obtained as a yellow solid, melting at 188.9-190.0°C. It showed the same molecular formula as PP3. In addition, its IR (Figure 85) and UV (Figure 84) spectra were almost identical to those of PP3. Surprisingly, ¹H NMR and ¹³C NMR signals observed in the NMR spectra of PP3 (Figures 86 and 87) (Table 56) and PP4 were alike except for chemical-shift values of ¹H and ¹³C signals of a

2,3,3-trimethylhydrofuran unit. The attachment of all substituents was found to be identical to **PP3** according to the HMBC data (Figure 92) (Table 56). The NOE enhancement observed between the methine proton (δ_{H} 4.55, H-10) and the methyl protons (δ_{H} 1.42, Me-12) (Figure 89) and between the methyl protons (δ_{H} 1.49, Me-13) and the methylene proton (δ_{H} 2.55, H_b-15) of the C-5 prenyl group (Figure 90) suggested that H-10 was at β -position, which was opposite to that of **PP3**. Therefore, **PP4** had the structure 11, a new naturally occurring caged-triprenylated xanthone of which the structure differed from **PP3** in the stereochemistry of C-10.



11

Table 56 The NMR data of compound **PP4**

Position	δ_{H} (<i>mult.</i> , J_{Hz})	δ_{C} (C-type)	HMBC correlation
1-OH	13.09 (<i>s</i>)	166.37 (C)	C-1, C-2, C-3, C-9a
2	6.03 (<i>s</i>)	92.80 (CH)	C-1, C-3, C-4, C-9a
3		168.47 (C)	
4		112.58 (C)	

Table 56 (Continued)

Position	δ_{H} (mult., J_{Hz})	δ_{C} (C-type)	HMBC correlation
4a		156.34 (C)	
4b		89.60 (C)	
5		84.42 (C)	
6		202.07 (C=O)	
7		84.91 (C)	
7-OCH ₃	3.64 (<i>s</i>)	53.95 (CH ₃)	C-7
8	7.52 (<i>d</i> , 1.0)	134.36 (CH)	C-4b, C-5, C-6, C-8a, C-9, C-20, C-21
8a		132.07 (C)	
9		178.12 (C=O)	
9a		101.39 (C)	
10	4.55 (<i>q</i> , 6.5)	91.69 (CH)	C-3, C-4, C-12, C-13
11		43.39 (C)	
12	1.42 (<i>s</i>)	28.16 (CH ₃)	C-4, C-10, C-11, C-13, C-14
13	1.49 (<i>s</i>)	20.04 (CH ₃)	C-4, C-10, C-11, C-12
14	1.30 (<i>d</i> , 6.5)	16.30 (CH ₃)	C-10, C-11
15	H _a : 2.68 (<i>md</i> , 14.5) H _b : 2.55 (<i>dd</i> , 14.5 and 11.0)	28.98 (CH ₂)	C-5, C-16, C-17 C-5, C-6, C-16, C-17
16	4.36 (<i>md</i> , 11.0)	117.32 (CH)	
17		135.56 (C)	
18	1.38 (<i>brs</i>)	25.52 (CH ₃)	C-16, C-17, C-19
19	1.07 (<i>brs</i>)	16.76 (CH ₃)	C-16, C-17, C-18
20	H _a : 2.36 (<i>dd</i> , 13.0 and 1.0) H _b : 1.67 (<i>dd</i> , 13.0 and 9.5)	30.69 (CH ₂)	C-4b, C-7, C-8, C-21, C-22 C-6, C-7, C-8, C-21, C-22
21	2.61 (<i>d</i> , 9.5)	49.99 (CH)	C-4b, C-7, C-20
22		83.22 (C)	

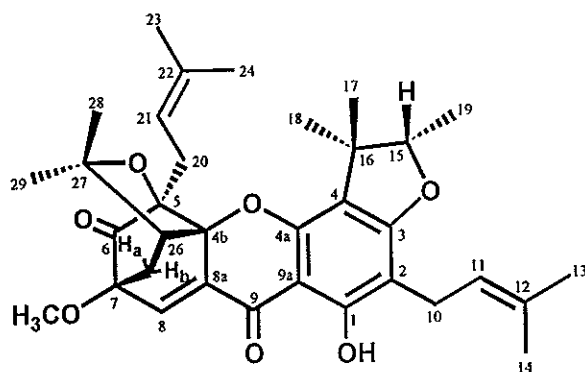
Table 56 (Continued)

Position	δ_{H} (mult., J _{Hz})	δ_{C} (C-type)	HMBC correlation
23	1.72 (s)	30.99 (CH ₃)	C-21, C-22, C-24
24	1.29 (s)	29.01 (CH ₃)	C-22, C-23

3.3 Structural determination of compounds isolated from the stem bark of *G. scortechinii*

3.3.1 Compound PP13

Compound PP13 was obtained as a yellow gum. Its IR (Figure 94) and UV (Figure 93) spectral data were similar to those of scortechinone A. Its ¹H NMR spectrum (Figure 95) (Table 57) indicated that PP13 contained identical substituents to scortechinone A: one chelated hydroxyl group, one methoxyl group, two units of a 3-methylbut-2-enyl group and one unit of a 2,3,3-trimethylhydrofuran ring. The minor differences were signals of the methine proton (H-15) and the methyl proton (Me-17) of the 2,3,3-trimethylhydrofuran ring which were shifted to lower field whereas the methyl protons (Me-18 and Me-19) were shifted to higher field. Comparison of its ¹H NMR data with those of GF3 (12) (Table 57) isolated from the fruits of *G. scortechinii* (Sukpondma, 2002) suggested that PP13 had the same structure as GF3 (12) of which the structure differed from scortechinone A only in the stereochemistry at C-15.



12

Table 57 The ^1H NMR data of PP13 and GF3

Position	PP13 (δ_{H})	GF3 (δ_{H})
1-OH	13.24 (<i>s</i> , 1H)	13.24 (<i>s</i> , 1H)
7-OCH ₃	3.64 (<i>s</i> , 3H)	3.64 (<i>s</i> , 3H)
H-8	7.51 (<i>d</i> , $J=1.0$ Hz, 1H)	7.51 (<i>d</i> , $J=1.5$ Hz, 1H)
H-10	3.22 (<i>d</i> , $J=7.0$ Hz, 2H)	3.22 (<i>d</i> , $J=7.0$ Hz, 2H)
H-11	5.22 (<i>mt</i> , $J=7.0$ Hz, 1H)	5.23 (<i>mt</i> , $J=7.0$ Hz, 1H)
Me-13	1.68 (<i>brs</i> , 3H)	1.68 (<i>d</i> , $J=1.0$ Hz, 3H)
Me-14	1.75 (<i>s</i> , 3H)	1.76 (<i>s</i> , 3H)
H-15	4.54 (<i>q</i> , $J=7.0$ Hz, 1H)	4.55 (<i>q</i> , $J=6.5$ Hz, 1H)
Me-17	1.41 (<i>s</i> , 3H)	1.42 (<i>s</i> , 3H)
Me-18	1.49 (<i>s</i> , 3H)	1.49 (<i>s</i> , 3H)
Me-19	1.30 (<i>d</i> , $J=7.0$ Hz, 3H)	1.30 (<i>d</i> , $J=6.5$ Hz, 3H)
H _a -20	2.67 (<i>md</i> , $J=14.5$ Hz, 1H)	2.67 (<i>md</i> , $J=14.5$ Hz, 1H)
H _b -20	2.54 (<i>dd</i> , $J=14.5, 10.5$ Hz, 1H)	2.54 (<i>dd</i> , $J=14.5, 10.5$ Hz, 1H)
H-21	4.36 (<i>md</i> , $J=10.5$ Hz, 1H)	4.36 (<i>md</i> , $J=10.5$ Hz, 1H)
Me-23	1.36 (<i>brs</i> , 3H)	1.36 (<i>s</i> , 3H)
Me-24	1.02 (<i>s</i> , 3H)	1.02 (<i>s</i> , 3H)

Table 57 (Continued)

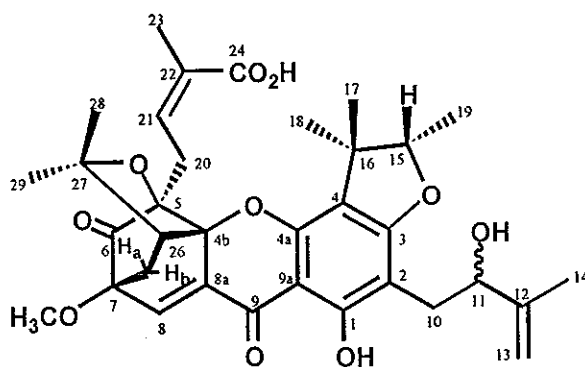
Position	PP13 (δ_{H})	GF3 (δ_{H})
H _a -25	2.34 (<i>d</i> , $J=13.0$ Hz, 1H)	2.34 (<i>d</i> , $J=13.5$ Hz, 1H)
H _b -25	1.66 (<i>dd</i> , $J=13.0, 9.5$ Hz, 1H)	1.67 (<i>dd</i> , $J=13.5, 9.5$ Hz, 1H)
H-26	2.58 (<i>d</i> , $J=9.5$ Hz, 1H)	2.57 (<i>d</i> , $J=9.5$ Hz, 1H)
Me-28	1.72 (<i>s</i> , 3H)	1.72 (<i>s</i> , 3H)
Me-29	1.29 (<i>s</i> , 3H)	1.29 (<i>s</i> , 3H)

3.3.2 Compound PP14

Compound PP14 was isolated as a yellow gum. The EIMS at m/z 608 (Figure 96) established a molecular formula of C₃₄H₄₀O₁₀. Its IR absorption bands (Figure 98) at 3600-2500 (a hydroxyl group of a carboxylic acid), 1745 (an unconjugated carbonyl group), 1694 (an α,β -unsaturated carboxyl group) and 1634 cm⁻¹ (a chelated *ortho*-hydroxyl carbonyl group) indicated that PP14 had three carbonyl functionalities. The presence of a ketone carbonyl group, an α,β -unsaturated carboxyl group and a chelated *ortho*-hydroxyl carbonyl group was confirmed by carbon signals at δ 203.08, 167.90 and 177.82, respectively, in the ¹³C NMR spectrum (Figure 100) (Table 59). Its UV spectrum (Figure 97) showed an absorption band due to a conjugated chromophore at λ_{max} 366 nm. The caged structure was evident by the signals of -OC(Me)₂-CHCH₂-C- unit [δ_{H} 2.63 (*d*, $J=9.5$ Hz, 1H, H-26), 2.32 (*d*, $J=13.6$ Hz, 1H, H_a-25), 1.72 (*dd*, $J=13.6, 9.5$ Hz, 1H, H_b-25), 1.72 (*s*, 3H, Me-28) and 1.28 (*s*, 3H, Me-29)] in the ¹H NMR spectrum (Figure 99) (Table 58). In addition, it contained one olefinic proton (δ_{H} 7.52, *d*, $J=1.3$ Hz, H-8), one methoxyl group (δ_{H}

3.63, *s*, 7-OCH₃), characteristic signals of a 2-hydroxy-3-methylbut-3-enyl group [δ_{H} 5.03 (*brs*, 1H, H_a-13), 4.88 (*brs*, 1H, H_b-13), 4.50 (*dd*, $J=10.8, 3.0$ Hz, 1H, H-11), 2.92 (*dd*, $J=14.3, 10.8$ Hz, 1H, H_a-10), 2.68 (*dd*, $J=14.3, 3.0$ Hz, 1H, H_b-10) and 1.84 (*s*, 3H, Me-14)], one unit of a 3-carboxybut-2-enyl group [δ_{H} 5.43 (*md*, $J=10.4$ Hz, 1H, H-21), 3.51 (*dd*, $J=15.6, 10.4$ Hz, 1H, H_a-20), 2.75 (*md*, $J=15.6$ Hz, 1H, H_b-20) and 1.67 (*brs*, 3H, Me-23)] and one unit of a 2,3,3-trimethylhydrofuran ring [δ_{H} 4.55 (*q*, $J=6.6$ Hz, 1H, H-15), 1.46 (*s*, 3H, Me-18), 1.39 (*s*, 3H, Me-17) and 1.37 (*d*, $J=6.6$ Hz, 3H, Me-19)]. These data were similar to those of scortechinone C (Rukachaisirikul, 2000a). Its HMBC data (Figure 107) (Table 60) revealed that all substituents were located at the same positions as scortechinone C. Irradiation of the methyl protons (Me-14) of the 2-hydroxy-3-methylbut-3-enyl unit (Figure 104) enhanced the signal of the olefinic proton (H_b-13), suggesting that Me-14 was *cis* to H_b-13. The configuration at C-21/C-22 double bond was assigned to be *Z* as irradiation of the olefinic proton (H-21) (Figure 102) enhanced the signal of Me-23. The relative stereochemistry at C-15 was established to be identical to that of scortechinone C by the NOEDIFF experiments. Irradiation of the oxymethine proton (H-15) (Figure 103) enhanced the *singlet* signal of the methyl protons (Me-17) and the *doublet* signal of the methyl protons (Me-19) while irradiation of the methyl protons (Me-18) (Figure 105) enhanced the signals of Me-19 and the methylene proton (H_a-20) of an α,β -unsaturated carboxylic acid unit. These results suggested the location of H-15 at β -position. Comparison of its 1D and 2D NMR data with those of scortechinone C (Tables 58, 59 and 60) revealed almost identical results. The minor difference was found in the 2-hydroxy-3-methylbut-3-enyl group which its oxymethine proton (H-11) was shifted to lower field than that of scortechinone C.

Furthermore, TLC chromatograms of **PP14** and scortechinone C, using 2% MeOH/CHCl₃ as mobile phase, indicated that they had different R_f values (R_f 0.28 and 0.38 for **PP14** and scortechinone C, respectively). Thus, **PP14** was assigned to have the structure **13** which differed from scortechinone C only in the stereochemistry of C-11.



13

Table 58 The ¹H NMR data of scortechinone C and **PP14**

Position	Scortechinone C (δ_H)	PP14 (δ_H)
1-OH	13.15 (s, 1H)	-
7-OCH ₃	3.65 (s, 3H)	3.63 (s, 3H)
H-8	7.51 (d, $J=1.4$ Hz, 1H)	7.52 (d, $J=1.3$ Hz, 1H)
H _a -10	2.98 (dd, $J=14.0, 3.4$ Hz, 1H)	2.92 (dd, $J=14.3, 10.8$ Hz, 1H)
H _b -10	2.64 (dd, $J=14.0, 11.1$ Hz, 1H)	2.68 (dd, $J=14.3, 3.0$ Hz, 1H)
H-11	4.32 (brdd, $J=11.1, 3.4$ Hz, 1H)	4.50 (dd, $J=10.8, 3.0$ Hz, 1H)
H _a -13	5.07 (m, 1H)	5.03 (brs, 1H)
H _b -13	4.92 (m, 1H)	4.88 (brs, 1H)
Me-14	1.87 (s, 3H)	1.84 (s, 3H)

Table 58 (Continued)

Position	Scortechinone C (δ_H)	PP14 (δ_H)
H-15	4.56 (<i>q</i> , $J=6.6$ Hz, 1H)	4.55 (<i>q</i> , $J=6.6$ Hz, 1H)
Me-17	1.37 (<i>s</i> , 3H)	1.39 (<i>s</i> , 3H)
Me-18	1.56 (<i>s</i> , 3H)	1.46 (<i>s</i> , 3H)
Me-19	1.45 (<i>d</i> , $J=6.6$ Hz, 3H)	1.37 (<i>d</i> , $J=6.6$ Hz, 3H)
H _a -20	3.81 (<i>dd</i> , $J=15.2, 11.8$ Hz, 1H)	3.51 (<i>dd</i> , $J=15.6, 10.4$ Hz, 1H)
H _b -20	2.73 (<i>ddq</i> , $J=15.2, 3.4, 2.5$ Hz, 1H)	2.75 (<i>md</i> , $J=15.6$ Hz, 1H)
H-21	5.20 (<i>ddq</i> , $J=11.4, 3.4, 1.4$ Hz, 1H)	5.43 (<i>md</i> , $J=10.4$ Hz, 1H)
Me-23	1.65 (<i>dd</i> , $J=2.5, 1.4$ Hz, 3H)	1.67 (<i>brs</i> , 3H)
H _a -25	2.35 (<i>dd</i> , $J=13.0, 1.4$ Hz, 1H)	2.32 (<i>d</i> , $J=13.6$ Hz, 1H)
H _b -25	1.70 (<i>dd</i> , $J=13.0, 9.3$ Hz, 1H)	1.72 (<i>dd</i> , $J=13.6, 9.5$ Hz, 1H)
H-26	2.64 (<i>d</i> , $J=9.3$ Hz, 1H)	2.63 (<i>d</i> , $J=9.5$ Hz, 1H)
Me-28	1.71 (<i>s</i> , 3H)	1.72 (<i>s</i> , 3H)
Me-29	1.29 (<i>s</i> , 3H)	1.28 (<i>s</i> , 3H)

Table 59 The ^{13}C NMR data of scortechinone C and PP14

Position	C-type	Scortechinone C (δ_C)	PP14 (δ_C)
1-OH	C	163.83	164.12
2	C	101.66	102.36
3	C	167.71	167.68
4	C	112.50	112.72
4a	C	155.78	155.00
4b	C	89.20	89.18
5	C	84.35	84.08

Table 59 (Continued)

Position	C-type	Scortechinone C (δ_c)	PP14 (δ_c)
6	C=O	203.20	203.08
7	C	85.15	85.10
7-OCH ₃	CH ₃	53.82	53.84
8	CH	134.79	134.80
8a	C	132.54	132.50
9	C=O	178.18	177.82
9a	C	101.38	101.32
10	CH ₂	28.80	28.50
11	CH	73.72	74.88
12	C	146.84	147.13
13	CH ₂	110.31	110.58
14	CH ₃	18.66	18.25
15	CH	92.43	92.07
16	C	43.94	43.49
17	CH ₃	28.66	27.98
18	CH ₃	19.28	19.68
19	CH ₃	16.77	16.19
20	CH ₂	29.07	29.00
21	CH	135.65	135.81
22	C	129.58	129.45
23	CH ₃	21.11	21.09
24	C=O	166.63	167.90
25	CH ₂	30.42	30.44
26	CH	49.74	49.69
27	C	83.46	83.56

Table 59 (Continued)

Position	C-type	Scortechinone C (δ_c)	PP14 (δ_c)
28	CH ₃	30.81	30.91
29	CH ₃	28.88	28.69

Table 60 The HMBC correlations of scortechinone C and PP14

Proton	Scortechinone C (Carbon)	PP14 (Carbon)
1-OH	C-1, C-2, C-3, C-9a	-
7-OCH ₃	C-7	C-7
H-8	C-4b, C-6, C-7, C-8a, C-9, C-25	C-4b, C-5, C-6, C-7, C-8a, C-9, C-25, C-26
H _a -10	C-1, C-2, C-3, C-11, C-12	C-1, C-2, C-3, C-11, C-12
H _b -10	C-1, C-2, C-3, C-11, C-12	C-1, C-2, C-3, C-11, C-12
H-11	C-10, C-12, C-13, C-14	C-2, C-10, C-12, C-13, C-14
H _a -13	C-11, C-12, C-14	C-11, C-12, C-14
H _b -13	C-11, C-12, C-14	C-11, C-12, C-14
Me-14	C-11, C-12, C-13	C-11, C-12, C-13
H-15	C-3, C-4, C-16, C-17, C-18, C-19	C-3, C-4, C-17, C-18
Me-17	C-4, C-15, C-16, C-18	C-4, C-15, C-16, C-18
Me-18	C-4, C-15, C-16, C-17	C-4, C-15, C-16, C-17
Me-19	C-15, C-16	C-15, C-16
H _a -20	C-4b, C-5, C-6, C-21, C-22	C-4b, C-5, C-6, C-21, C-22
H _b -20	C-4b, C-5, C-6, C-21, C-22	C-5, C-6, C-21, C-22
H-21	C-22, C-23	C-5, C-23
Me-23	C-21, C-22, C-24	C-21, C-22, C-24

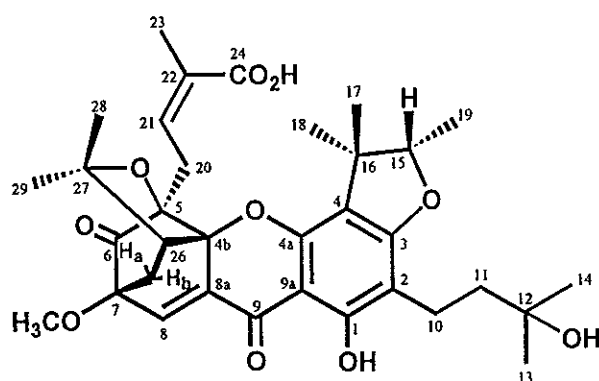
Table 60 (Continued)

Proton	Scortechinone C (Carbon)	PP14 (Carbon)
H _a -25	C-4b, C-6, C-7, C-8, C-26, C-27	C-4b, C-7, C-8, C-26
H _b -25	C-6, C-7, C-8, C-27	C-6, C-7, C-8, C-26, C-27
H-26	C-4b, C-5, C-7, C-27, C-28	C-4b, C-5, C-7, C-28
Me-28	C-26, C-27, C-29	C-26, C-27, C-29
Me-29	C-26, C-27, C-28	C-26, C-27, C-28

3.3.3 Compound PP15

Compound PP15 was obtained as a yellow gum. The molecular ion at m/z 610 in the EIMS spectrum (Figure 108) corresponded to a molecular formula of $C_{34}H_{42}O_{10}$. The IR spectrum (Figure 110) exhibited absorption bands at 3600-2500 (a hydroxyl group of a carboxylic acid), 1745 (an unconjugated carbonyl group), 1690 (an α,β -unsaturated carboxyl group) and 1634 cm^{-1} (a chelated *ortho*-hydroxyl carbonyl group). The UV absorption band at λ_{max} 367 nm (Figure 109) suggested that PP15 had the same chromophore as PP14. Its ^1H (Figure 111) (Table 61) and ^{13}C NMR data (Figure 112) (Table 61) were similar to those of PP14 except that PP15 contained none of signals for a 2-hydroxy-3-methylbut-3-enyl substituent. These signals were replaced by signals which could be ascribed to a 3-hydroxy-3-methylbutyl group [δ_{H} 2.72 (*ddd*, $J=14.7, 7.2, 3.2$ Hz, 1H, H_a-10), 2.61 (*dd*, $J=14.7, 3.2$ Hz, 1H, H_b-10), 2.05 (*ddd*, $J=13.5, 7.2, 3.2$ Hz, 1H, H_a-11), 1.73-1.66 (*m*, 1H, H_b-11), 1.40 (*s*, 3H, Me-13), 1.24 (*s*, 3H, Me-14); δ_{C} 17.27 (C-10), 39.42 (C-11), 73.18 (C-12), 27.60 (C-13) and 30.04 (C-14)]. This substituent was assigned to be at C-2 (δ

105.98) by HMBC correlations (Figure 118) (Table 61) of its methylene protons (H_a -10 and H_b -10) with C-1 (δ 163.73), C-2 and C-3 (δ 165.86). The attachment of other substituents was identical to PP14 by the HMBC data. Irradiation of the methyl protons (δ_H 1.42, Me-19) of the 2,3,3-trimethylhydrofuran ring (Figure 116) enhanced the signals of the methine proton (δ_H 4.60, H-15) and the methyl protons (δ_H 1.52, Me-18). When Me-18 was irradiated (Figure 115), the signals of the methylene proton (δ_H 3.79, H_a -20) of the C-5 3-carboxybut-2-enyl substituent and Me-19 were enhanced. These results indicated that Me-18 and Me-19 were located on the same side as the α,β -unsaturated carboxylic acid unit at C-5. Thus, the methine proton (H-15) was on the same face (β -face) as PP14. The configuration at C-21/C-22 double bond was determined as *Z* by the NOE enhancement observed between the olefinic proton (δ_H 5.20, H-21) and the methyl protons (δ_H 1.63, Me-23) (Figure 114). Therefore, PP15 had the structure 14, a new caged-tetraprenylated xanthone.



14

Table 61 The NMR data of compound PP15

Position	δ_{H} (<i>mult.</i> , J_{Hz})	δ_{C} (C-type)	HMBC correlation
1-OH		163.73 (C)	
2		105.98 (C)	
3		165.86 (C)	
4		112.24 (C)	
4a		154.31 (C)	
4b		89.09 (C)	
5		84.32 (C)	
6		202.90 (C=O)	
7		85.09 (C)	
7-OCH ₃	3.64 (<i>s</i>)	53.79 (CH ₃)	C-7
8	7.52 (<i>d</i> , 2.4)	134.68 (CH)	C-4b, C-5, C-6, C-8a, C-9, C-25, C-26
8a		132.48 (C)	
9		178.09 (C=O)	
9a		101.46 (C)	
10	H _a : 2.72 (<i>ddd</i> , 14.7, 7.2 and 3.2) H _b : 2.61 (<i>dd</i> , 14.7 and 3.2)	17.27 (CH ₂)	C-1, C-2, C-3, C-11, C-12 C-1, C-2, C-3, C-11, C-12
11	H _a : 2.05 (<i>ddd</i> , 13.5, 7.2 and 3.2) H _b : 1.73-1.66 (<i>m</i>)	39.42 (CH ₂)	C-2, C-10, C-12, C-13, C-14 C-2, C-10, C-12
12-OH		73.18 (C)	
13	1.40 (<i>s</i>)	27.60 (CH ₃)	C-11, C-12, C-14
14	1.24 (<i>s</i>)	30.04 (CH ₃)	C-11, C-12, C-13
15	4.60 (<i>q</i> , 6.8)	92.19 (CH)	C-3, C-4, C-16, C-17, C-18
16		43.74 (C)	
17	1.38 (<i>s</i>)	28.77 (CH ₃)	C-4, C-15, C-16, C-18

Table 61 (Continued)

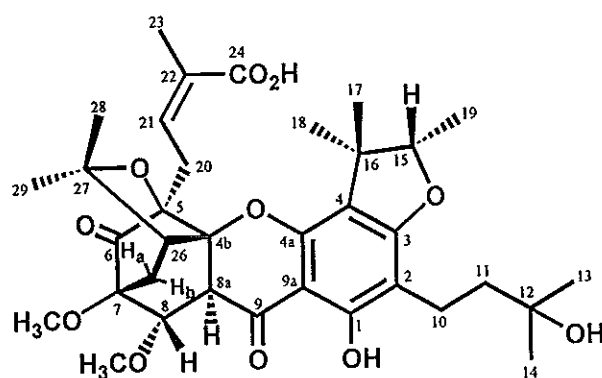
Position	δ_{H} (<i>mult.</i> , J_{Hz})	δ_{C} (C-type)	HMBC correlation
18	1.52 (<i>s</i>)	19.38 (CH ₃)	C-4, C-15, C-16, C-19
19	1.42 (<i>d</i> , 6.8)	16.83 (CH ₃)	C-15, C-16, C-18
20	H _a : 3.79 (<i>dd</i> , 16.2 and 12.0)	29.10 (CH ₂)	C-4b, C-5, C-6, C-21, C-22
	H _b : 2.71 (<i>md</i> , 16.2)		C-4b, C-5, C-21, C-22, C-23
21	5.20 (<i>md</i> , 12.0)	135.38 (CH)	C-23
22		129.88 (C)	
23	1.63 (<i>dd</i> , 2.3 and 1.4)	21.01 (CH ₃)	C-5, C-21, C-22, C-24
24		167.67 (C=O)	
25	H _a : 2.35 (<i>d</i> , 13.5)	30.35 (CH ₂)	C-4b, C-6, C-7, C-8, C-26, C-27
	H _b : 1.69 (<i>dd</i> , 13.5 and 9.6)		C-6, C-7, C-8, C-26, C-27
26	2.62 (<i>d</i> , 9.6)	49.78 (CH)	C-4b, C-5, C-7, C-25, C-28
27		83.41 (C)	
28	1.70 (<i>s</i>)	30.83 (CH ₃)	C-26, C-27, C-29
29	1.28 (<i>s</i>)	28.89 (CH ₃)	C-26, C-27, C-28

3.3.4 Compound PP16

Compound PP16 was obtained as a pale yellow gum. The IR spectrum (Figure 120) exhibited absorption bands at 3690-2350 (a hydroxyl group of a carboxylic acid), 1751 (an unconjugated carbonyl group), 1692 (an α,β -unsaturated carboxyl group) and 1633 cm^{-1} (a chelated *ortho*-hydroxyl carbonyl group). Its UV absorption band at λ_{max} 304 nm (Figure 119) was similar to that of PP8, indicating that PP16 had the same chromophore as PP8. Its ¹H NMR (Figure 121) (Table 62)

and ^{13}C NMR (Figure 122) (Table 62) spectral data were also similar to those of PP8 except for the fact that signals for a 3-methylbut-2-enyl group were replaced by signals for a 3-hydroxy-3-methylbutyl group [δ_{H} 2.63-2.59 (*m*, 2H, H-10), 1.72-1.68 (*m*, 2H, H-11), 1.29 (*s*, 3H), 1.28 (*s*, 3H); δ_{C} 17.18 (C-10), 42.18 (C-11), 71.03 (C-12), 29.09 (C-13) and 29.06 (C-14)]. This group was assigned to be at C-2 (δ_{C} 106.10) by the HMBC correlations (Figure 129) (Table 62) between its methylene protons (H-10) with C-1 (δ_{C} 161.50), C-2 and C-3 (δ_{C} 166.64). The attachment of other substituents was identical to PP8 based on the HMBC data. Irradiation of the oxymethine proton (δ_{H} 4.40, H-15) (Figure 125) enhanced a *singlet* signal of the methyl protons (δ_{H} 1.44, Me-17) and a *doublet* signal of the methyl protons (δ_{H} 1.35, Me-19), indicating that H-15 was *cis* to Me-17. When the methyl protons (δ_{H} 1.11, Me-18) were irradiated (Figure 127), signals of Me-17, Me-19, the methylene protons [δ_{H} 3.21 (H_a-20) and 3.12 (H_b-20)], the olefinic proton (δ_{H} 6.60, H-21) and the methyl protons (δ_{H} 1.97, Me-23) of a C-5 α,β -unsaturated carboxylic acid unit were enhanced. These results indicated that Me-18, Me-19 and the C-5 α,β -unsaturated carboxylic acid unit were located on the same side of the molecule, the α -side, and H-15 was on β -side. The configuration of C-21/C-22 double bond was assigned to be *Z* since irradiation of H-21 (Figure 124) enhanced a signal of Me-23. The relative stereochemistry at C-8 and C-8a was found to be the same as PP8 according to the following NOEDIFF results. Irradiation of H-21 of the C-5 substituent enhanced a signal of the methine proton (δ_{H} 3.18, H-8a), suggesting that H-8a was on α -side. Irradiation of the methylene proton (δ_{H} 1.65, H_b-25) (Figure 126) caused NOE enhancement with the methylene proton (δ_{H} 2.02, H_a-25), the methine proton (δ_{H}

2.70, H-26) and the oxymethine proton (δ_{H} 4.47, H-8) but did not affect signals of the methoxy protons (δ_{H} 3.38, 8-OCH₃) and H-8a. These results indicated that H-8 was *trans* to H-8a. Therefore, PP16 had the structure **15**, a new caged-tetraprenylated xanthone.



15

Table 62 The NMR data of compound PP16

Position	δ_{H} (<i>mult.</i> , J_{Hz})	δ_{C} (C-type)	HMBC correlation
1-OH	12.11 (<i>s</i>)	161.50 (C)	C-1, C-2, C-9a
2		106.10 (C)	
3		166.64 (C)	
4		113.75 (C)	
4a		152.17 (C)	
4b		87.03 (C)	
5		86.42 (C)	
6		205.50 (C=O)	
7		81.40 (C)	

Table 62 (Continued)

Position	δ_{H} (<i>mult.</i> , J_{Hz})	δ_{C} (C-type)	HMBC correlation
7-OCH ₃	3.51 (<i>s</i>)	52.39 (CH ₃)	C-7
8	4.47 (<i>d</i> , 1.0)	75.10 (CH)	C-4b, C-6, C-7, 8-OCH ₃ , C-8a, C-9, C-25
8-OCH ₃	3.38 (<i>s</i>)	57.41 (CH ₃)	C-8
8a	3.18 (<i>brs</i>)	48.90 (CH)	C-4b, C-7, C-8, C-9, C-26
9		192.09 (C=O)	
9a		102.37 (C)	
10	2.63-2.59 (<i>m</i>)	17.18 (CH ₂)	C-1, C-2, C-3, C-11, C-12
11	1.72-1.68 (<i>m</i>)	42.18 (CH ₂)	C-2, C-10, C-12, C-13, C-14
12-OH		71.03 (C)	
13	1.29 (<i>s</i>)	29.09* (CH ₃)	C-11, C-12, C-14
14	1.28 (<i>s</i>)	29.06* (CH ₃)	C-11, C-12, C-13
15	4.40 (<i>q</i> , 6.5)	90.31 (CH)	C-17, C-18
16		43.93 (C)	
17	1.44 (<i>s</i>)	26.08 (CH ₃)	C-4, C-15, C-16, C-18
18	1.11 (<i>s</i>)	22.11 (CH ₃)	C-4, C-15, C-16, C-17
19	1.35 (<i>d</i> , 6.5)	13.87 (CH ₃)	C-15, C-16
20	H _a : 3.21 (<i>mdd</i> , 17.0 and 7.0) H _b : 3.12 (<i>mdd</i> , 17.0 and 7.0)	28.42 (CH ₂)	C-5, C-6, C-21, C-22 C-5, C-6, C-21, C-22
21	6.60 (<i>mt</i> , 7.0)	137.77 (CH)	C-5, C-23, C-24
22		128.14 (C)	
23	1.97 (<i>d</i> , 1.0)	20.88 (CH ₃)	C-21, C-22, C-24
24		170.87 (C=O)	
25	H _a : 2.02 (<i>d</i> , 14.0) H _b : 1.65 (<i>dd</i> , 14.0 and 8.5)	23.92 (CH ₂)	C-4b, C-7, C-8, C-26, C-27 C-6, C-7, C-8, C-26, C-27

Table 62 (Continued)

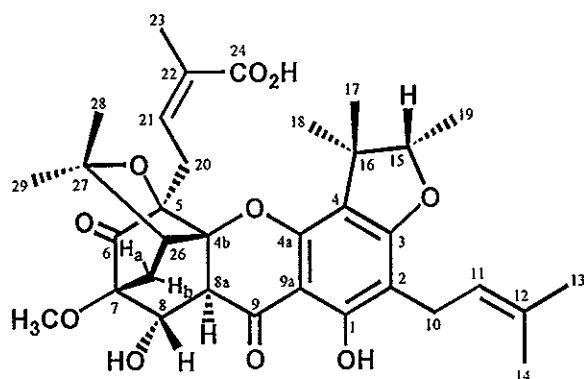
Position	δ_{H} (mult., J_{Hz})	δ_{C} (C-type)	HMBC correlation
26	2.70 (<i>d</i> , 8.5)	45.24 (CH)	C-4b, C-5, C-7, C-25, C-28
27		82.68 (C)	
28	1.43 (<i>s</i>)	30.46 (CH ₃)	C-26, C-27, C-29
29	1.21 (<i>s</i>)	27.19 (CH ₃)	C-26, C-27, C-28

* interchangeable

3.3.5 Compound PP17

Compound PP17 was isolated as a pale yellow gum. Its IR (Figure 131) and UV spectra (Figure 130) were almost identical to those of PP8. Its ¹H NMR spectrum (Figure 132) (Table 63) was also similar to that of PP8 except for the fact that PP17 contained only one methoxyl group (δ_{H} 3.48) which was assigned to be located at C-7 (δ_{C} 81.97) by its HMBC correlation (Figure 140) (Table 63) with C-7. In addition, the signal of the methine proton (δ_{H} 4.82, H-8) was shifted to lower field than that found in PP8. These results indicated that the substituent at C-8 in PP17 was a hydroxyl group, not a methoxyl group. Furthermore, the attachment of other substituents were found to be identical to those of PP8 by HMBC data. Irradiation of the methyl protons (δ_{H} 1.34, Me-19) of a 2,3,3-trimethylhydrofuran ring (Figure 137) enhanced the signals of the methine proton (δ_{H} 4.40, H-15) and the methyl protons (δ_{H} 1.10, Me-18), indicating that Me-19 was *cis* to Me-18. When Me-18 was irradiated (Figure 138), signals of Me-17, Me-19, the methylene protons (δ_{H} 3.24-3.17, H-20),

the olefinic proton (δ_{H} 6.64, H-21) and the methyl protons (δ_{H} 1.97, Me-23) of a C-5 α,β -unsaturated carboxylic acid unit were enhanced. These suggested that Me-18 and Me-19 were located on the same side, the α -side, as the C-5 α,β -unsaturated carboxylic acid unit. Thus, H-15 was located on the β -side. Irradiation of H-21 (Figure 135) caused a NOE enhancement of Me-23, suggesting that the configuration at C-21/C-22 double bond was *Z*. Irradiation of the methylene proton (δ_{H} 1.57, H_b-25) (Figure 136) enhanced the signal of H-8 but did not affect the signal of H-8a, indicating that H-8 was on the β -side and *trans* to H-8a. Therefore, PP17 was assigned to have the structure 16 which differed from PP8 only in the C-8 substituent.



16

Table 63 The NMR data of compound PP17

Position	δ_{H} (mult., J_{Hz})	δ_{C} (C-type)	HMBC correlation
1-OH	12.08 (<i>s</i>)	161.65 (C)	C-1, C-2, C-3, C-9a
2		105.34 (C)	
3		166.85 (C)	
4		113.62 (C)	
4a		152.10 (C)	
4b		86.97 (C)	
5		86.35 (C)	
6		206.43 (C=O)	
7		81.97 (C)	
7-OCH ₃	3.48 (<i>s</i>)	52.05 (CH ₃)	C-7
8	4.82 (<i>d</i> , 1.0)	67.24 (CH)	C-4b, C-6, C-7, C-8a, C-9, C-25
8a	3.19 (<i>s</i>)	49.70 (CH)	C-4b, C-7, C-8, C-9, C-26
9		191.72 (C=O)	
9a		102.41 (C)	
10	3.26-3.13 (<i>m</i>)	21.43 (CH ₂)	C-1, C-2, C-3, C-11, C-12
11	5.23 (<i>mt</i> , 7.0)	121.59 (CH)	C-2, C-10, C-13, C-14
12		132.16 (C)	
13	1.69 (<i>s</i>)	25.79 (CH ₃)	C-11, C-12, C-14
14	1.76 (<i>s</i>)	17.74 (CH ₃)	C-11, C-12, C-13
15	4.40 (<i>q</i> , 6.5)	90.18 (CH)	C-17, C-18
16		43.94 (C)	
17	1.43 (<i>s</i>)	26.09 (CH ₃)	C-4, C-15, C-16, C-18
18	1.10 (<i>s</i>)	22.12 (CH ₃)	C-4, C-15, C-16, C-17
19	1.34 (<i>d</i> , 6.5)	13.83 (CH ₃)	C-15, C-16
20	3.24-3.17 (<i>m</i>)	28.33 (CH ₂)	C-5, C-6, C-21, C-22

Table 63 (Continued)

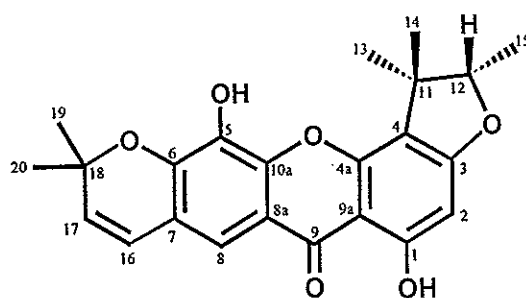
Position	δ_{H} (mult., J_{Hz})	δ_{C} (C-type)	HMBC correlation
21	6.64 (<i>mt</i> , 7.0)	138.66 (CH)	C-5, C-23, C-24
22		127.65 (C)	
23	1.97 (<i>d</i> , 1.0)	20.76 (CH ₃)	C-21, C-22, C-24
24		171.77 (C=O)	
25	H _a : 2.08 (<i>d</i> , 14.0) H _b : 1.57 (<i>dd</i> , 14.0 and 8.5)	22.59 (CH ₂)	C-4b, C-7, C-8, C-26 C-6, C-8 C-26, C-27
26	2.72 (<i>d</i> , 8.5)	45.44 (CH)	C-4b, C-7, C-25, C-28
27		82.54 (C)	
28	1.42 (<i>s</i>)	30.47 (CH ₃)	C-26, C-27, C-29
29	1.22 (<i>s</i>)	27.31 (CH ₃)	C-26, C-27, C-28

3.3.6 Compound PP11

Compound PP11 was obtained as a yellow solid, melting at 173.2-174.9°C. The xanthone chromophore was evident by its UV absorption bands (Figure 141) at 273, 331 and 373 nm while the pyrone carbonyl stretching frequency was found in the region of 1639 cm⁻¹ in the IR spectrum (Figure 142). Its ¹H NMR spectrum (Figure 143) (Table 64) showed signals of one chelated hydroxy proton (δ_{H} 13.28, *s*, 1-OH), one broad *singlet* signal for a hydroxyl group (δ_{H} 5.49), two olefinic protons [δ_{H} 7.49 (*s*, 1H) and 6.24 (*s*, 1H)], one unit of a dimethylchromene ring [δ_{H} 6.45 (*d*, $J=10.5$ Hz, 1H, H-16), 5.73 (*d*, $J=10.5$ Hz, 1H, H-17), 1.53 (*s*, 3H, Me-19) and 1.52 (*s*, 3H, Me-20)] and one unit of a 2,3,3-trimethylhydrofuran ring [δ_{H} 4.55 (*q*, $J=7.0$ Hz, 1H, H-

12), 1.60 (*s*, 3H, Me-14), 1.42 (*d*, $J=7.0$ Hz, 3H, Me-15) and 1.32 (*s*, 3H, Me-13)]. The ^{13}C NMR spectral data (Figure 144) (Table 64) deduced from DEPT (Figure 145) and HMQC (Figure 148) spectra showed 22 signals for 23 carbon atoms: 13 quaternary carbons, 5 methine carbons and 5 methyl carbons. In the HMBC spectrum (Figure 149) (Table 64), the chelated hydroxy proton (1-OH) showed a correlation with a methine aromatic carbon at δ 93.81 (C-2) which correlated to the aromatic proton at δ 6.24 (H-2) in the HMQC spectrum. In addition, H-2 showed cross peaks with C-1 (δ_{C} 164.16), C-3 (δ_{C} 165.89) and C-4 (δ_{C} 113.00). Two methyl-proton signals (Me-13 and Me-14) of the 2,3,3-trimethylhydrofuran ring showed a HMBC correlation with C-4, suggesting the attachment of this group at C-3 and C-4. The chemical-shift values of C-3 and C-4 showed that the hydrofuran ring was fused to the aromatic ring by linkage of its *gem*-dimethyl carbon and ring oxygen atom with C-4 and C-3, respectively. Irradiation of the methine proton (H-12) (Figure 147) enhanced the *singlet* signal of the methyl protons (Me-14) and the *doublet* signal of the methyl protons (Me-15), suggesting that H-12 was *cis* to Me-14. The lowest-field aromatic proton (δ_{H} 7.49) gave HMBC correlations with a carbonyl carbon (δ_{C} 180.10, C-9) and two *O*-linked carbons at δ 144.53 (C-6) and 132.30 (C-10a), indicating that this aromatic proton was located at a *peri*-position (C-8) to the carbonyl group. The olefinic proton (H-16) of the chromene unit showed the correlations with carbons at δ 144.53 (C-6), 117.52 (C-7) and 113.45 (C-8) in the HMBC spectrum, suggesting that the dimethylchromene ring was fused to C-6 and C-7 with an ether linkage at C-6. This was confirmed by irradiation of the olefinic proton (H-16) (Figure 146) which enhanced the signals of the olefinic proton (H-17) and the aromatic proton (H-8). The remaining hydroxyl group (δ_{H} 5.49) was assigned

to be at the remaining carbon signal, C-5 (δ_C 144.82). **PP11** was then assigned as 4'',5''-dihydro-1,5-dihydroxy-6',6'-dimethylpyrano(2',3':6,7)-4'',4'',5''-trimethylfurano(2'',3'':3,4)xanthone (**17**) which was previously isolated from *Rheedia blasiensis* (Delle Monache, 1984).



17

Table 64 The NMR data of **PP11** and 4'',5''-dihydro-1,5-dihydroxy-6',6'-dimethylpyrano(2',3':6,7)-4'',4'',5''-trimethylfurano(2'',3'':3,4)xanthone

Position	PP11		HMBC correlation	PP11 (reported data)
	δ_H (mult, J_{Hz})	δ_C (C-Type)		δ_H (mult, J_{Hz})*
1-OH	13.28 (s)	164.16 (C)	C-1, C-2, C-9a	12.10 (s)
2	6.24 (s)	93.81 (CH)	C-1, C-3, C-4, C-9a	6.20 (s)
3		165.89 (C)		
4		113.00 (C)		
4a		152.61 (C)		
5-OH	5.49 (brs)	144.82 (C)		5.10 (brs)
6		144.53 (C)		
7		117.52 (C)		

Table 64 (Continued)

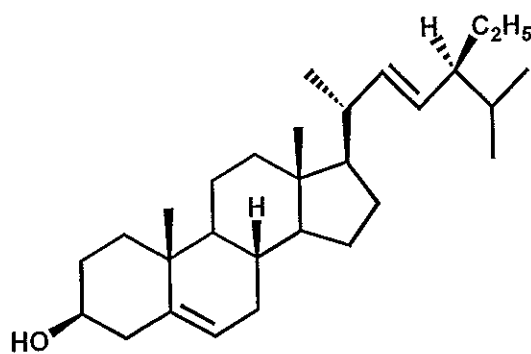
Position	PP11		HMBC correlation	PP11 (reported data)
	δ_{H} (mult, J_{Hz})	δ_{C} (C-Type)		δ_{H} (mult, J_{Hz}^*)
8	7.49 (s)	113.45 (CH)	C-6, C-9, C-10a, C-16	7.42 (s)
8a		114.75 (C)		
9		180.10 (C=O)		
9a		103.36 (C)		
10a		132.30 (C)		
11		43.75 (C)		
12	4.55 (q, 7.0)	90.88 (CH)	C-11, C-13, C-14	4.53 (q, 7.0)
13	1.32 (s)	21.25 (CH ₃)	C-4, C-11, C-12, C-14	1.32 (s)
14	1.60 (s)	25.55 (CH ₃)	C-4, C-11, C-12, C-13	1.59 (s)
15	1.42 (d, 7.0)	14.28 (CH ₃)	C-11, C-12	1.41 (d, 7.0)
16	6.45 (d, 10.5)	121.44 (CH)	C-6, C-7, C-8, C-18	6.40 (d, 10.0)
17	5.73 (d, 10.5)	130.77 (CH)	C-7, C-18, C-19, C-20	5.70 (d, 10.0)
18		78.87 (C)		
19	1.53 (s)	28.46 (CH ₃)	C-16, C-17, C-18, C-20	1.50 (s)
20	1.52 (s)	28.46 (CH ₃)	C-16, C-17, C-18, C-19	1.50 (s)

* ¹H NMR data of 4'',5''-dihydro-1,5-dihydroxy-6',6'-dimethylpyrano(2',3':6,7)-4'',4'',5''-trimethyl-furano(2'',3'':3,4)xanthone in CDCl₃.

3.3.7 Compound PP12

Compound PP12 was obtained as a white solid, melting at 154.3-156.1°C. Its IR spectrum (Figure 150) showed the absorption bands at 3341 (a hydroxyl group),

2958, 2936 and 2868 cm^{-1} (C-H bond). PP12 was identified as stigmasterol (**18**) by direct comparison of its ^1H NMR spectrum (Figure 151) and TLC chromatogram with authentic sample that was obtained from the twigs of *G. scortechinii* (Rukachaisirikul, 2000a).



18

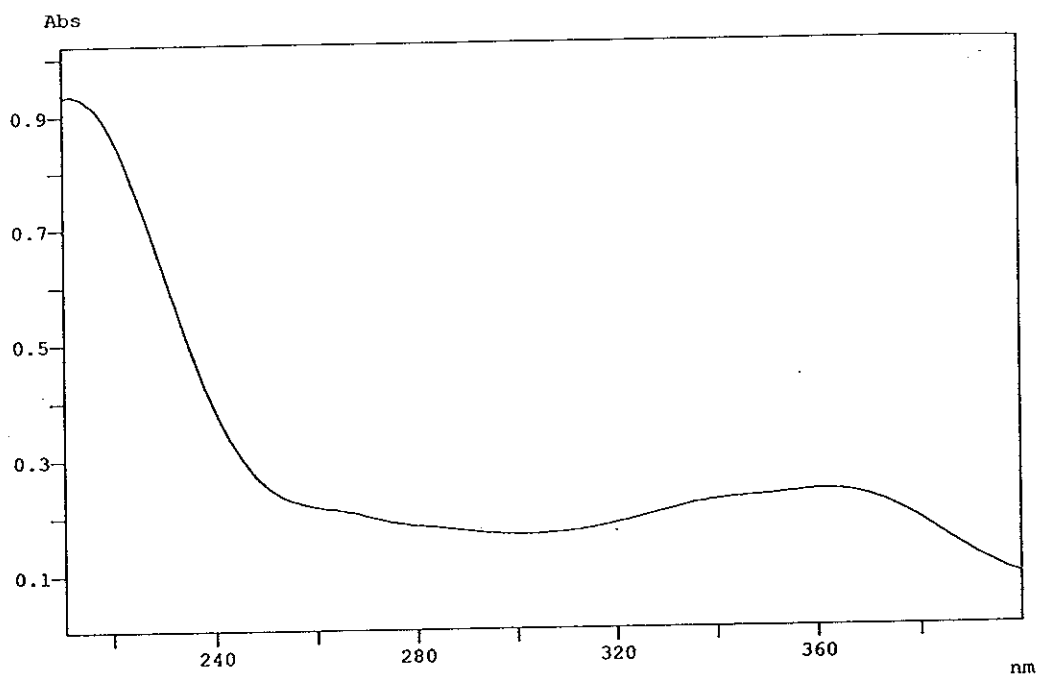


Figure 2 UV (MeOH) spectrum of PP7

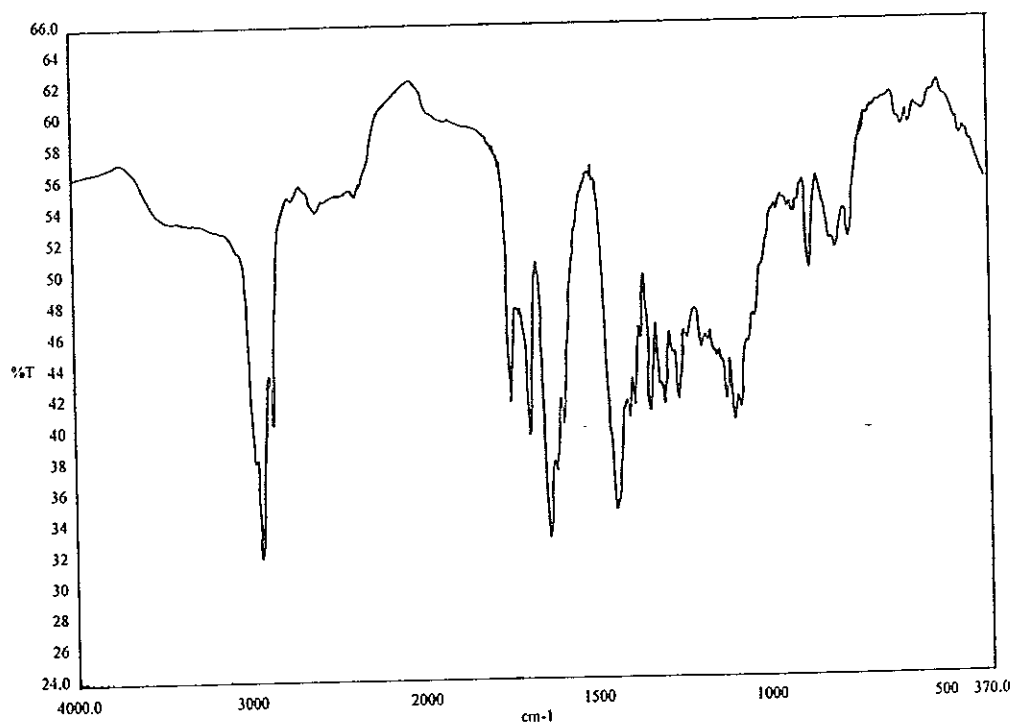


Figure 3 FT-IR (neat) spectrum of PP7

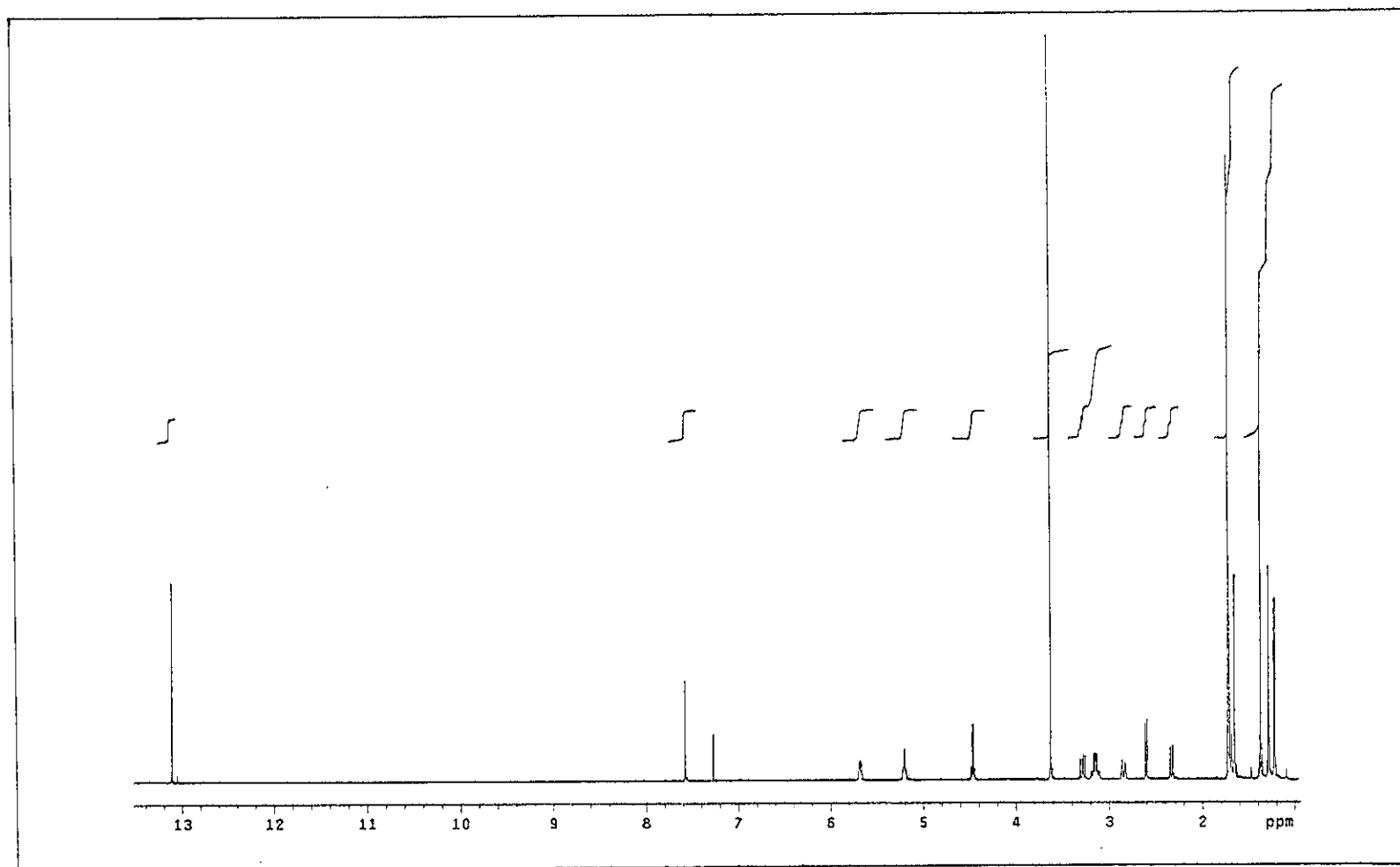


Figure 4 ^1H NMR (500 MHz) (CDCl_3) spectrum of PP7

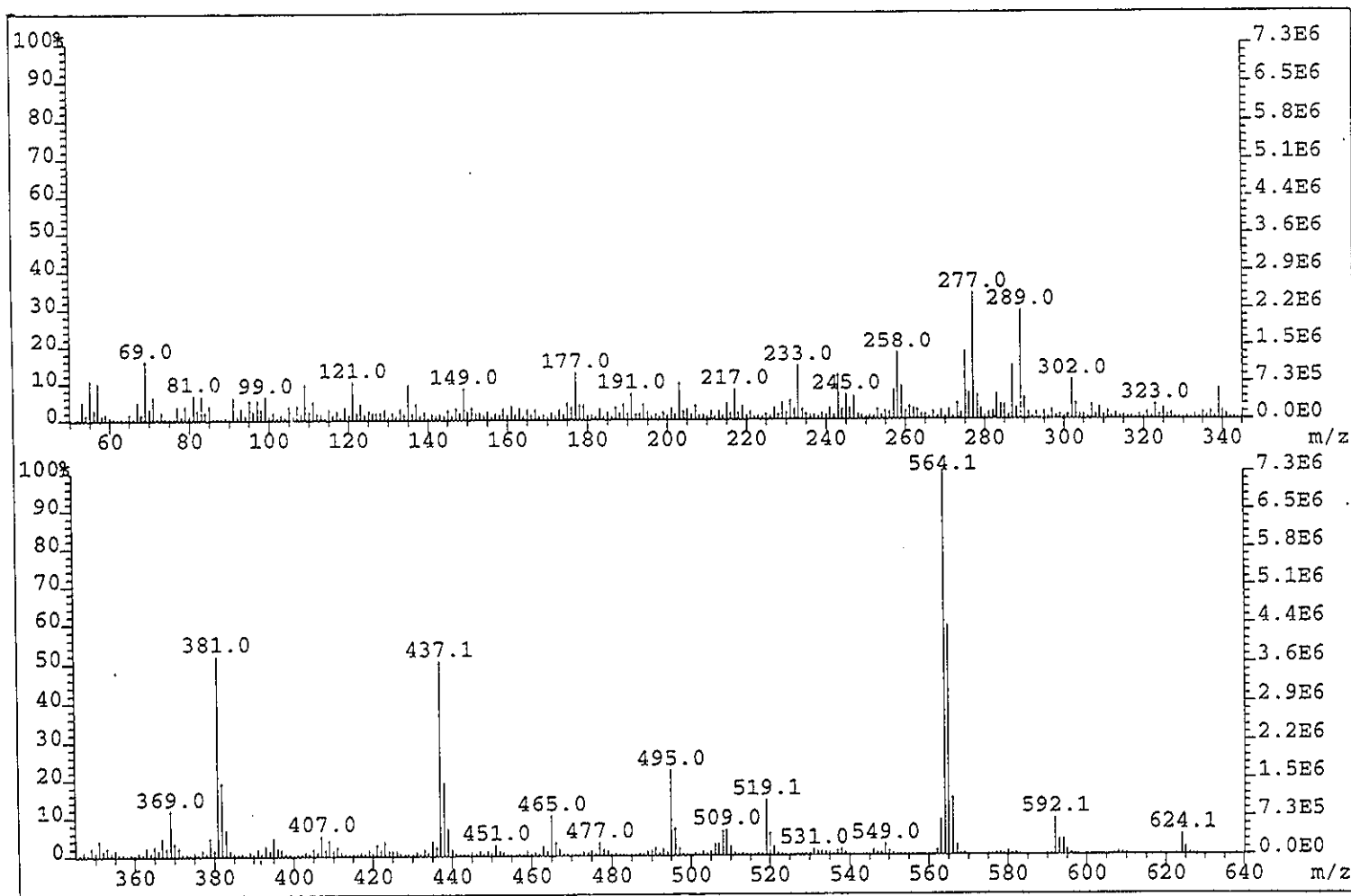


Figure 5 Mass spectrum of PP9

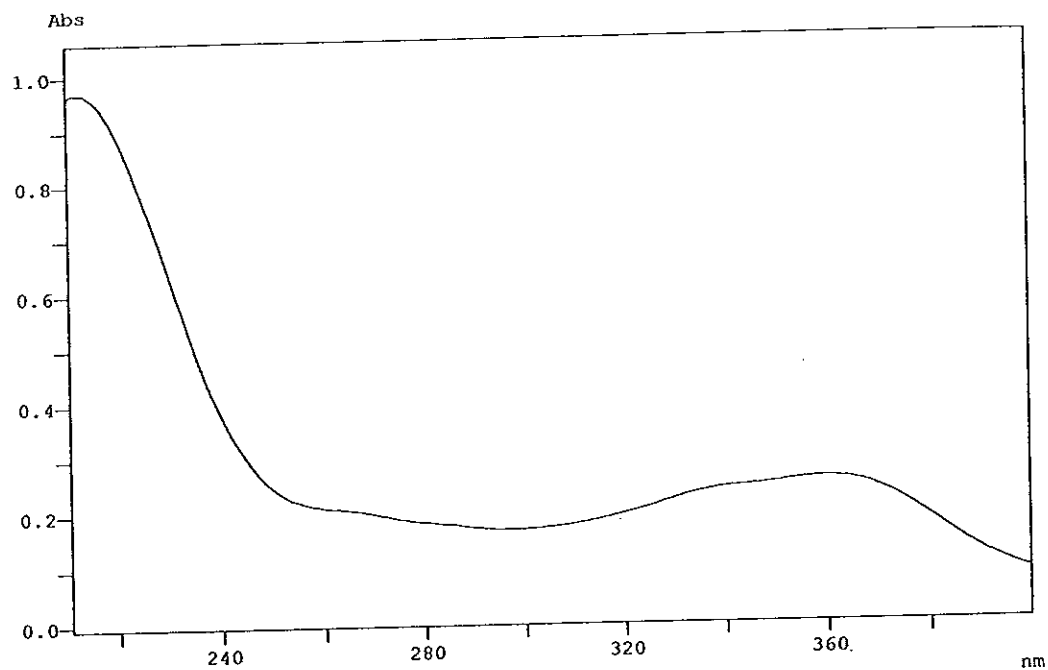


Figure 6 UV (MeOH) spectrum of PP9

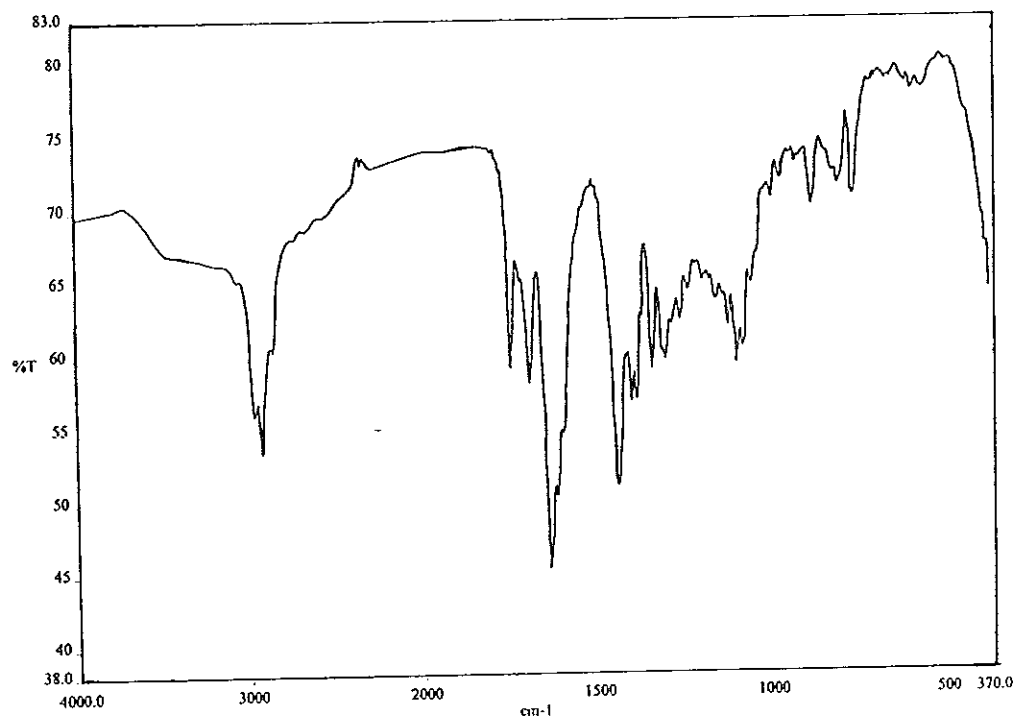


Figure 7 FT-IR (neat) spectrum of PP9

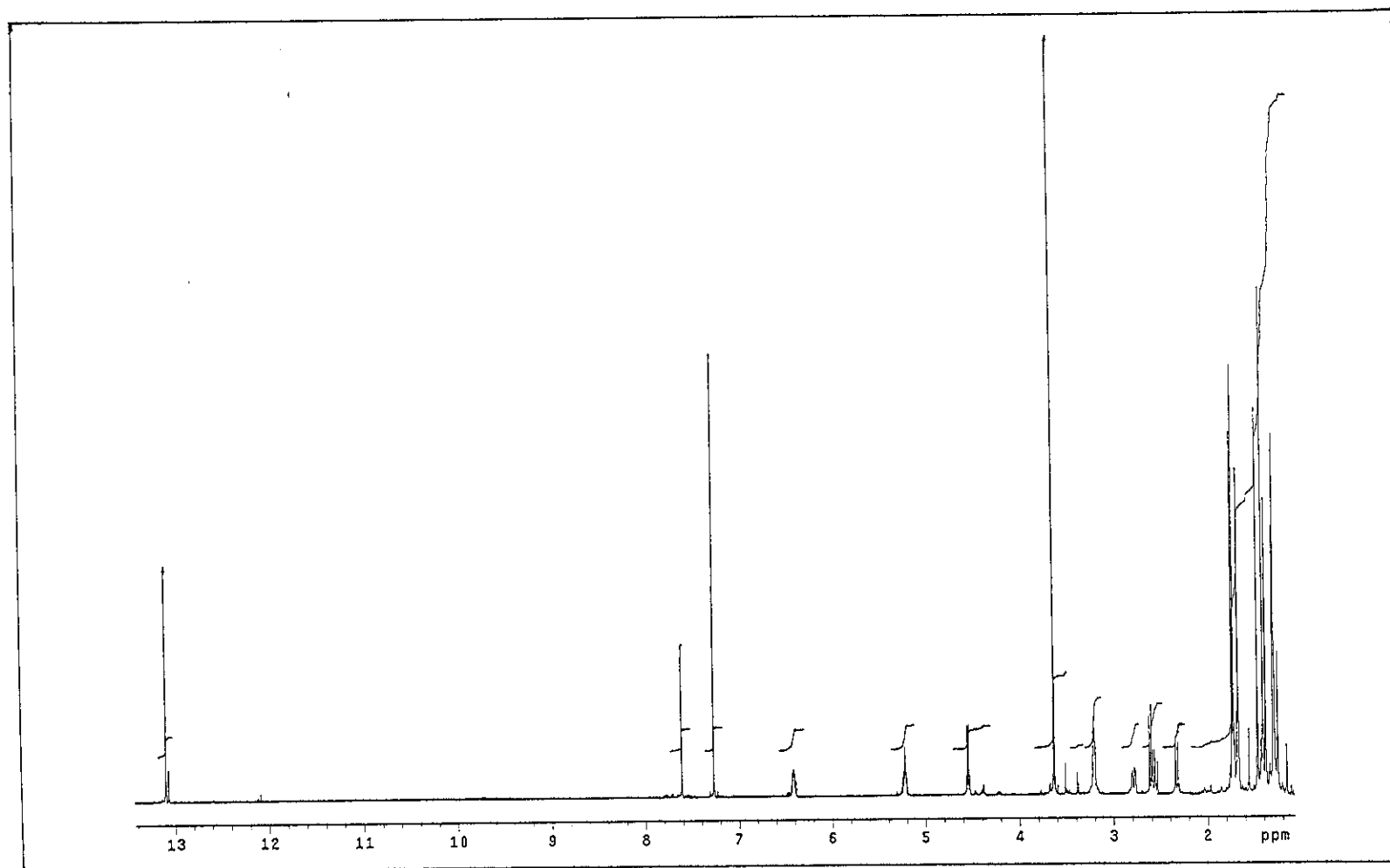


Figure 8 ^1H NMR (500 MHz) (CDCl_3) spectrum of PP9

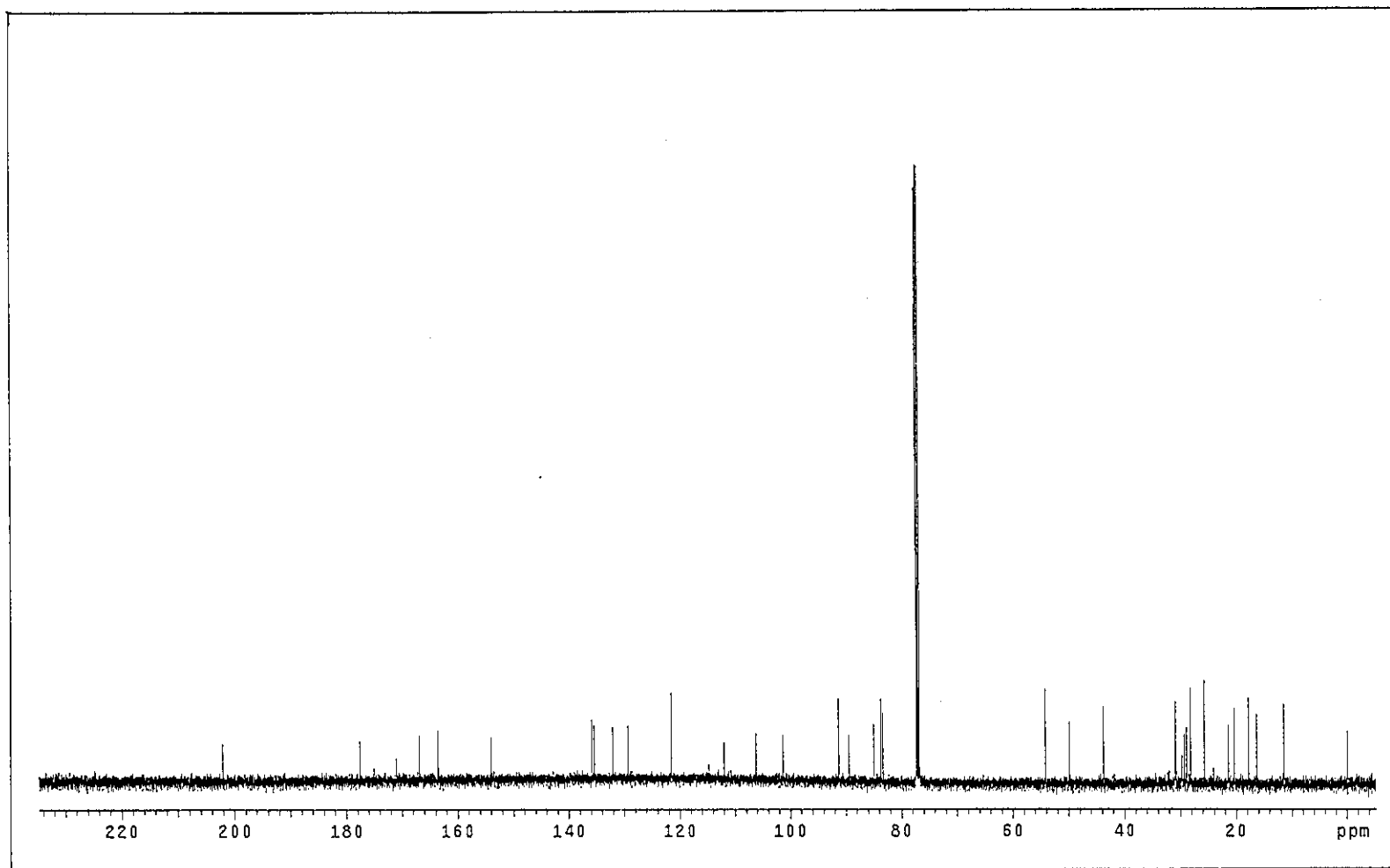


Figure 9 ^{13}C NMR (125 MHz) (CDCl_3) spectrum of PP9

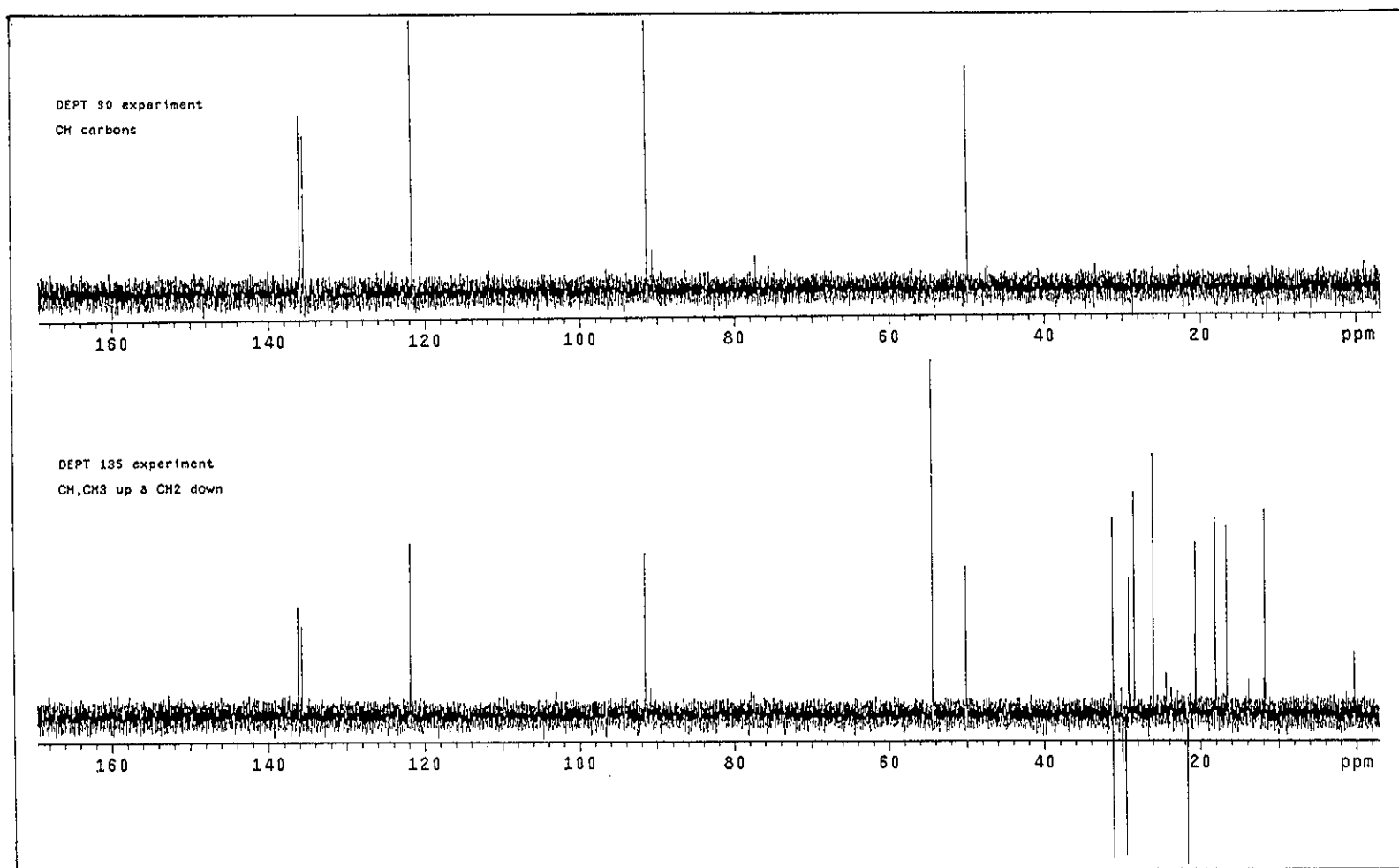


Figure 10 DEPT spectrum of PP9

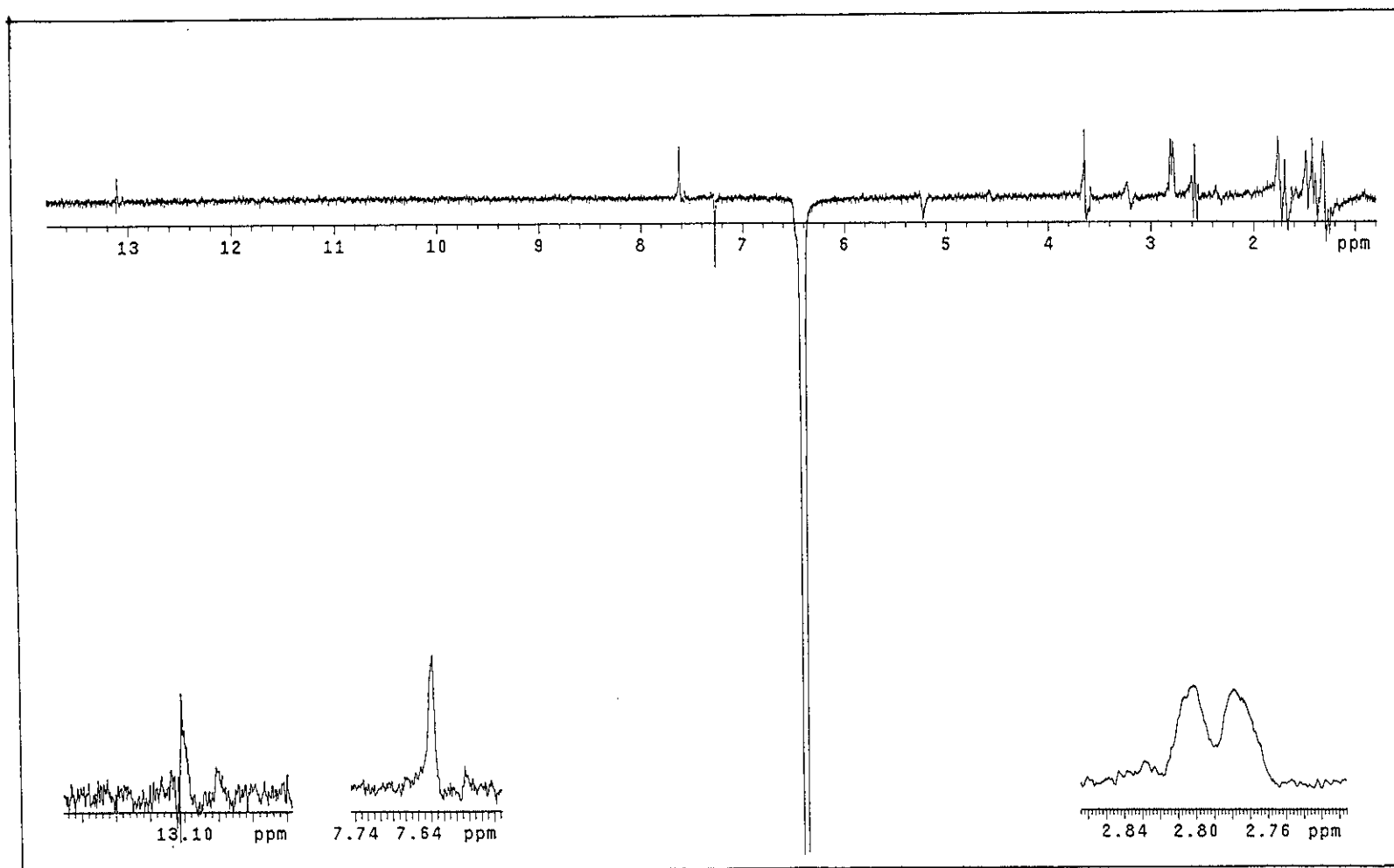


Figure 11 NOEDIFF spectrum of PP9 after irradiation at δ_H 6.41

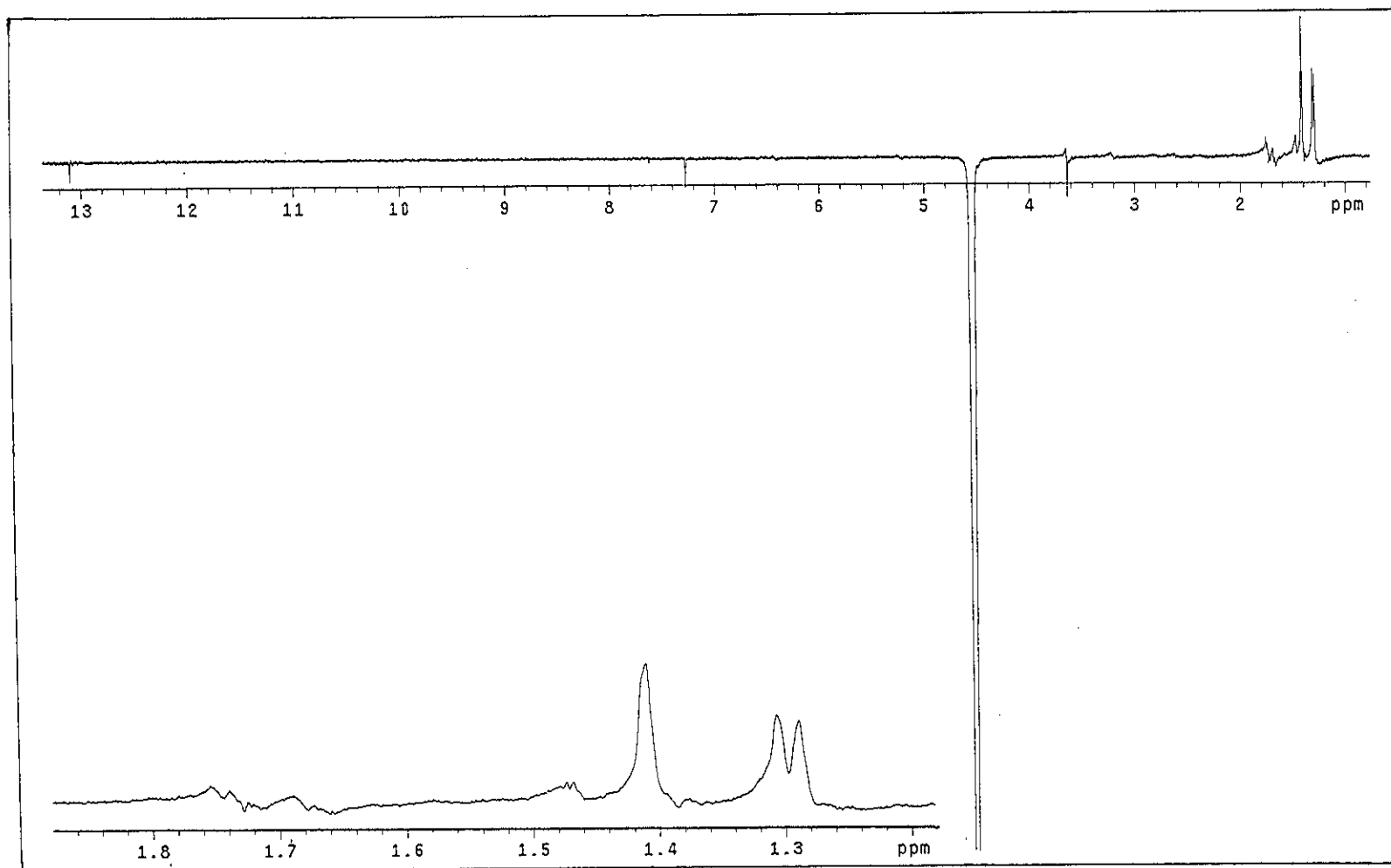


Figure 12 NOEDIFF spectrum of PP9 after irradiation at δ_H 4.54

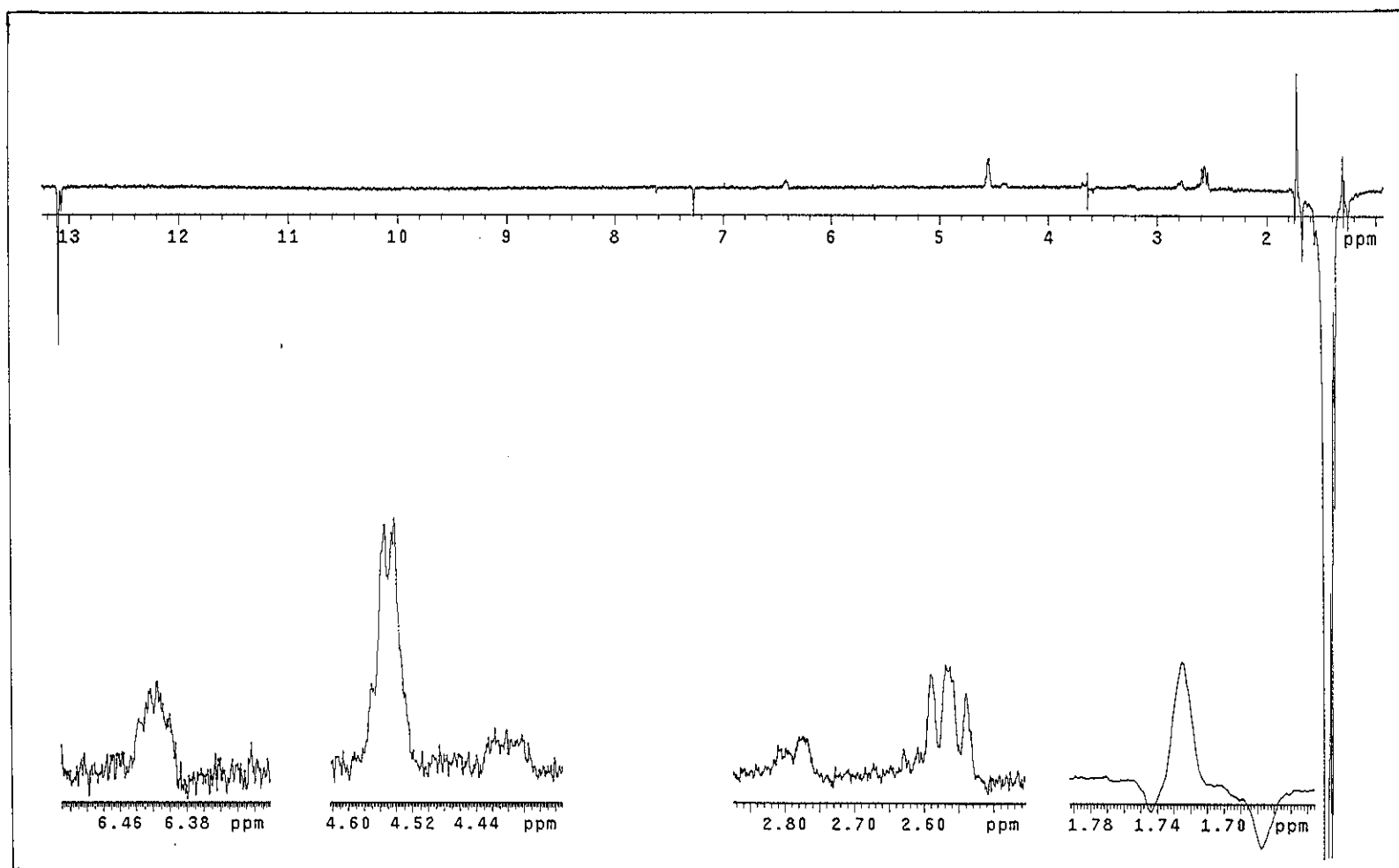


Figure 13 NOEDIFF spectrum of PP9 after irradiation at δ_H 1.46

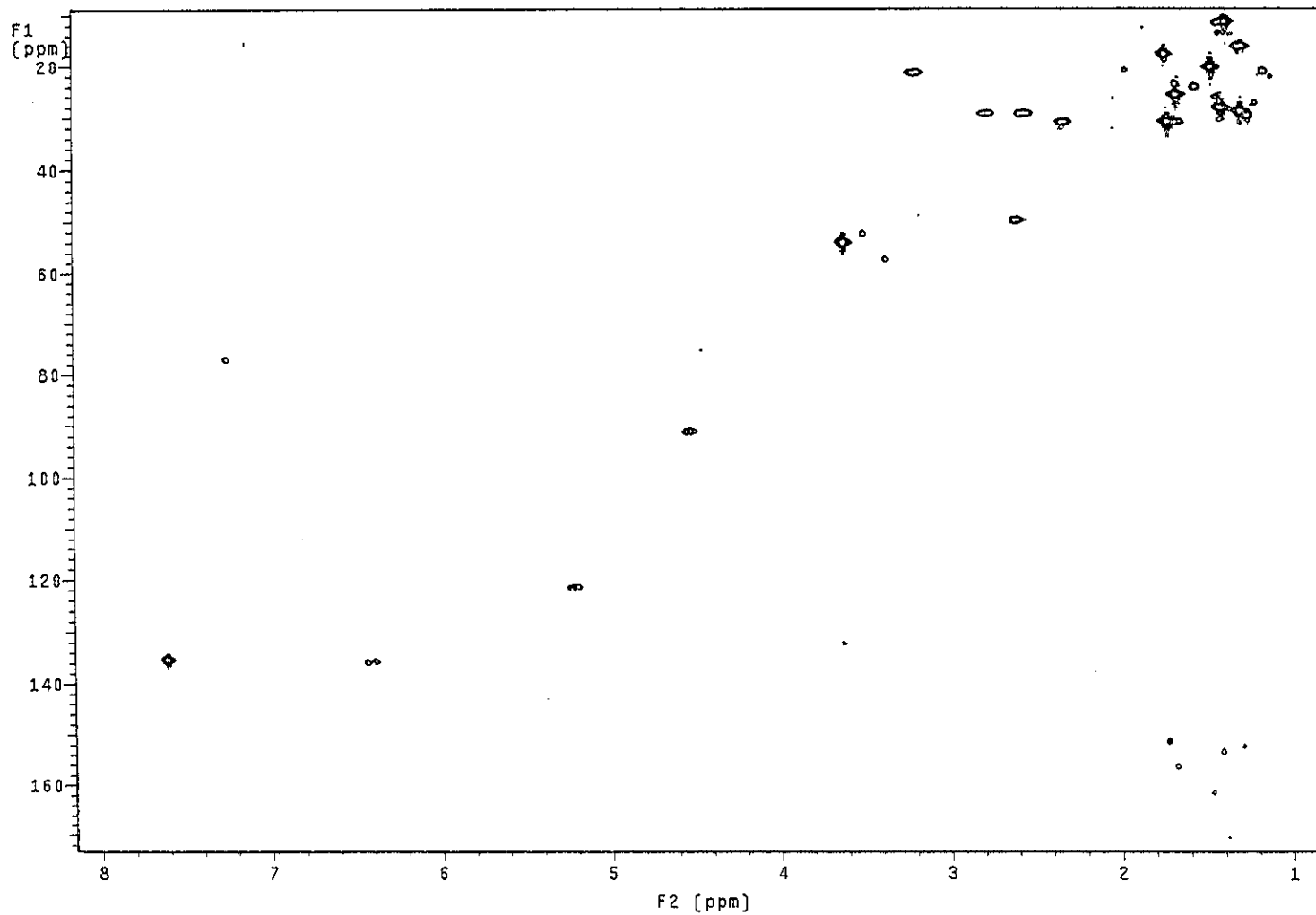


Figure 14 2D HMQC spectrum of PP9

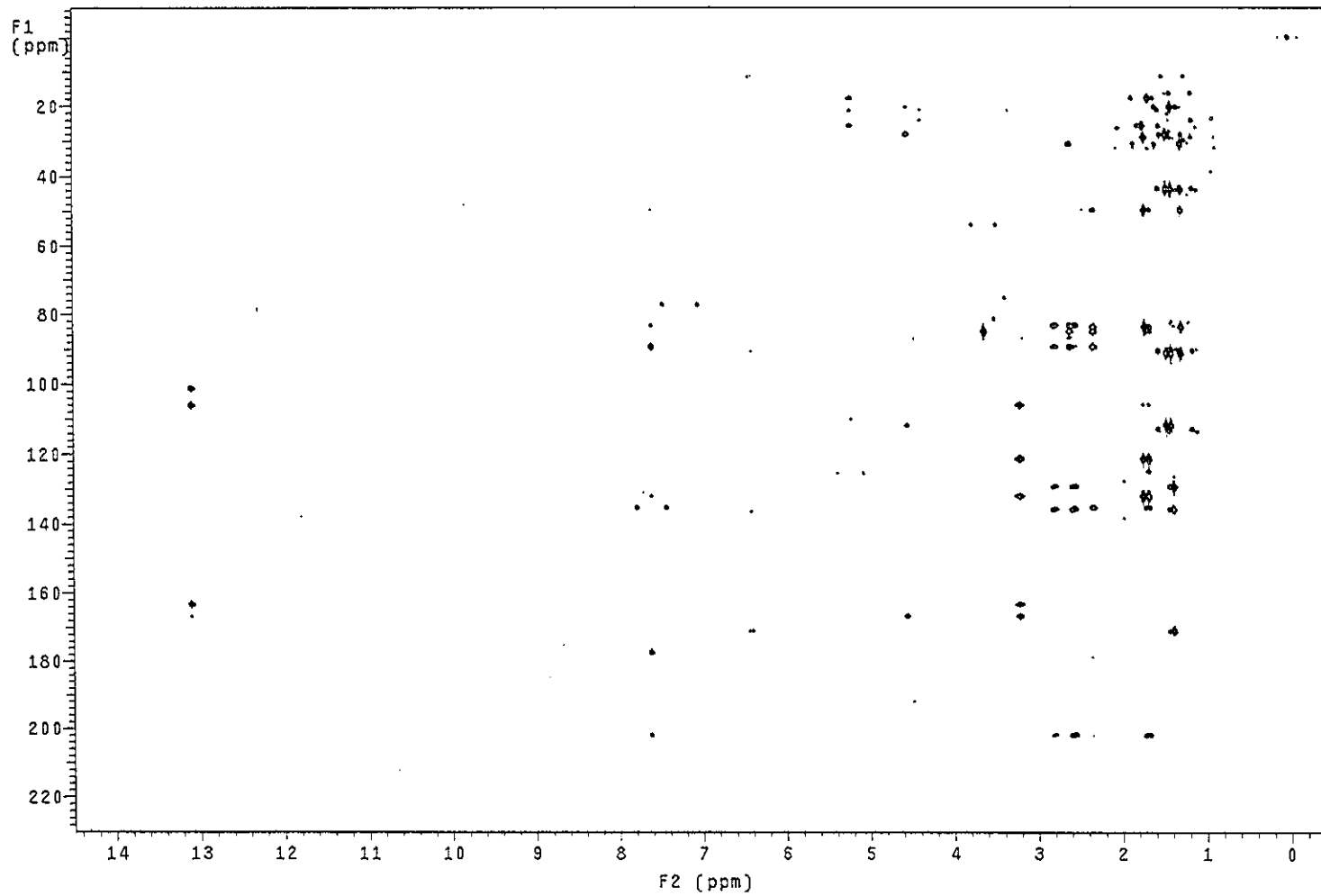


Figure 15 2D HMBC spectrum of PP9

Mass Peak # : 370 Ret. Time : (3.050 - 3.350)
Base Peak : 101.00 (69819) .

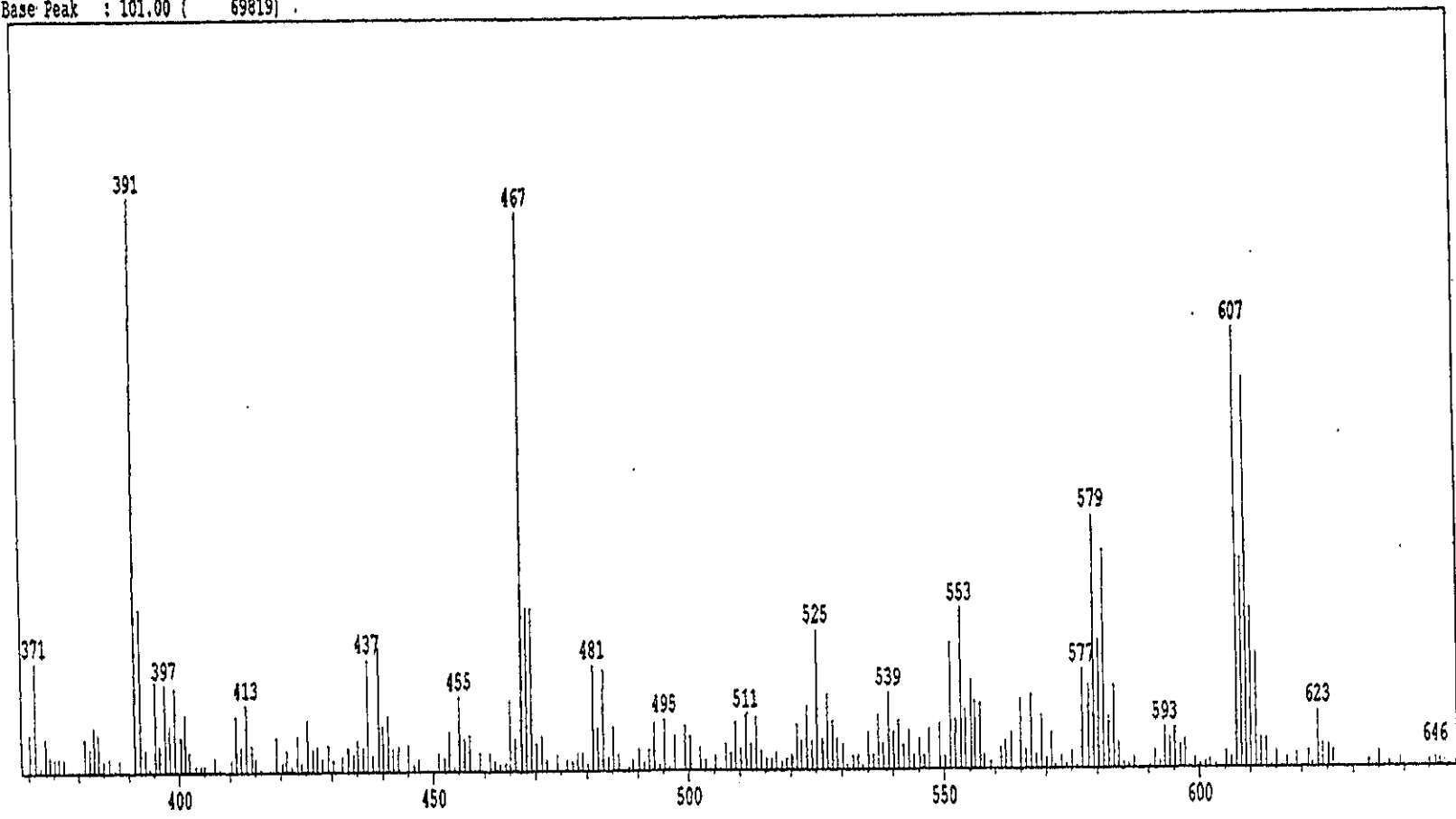


Figure 16 Mass spectrum of PP5

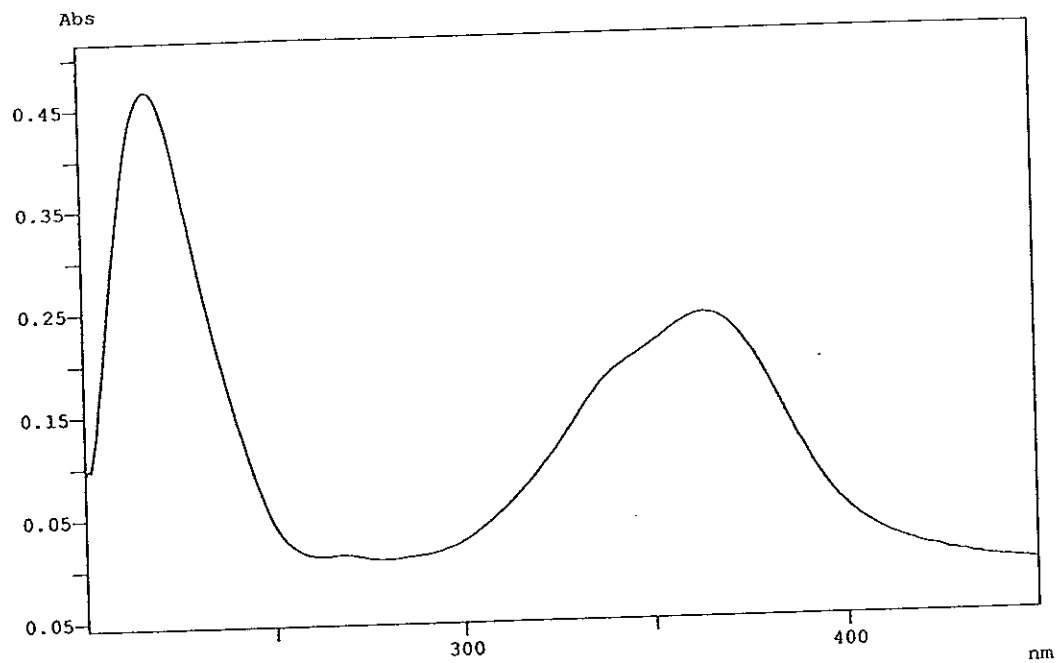


Figure 17 UV (MeOH) spectrum of PP5

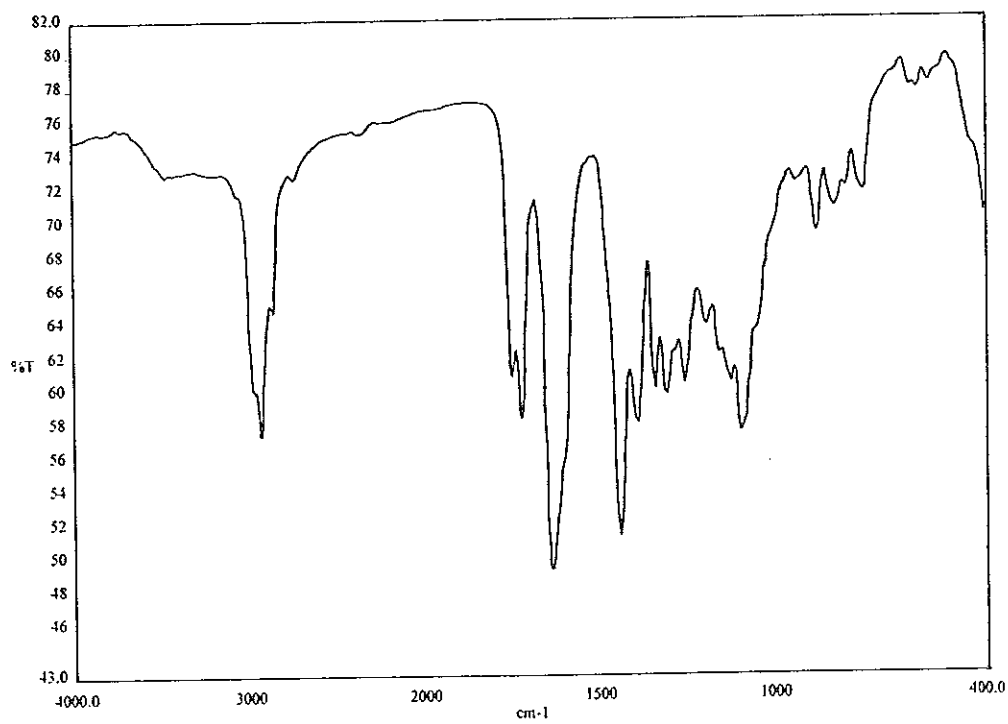


Figure 18 FT-IR (neat) spectrum of PP5

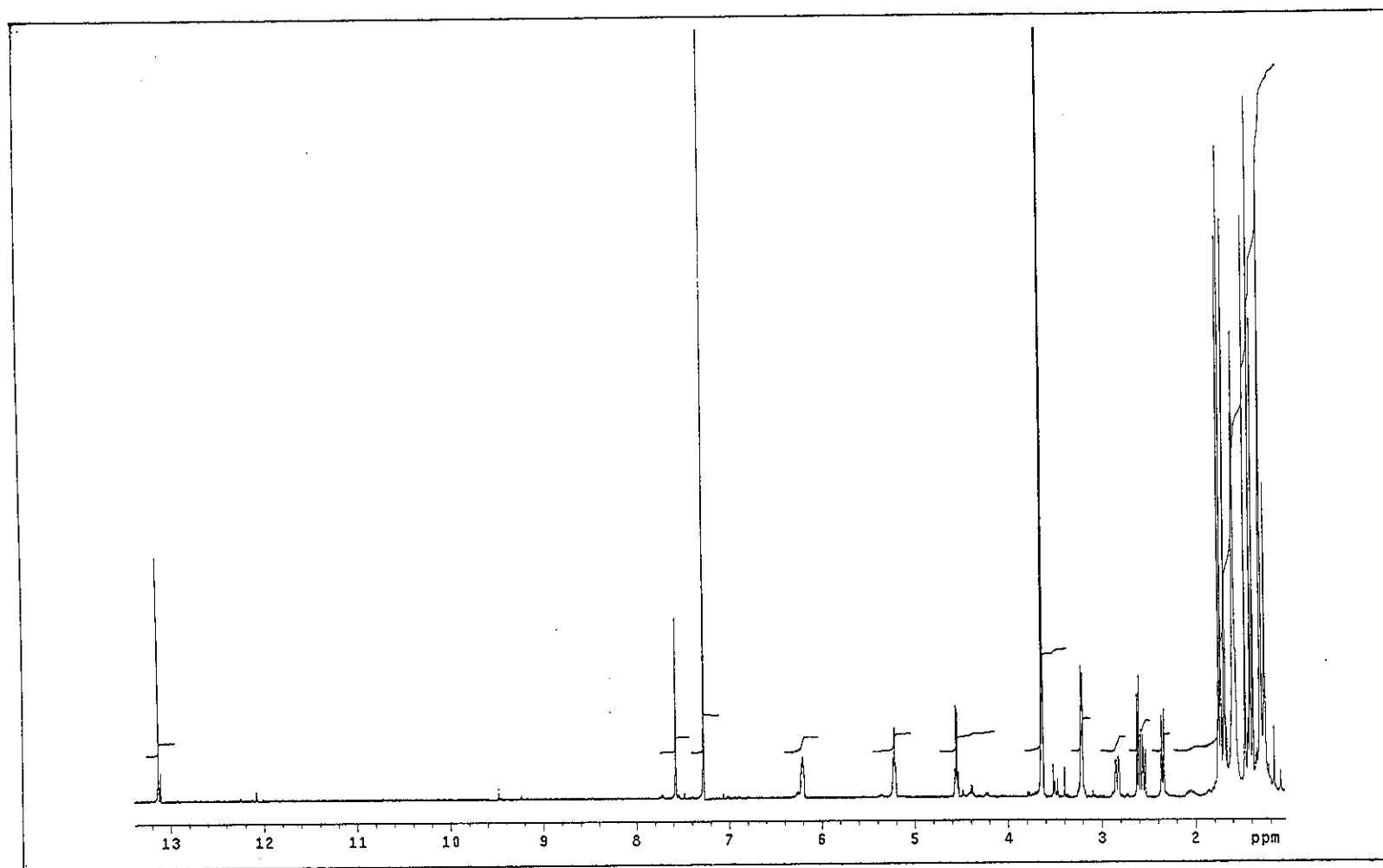


Figure 19 ^1H NMR (500 MHz) (CDCl_3) spectrum of PP5

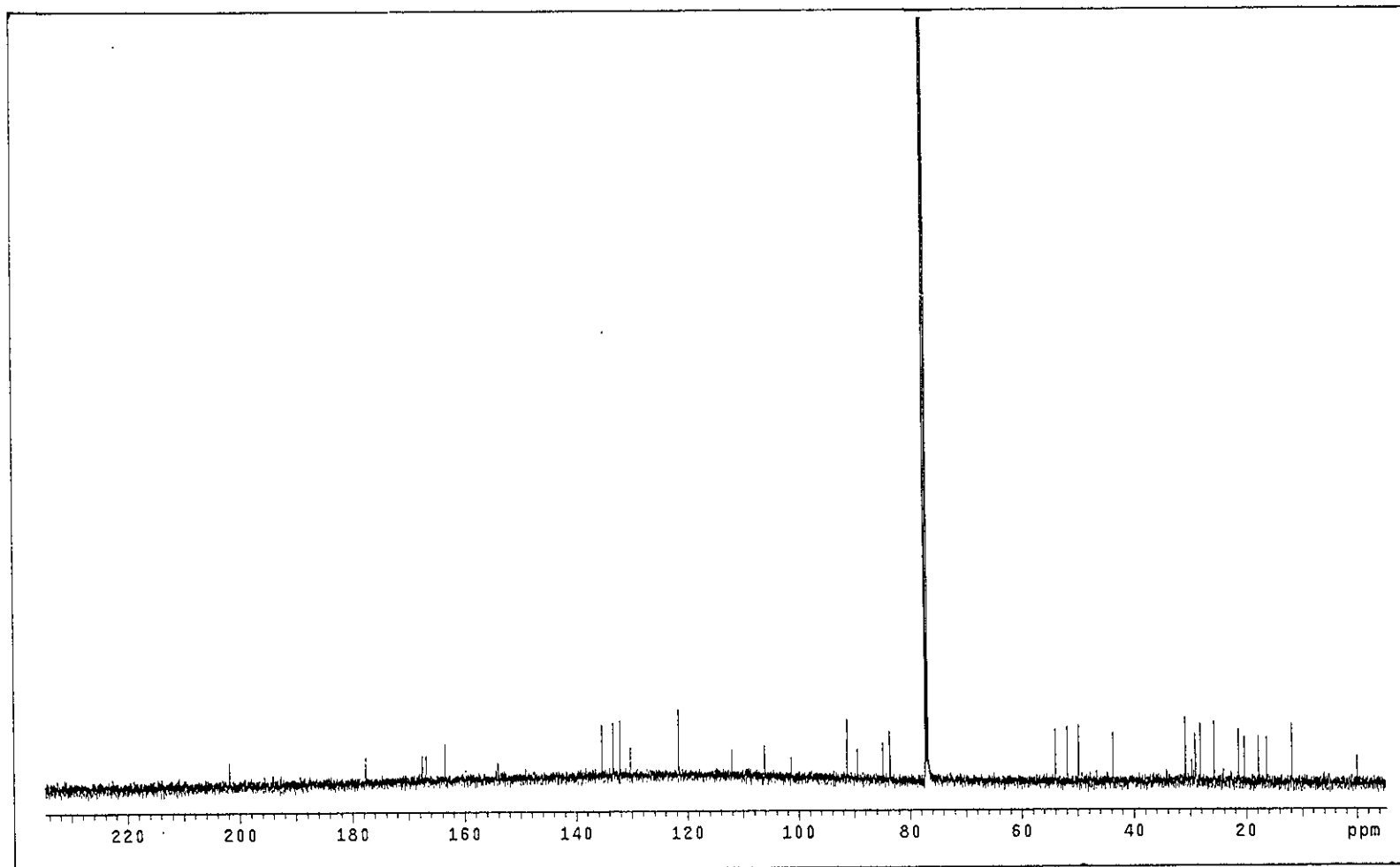


Figure 20 ^{13}C NMR (125 MHz) (CDCl_3) spectrum of PP5

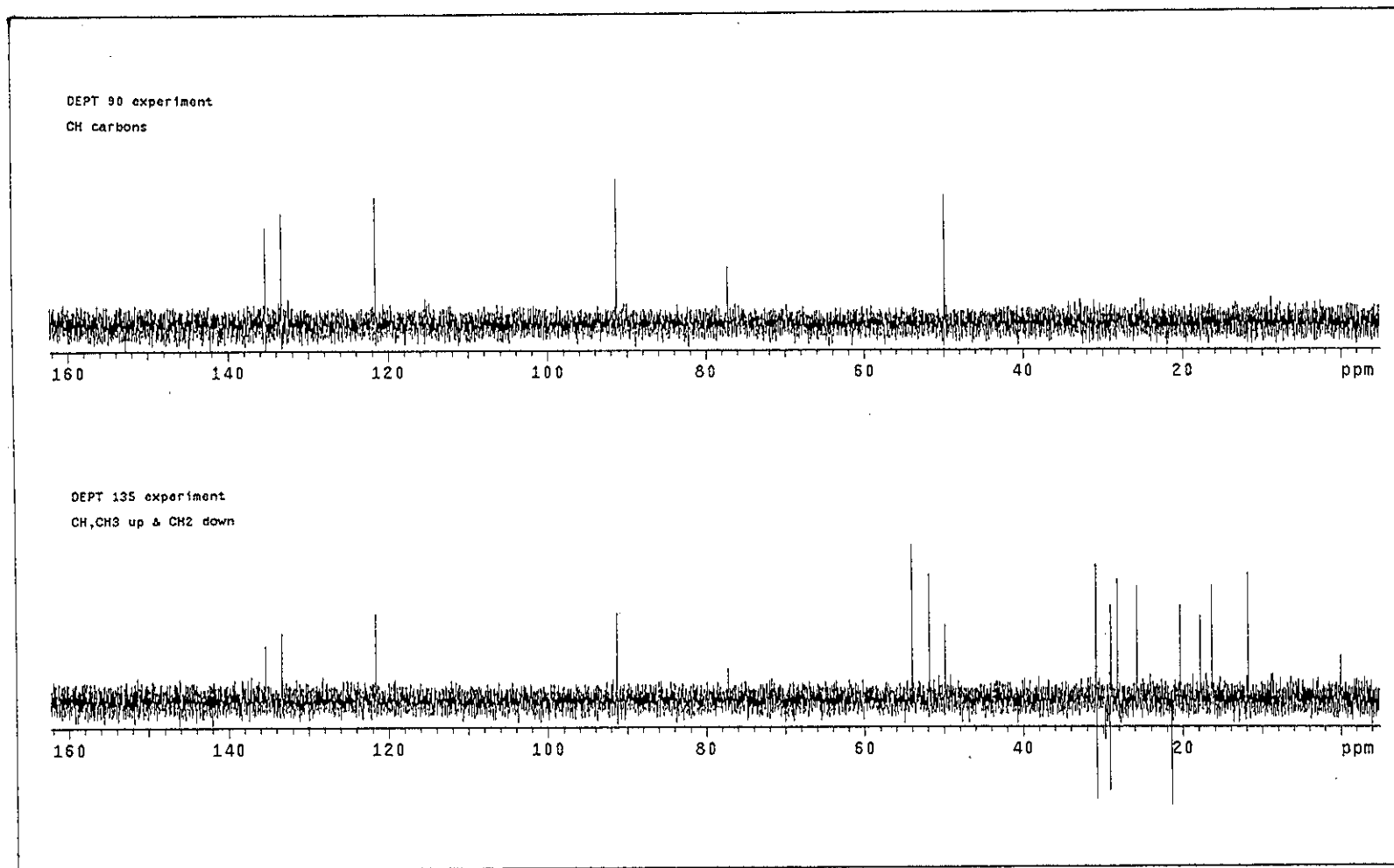


Figure 21 DEPT spectrum of PP5

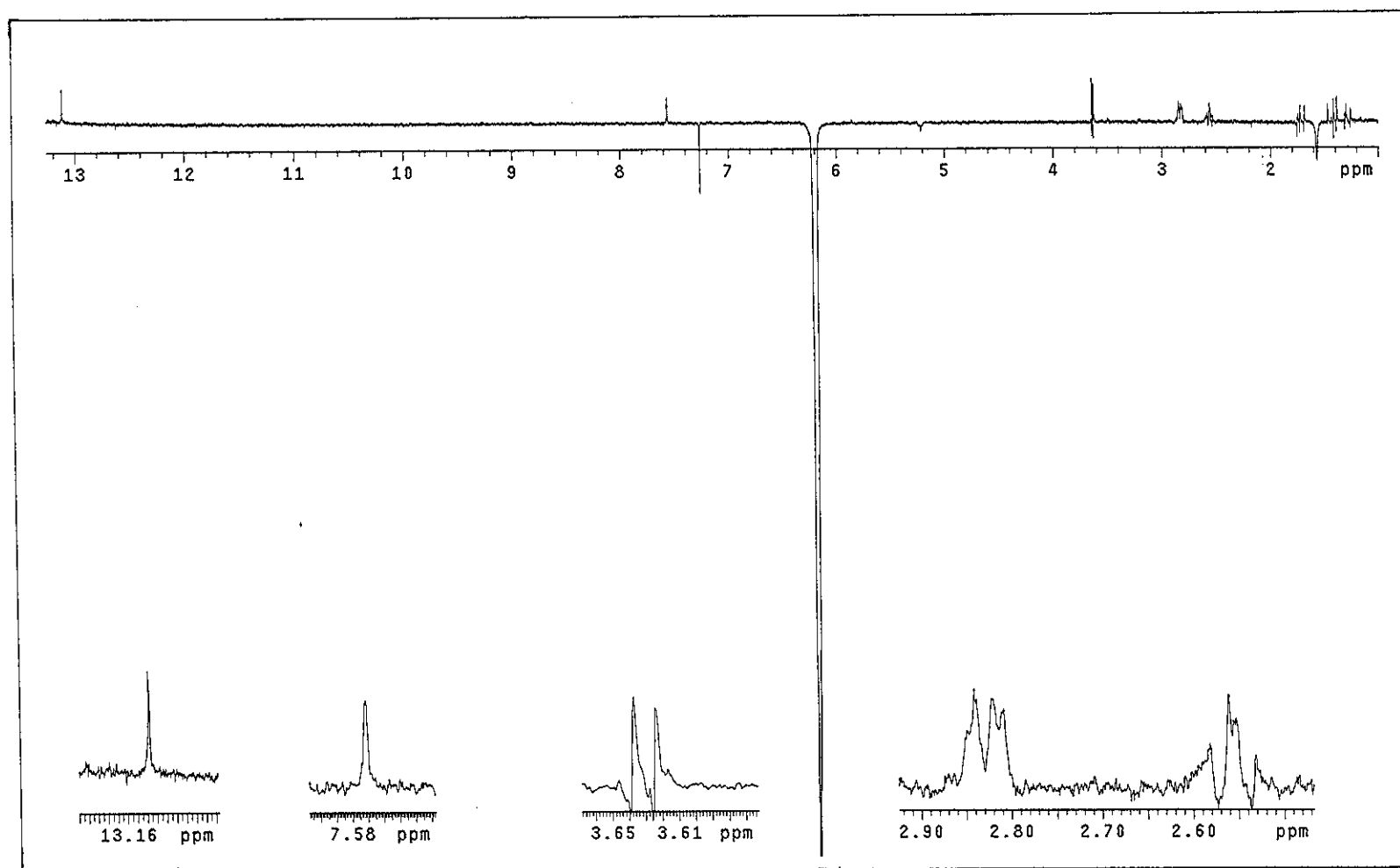


Figure 22 NOEDIFF spectrum of PP5 after irradiation at δ_H 6.20

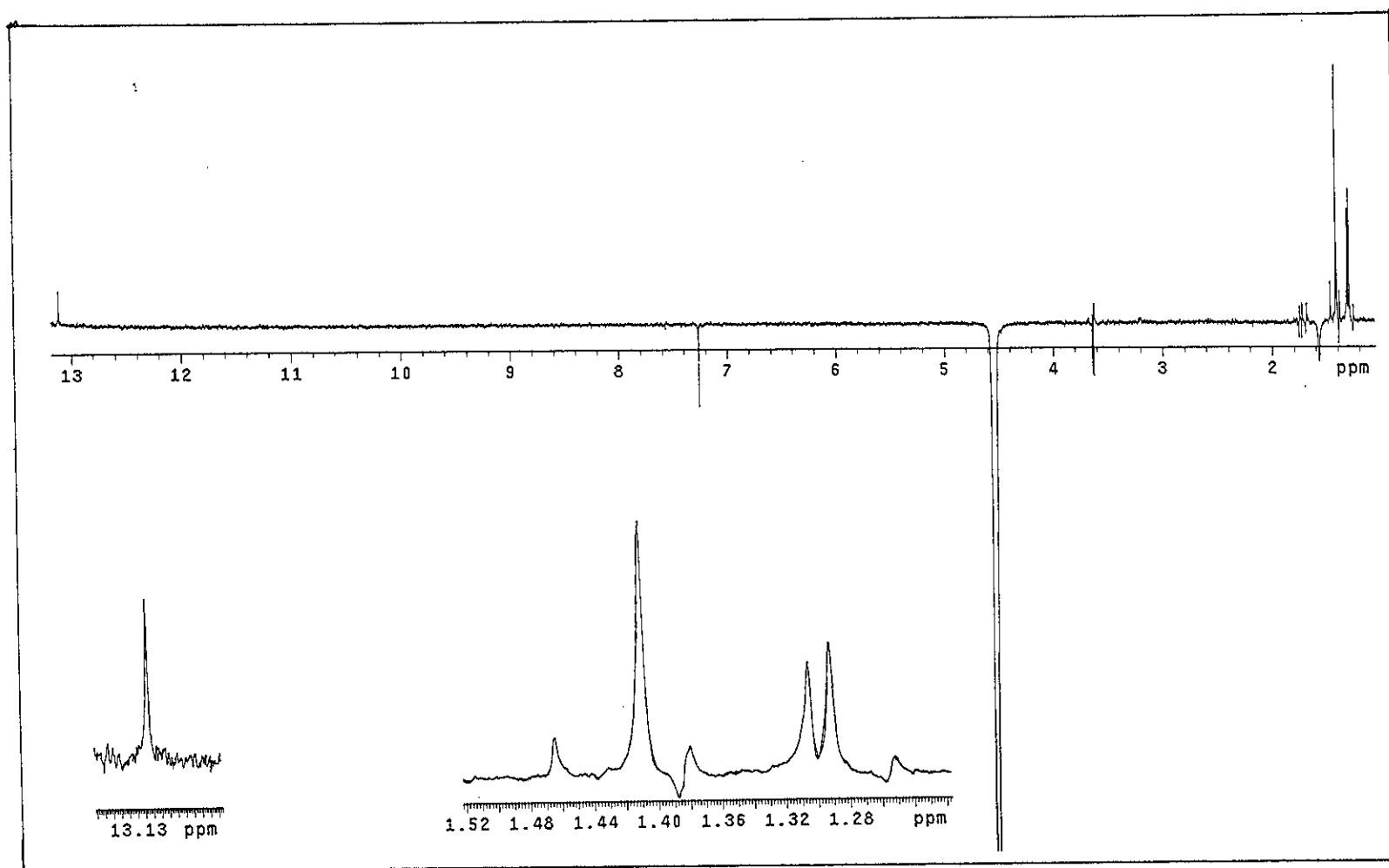


Figure 23 NOEDIFF spectrum of PP5 after irradiation at δ_H 4.55

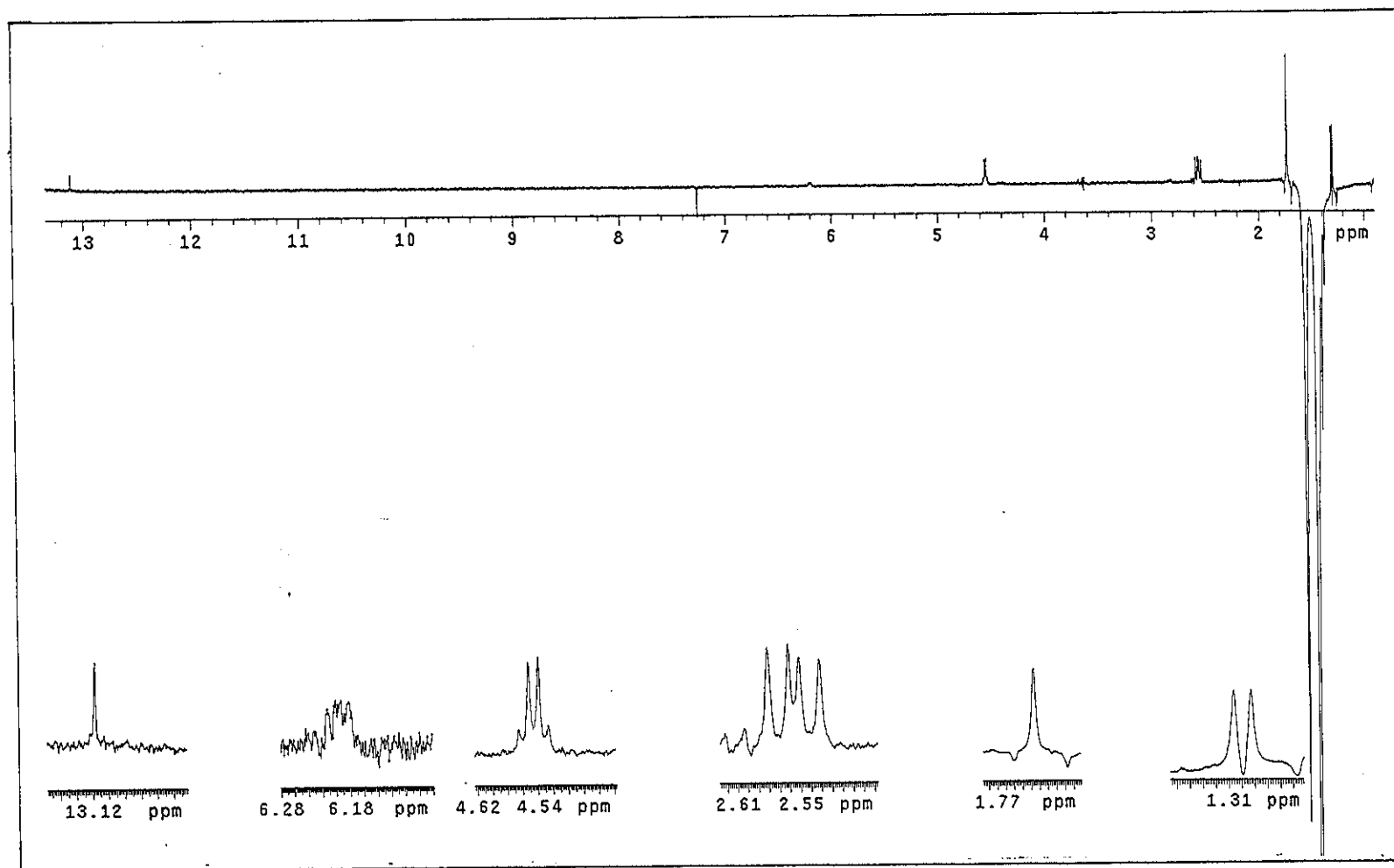


Figure 24 NOEDIFF spectrum of PP5 after irradiation at δ_H 1.47

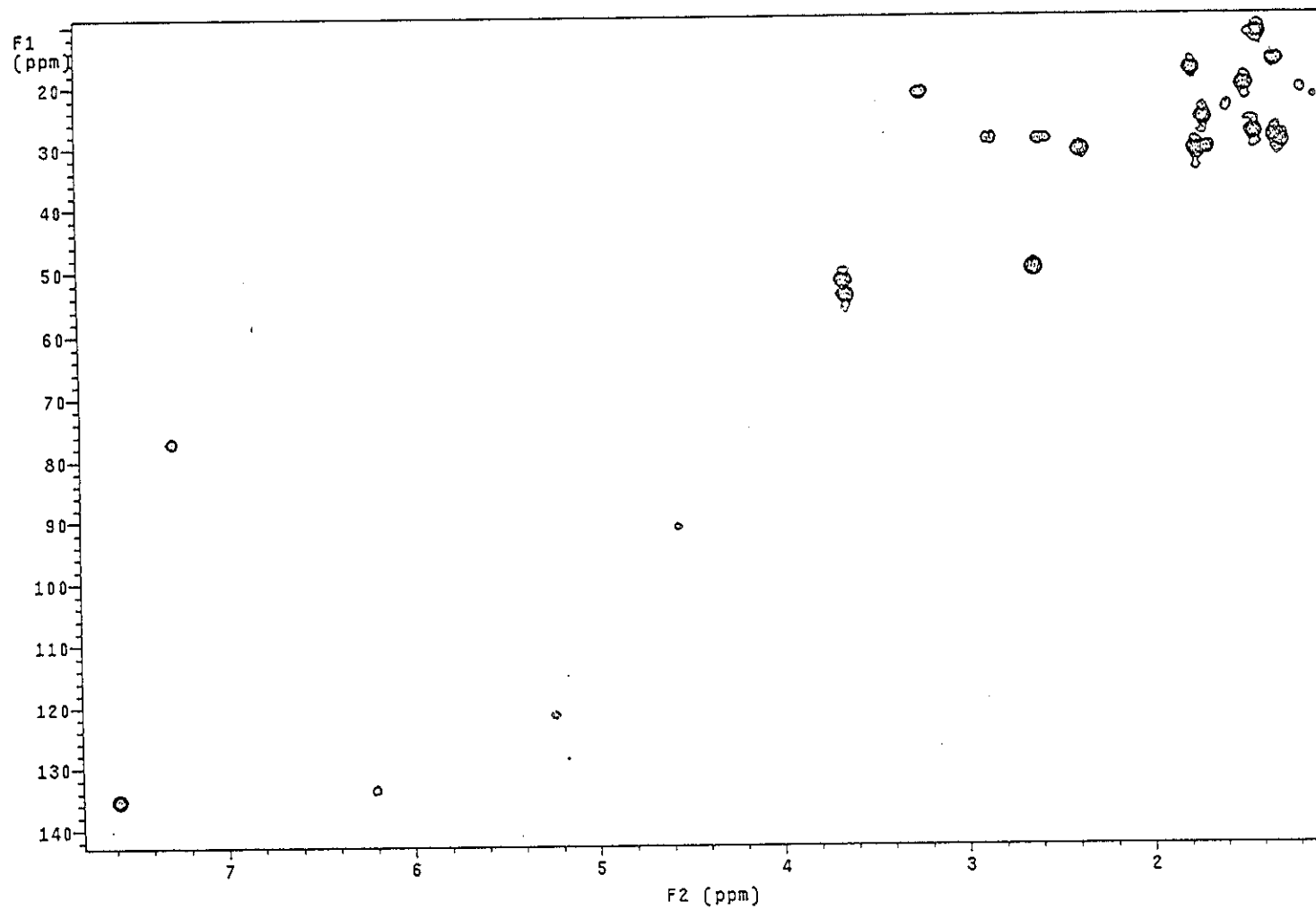


Figure 25 2D HMQC spectrum of PP5

Mass Peak #: 569 Ret. Time: (1.333 - 1.598)
Base Peak : 148.95 (10720722)

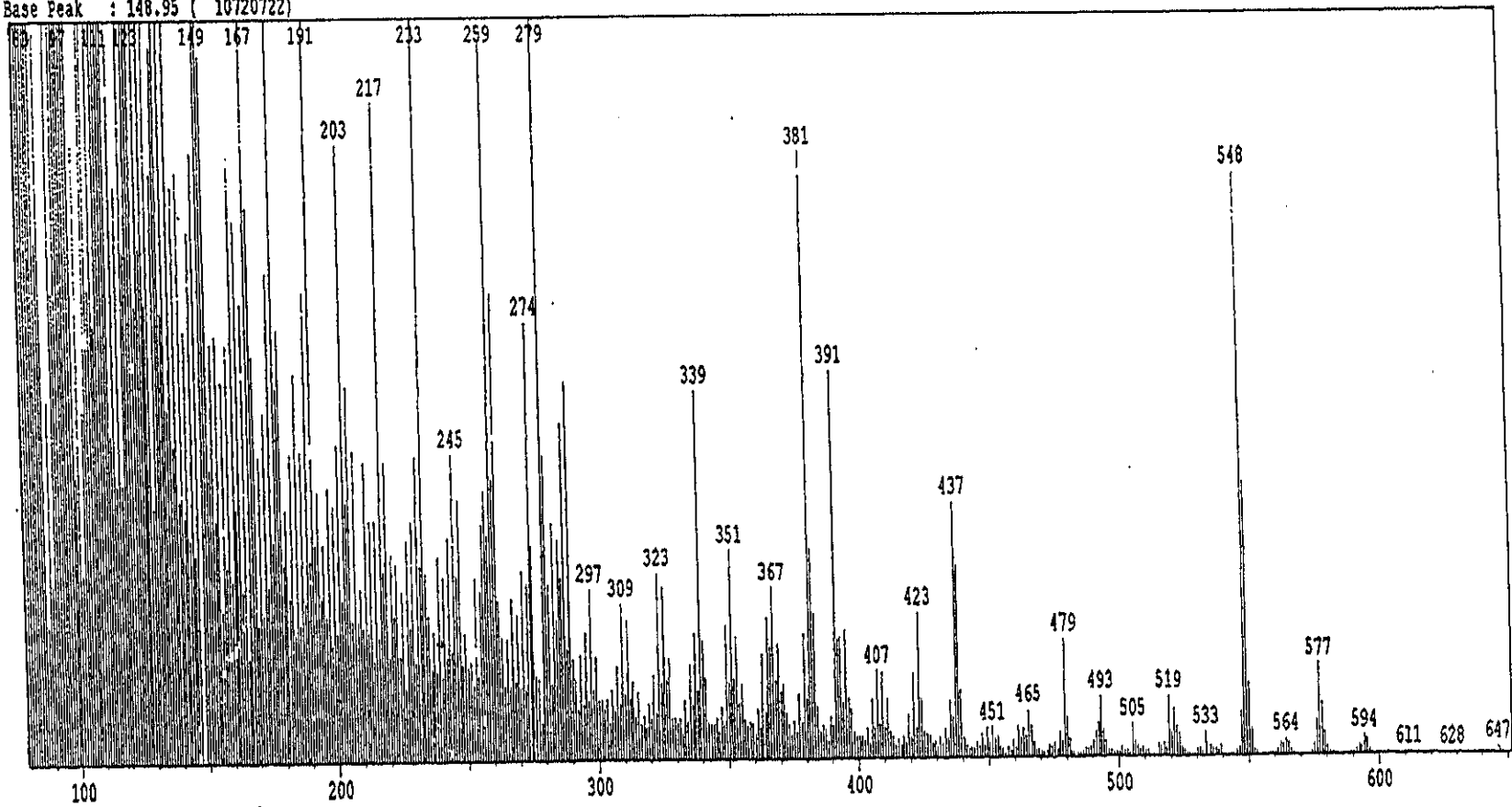


Figure 27 Mass spectrum of PP6

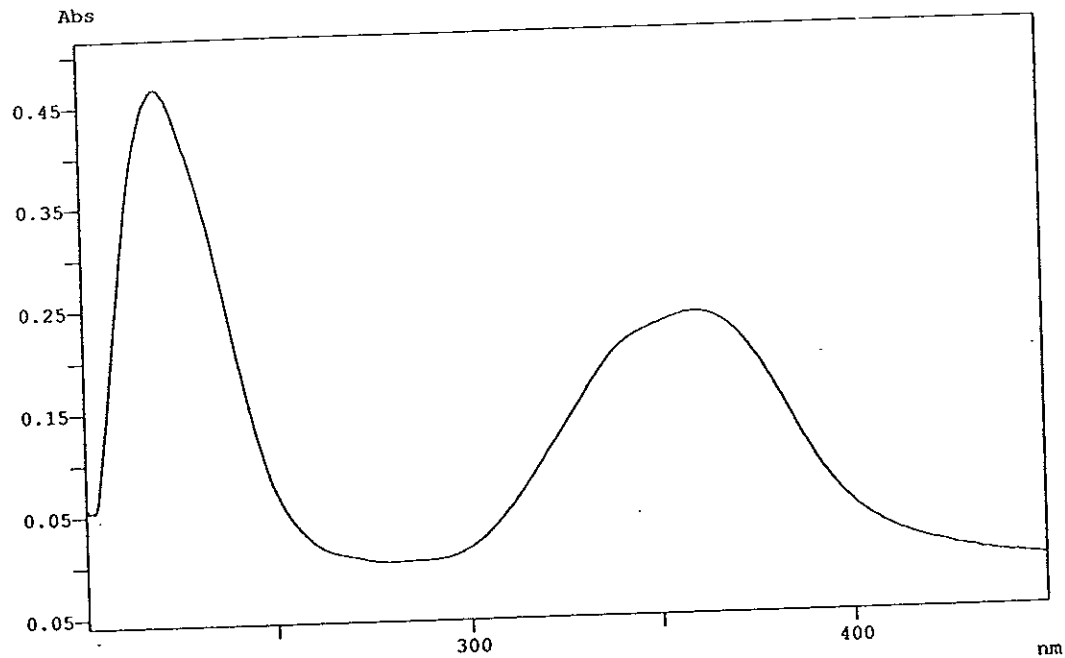


Figure 28 UV (MeOH) spectrum of PP6

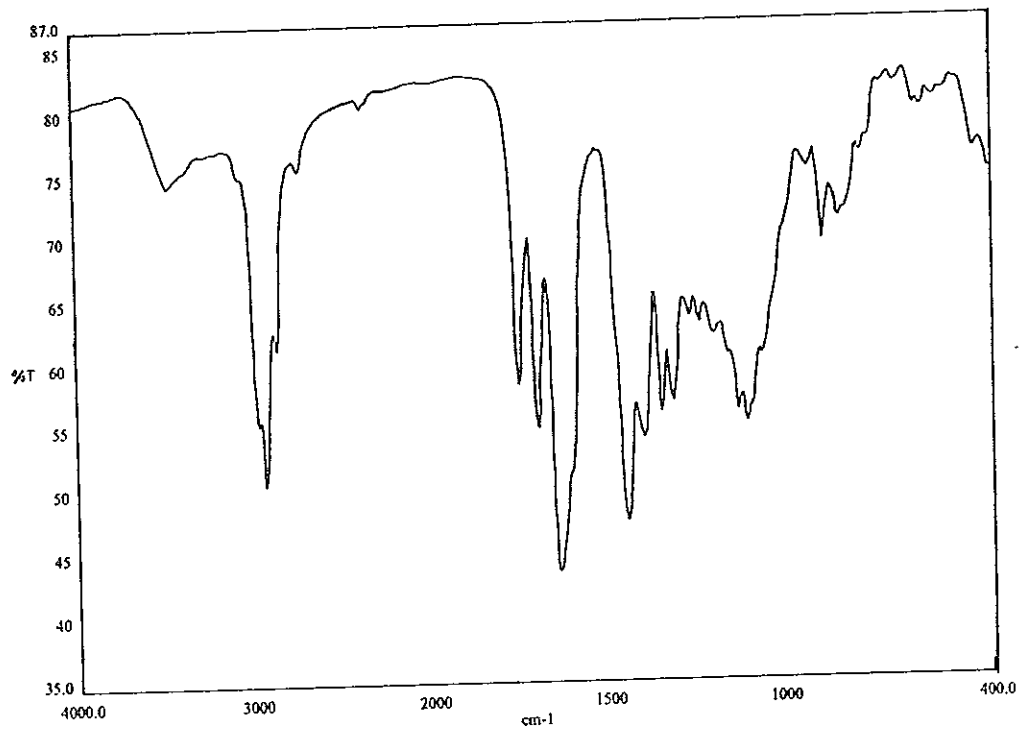


Figure 29 FT-IR (neat) spectrum of PP6

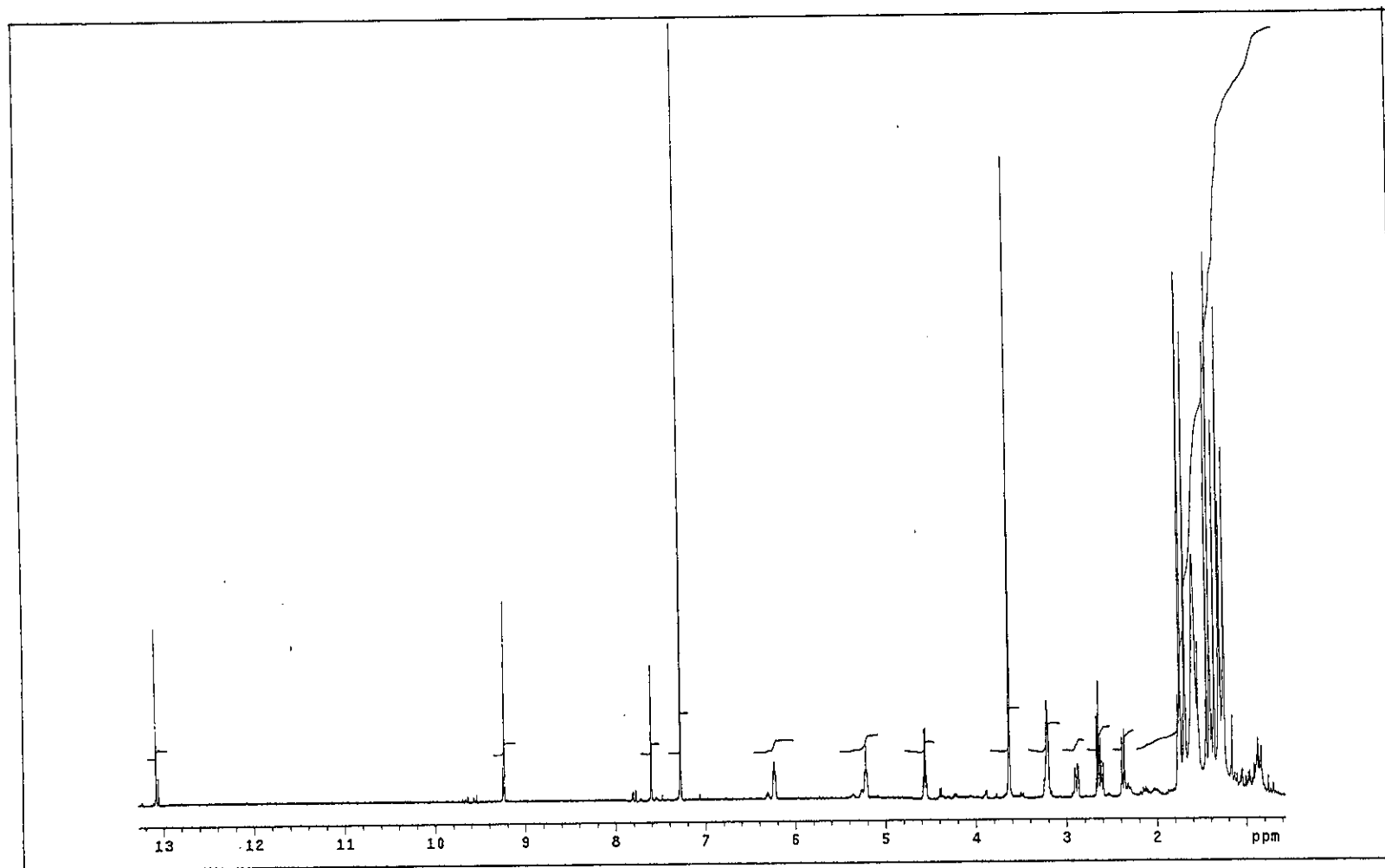


Figure 30 ^1H NMR (500 MHz) (CDCl_3) spectrum of PP6

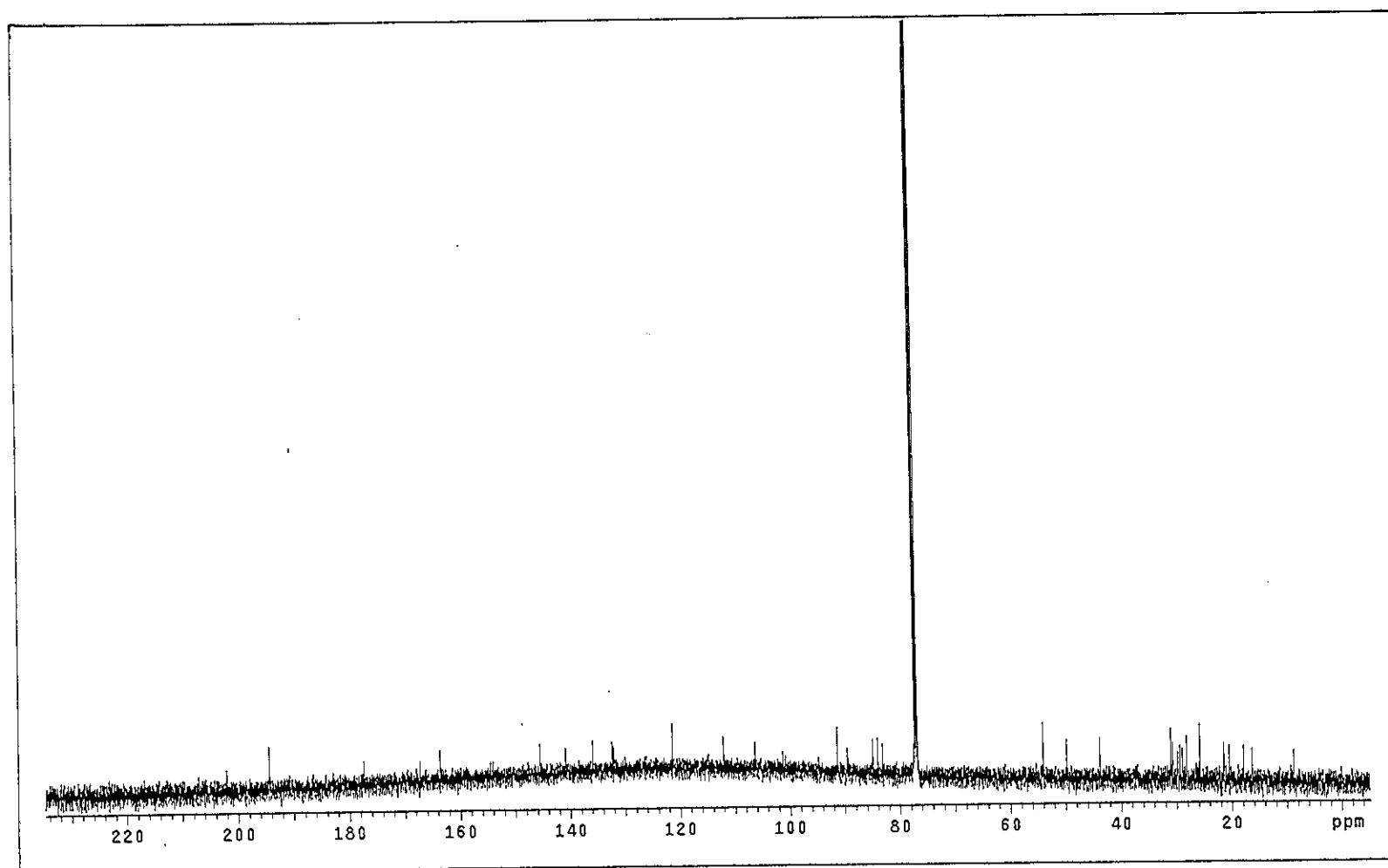


Figure 31 ^{13}C NMR (125 MHz) (CDCl_3) spectrum of PP6

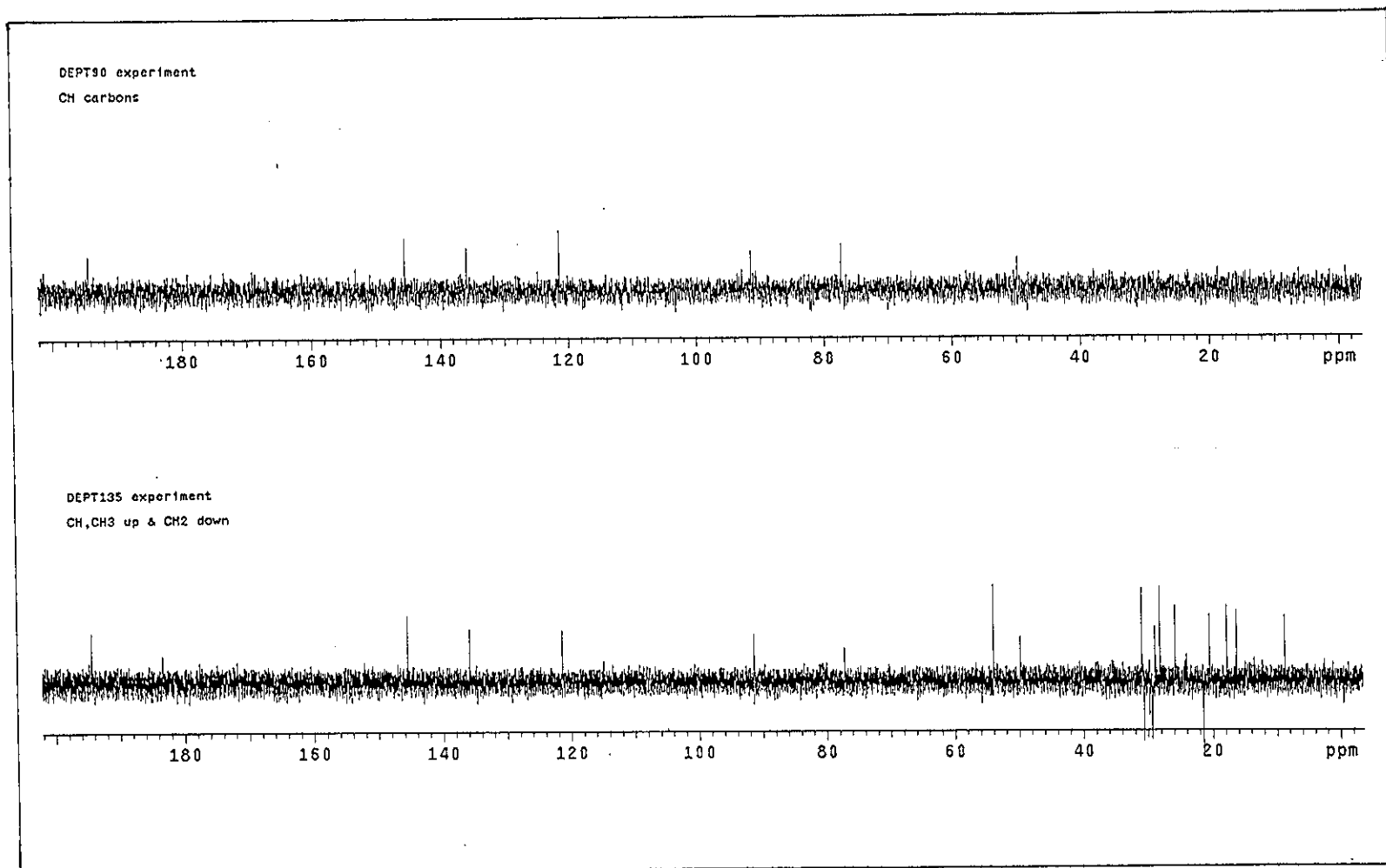


Figure 32 DEPT spectrum of PP6

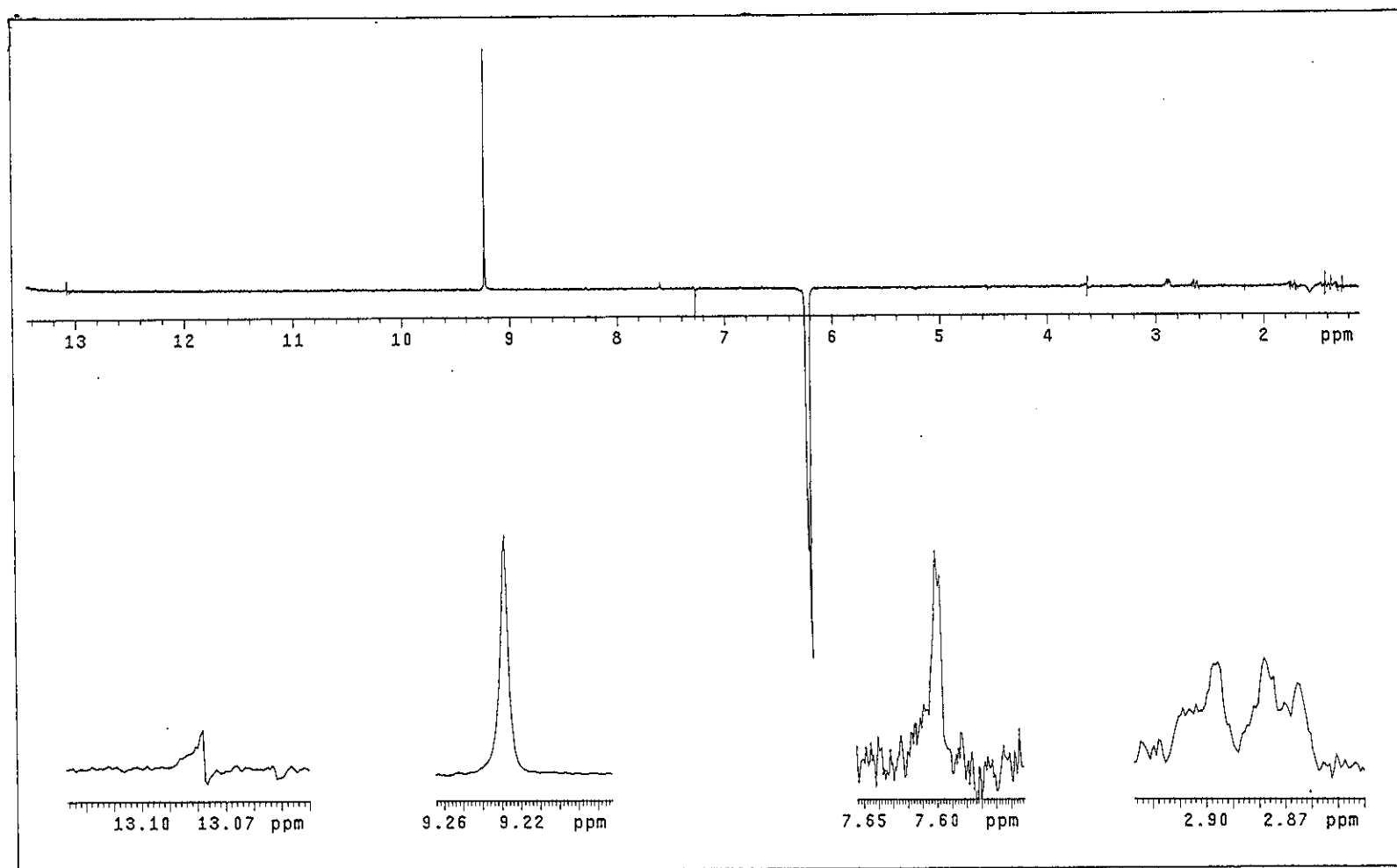


Figure 33 NOEDIFF spectrum of PP6 after irradiation at δ_H 6.23

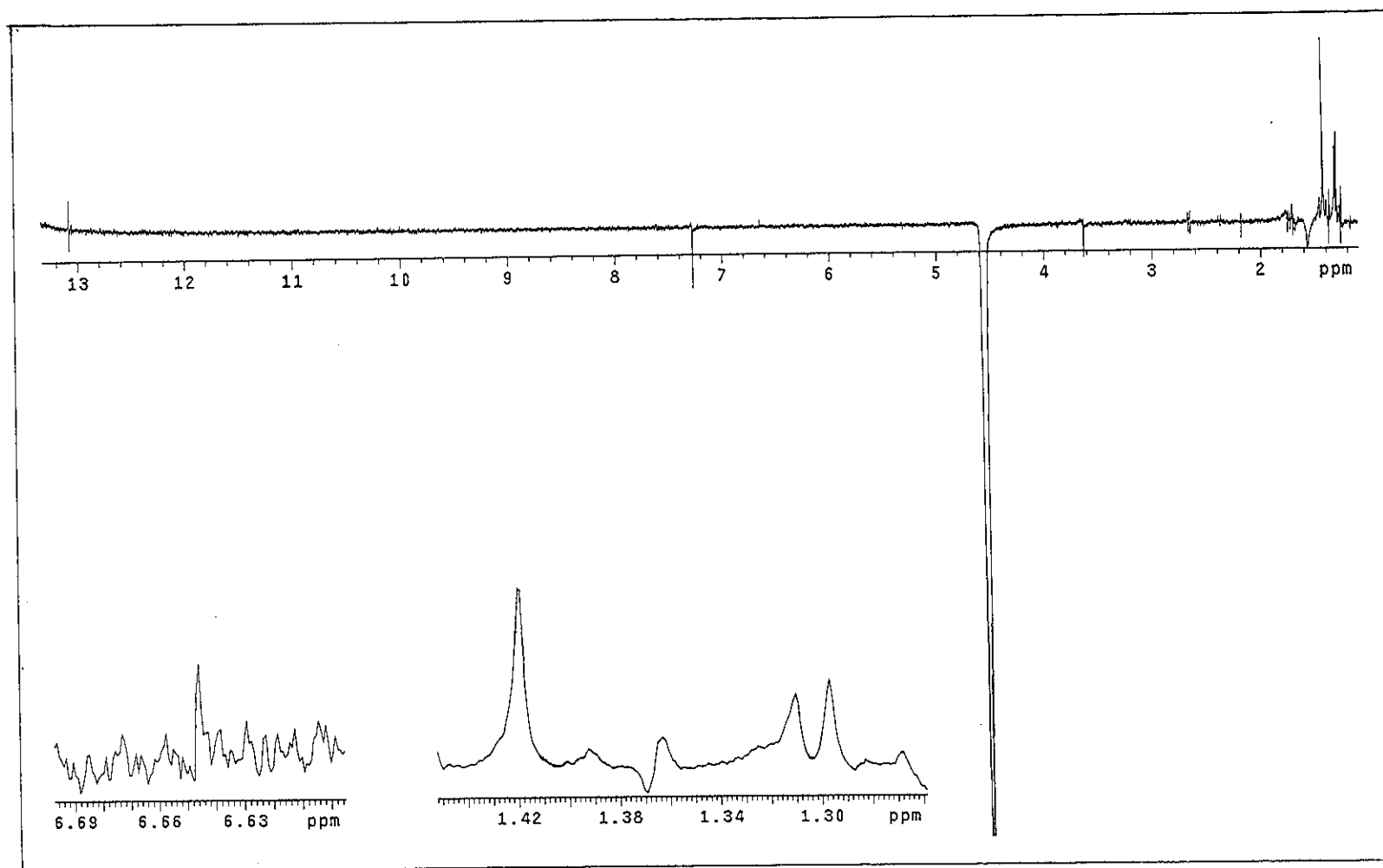


Figure 34 NOEDIFF spectrum of PP6 after irradiation at δ_H 4.56

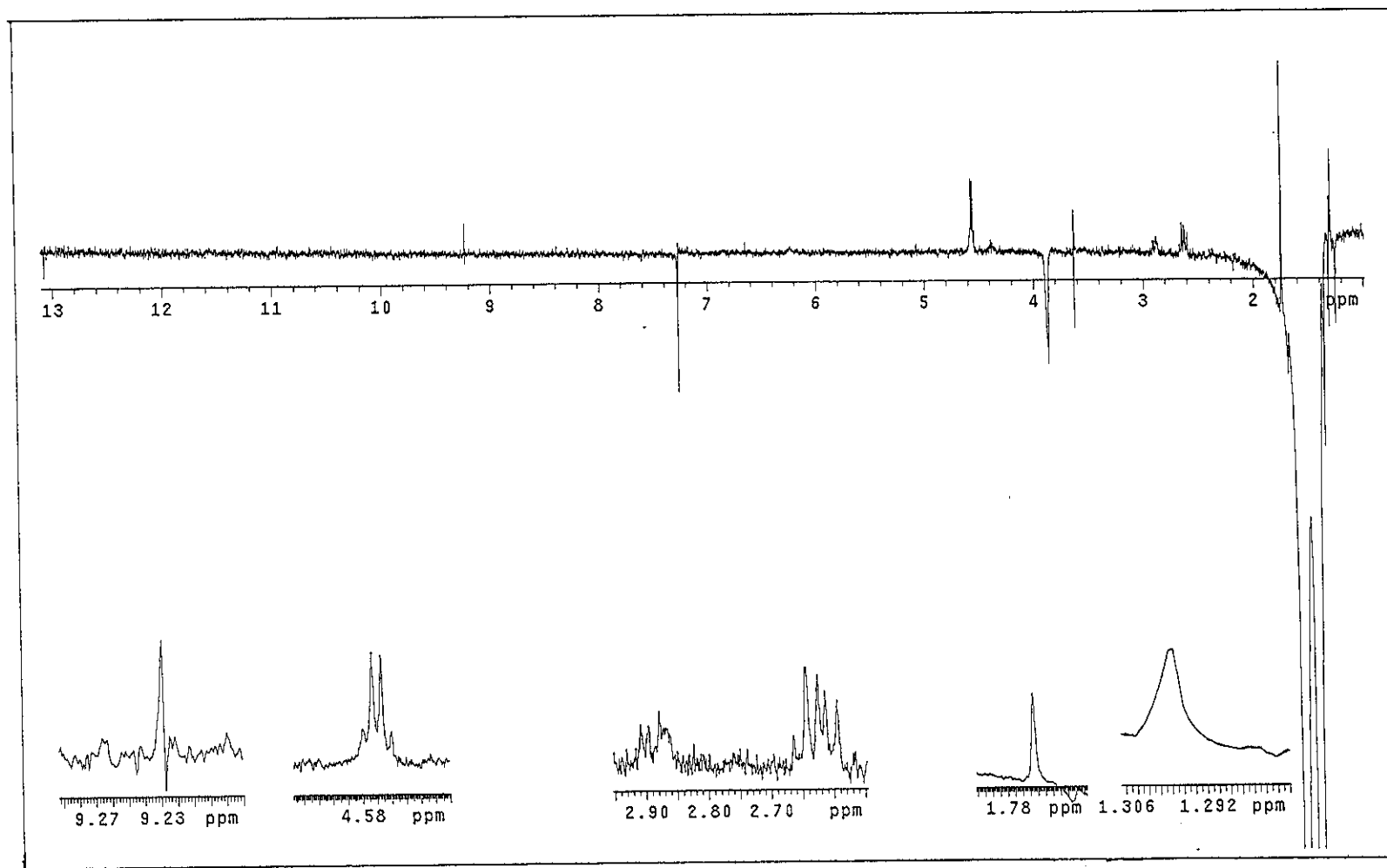


Figure 35 NOEDIFF spectrum of PP6 after irradiation at δ_H 1.45

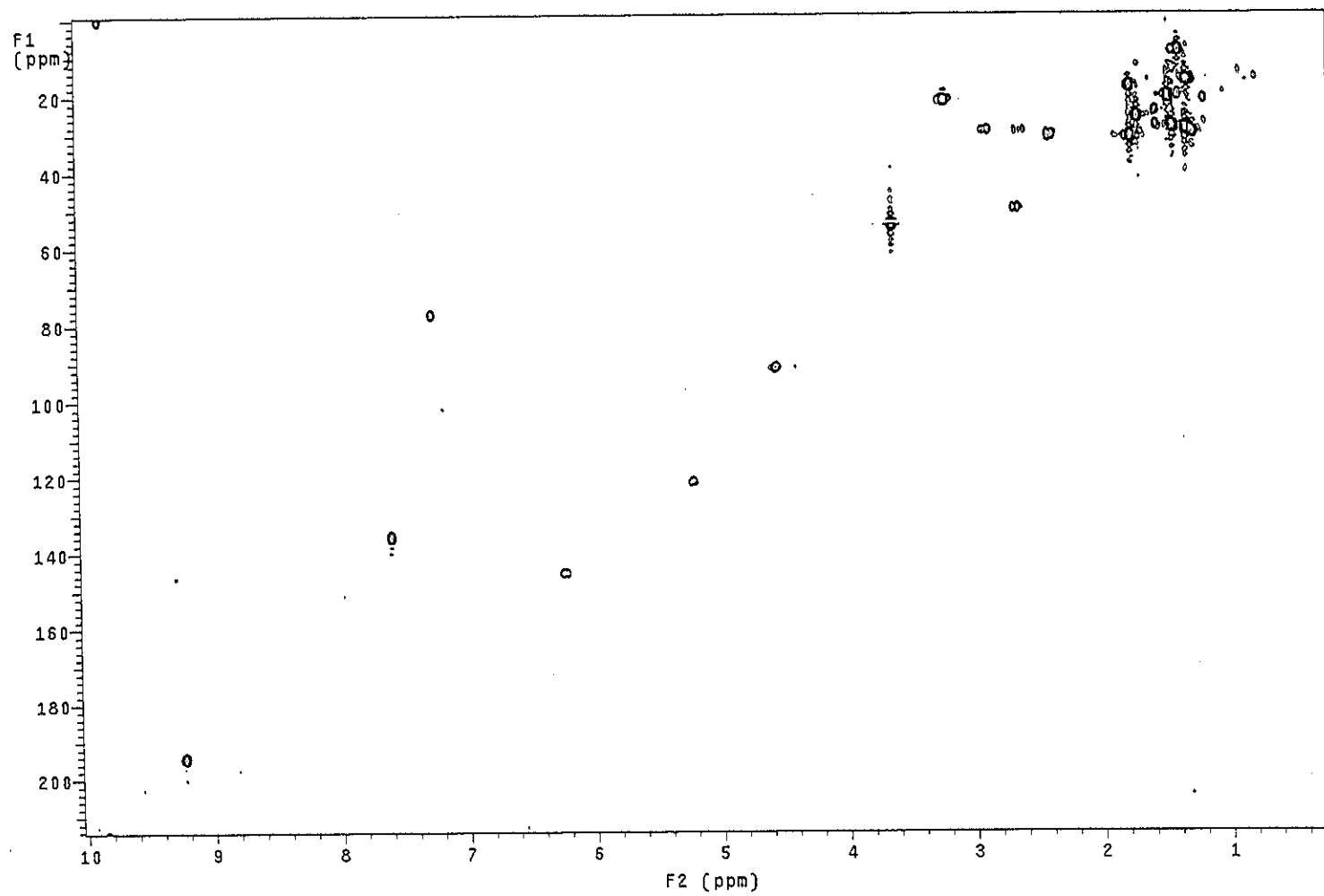


Figure 36 2D HMQC spectrum of PP6

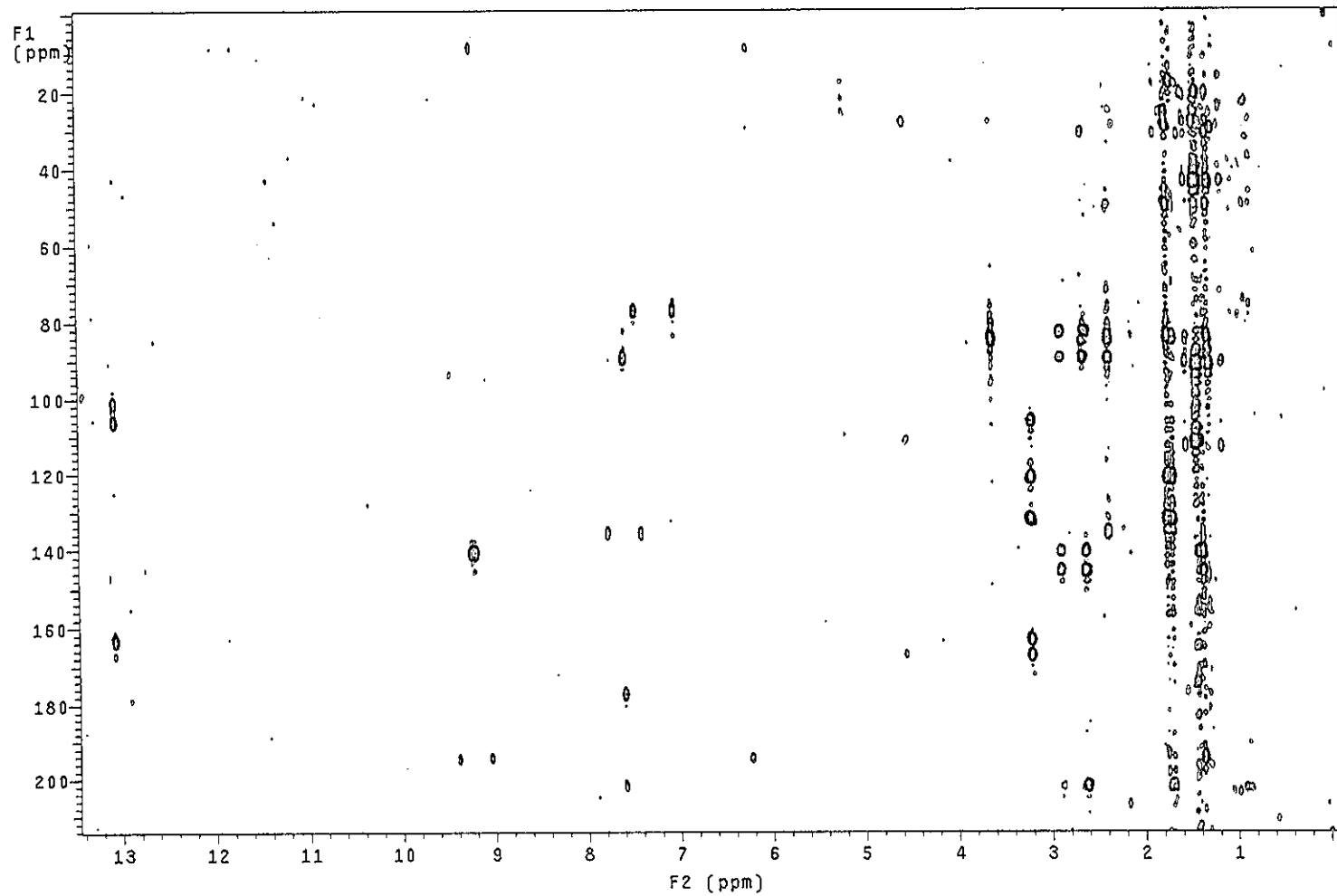


Figure 37 2D HMBC spectrum of PP6

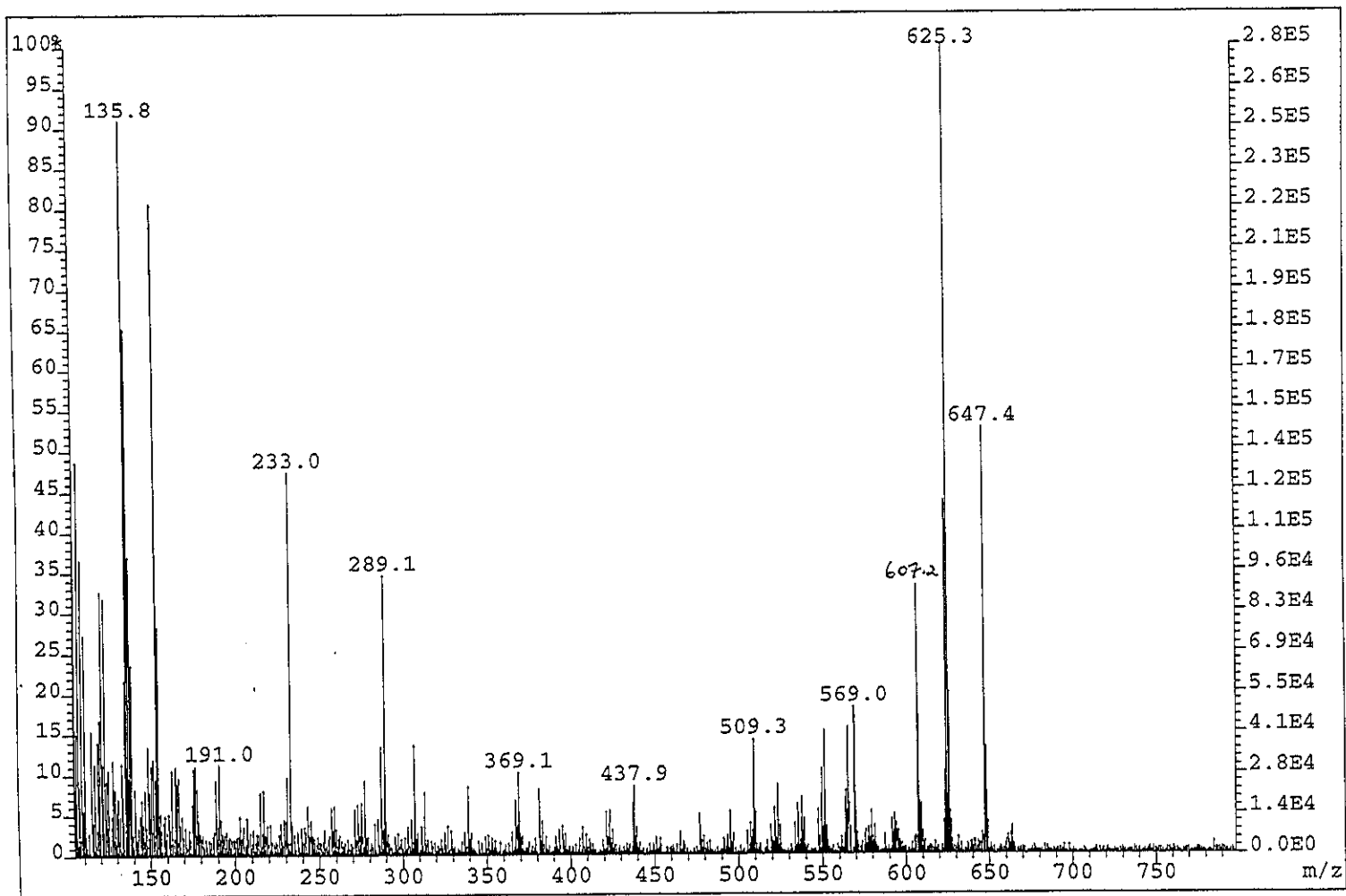


Figure 38 Mass spectrum of PP8

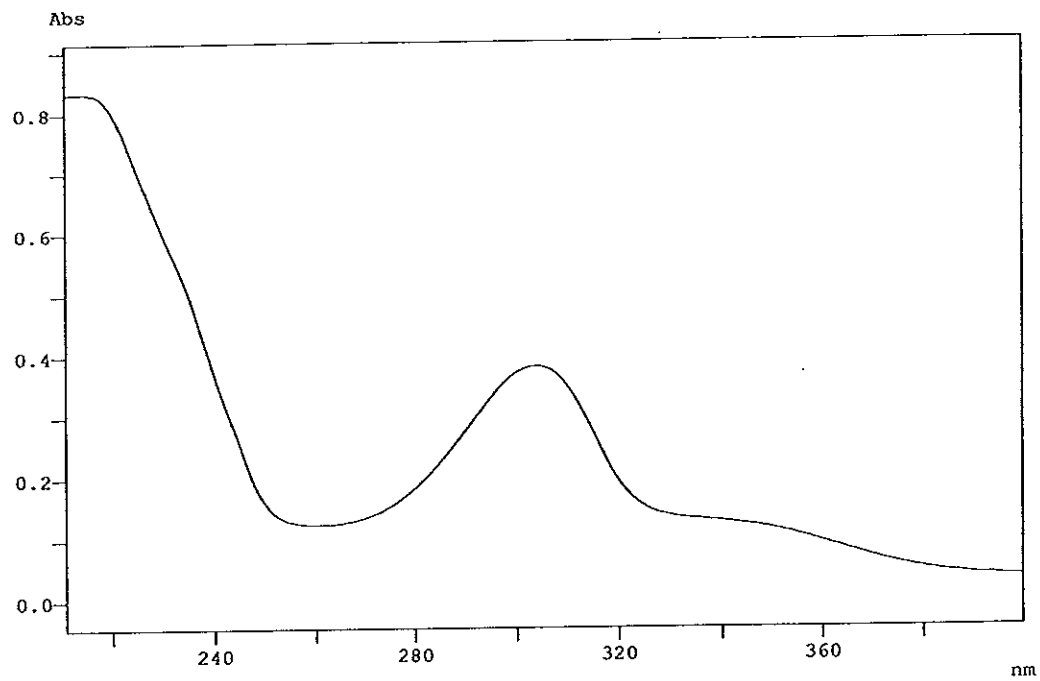


Figure 39 UV (MeOH) spectrum of PP8

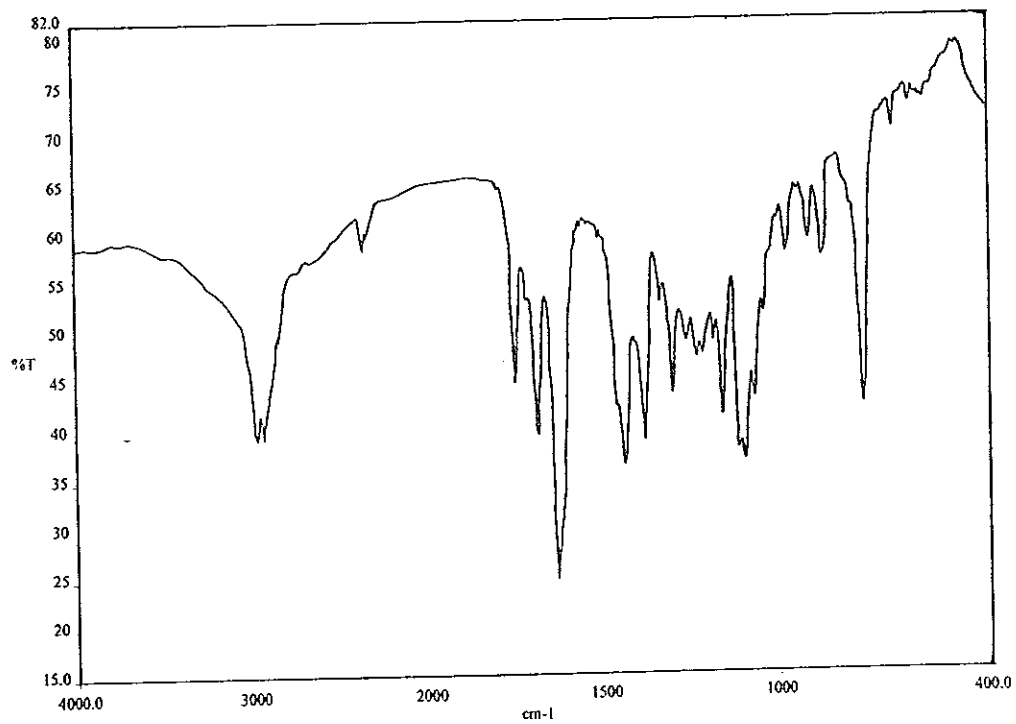


Figure 40 FT-IR (neat) spectrum of PP8

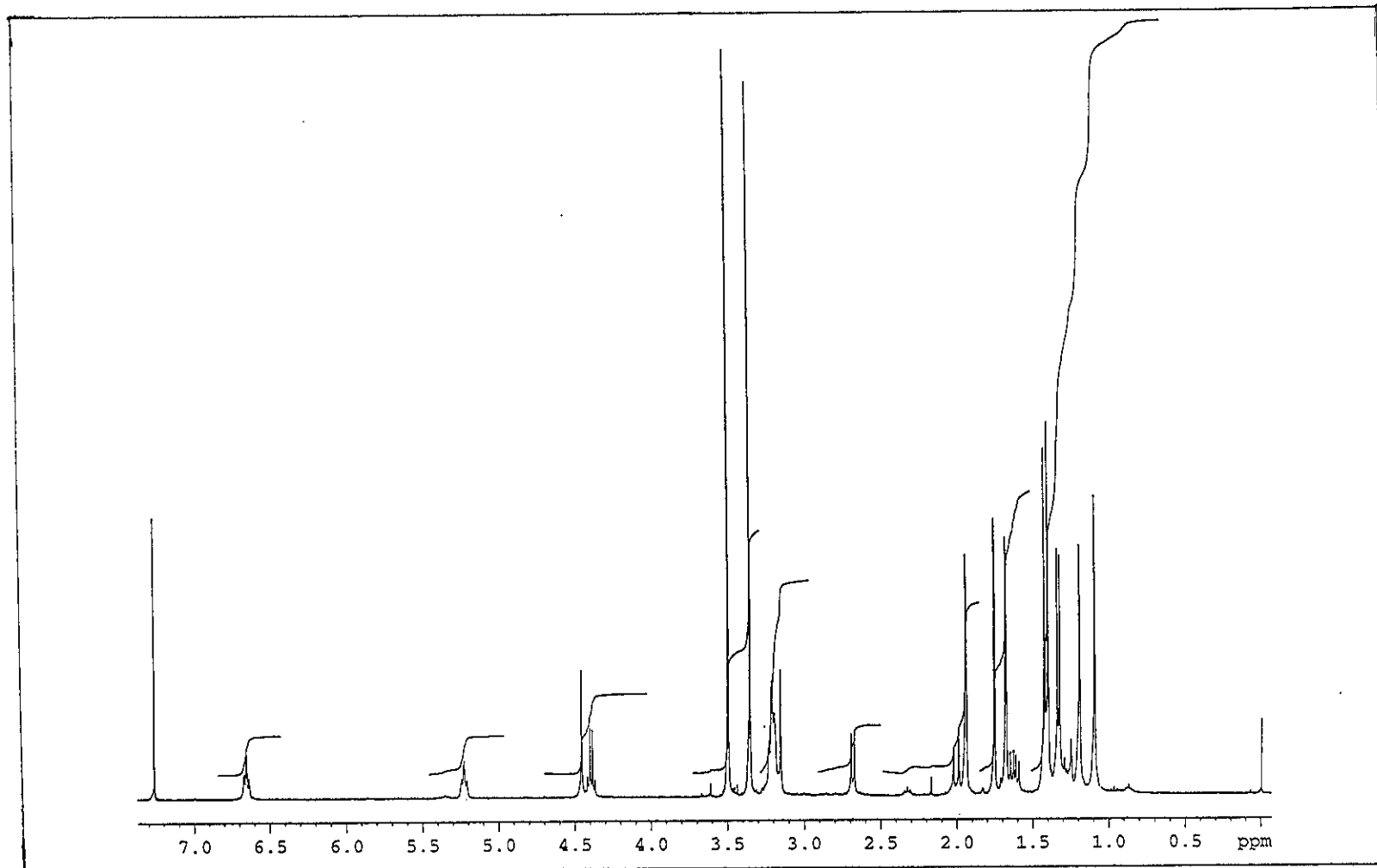


Figure 41 ^1H NMR (400 MHz) (CDCl_3) spectrum of PP8

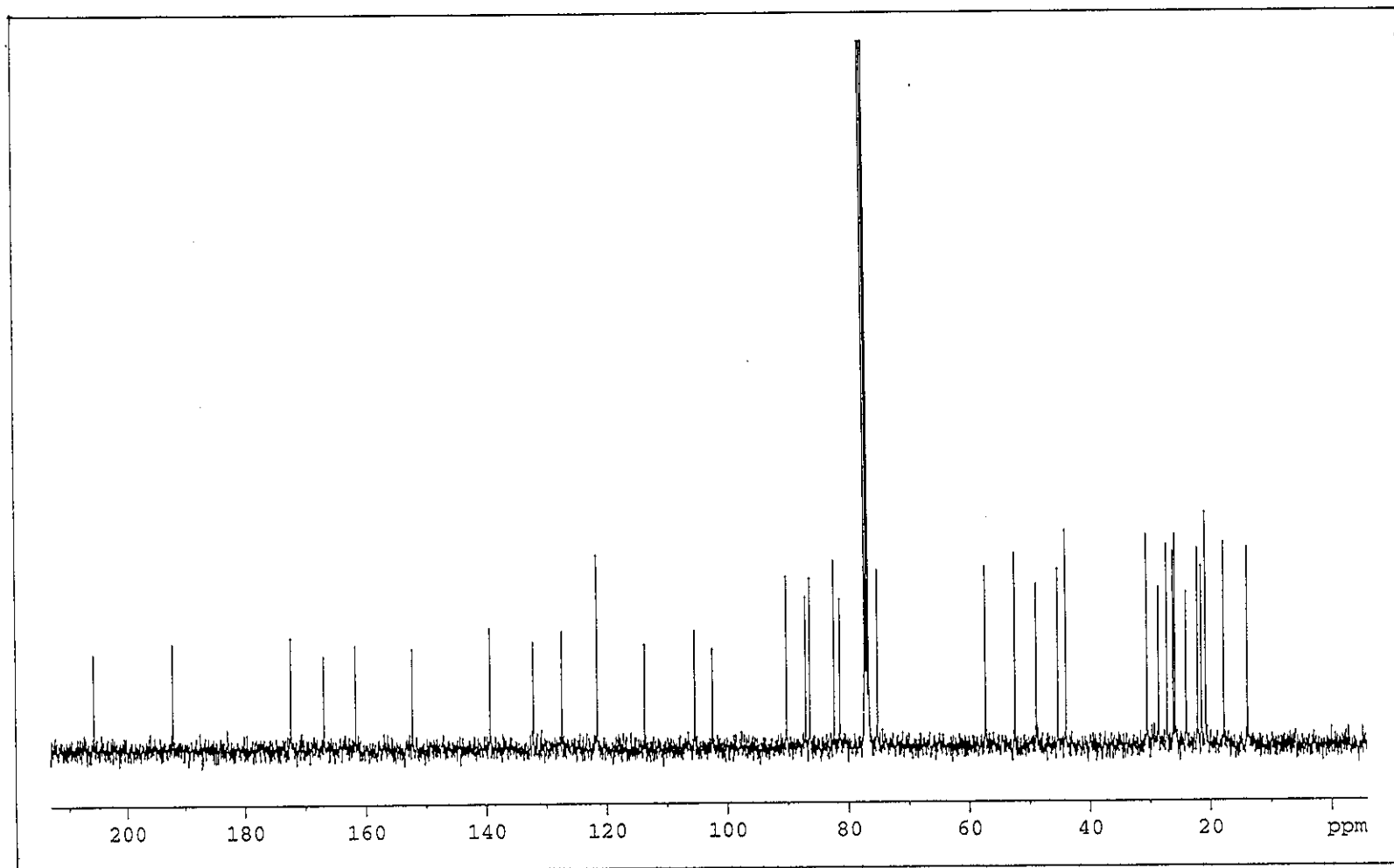


Figure 42 ^{13}C NMR (100 MHz) (CDCl_3) spectrum of PP8

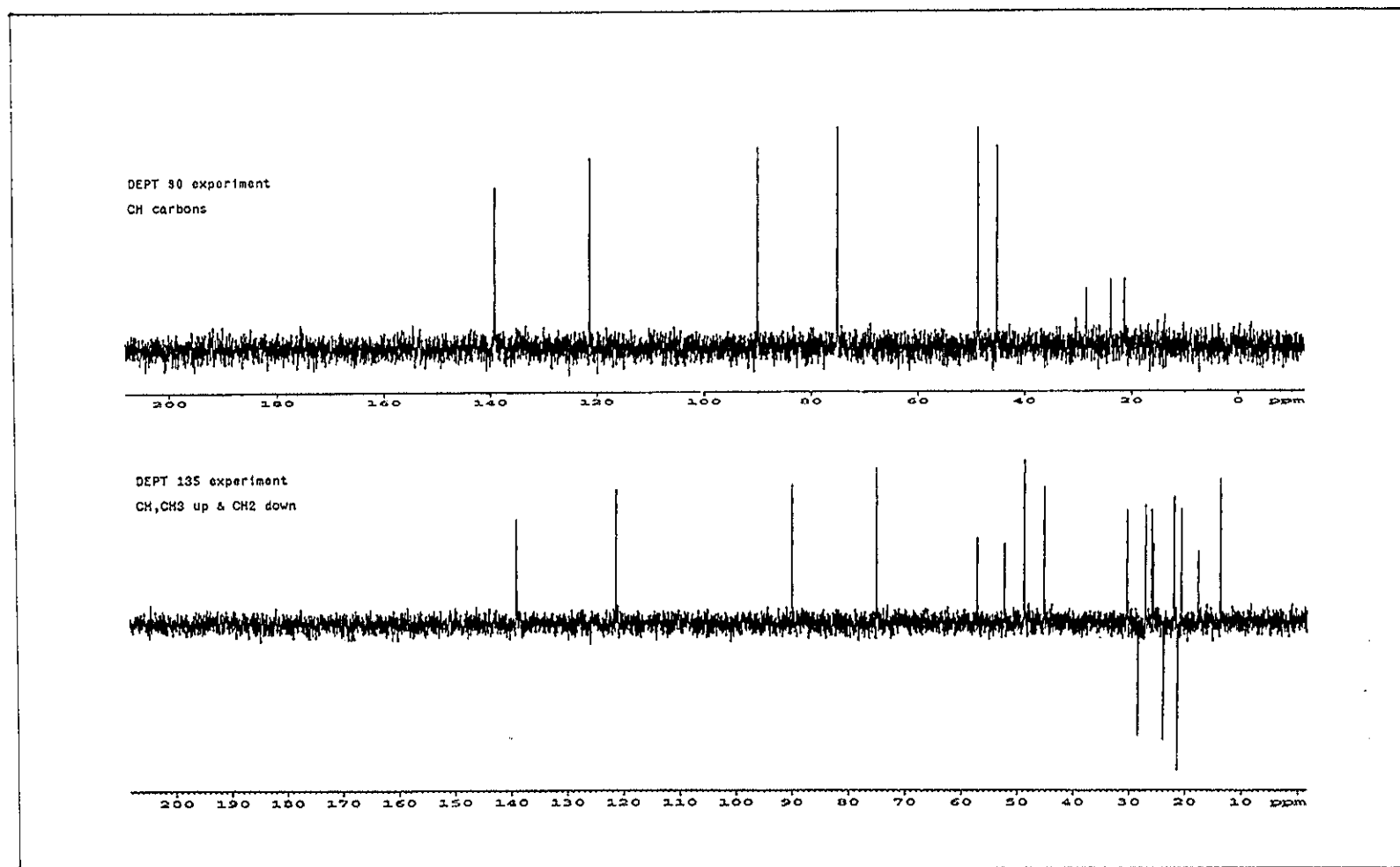


Figure 43 DEPT spectrum of PP8

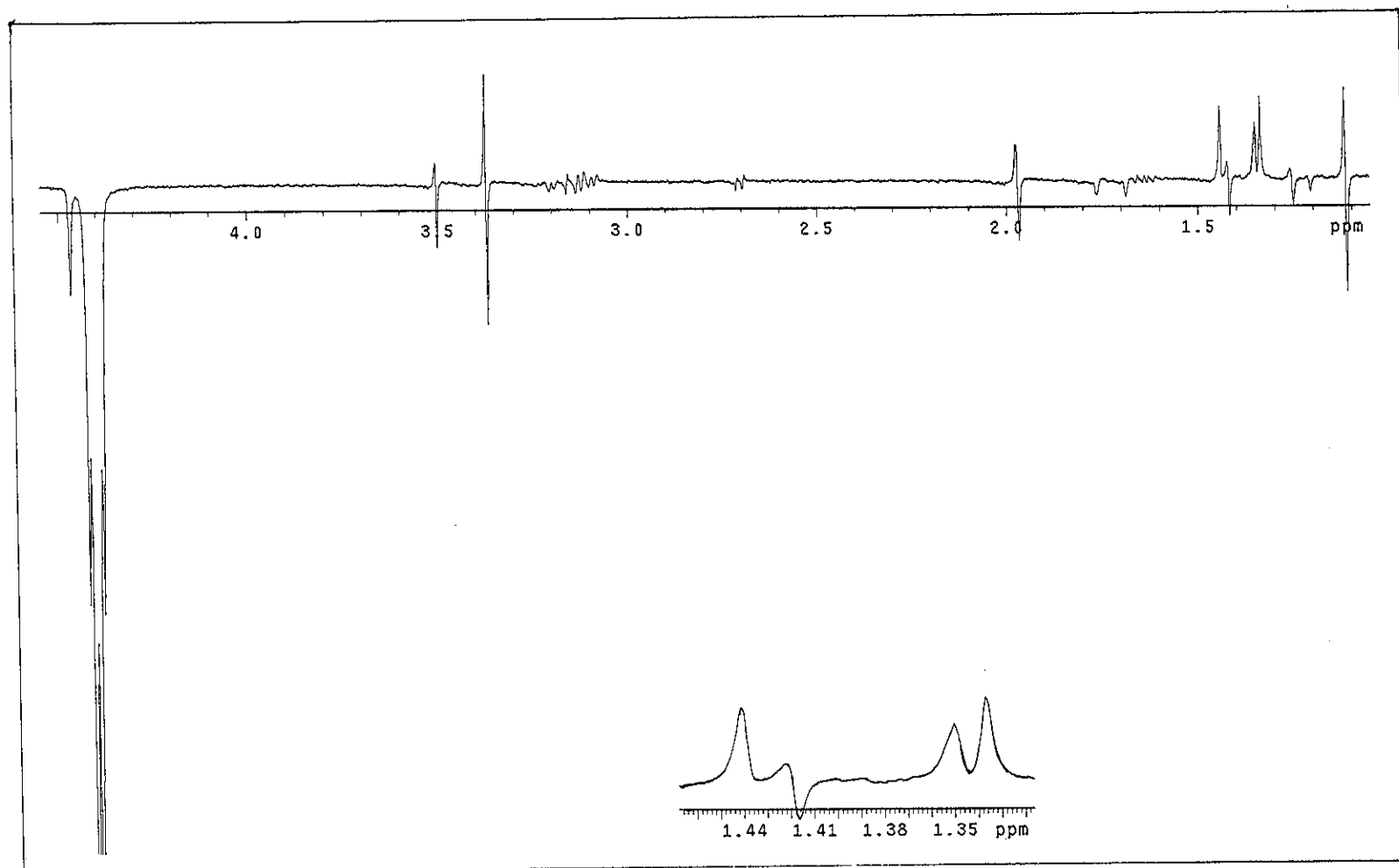


Figure 44 NOEDIFF spectrum of PP8 after irradiation at δ_H 4.40

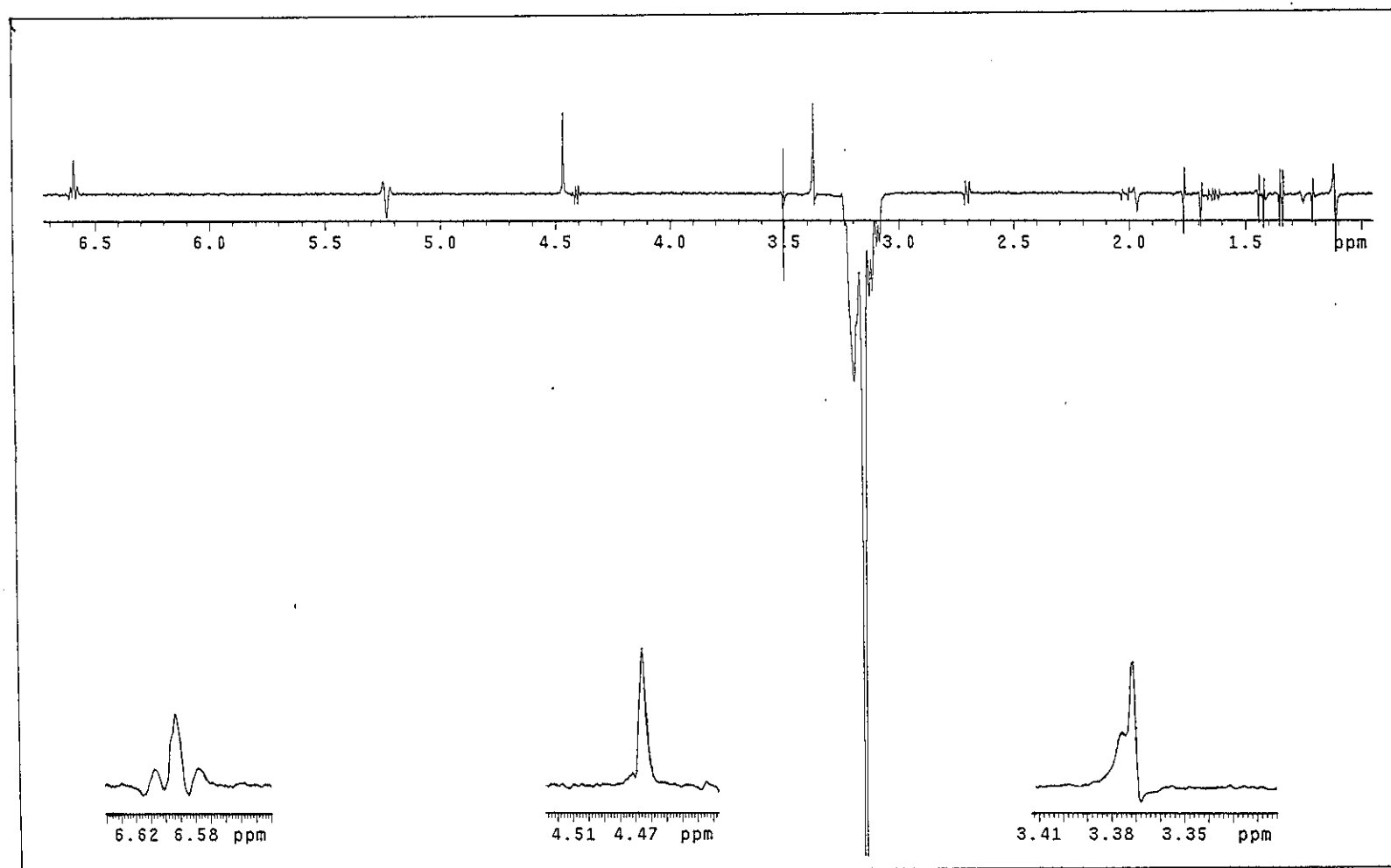


Figure 45 NOEDIFF spectrum of PP8 after irradiation at δ_H 3.16

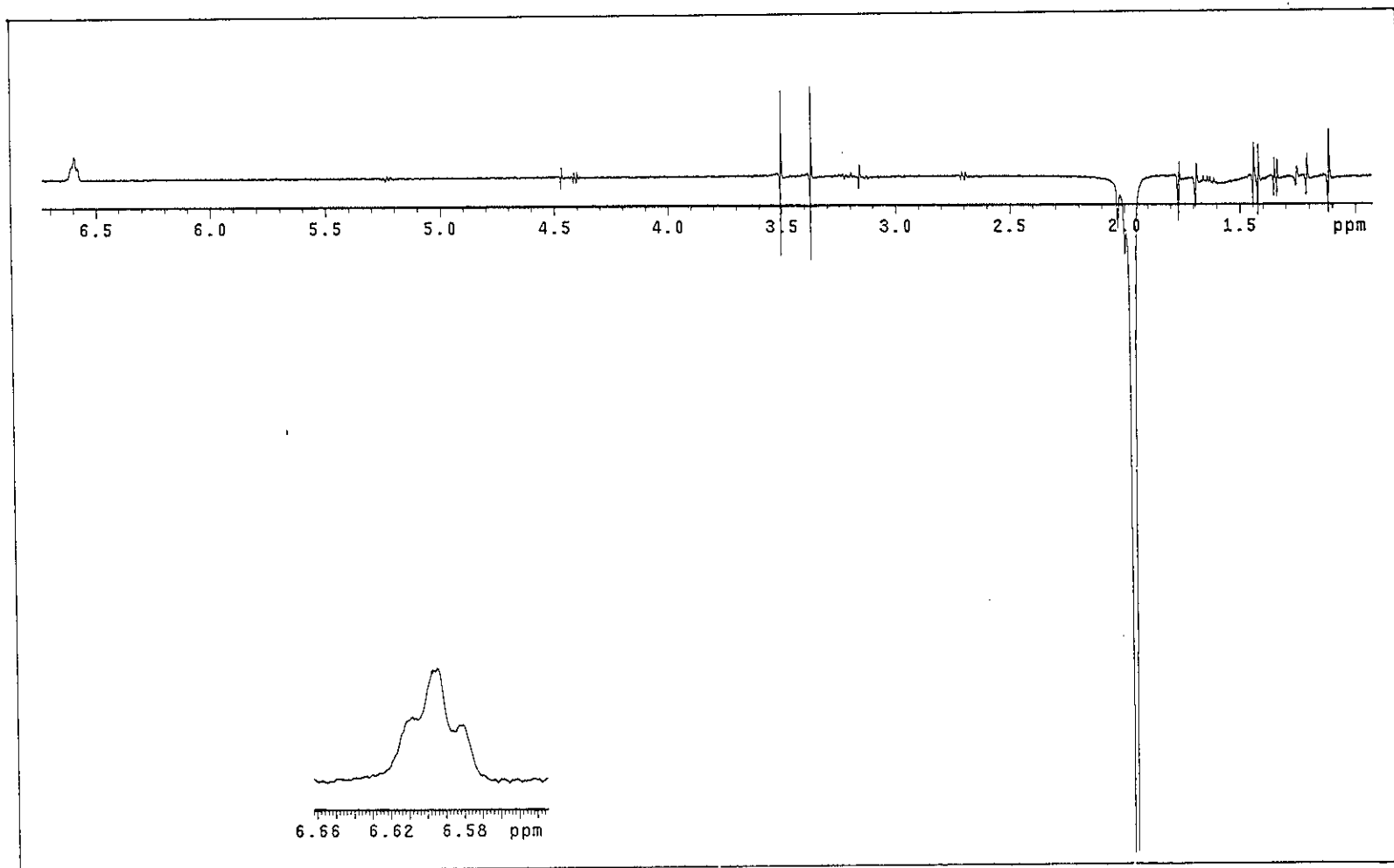


Figure 46 NOEDIFF spectrum of PP8 after irradiation at δ_H 1.98

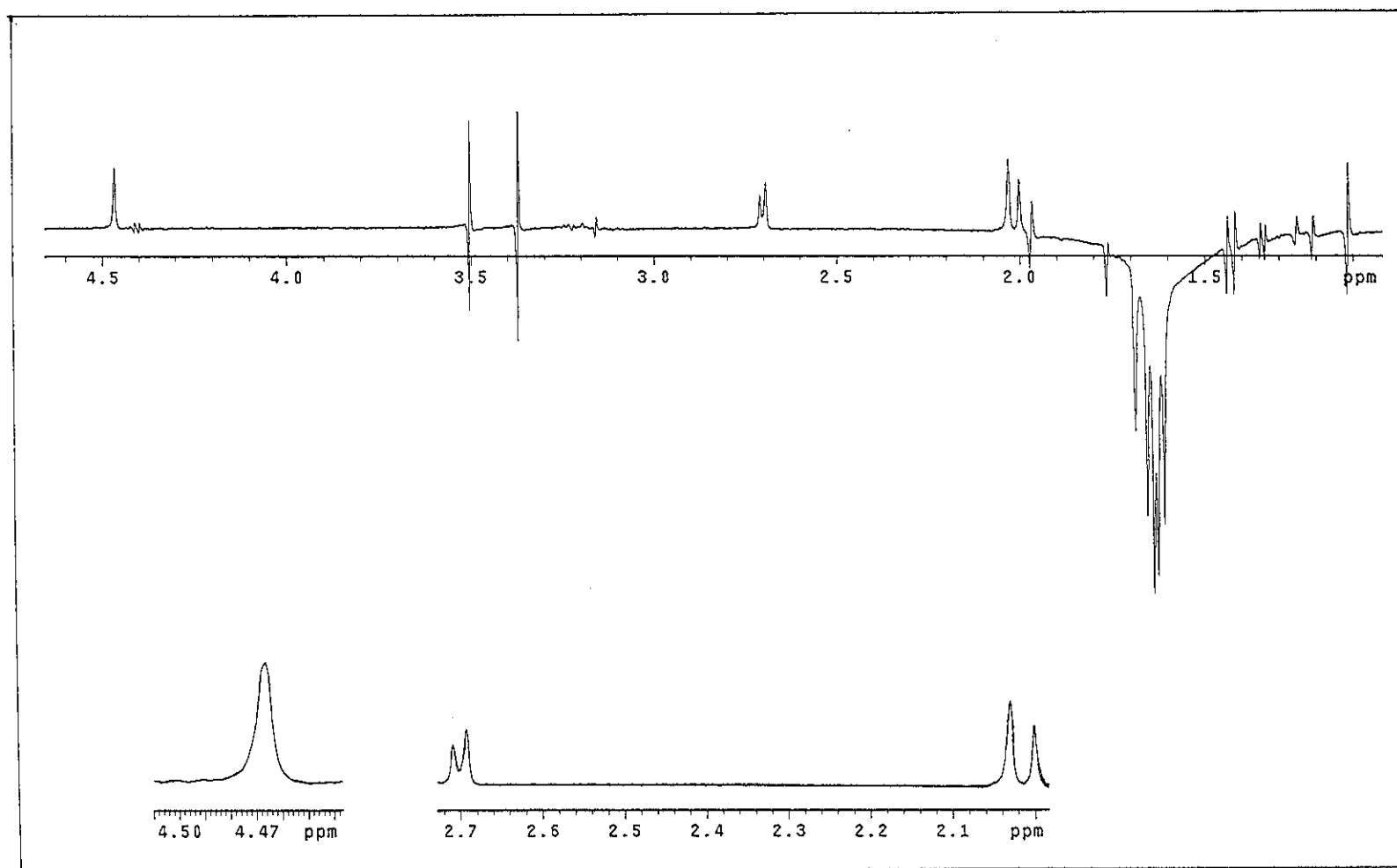


Figure 47 NOEDIFF spectrum of PP8 after irradiation at δ_H 1.63

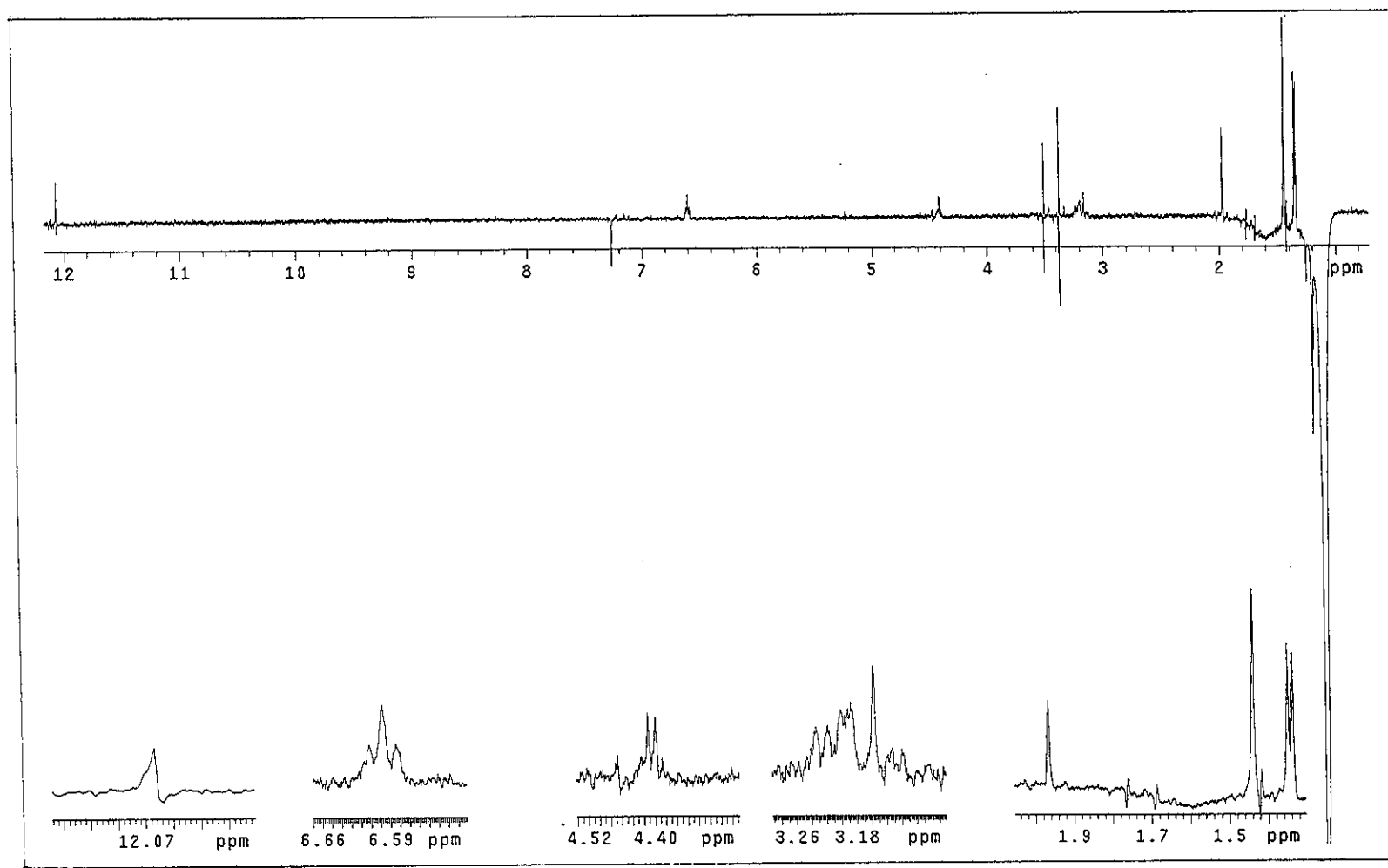


Figure 48 NOEDIFF spectrum of PPS after irradiation at $\delta_H 1.10$

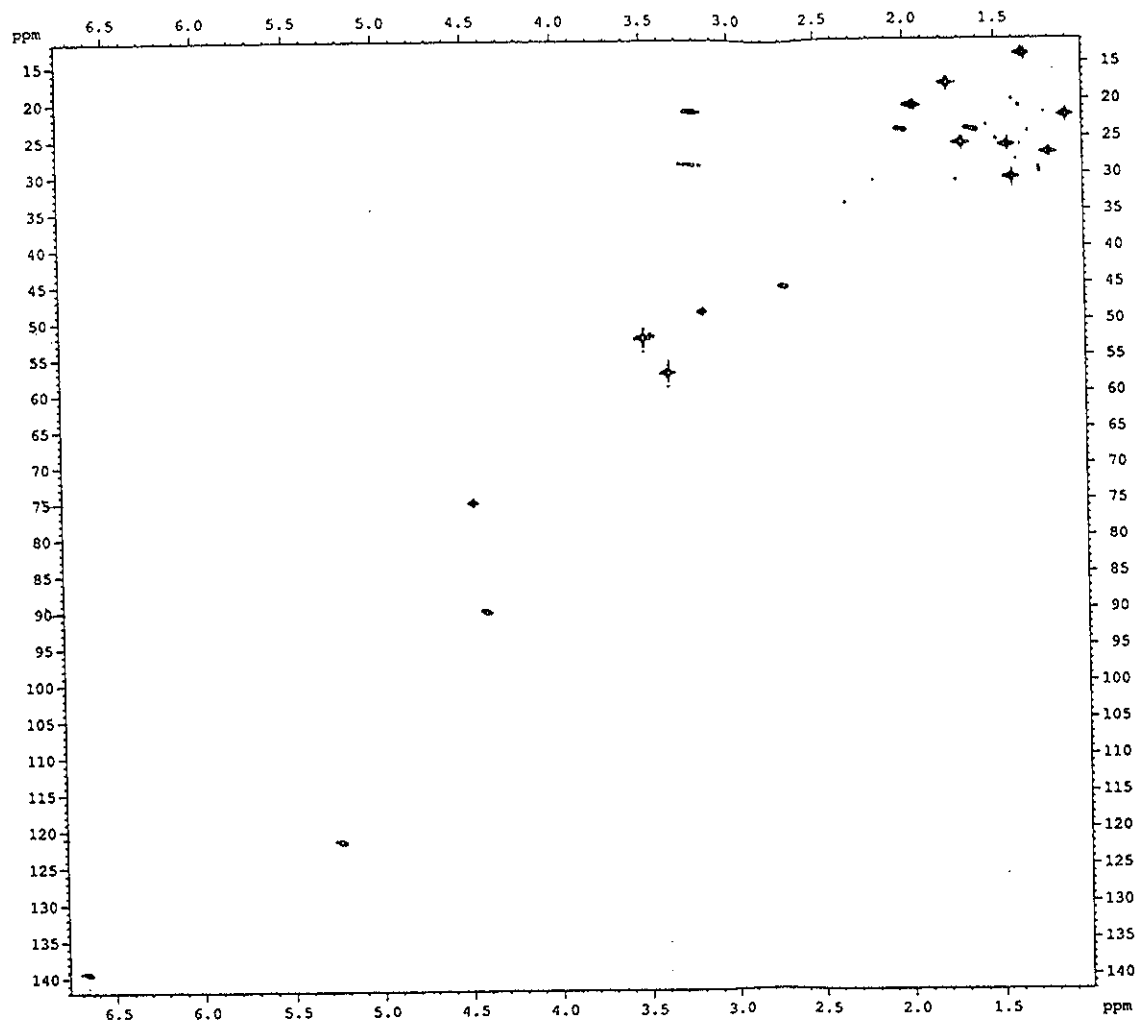


Figure 49 2D HMQC spectrum of PP8

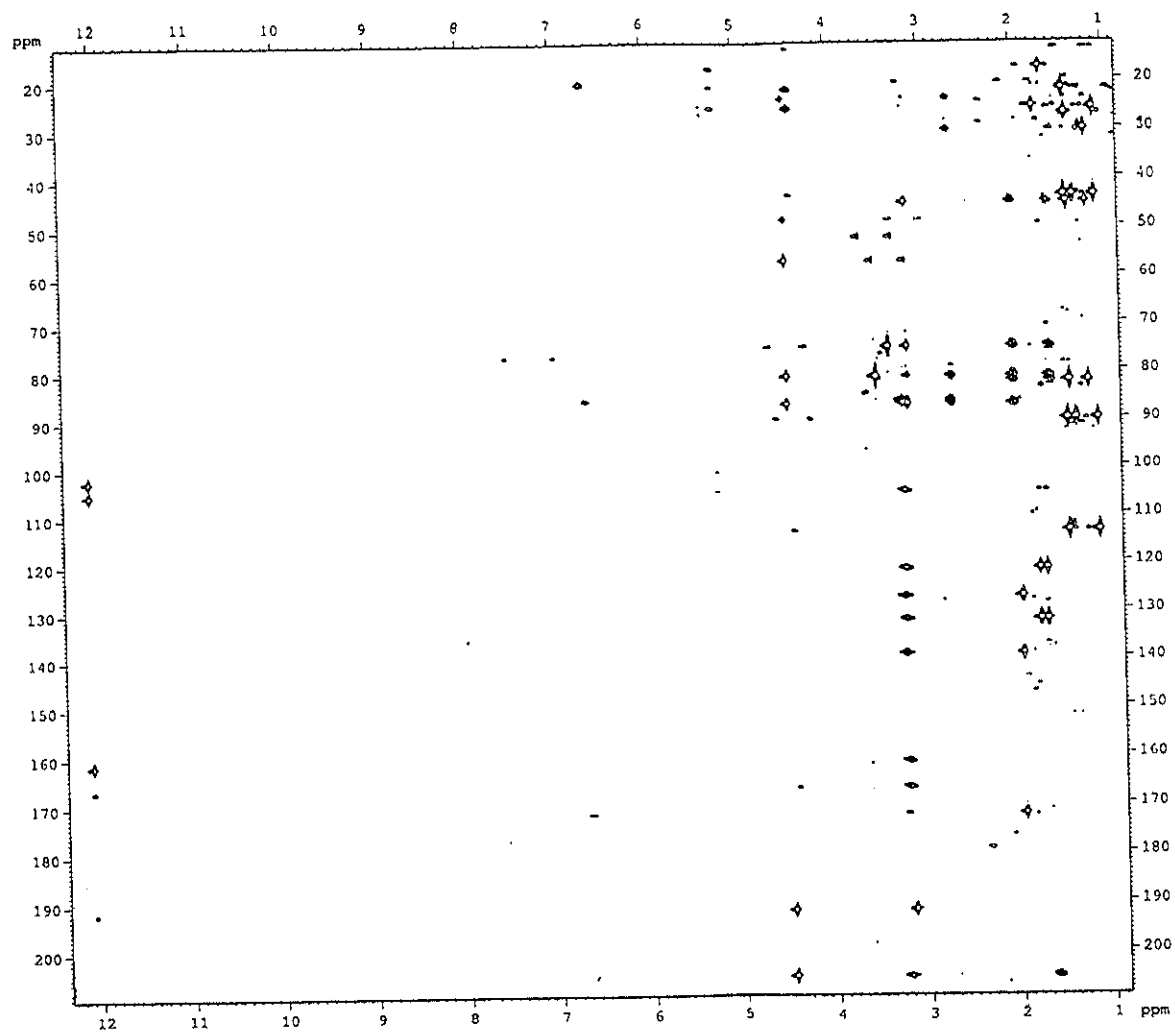


Figure 50 2D HMBC spectrum of PP8

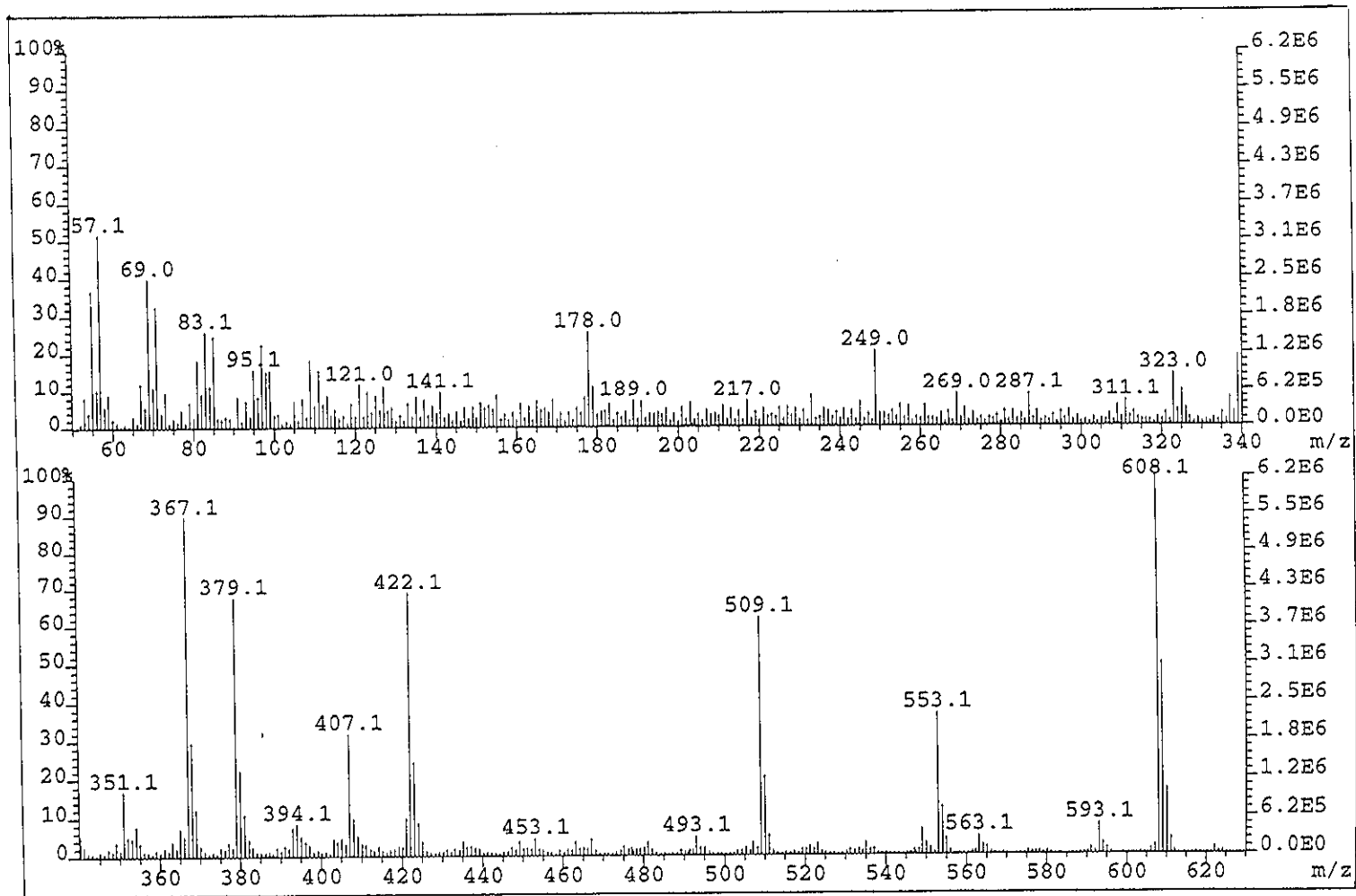


Figure 51 Mass spectrum of PP10

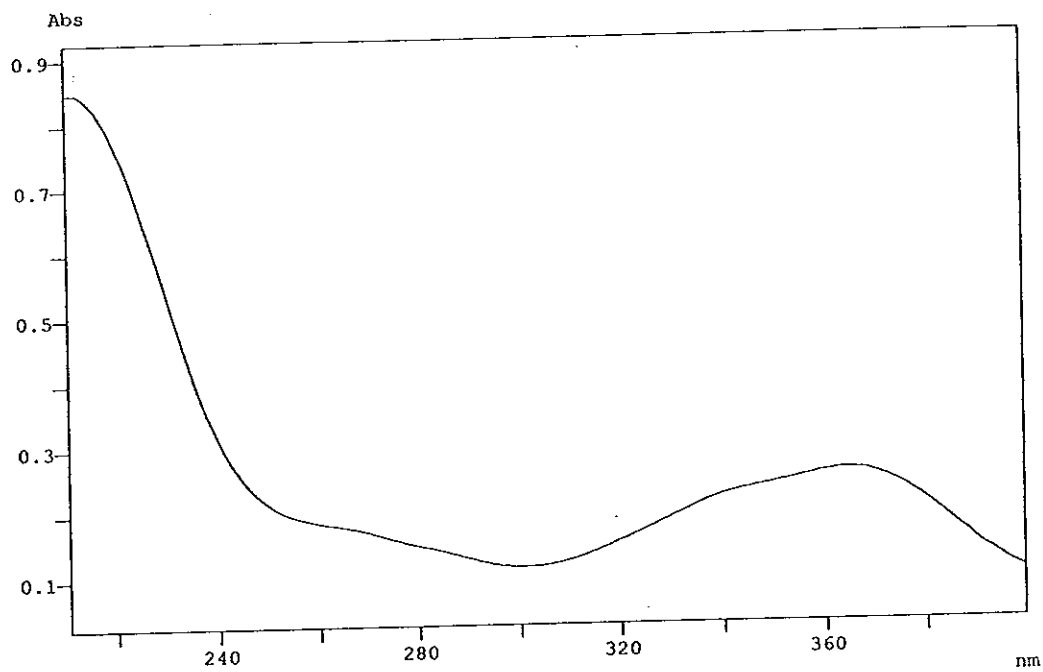


Figure 52 UV (MeOH) spectrum of PP10

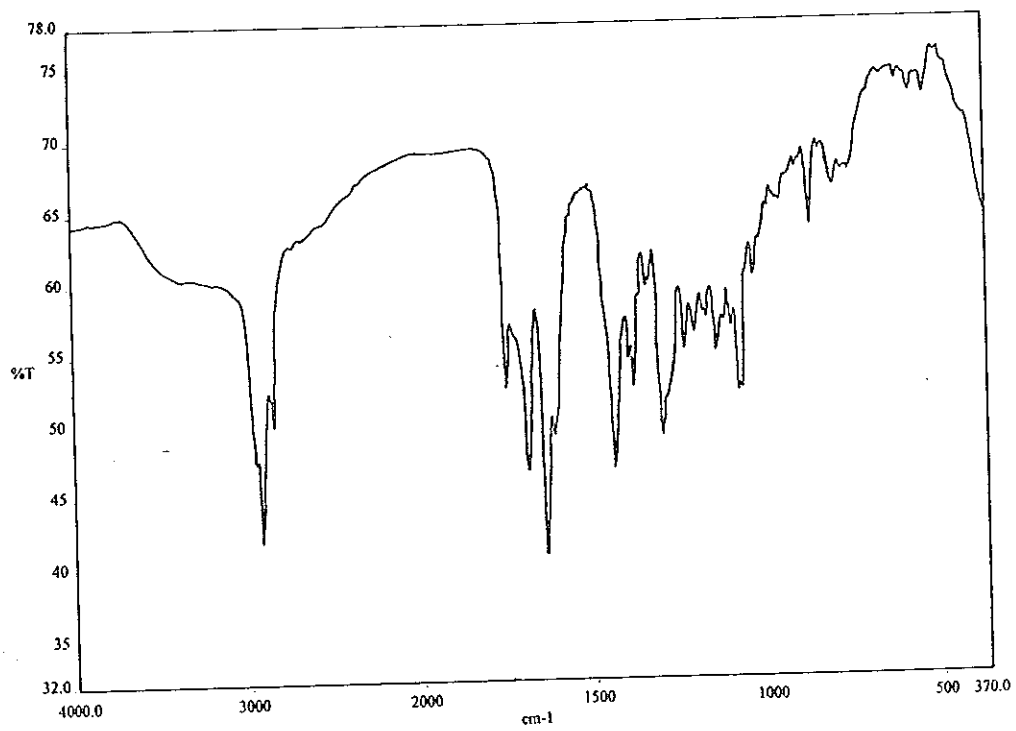


Figure 53 FT-IR (neat) spectrum of PP10

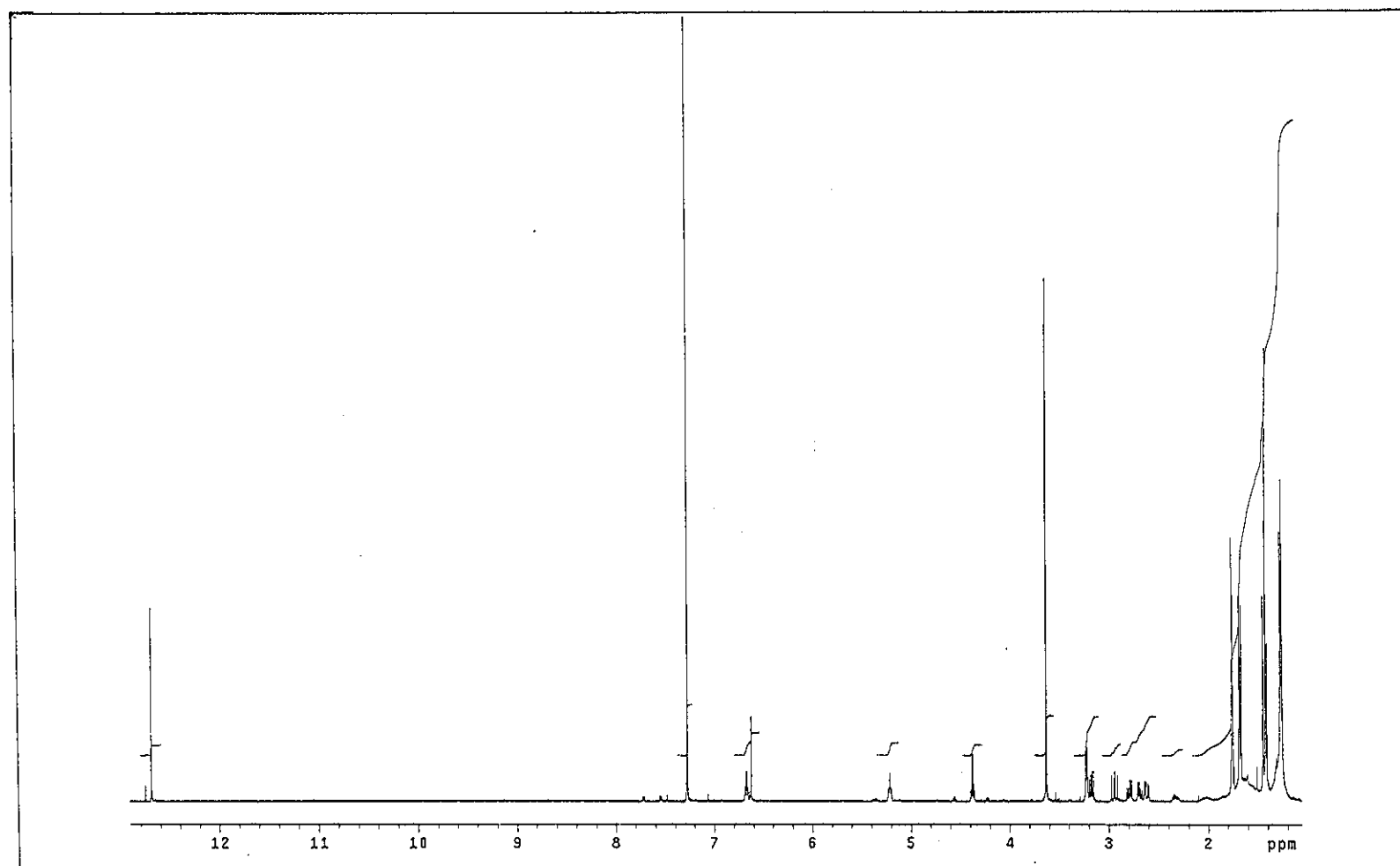


Figure 54 ^1H NMR (500 MHz) (CDCl_3) spectrum of PP10

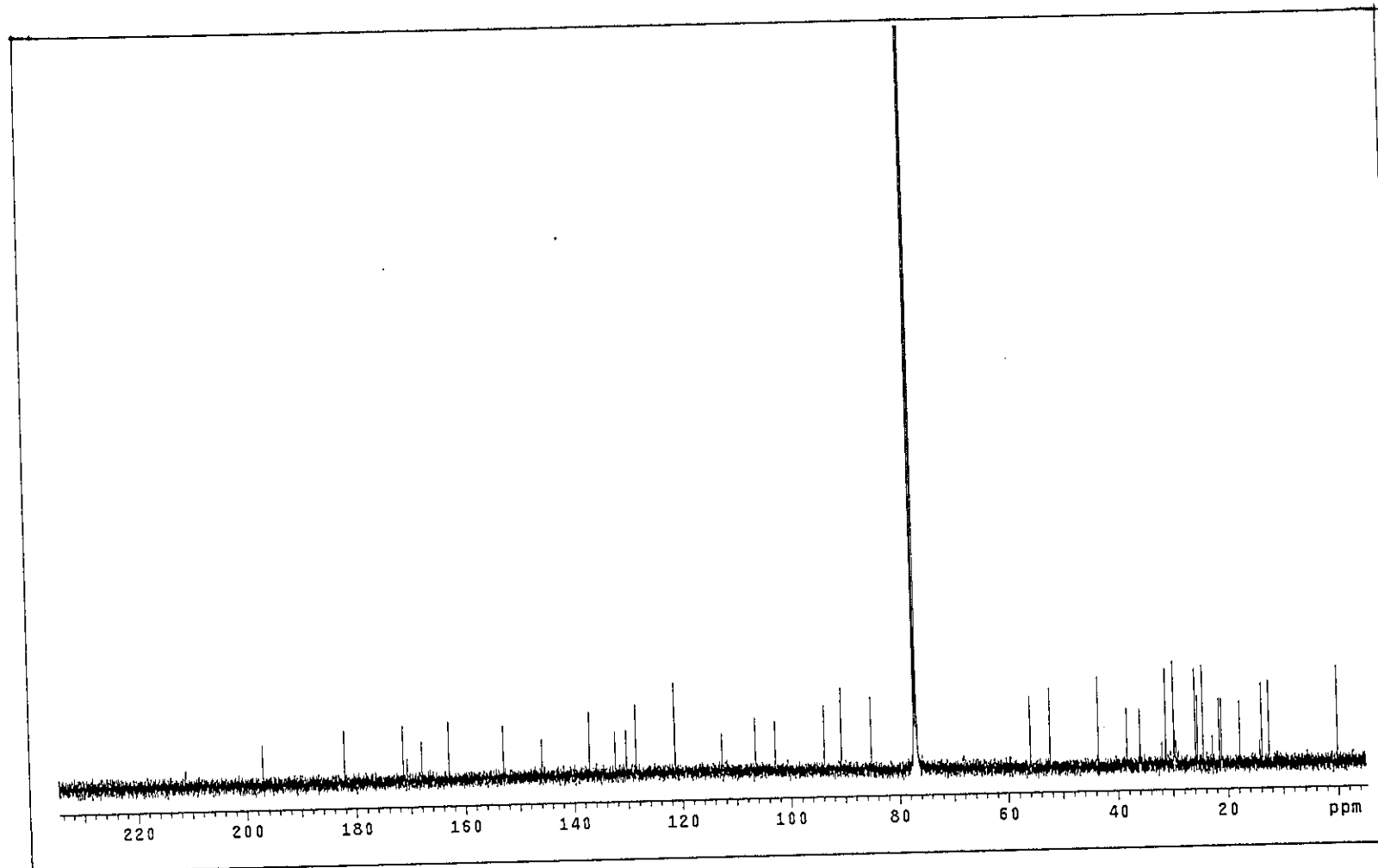


Figure 55 ^{13}C NMR (125 MHz) (CDCl_3) spectrum of PP10

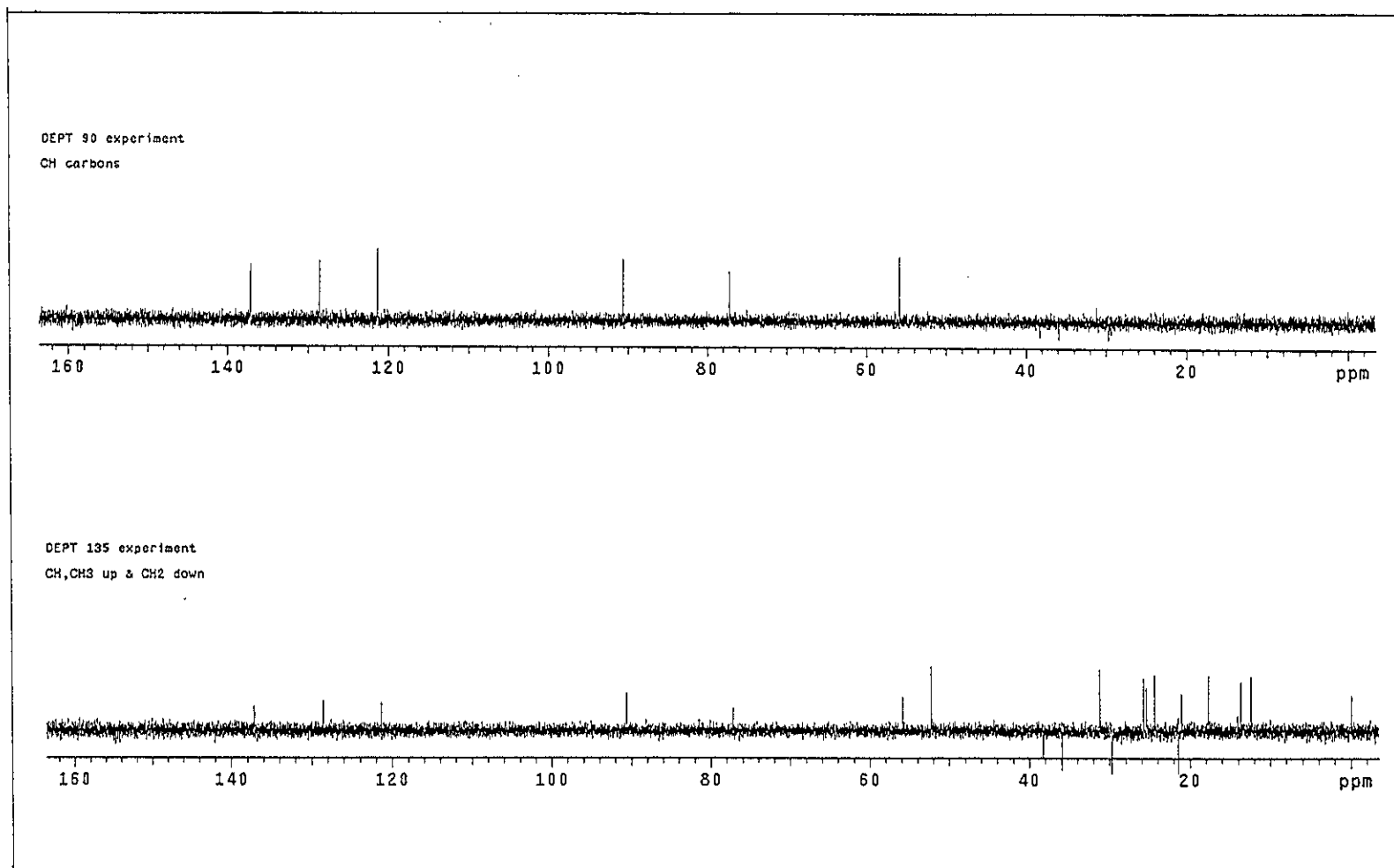


Figure 56 DEPT spectrum of PP10

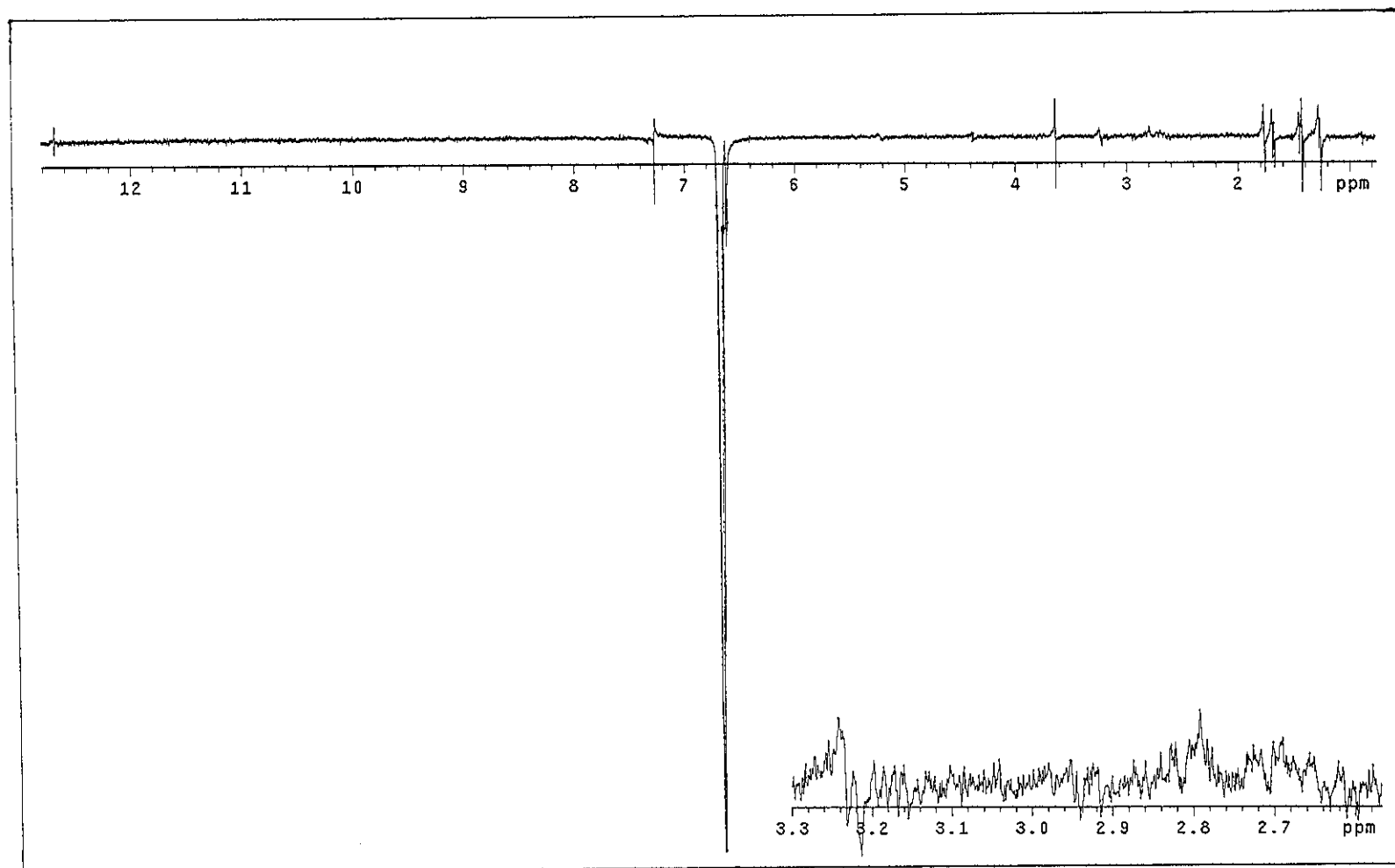


Figure 57 NOEDIFF spectrum of PP10 after irradiation at δ_H 6.67

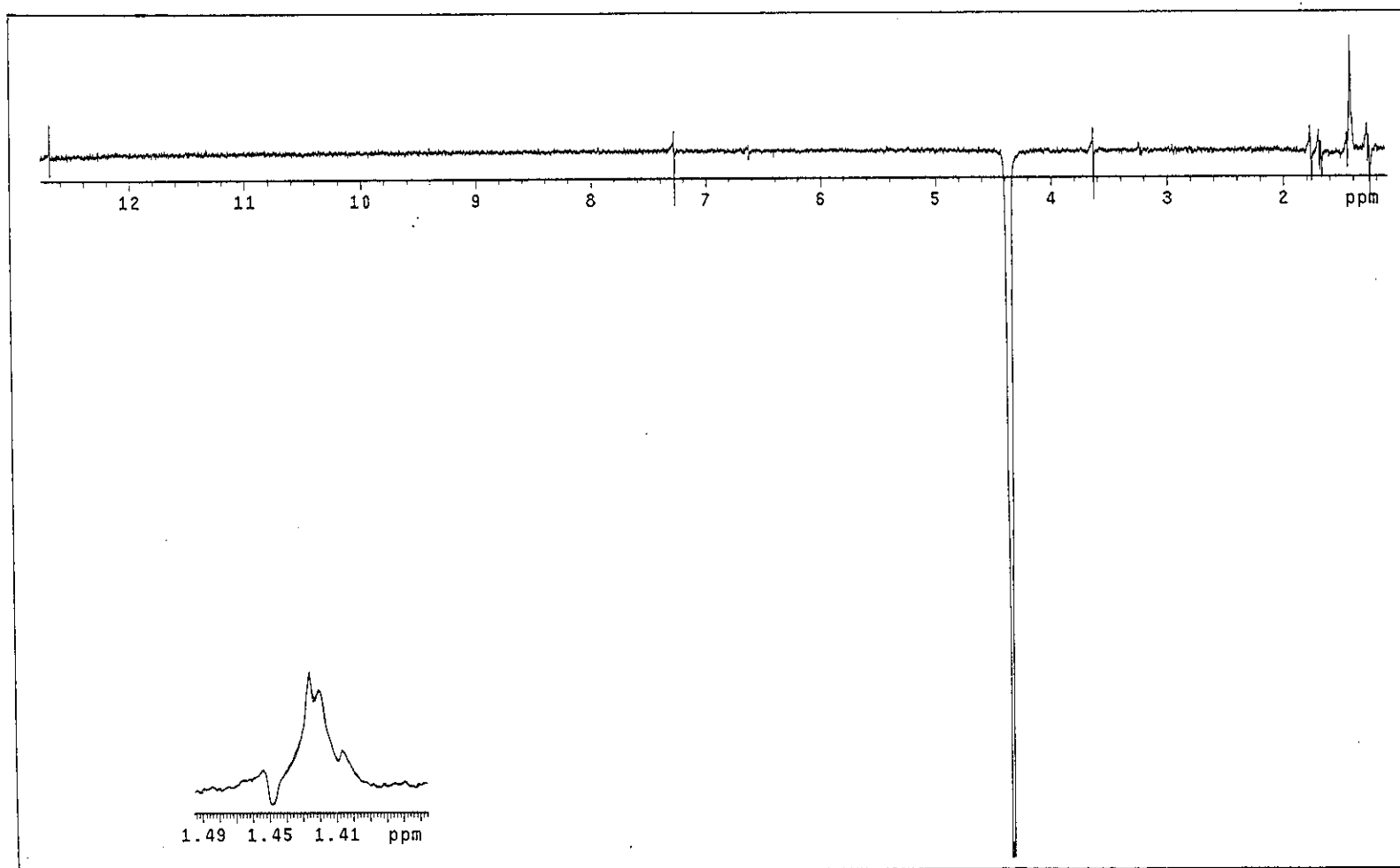


Figure 58 NOEDIFF spectrum of PP10 after irradiation at δ_H 4.37

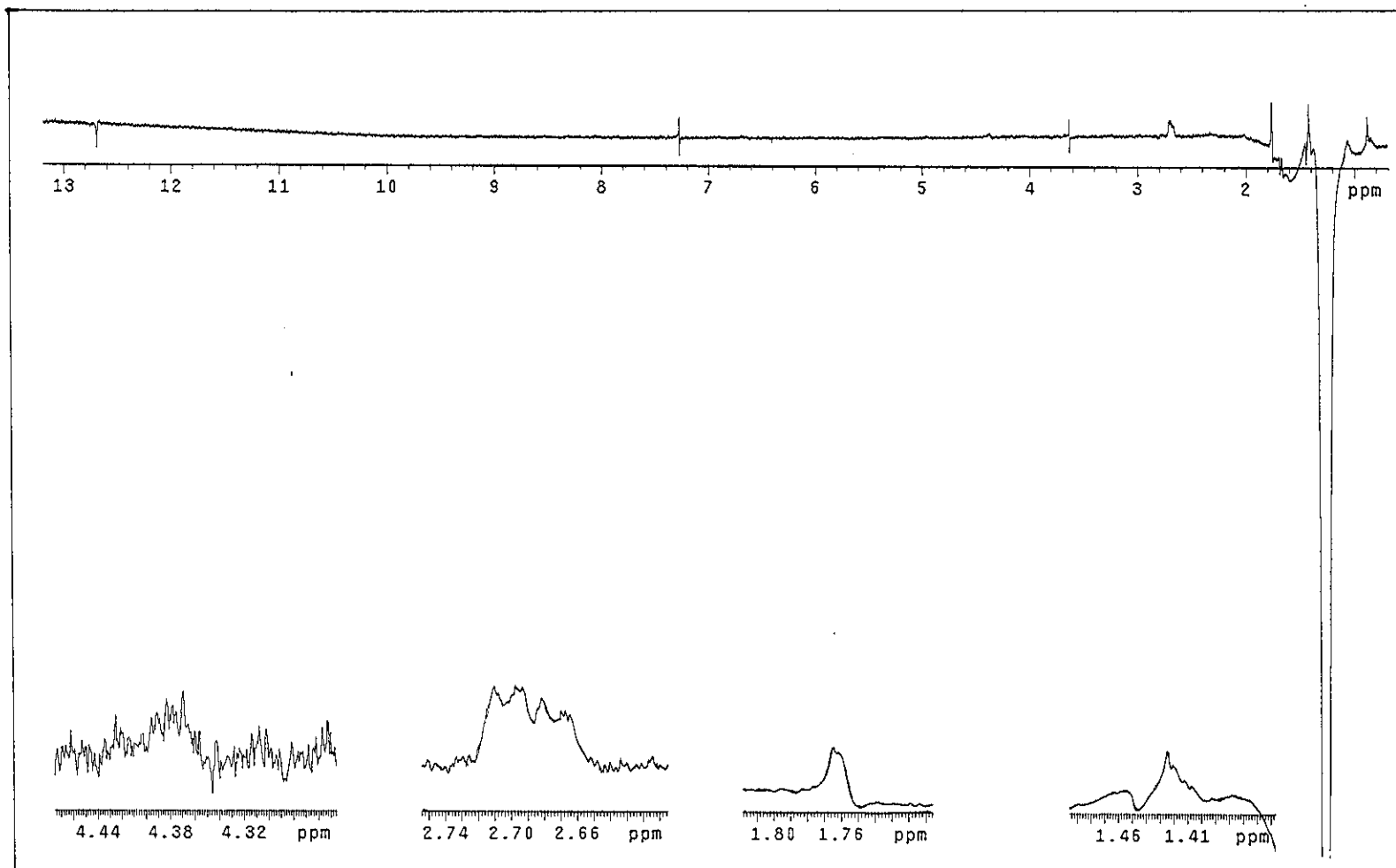


Figure 59 NOEDIFF spectrum of PP10 after irradiation at δ_H 1.27

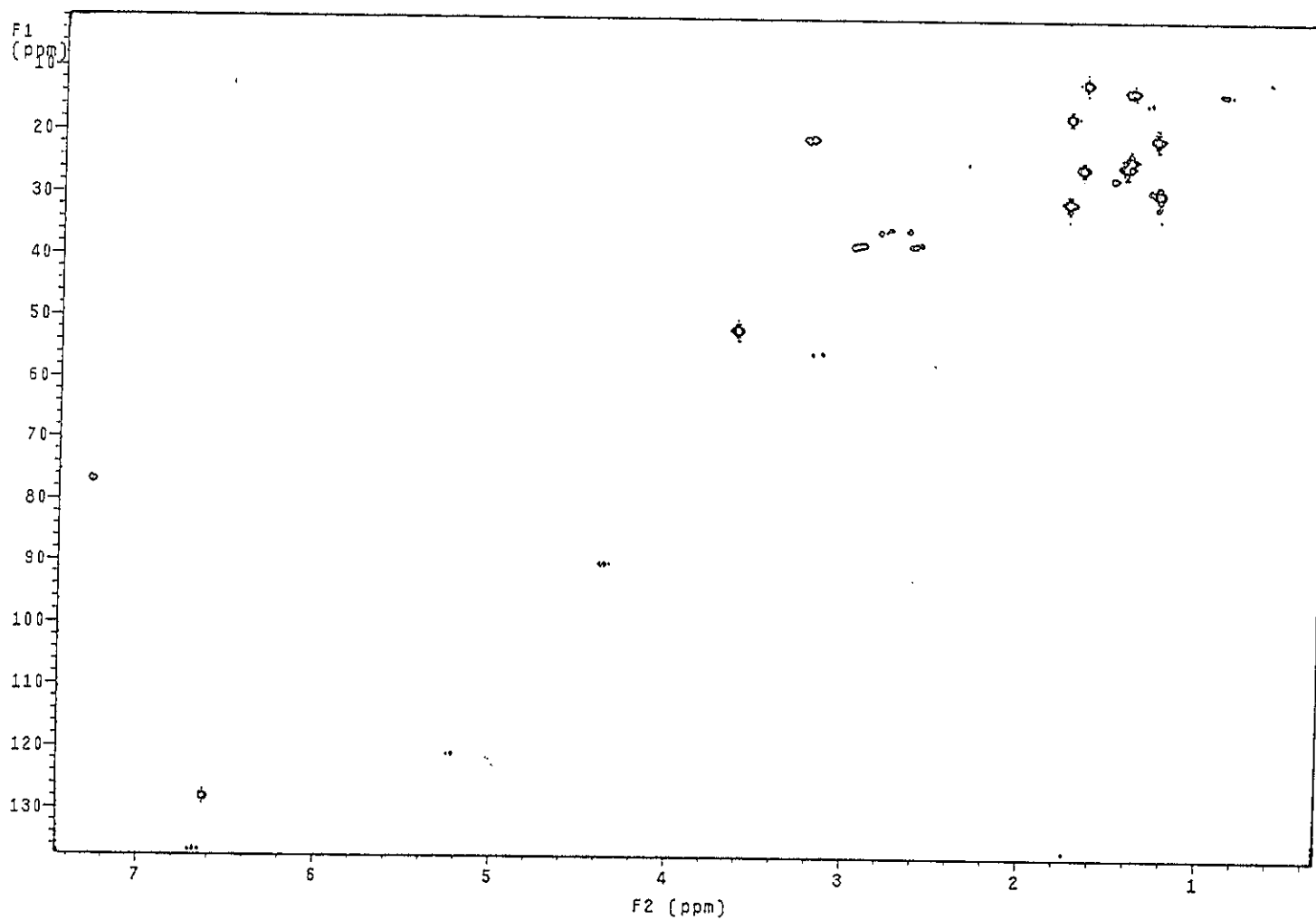


Figure 60 2D HMQC spectrum of PP10

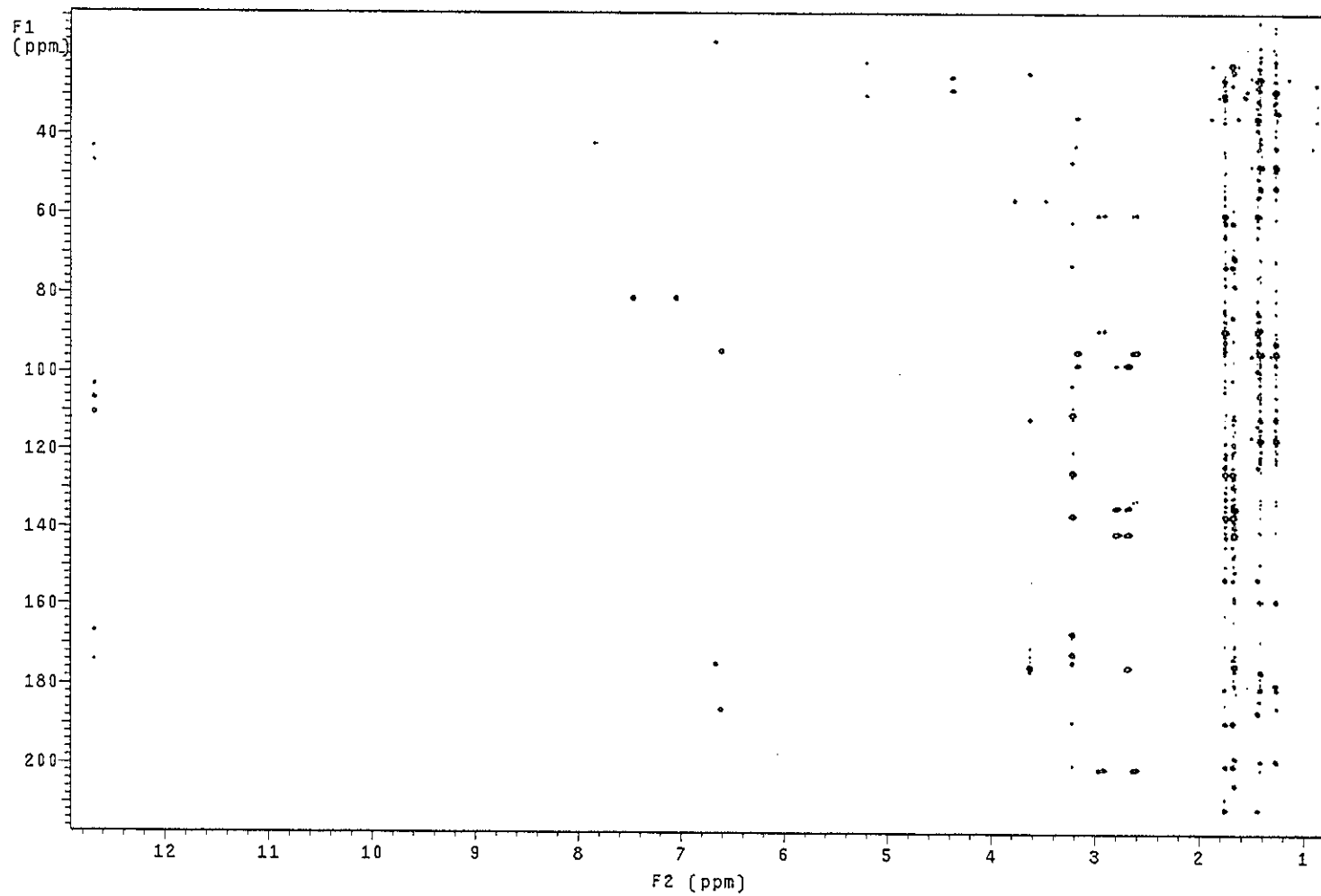


Figure 61 2D HMBC spectrum of PP10

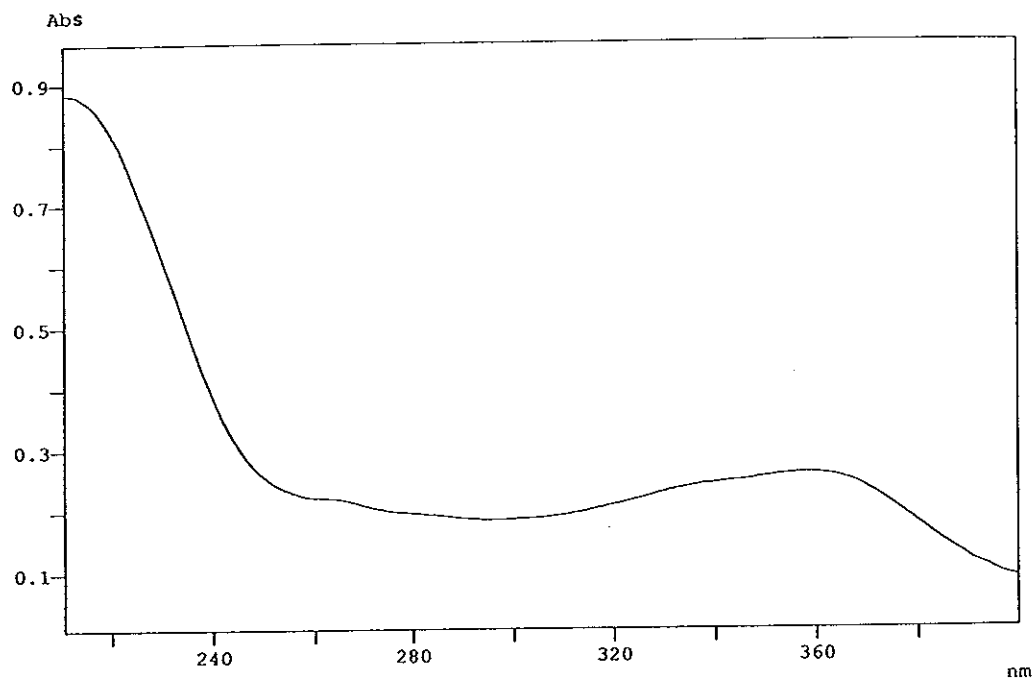


Figure 62 UV (MeOH) spectrum of PP2

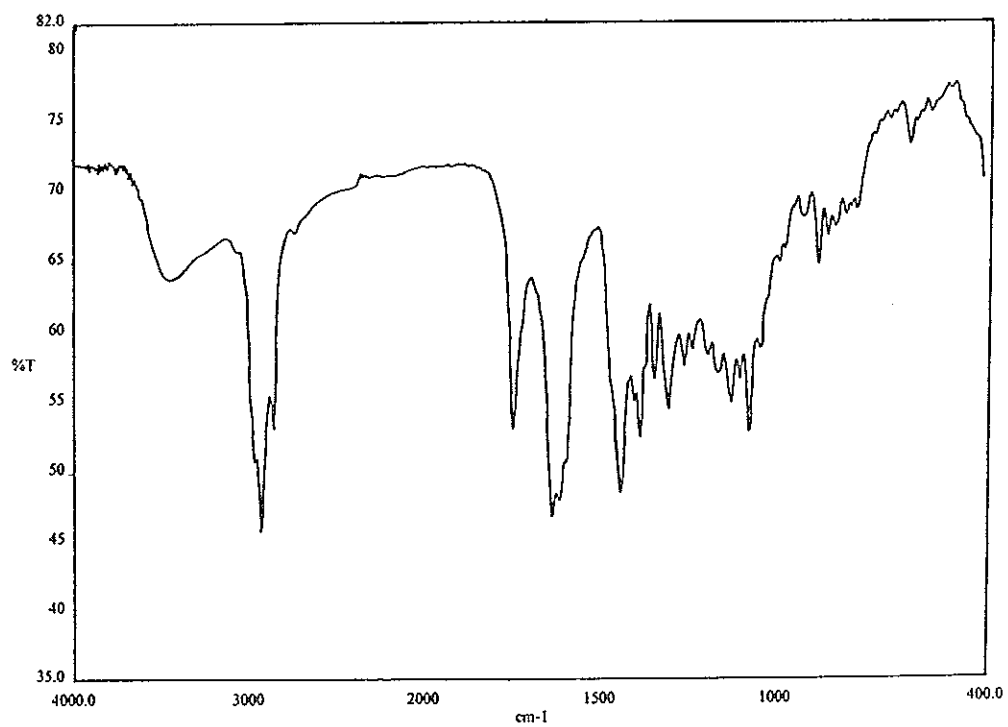


Figure 63 FT-IR (neat) spectrum of PP2

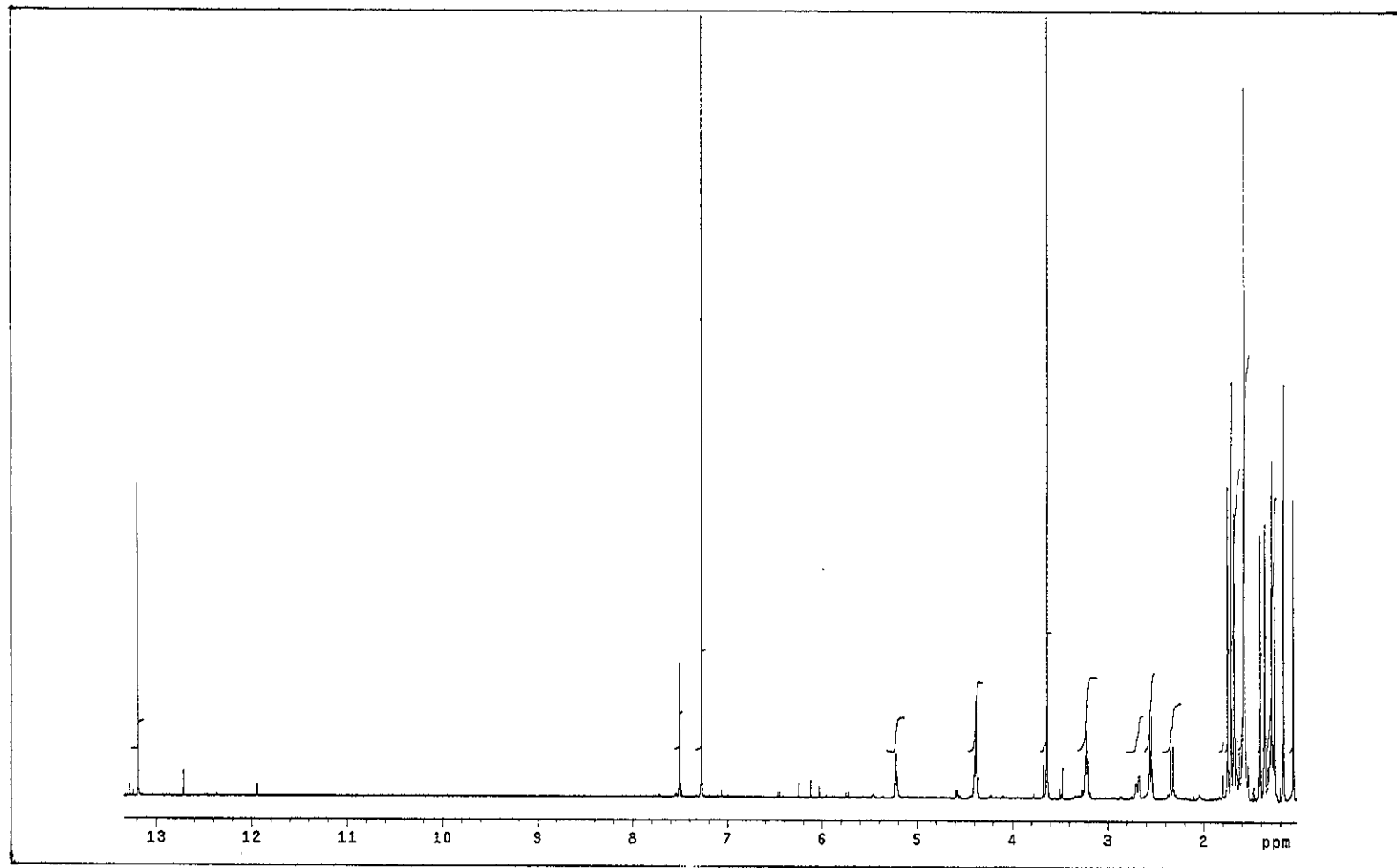


Figure 64 ¹H NMR (500 MHz) (CDCl₃) spectrum of PP2

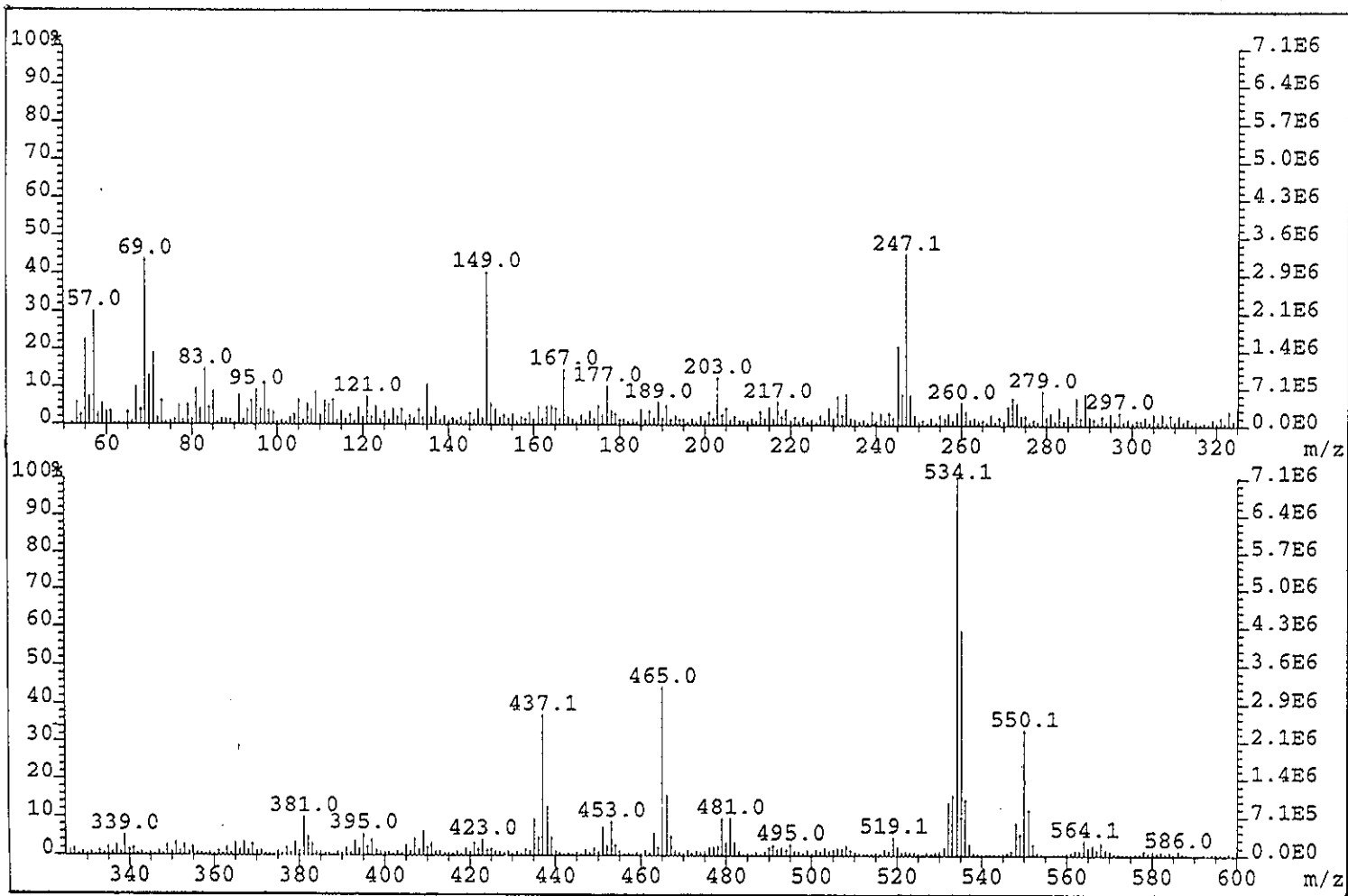


Figure 65 Mass spectrum of PP1

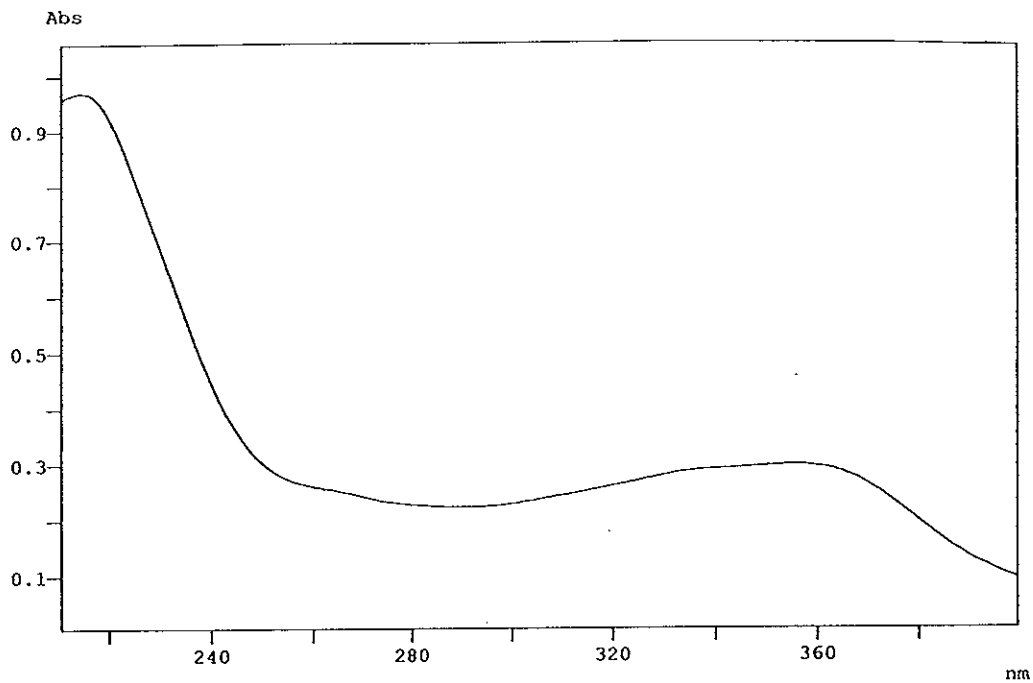


Figure 66 UV (MeOH) spectrum of PP1

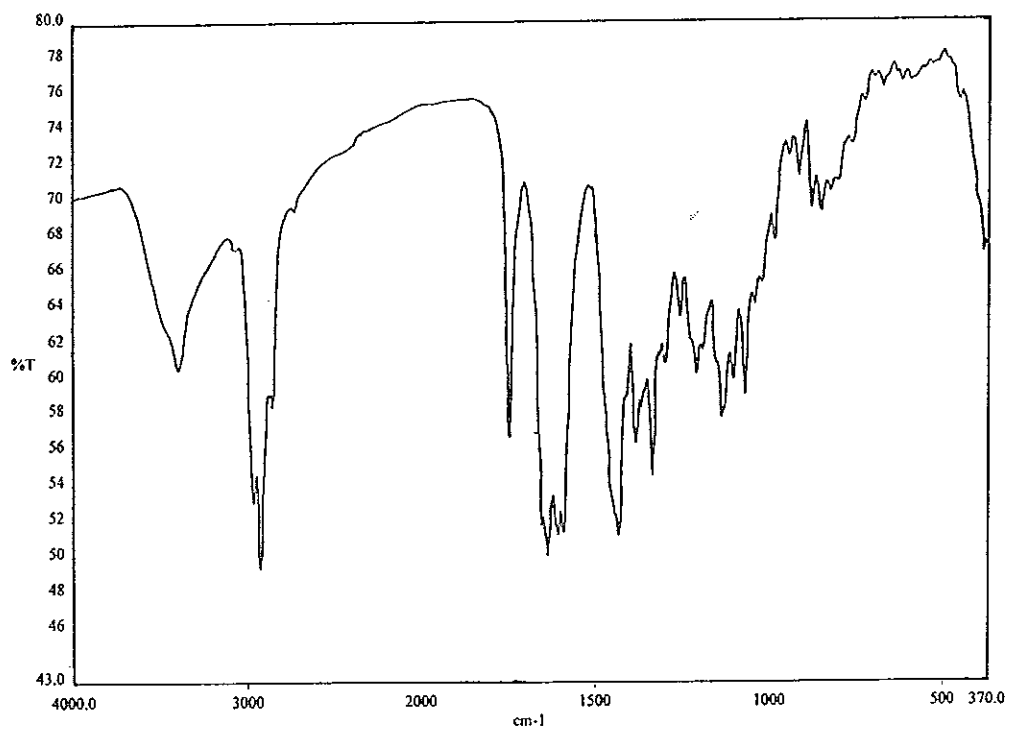


Figure 67 FT-IR (neat) spectrum of PP1

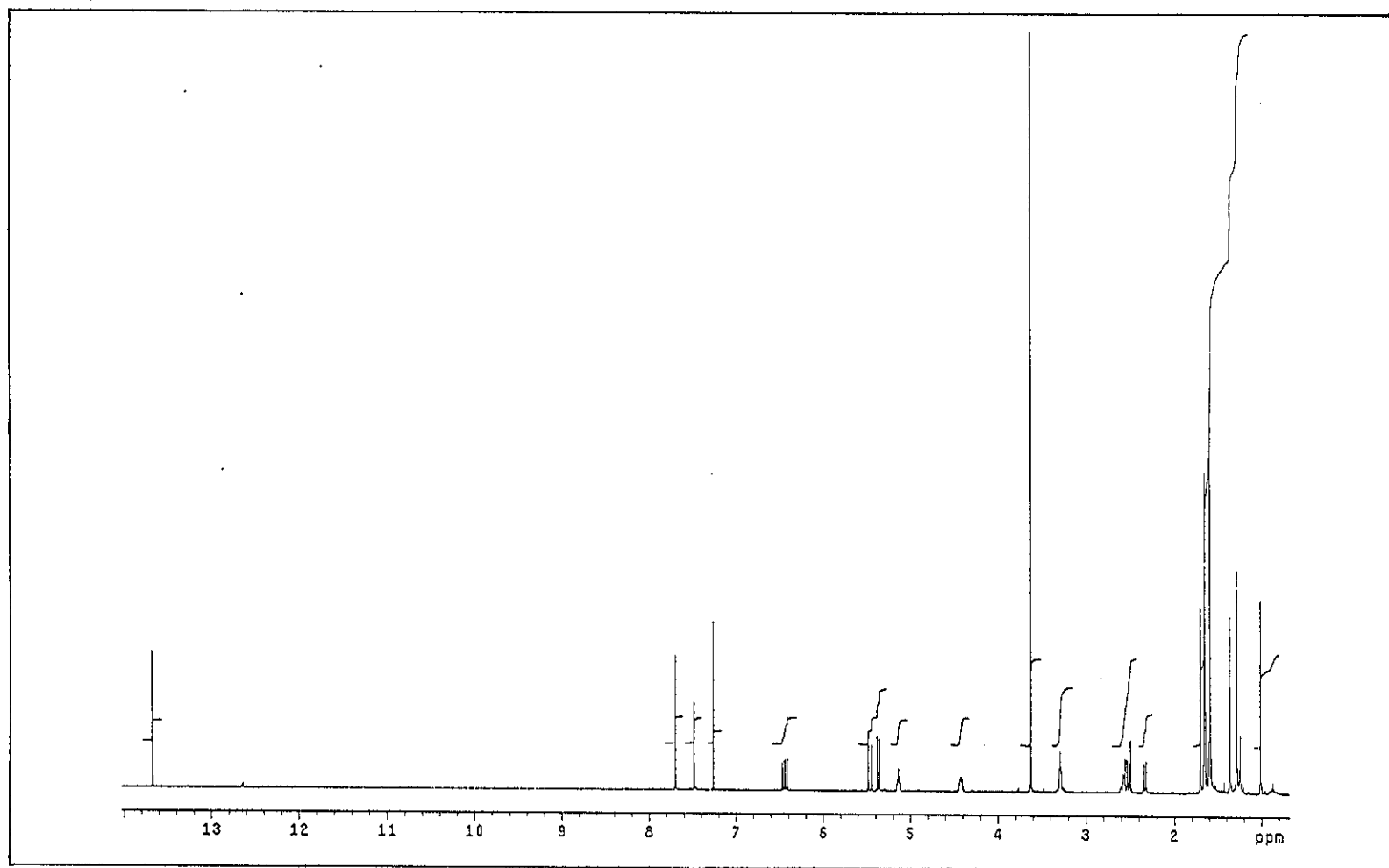


Figure 68 ^1H NMR (500 MHz) (CDCl_3) spectrum of PP1

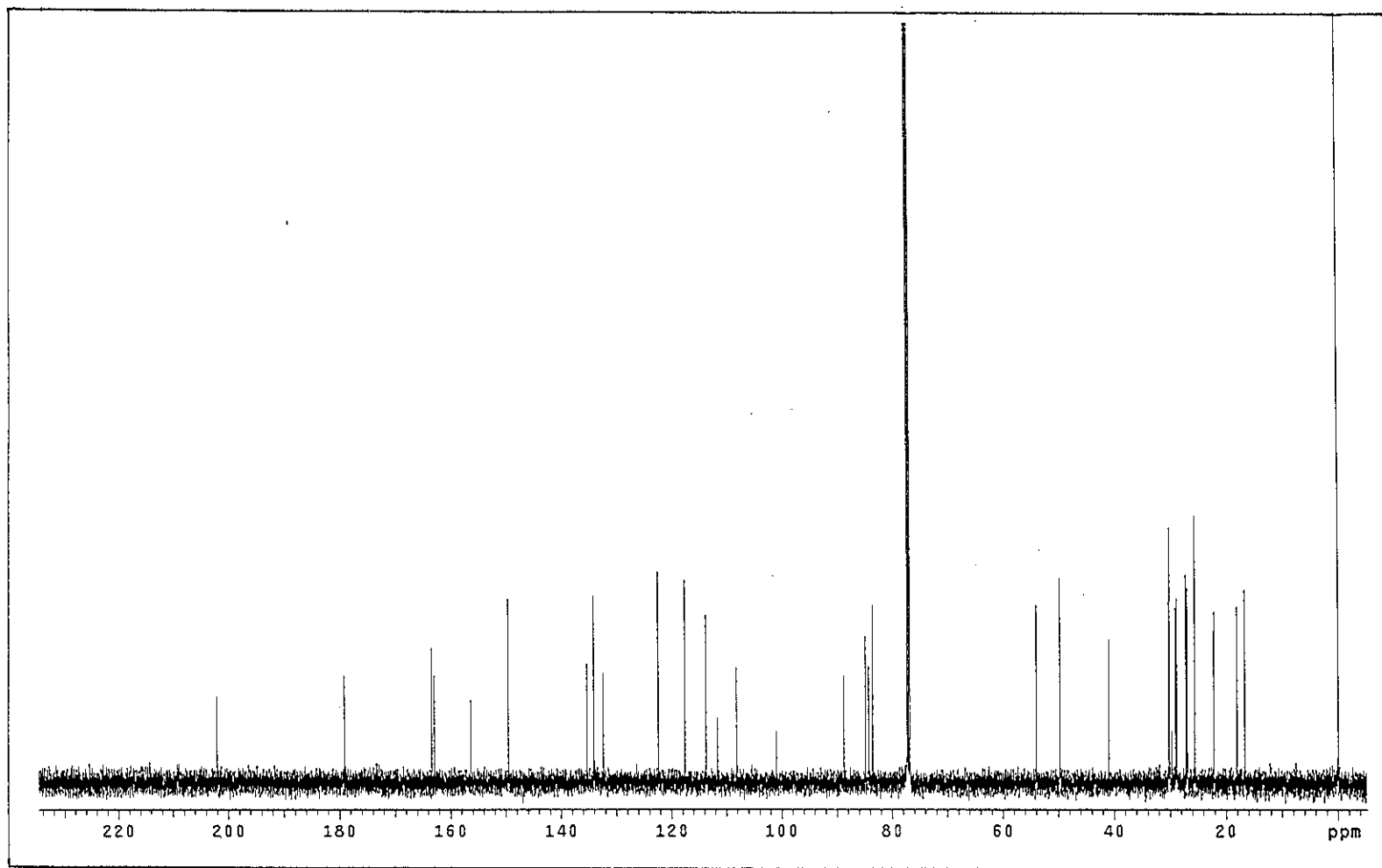


Figure 69 ^{13}C NMR (125 MHz) (CDCl_3) spectrum of PP1

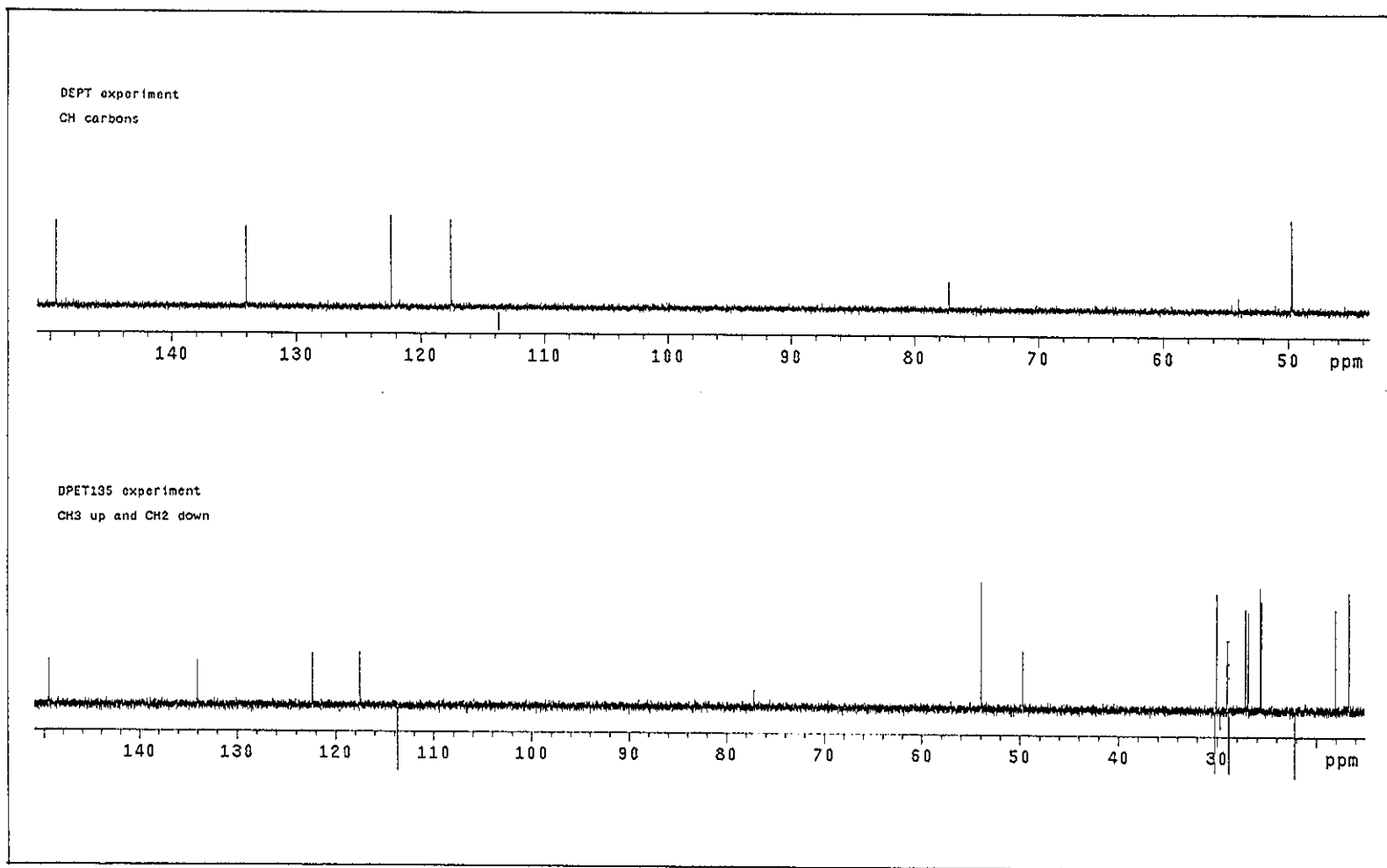


Figure 70 DEPT spectrum of PP1

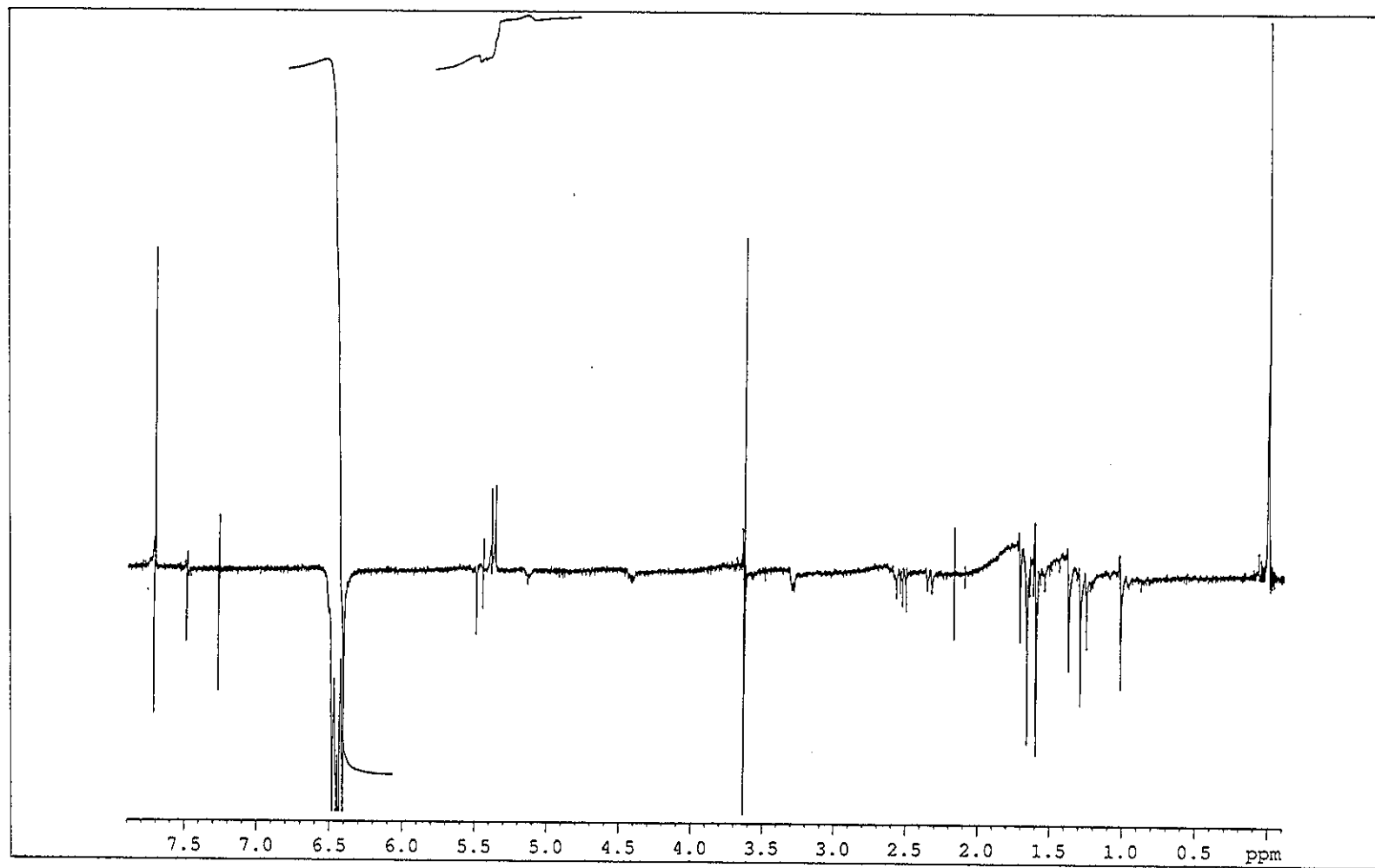


Figure 71 NOEDIFF spectrum of PP1 after irradiation at δ_H 6.43

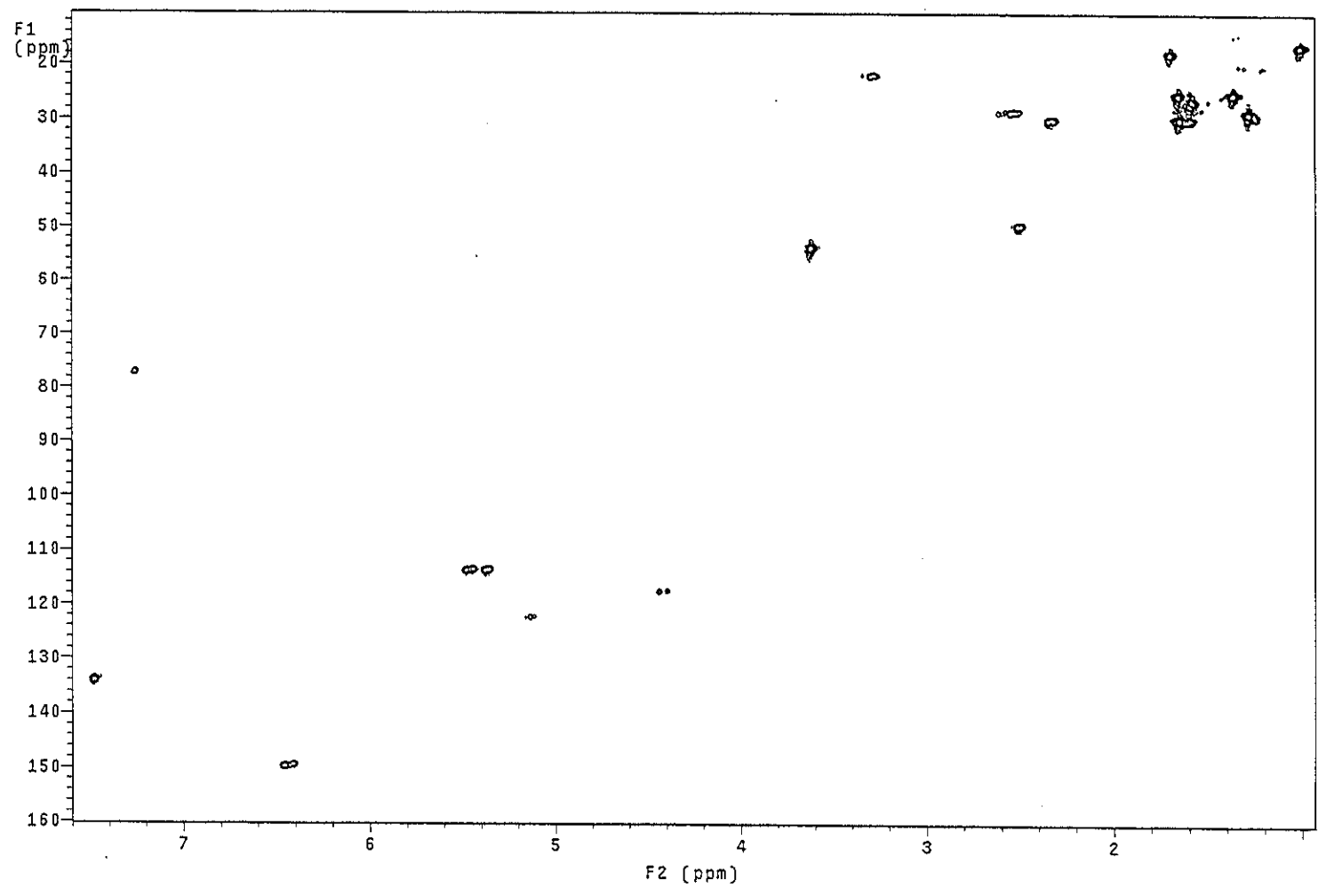


Figure 72 2D HMQC spectrum of PP1

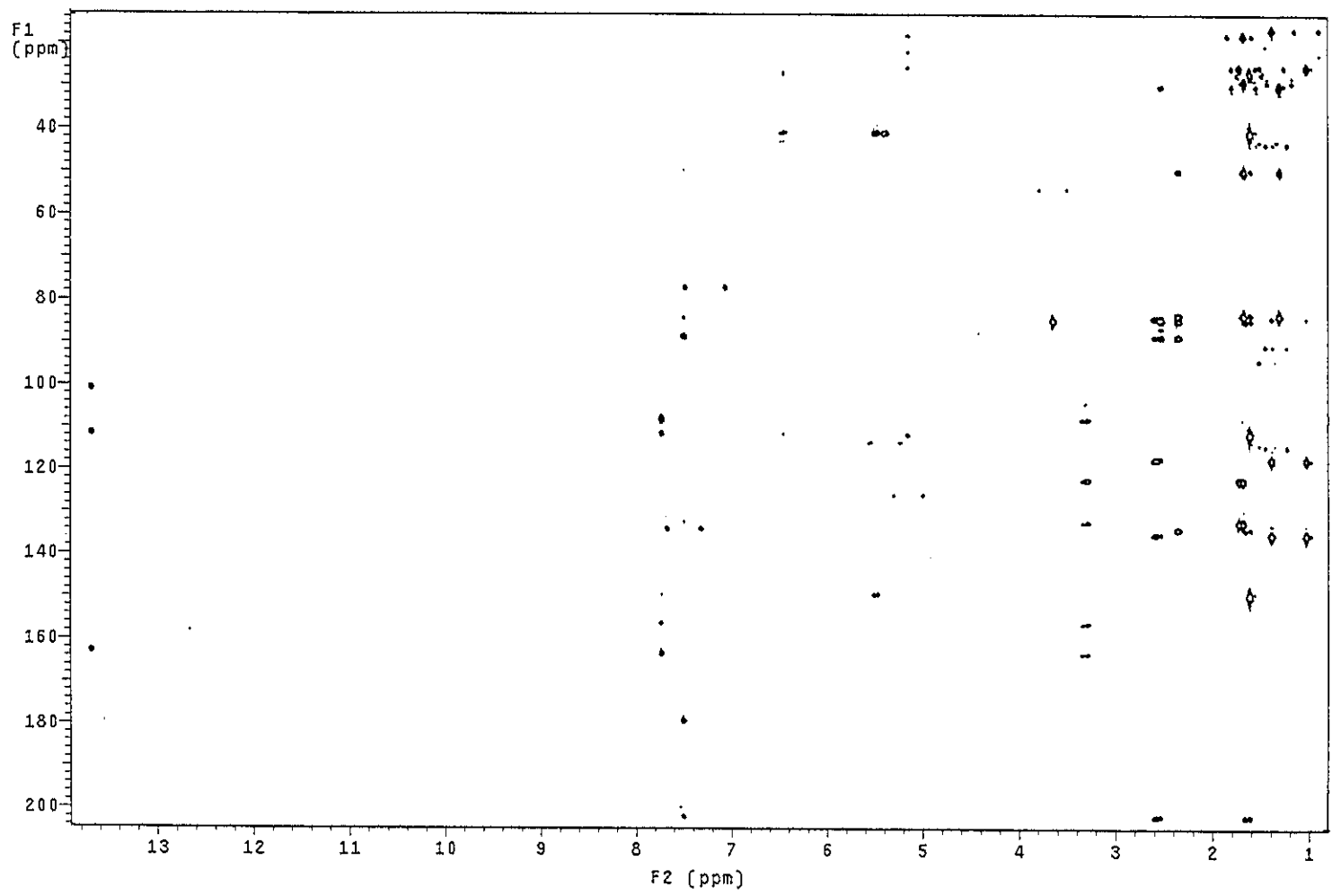


Figure 73 2D HMBC spectrum of PP1

Mass Peak #: 563 Ret. Time: (0.619 - 3.196)
Base Peak : 85.05 (812497)

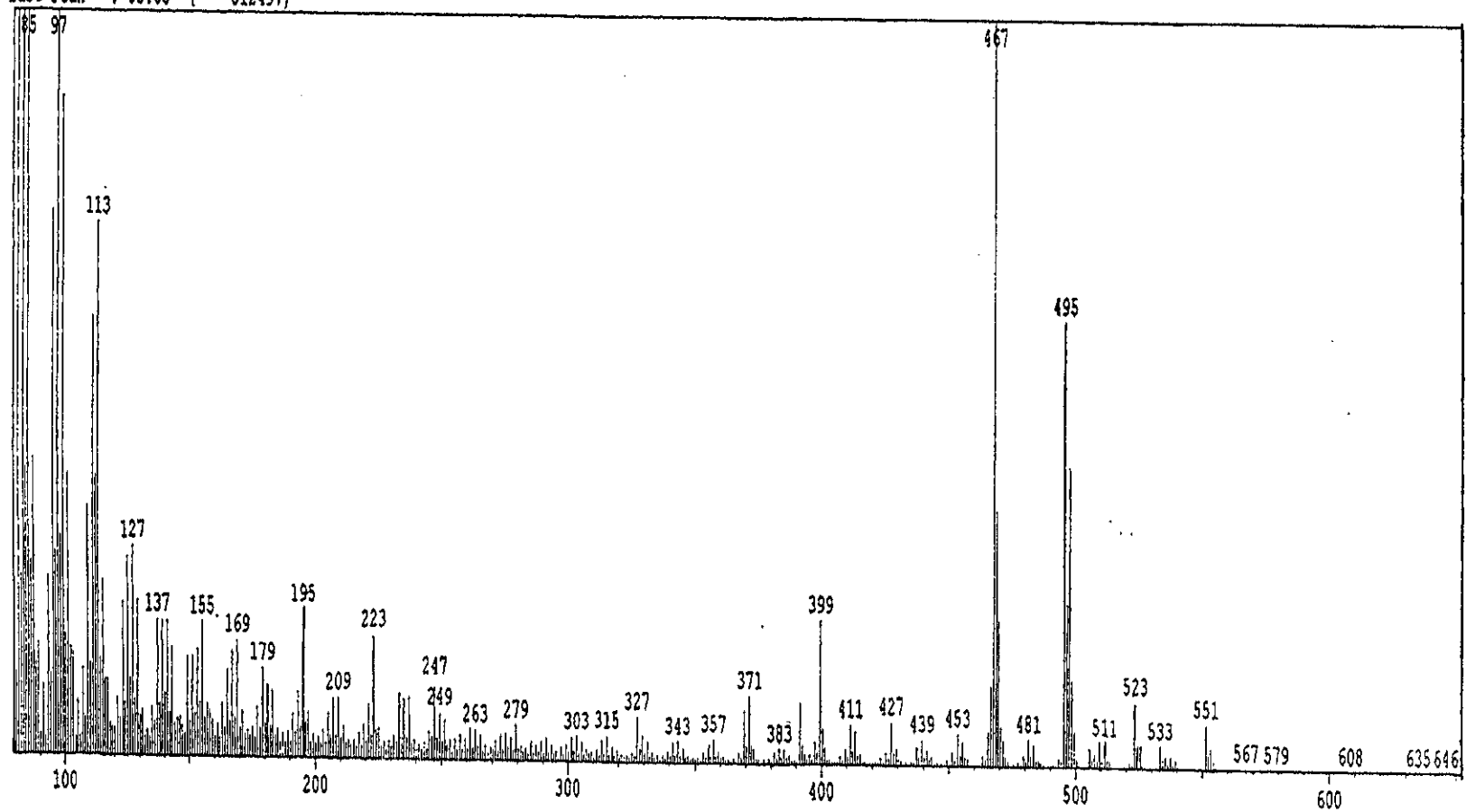


Figure 74 Mass spectrum of PP3

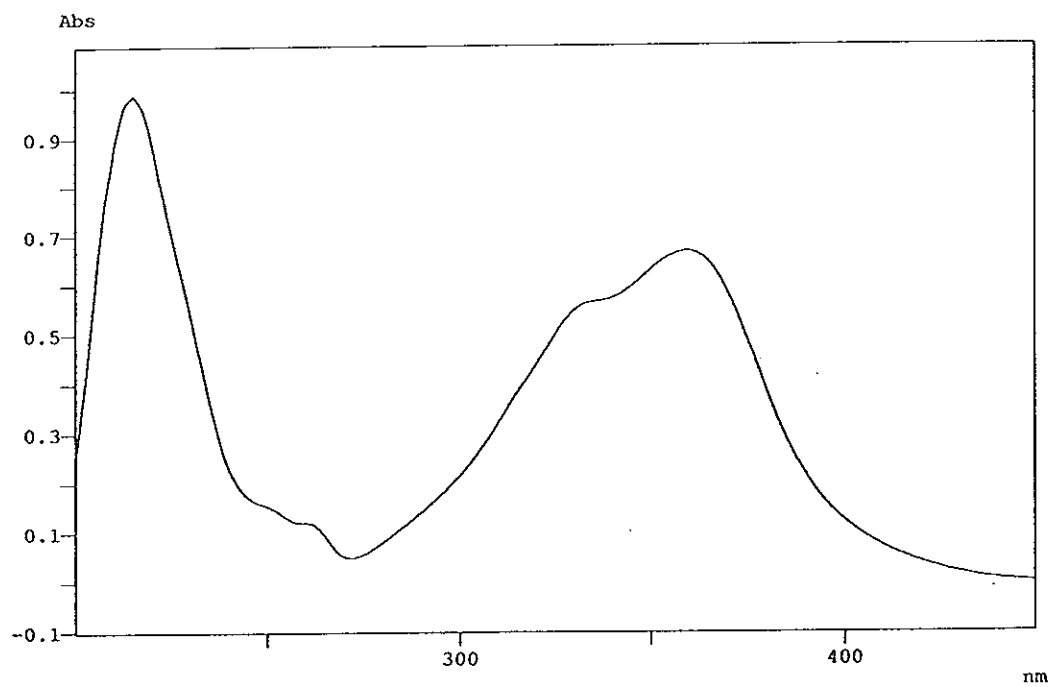


Figure 75 UV (MeOH) spectrum of PP3

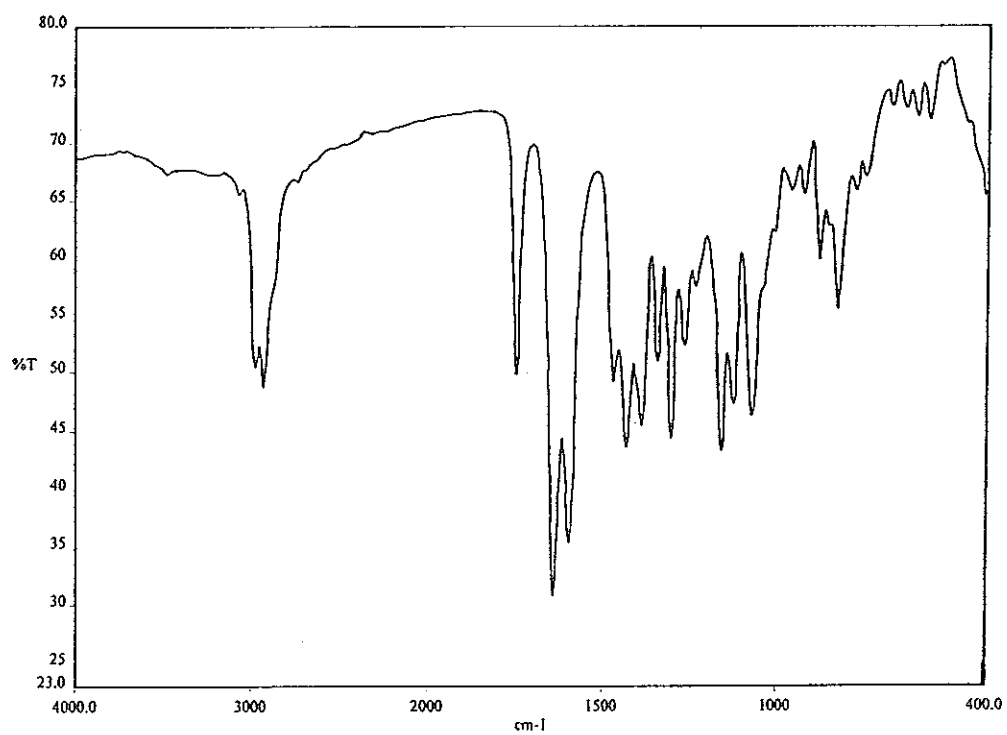


Figure 76 FT-IR (neat) spectrum of PP3

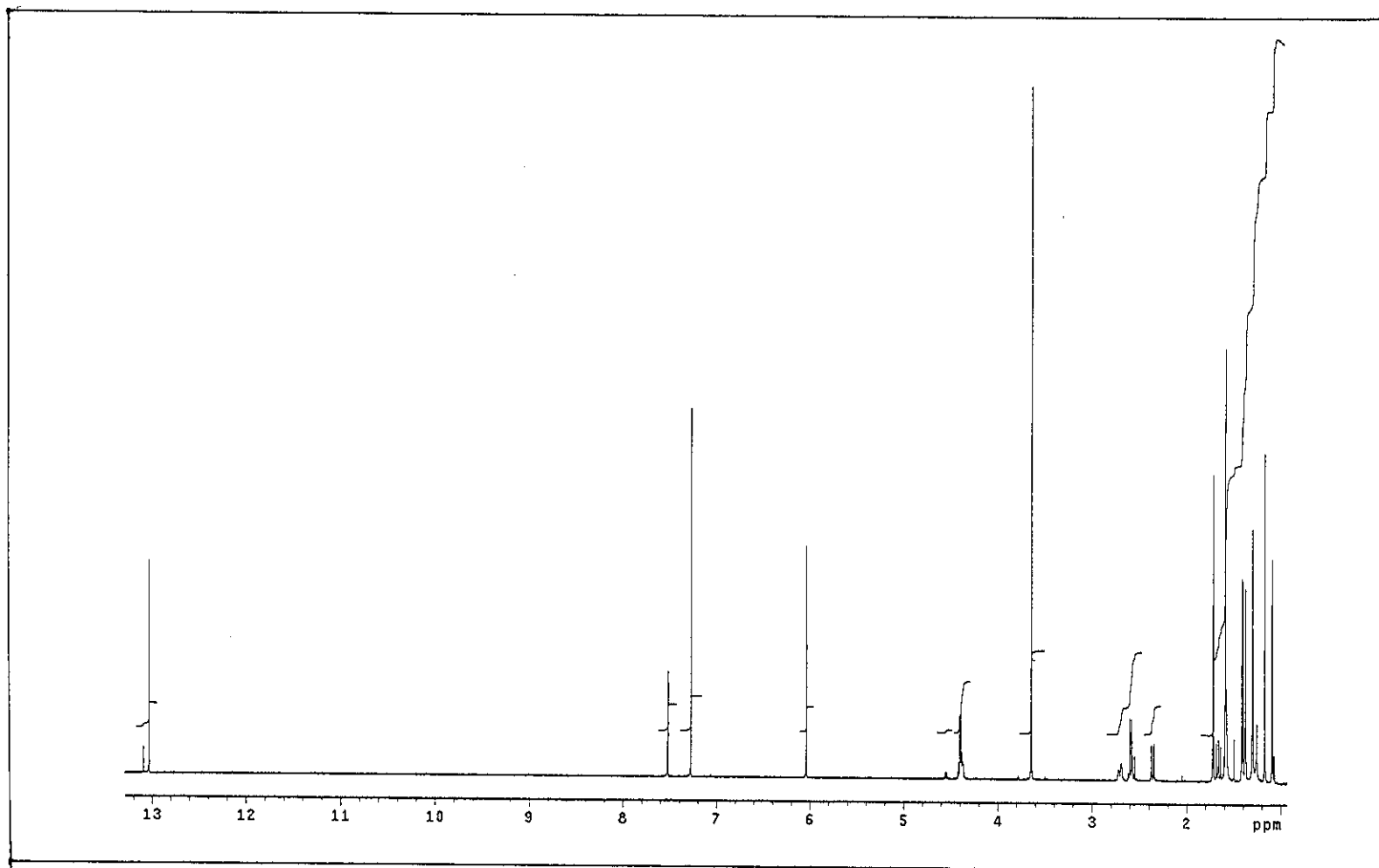


Figure 77 ^1H NMR (500 MHz) (CDCl_3) spectrum of PP3

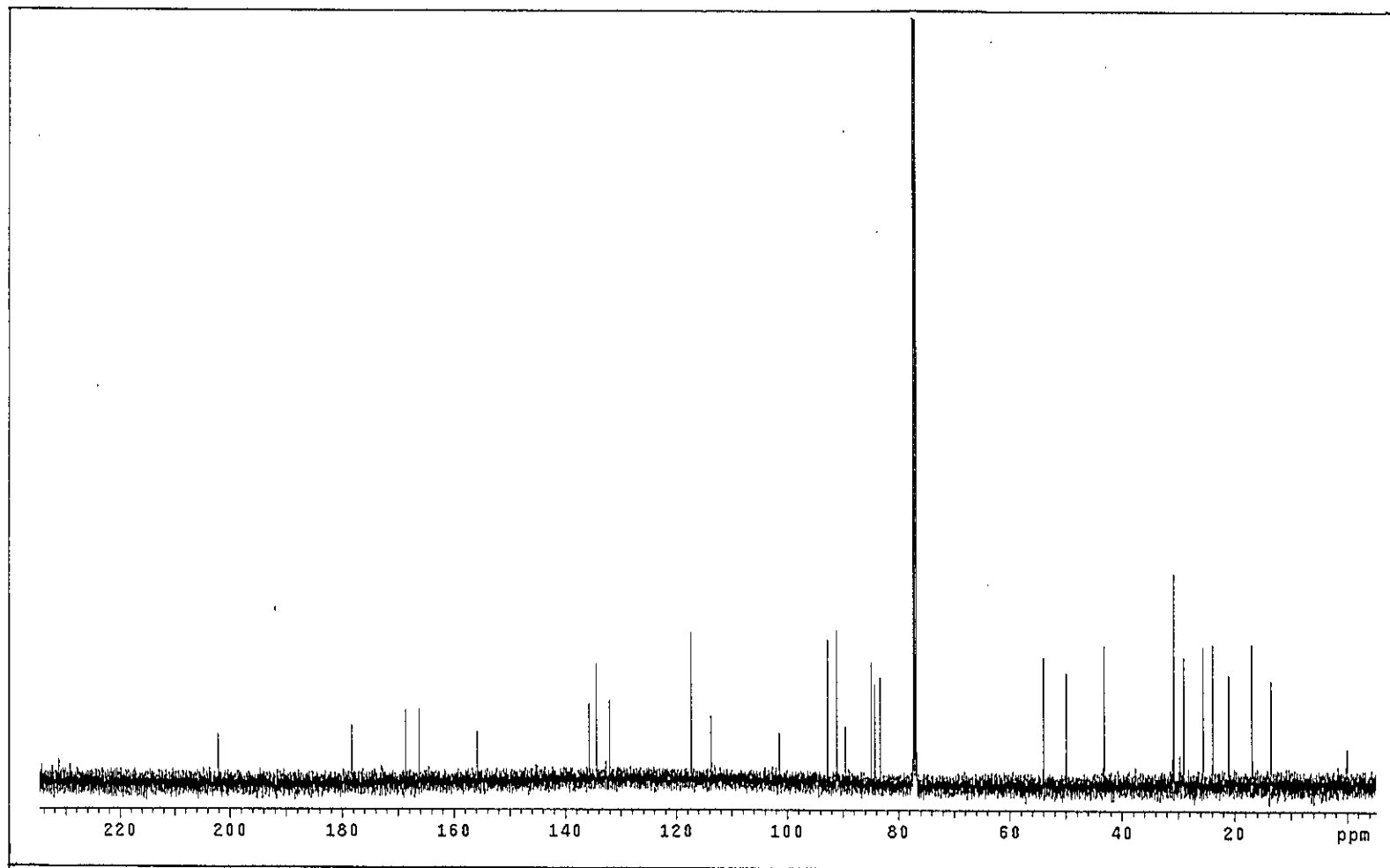


Figure 78 ^{13}C NMR (125 MHz) (CDCl_3) spectrum of PP3

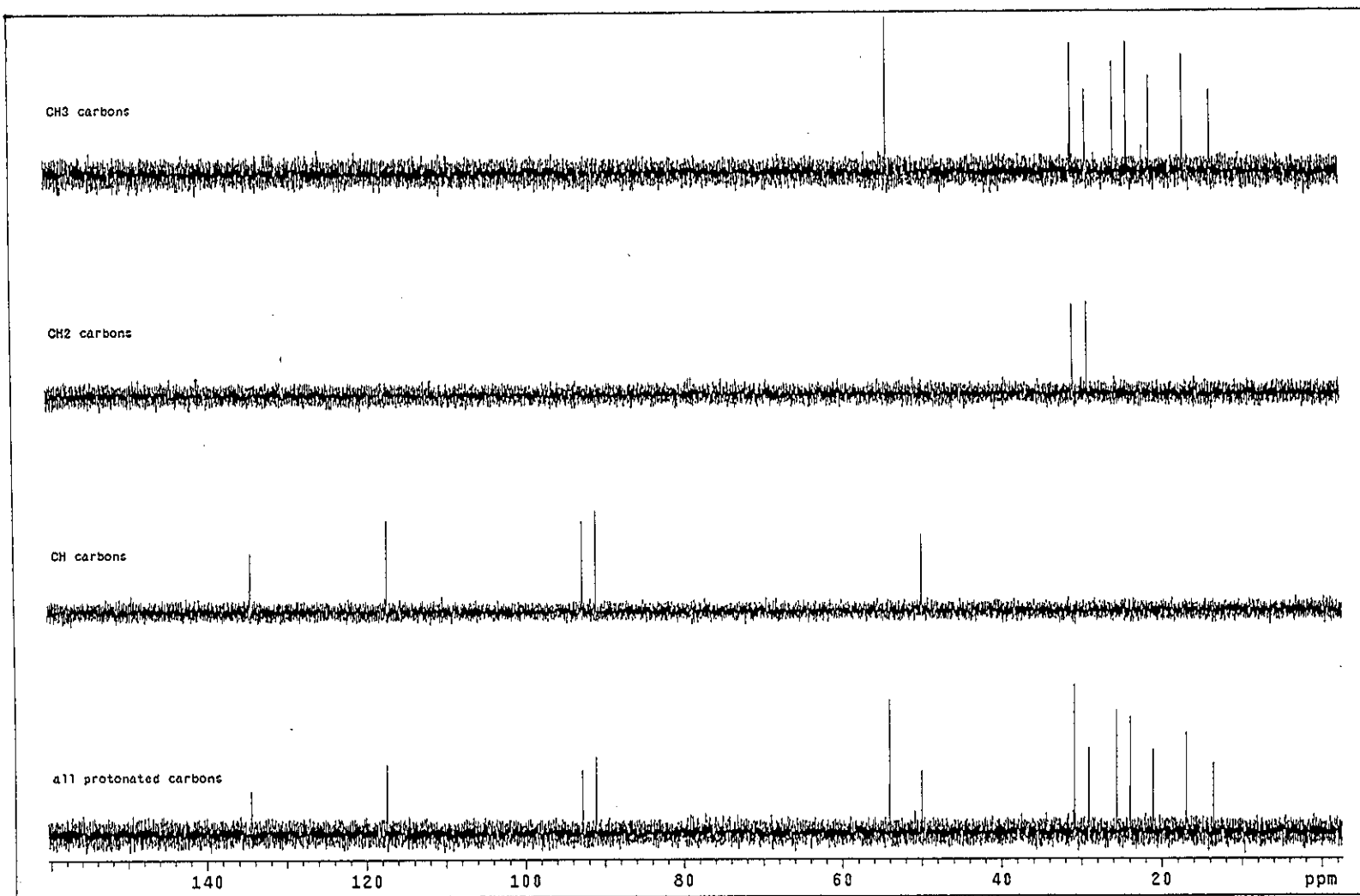


Figure 79 DEPT spectrum of PP3

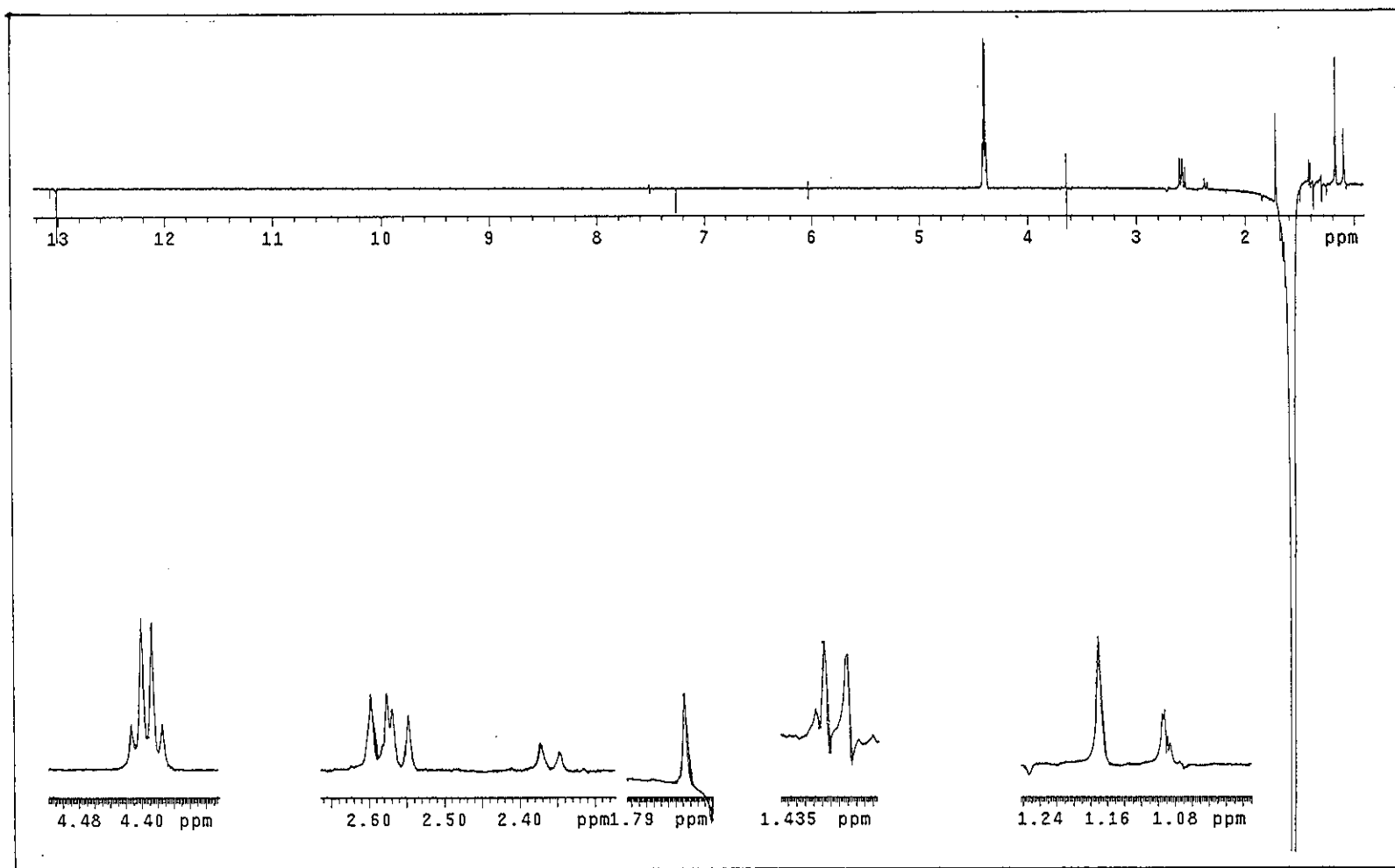


Figure 80 NOEDIFF spectrum of PP3 after irradiation at δ_H 1.59

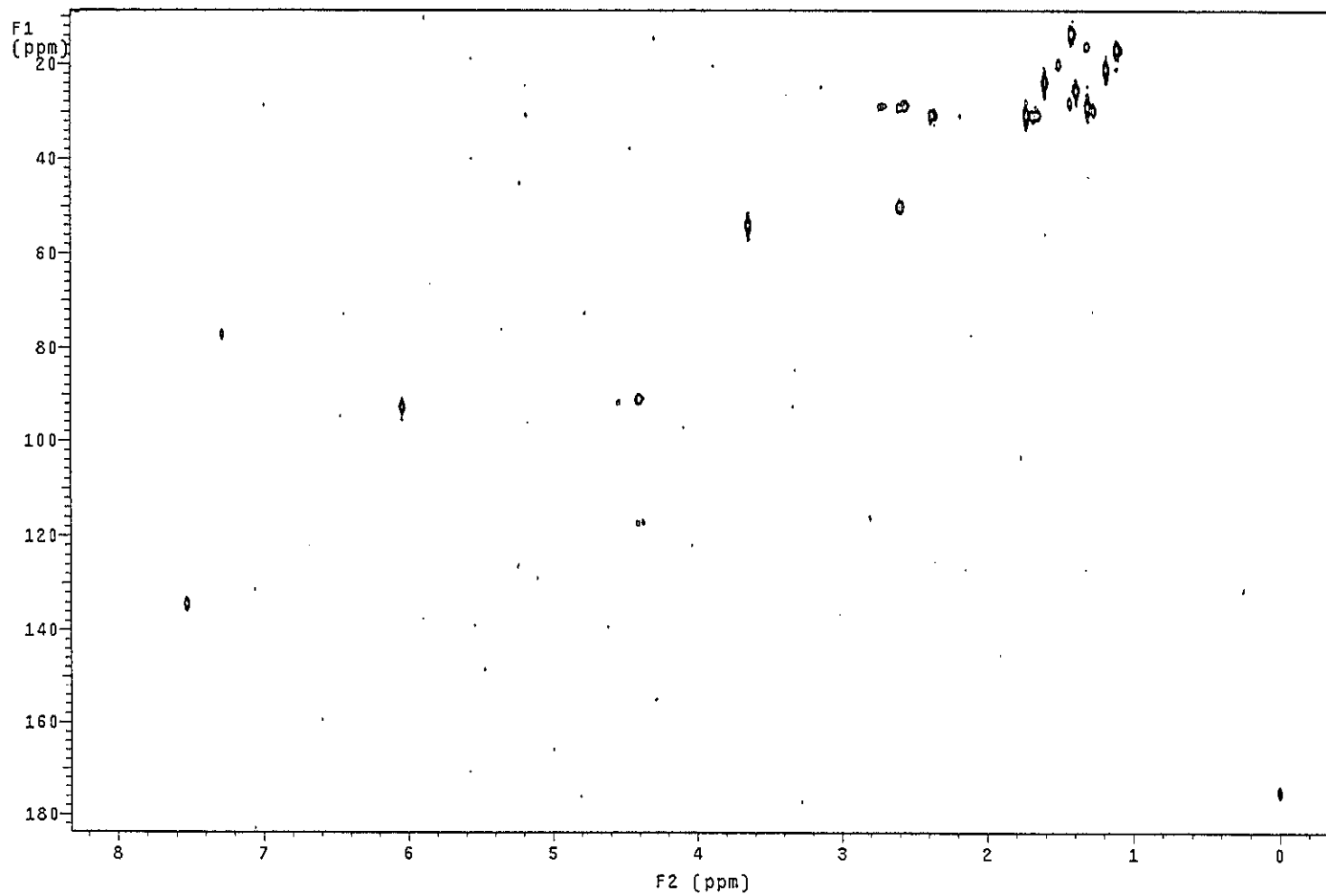


Figure 81 2D HMQC spectrum of PP3

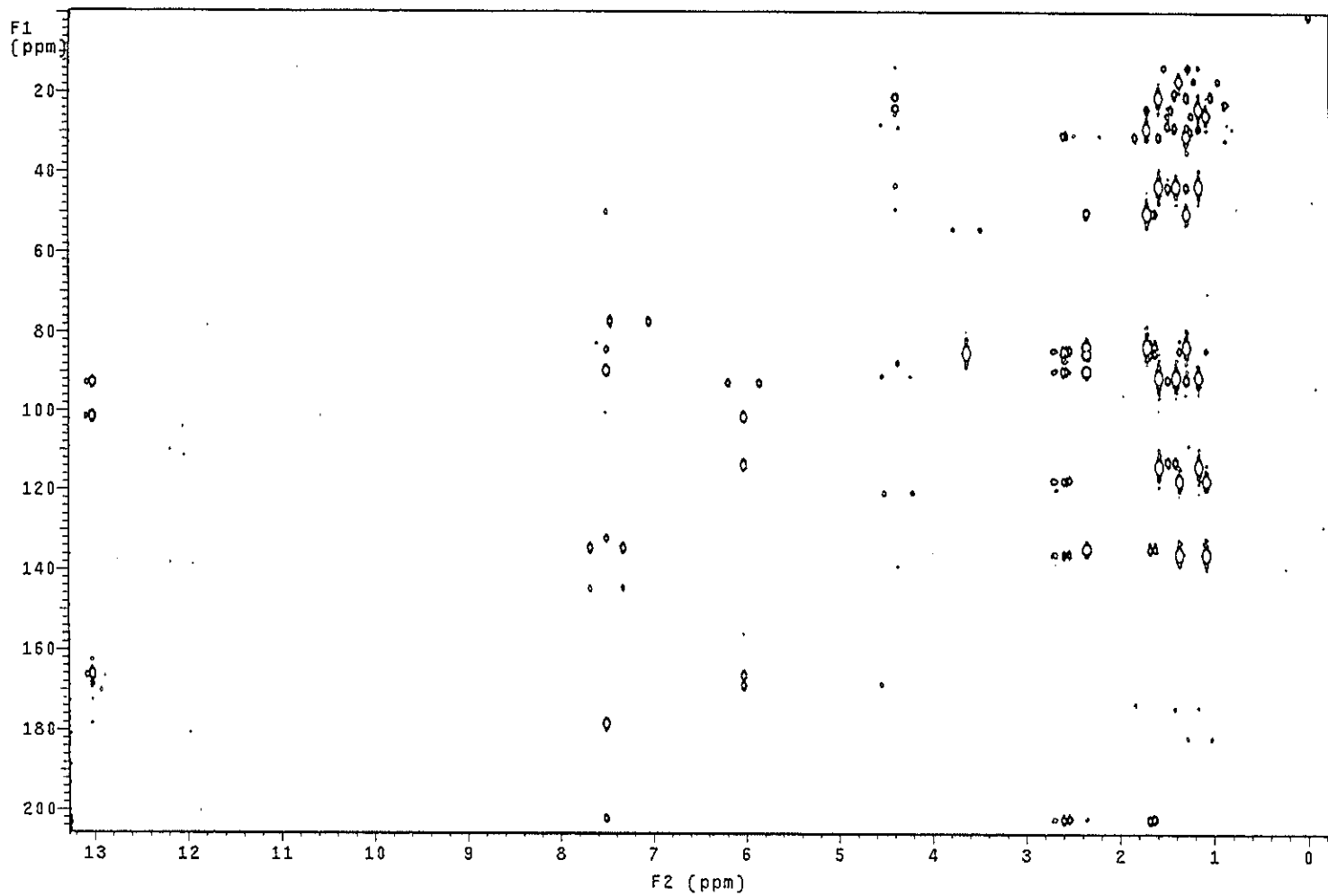


Figure 82 2D HMBC spectrum of PP3

Mass Peak #: 524 Ret. Time: (0.194 - 0.871)
Base Peak : 85.05 (473705)

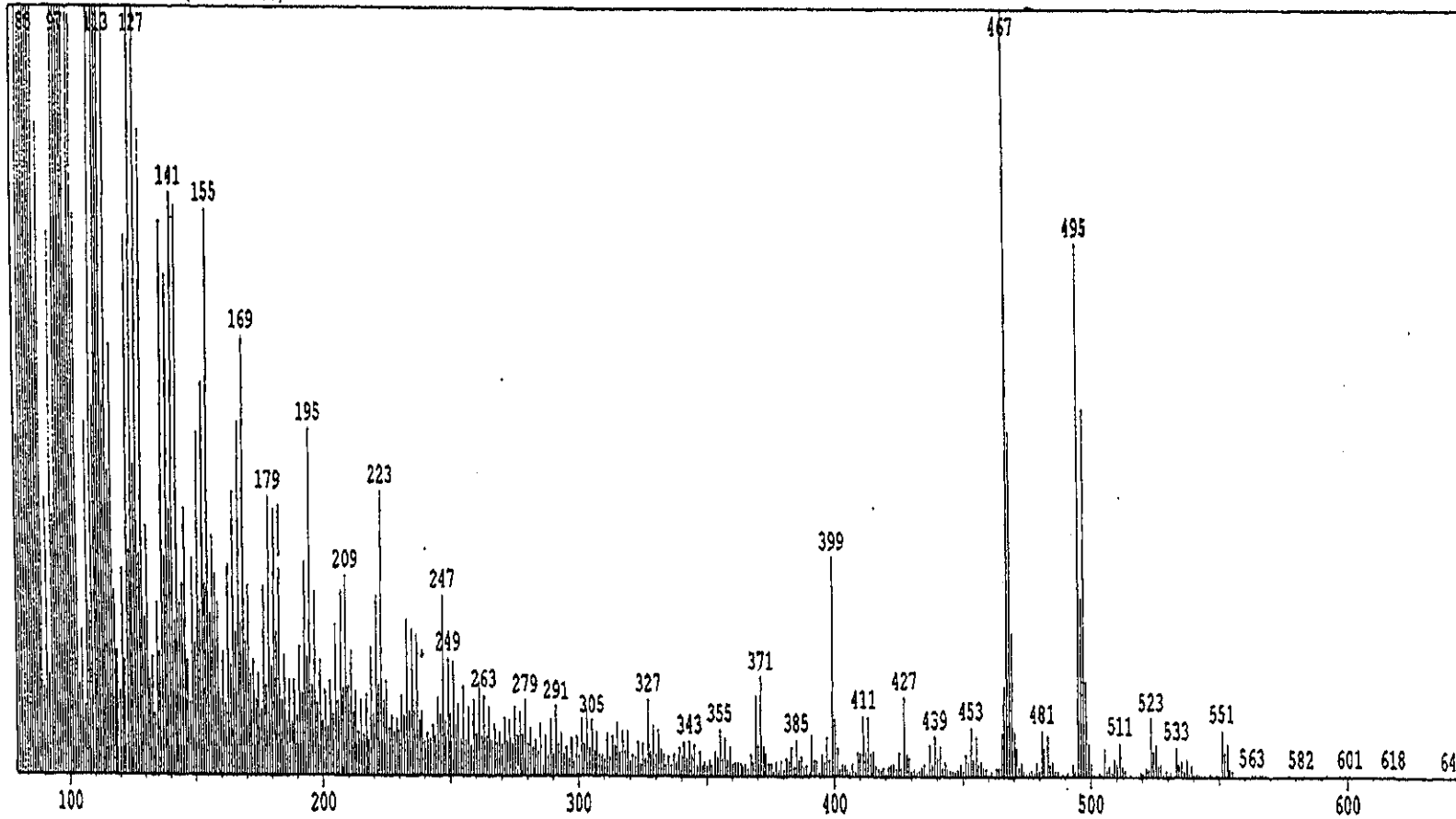


Figure 83 Mass spectrum of PP4

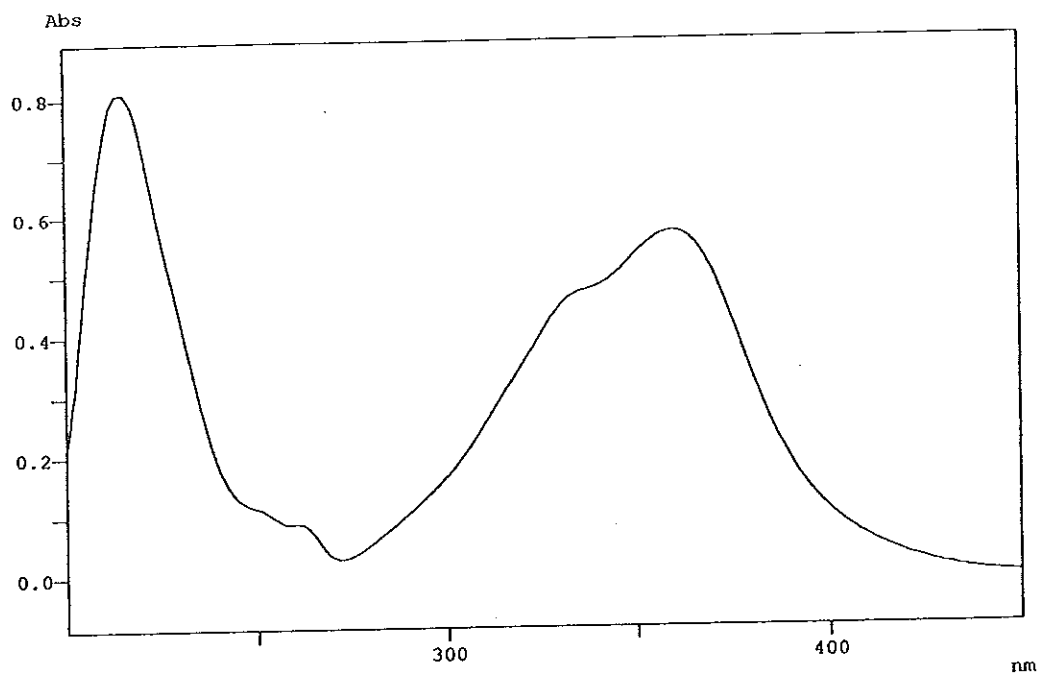


Figure 84 UV (MeOH) spectrum of PP4

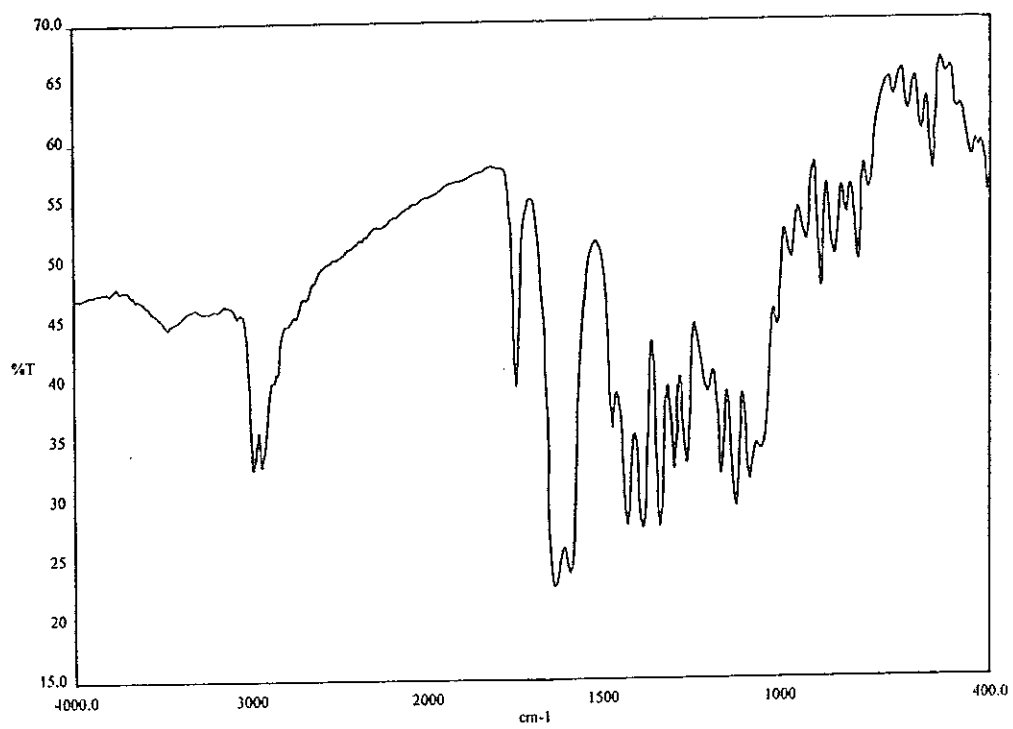


Figure 85 FT-IR (neat) spectrum of PP4

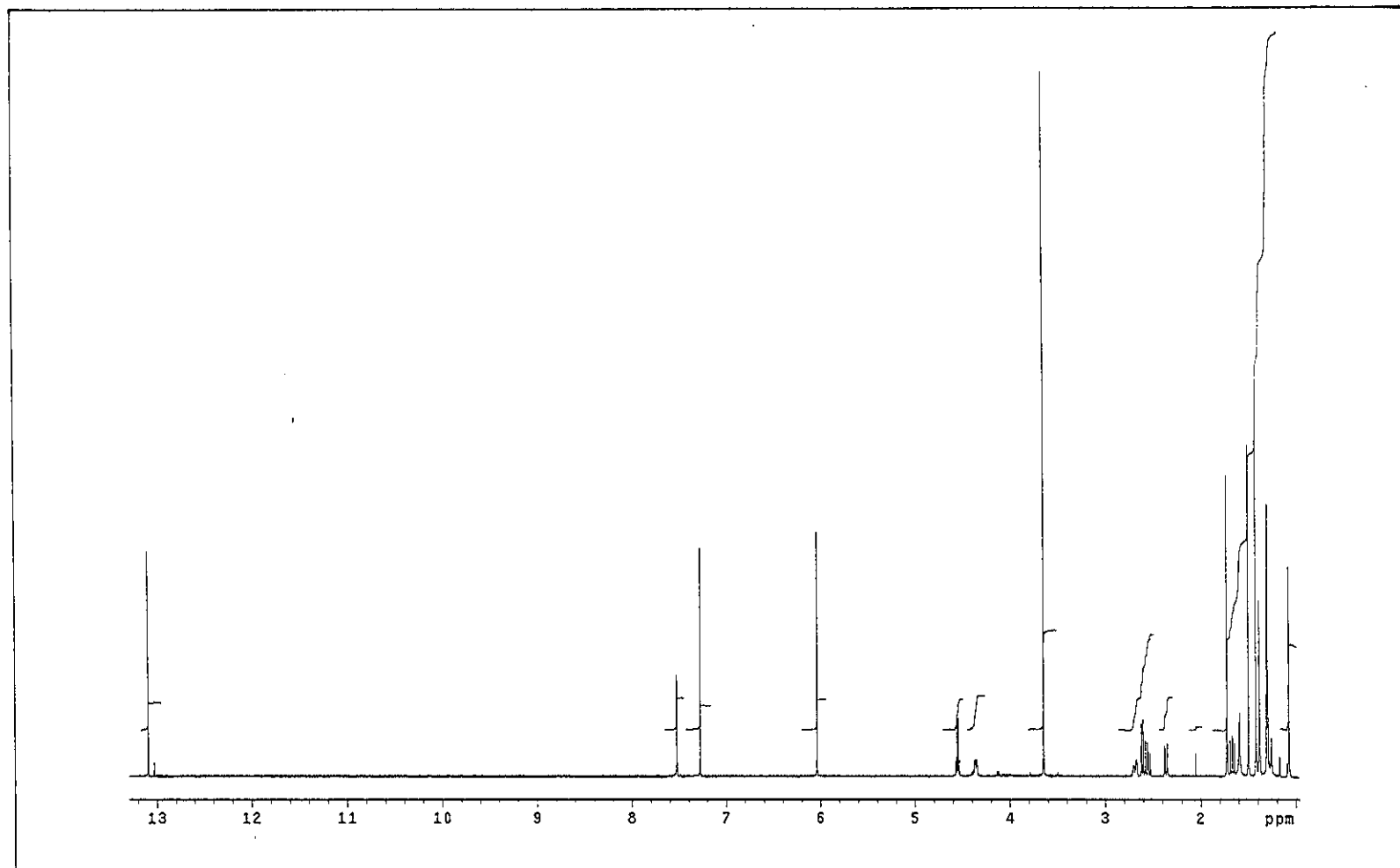


Figure 86 ^1H NMR (500 MHz) (CDCl_3) spectrum of PP4

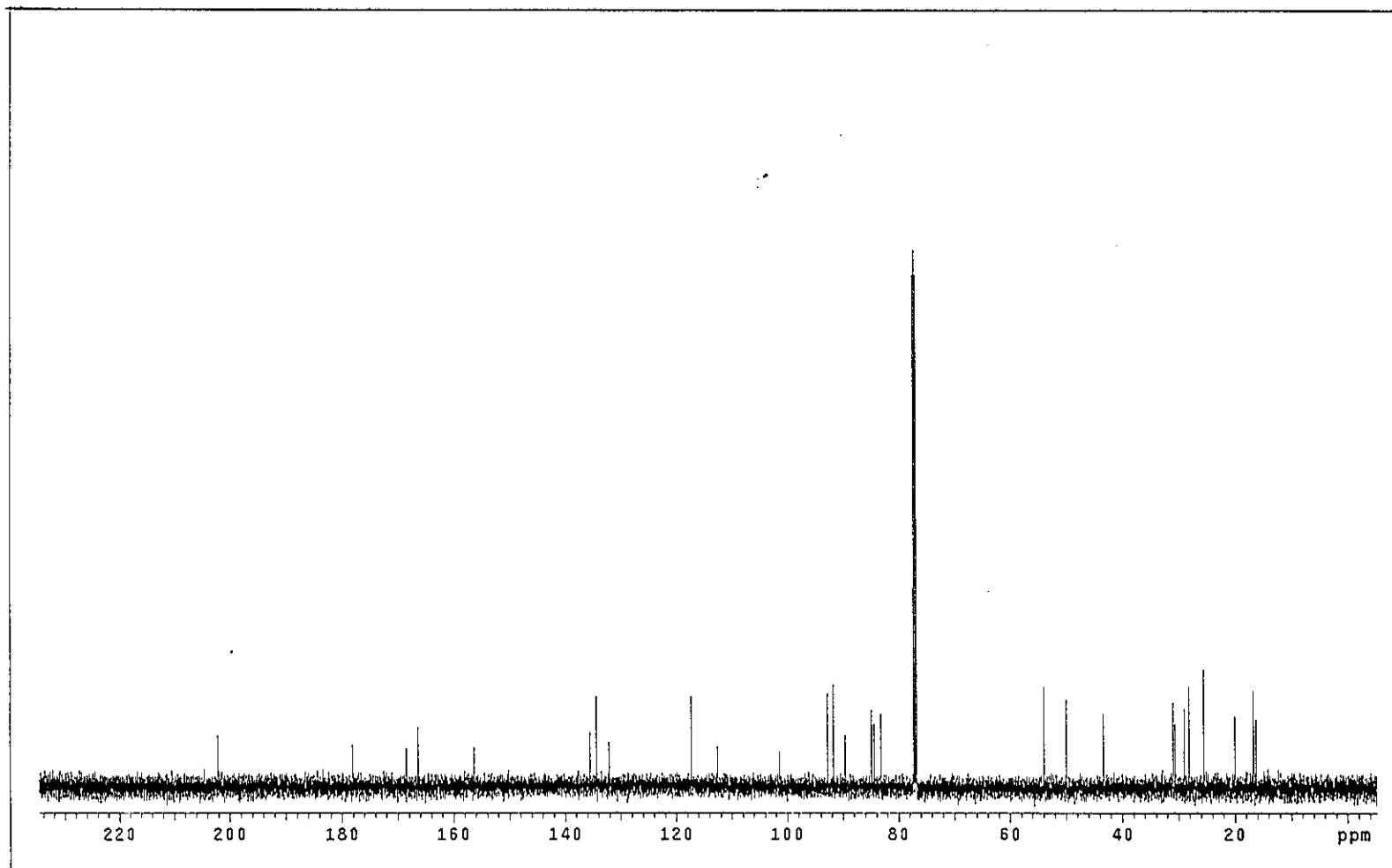


Figure 87 ^{13}C NMR (125 MHz) (CDCl_3) spectrum of PP4

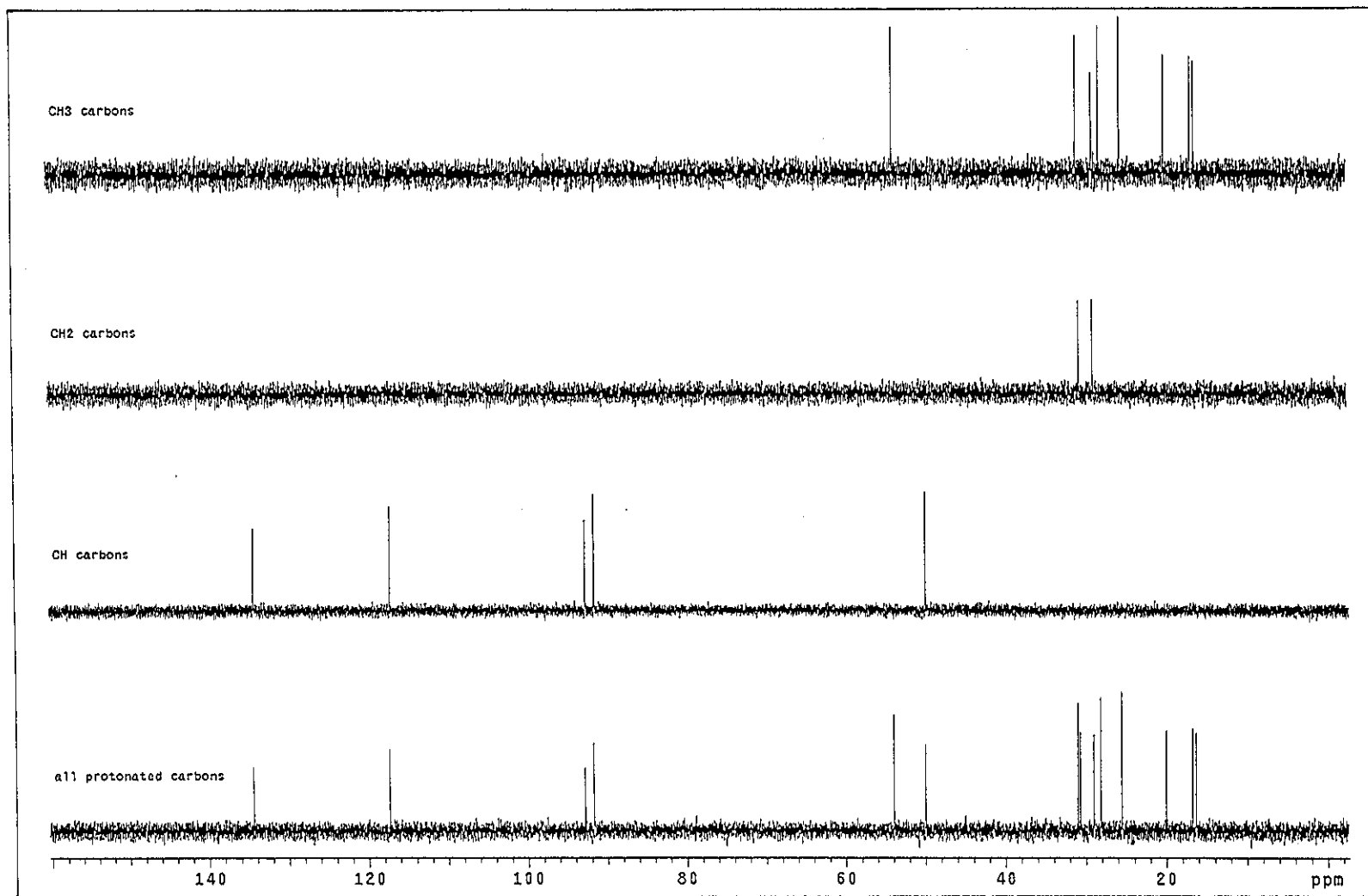


Figure 88 DEPT spectrum of PP4

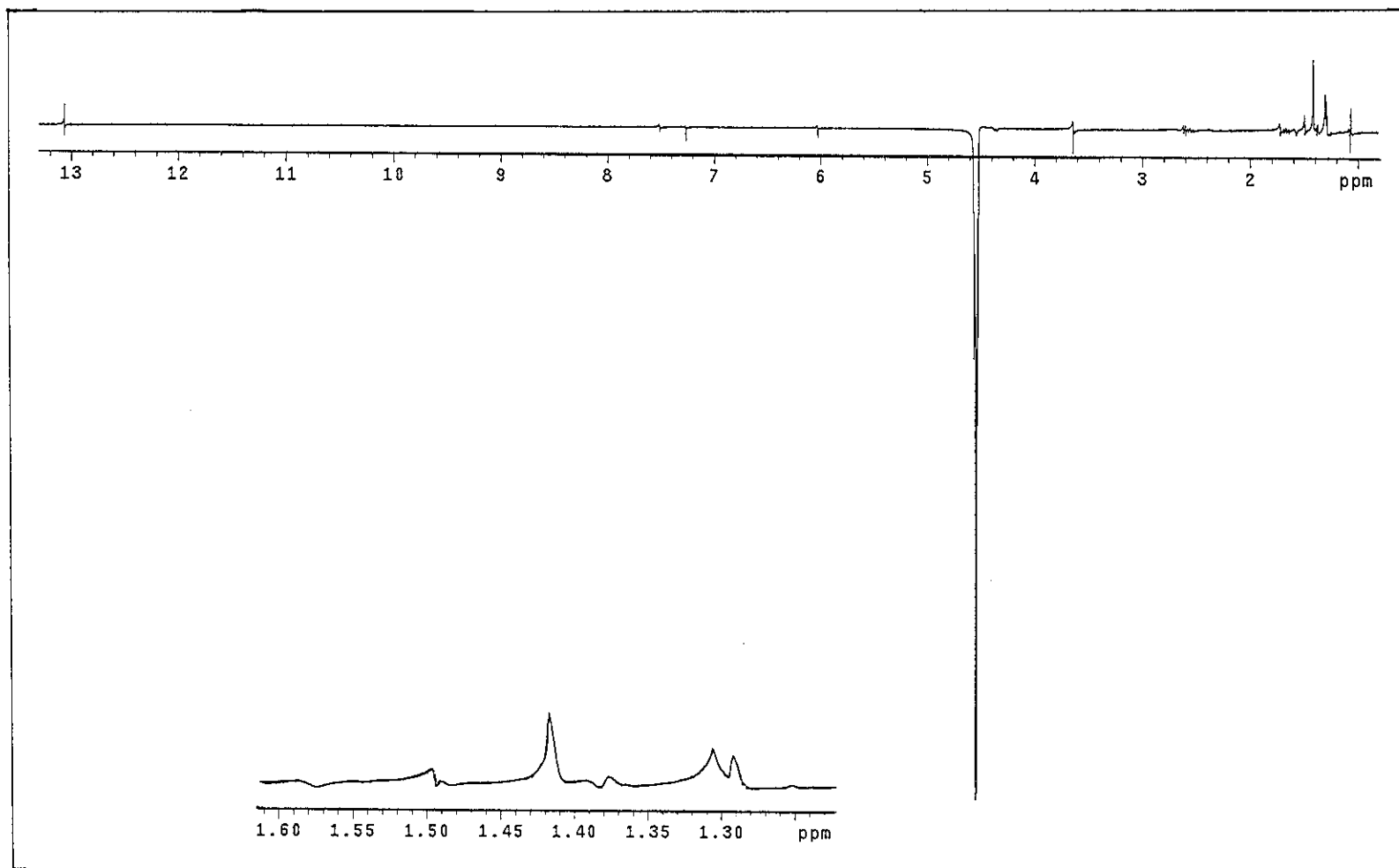


Figure 89 NOEDIFF spectrum of PP4 after irradiation at δ_H 4.55

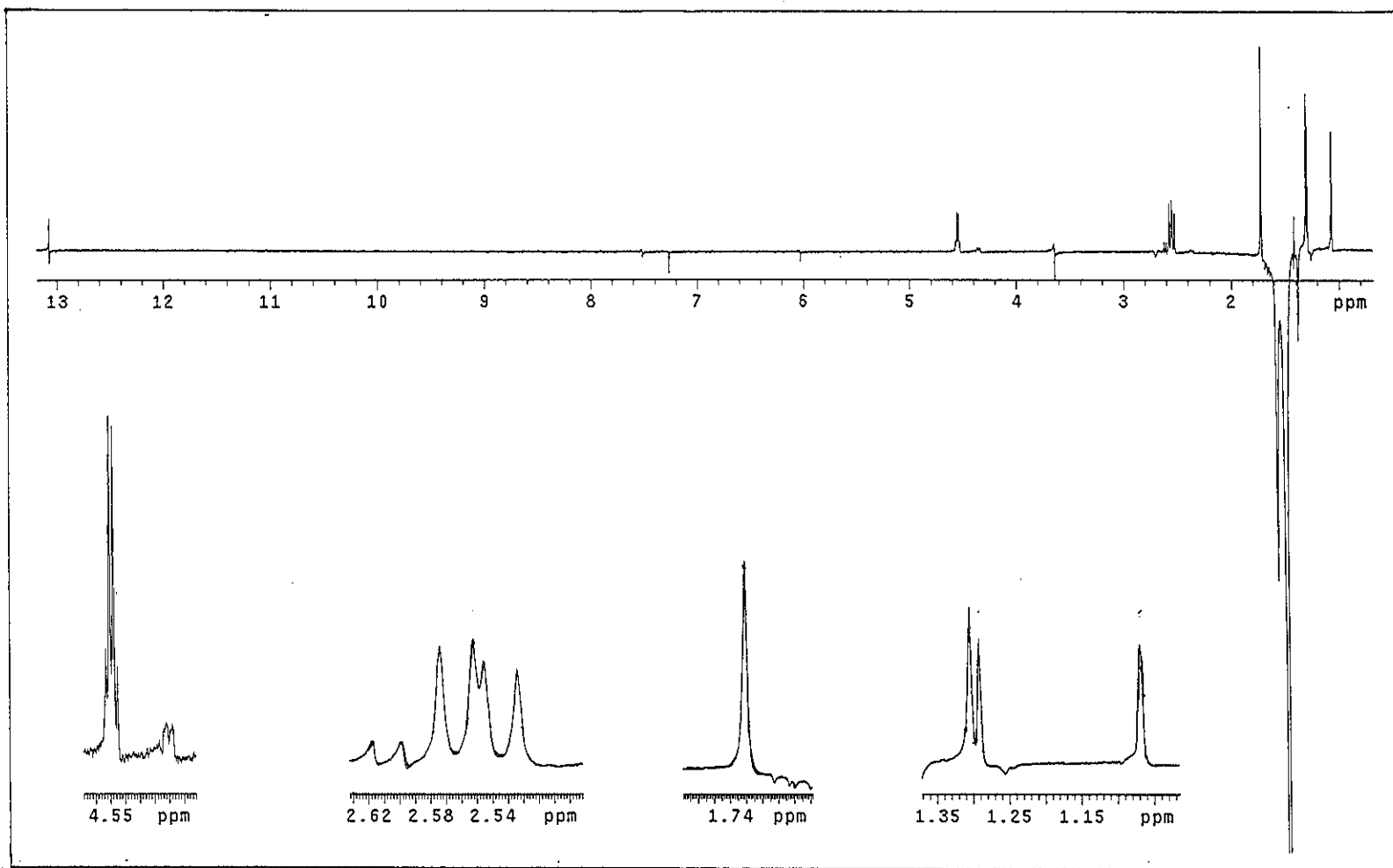


Figure 90 NOEDIFF spectrum of PP4 after irradiation at δ_H 1.49

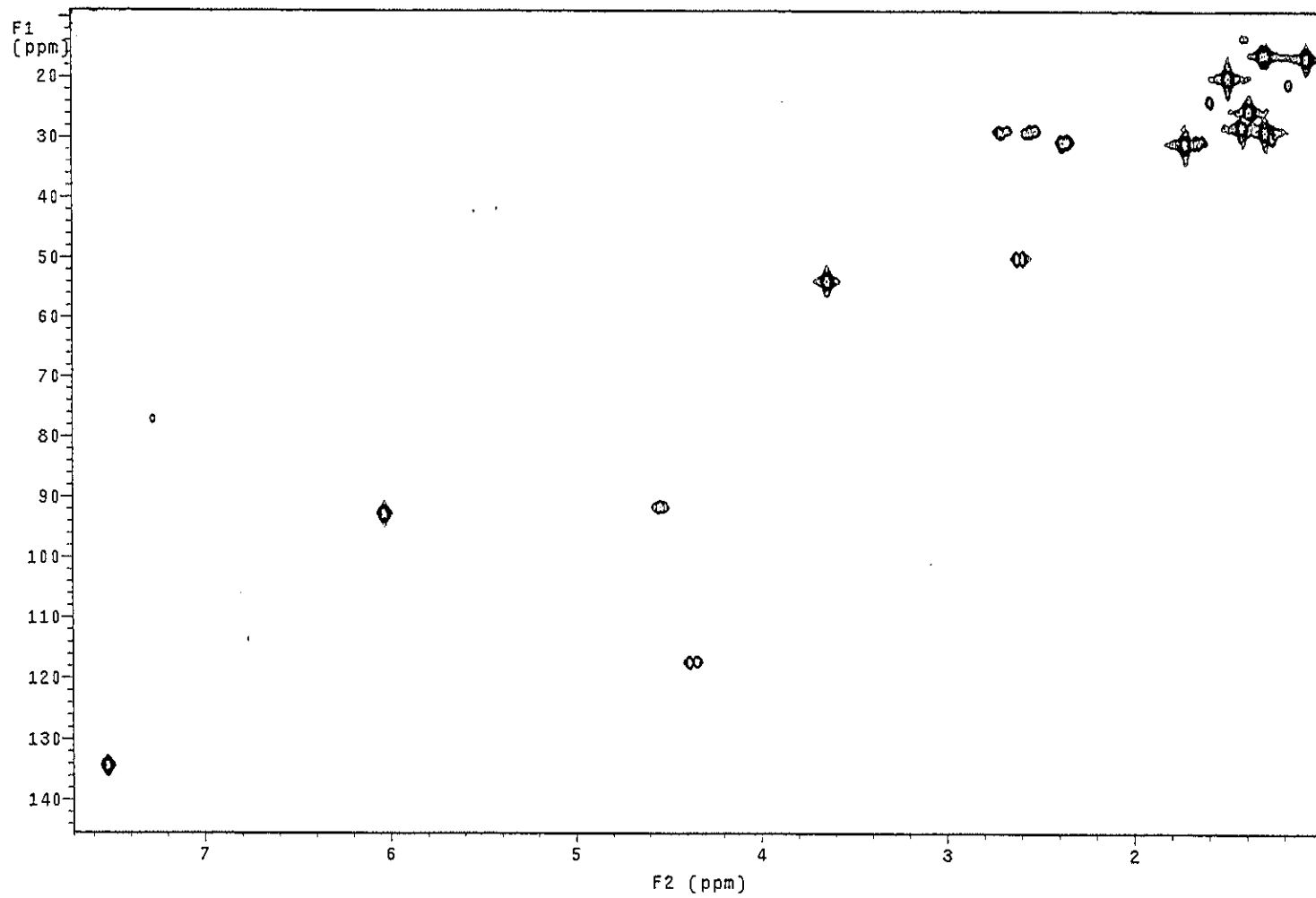


Figure 91 2D HMQC spectrum of PP4

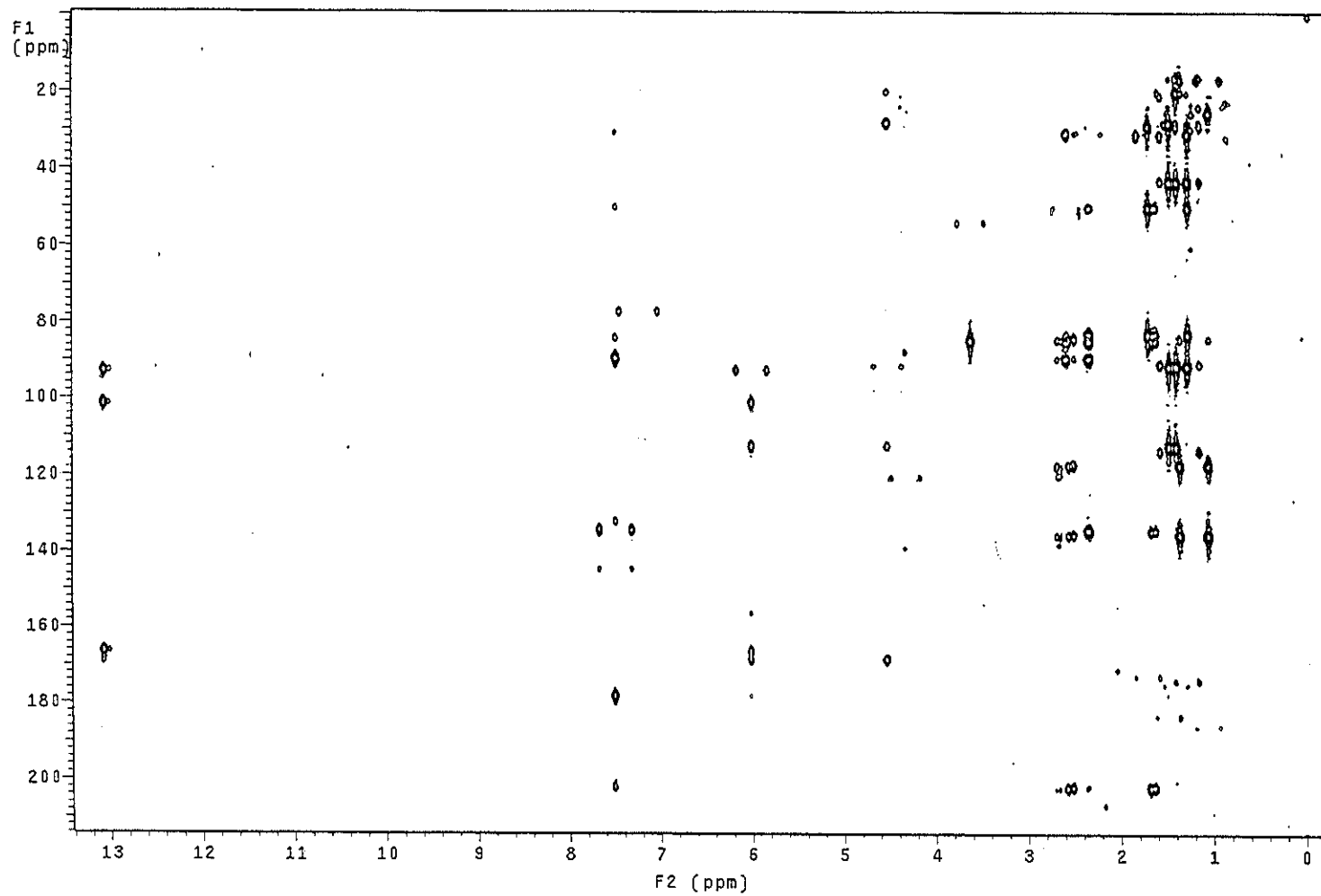


Figure 92 2D HMBC spectrum of PP4

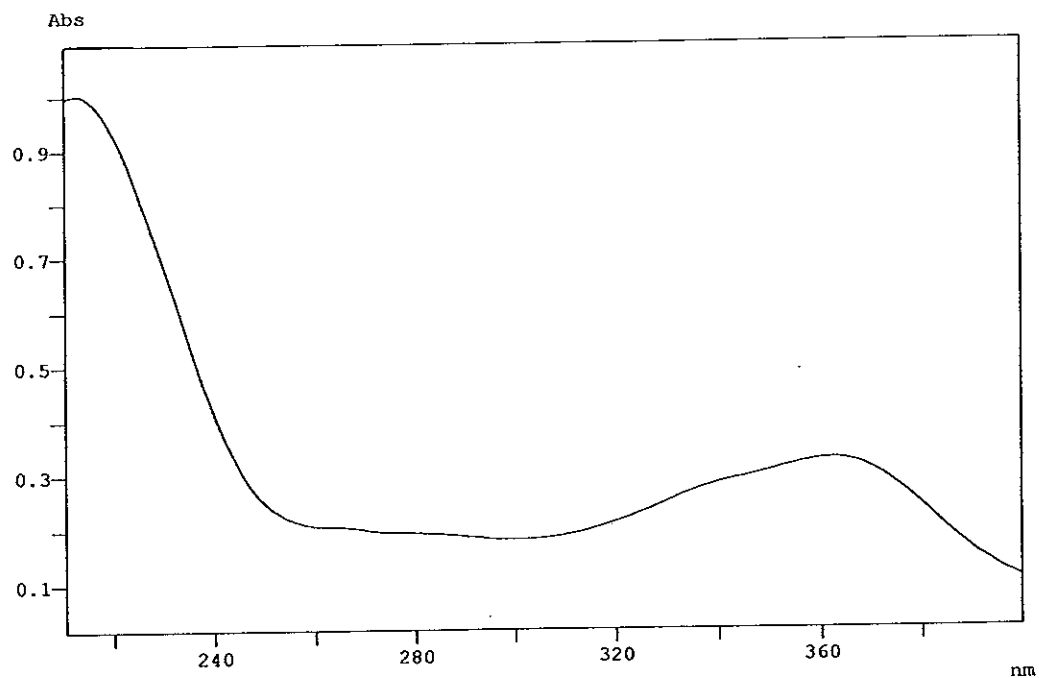


Figure 93 UV (MeOH) spectrum of PP13

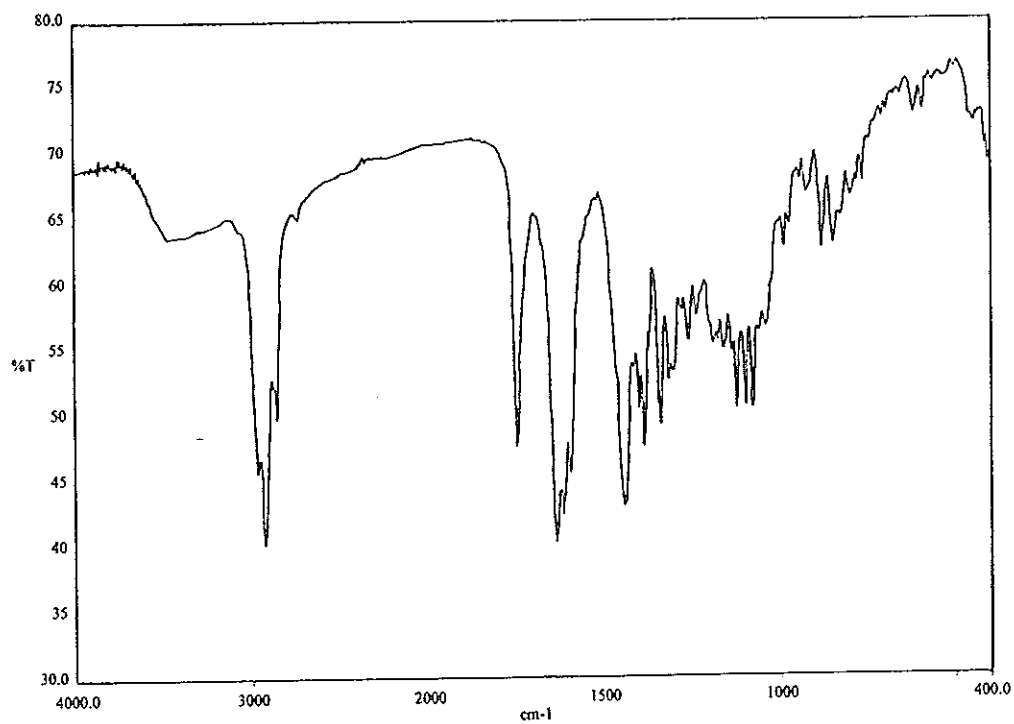


Figure 94 FT-IR (neat) spectrum of PP13

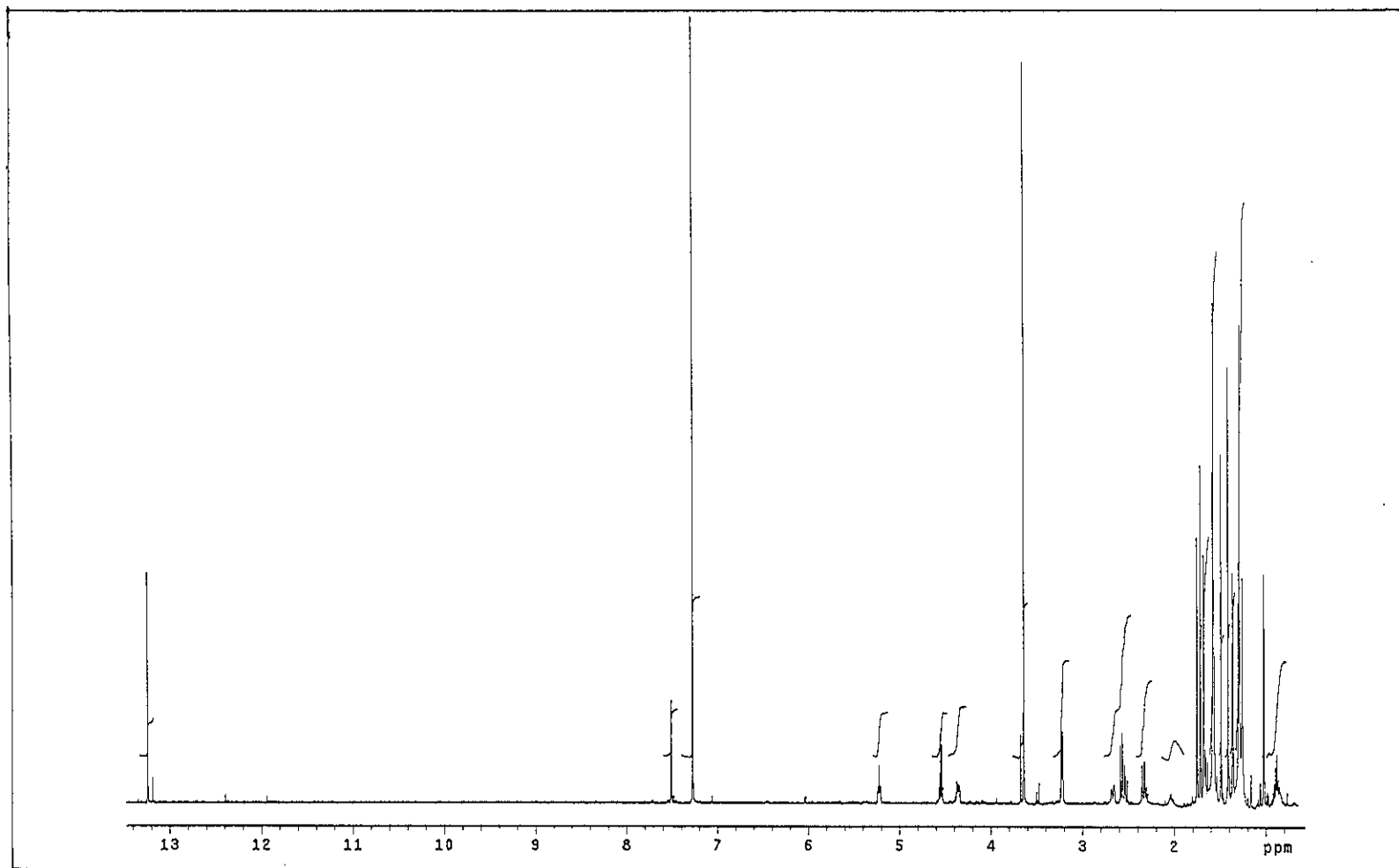


Figure 95 ^1H NMR (500 MHz) (CDCl_3) spectrum of PP13

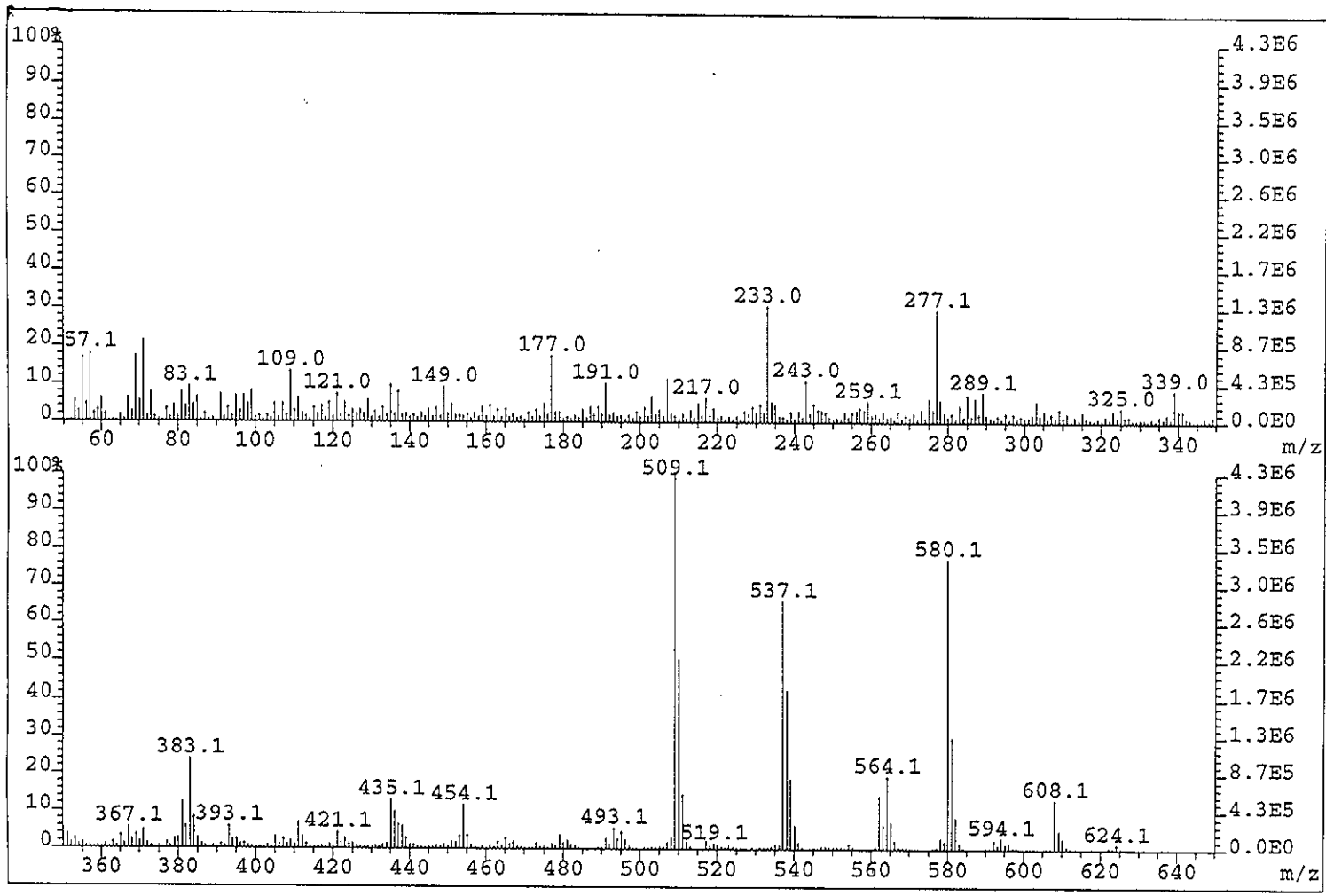


Figure 96 Mass spectrum of PP14

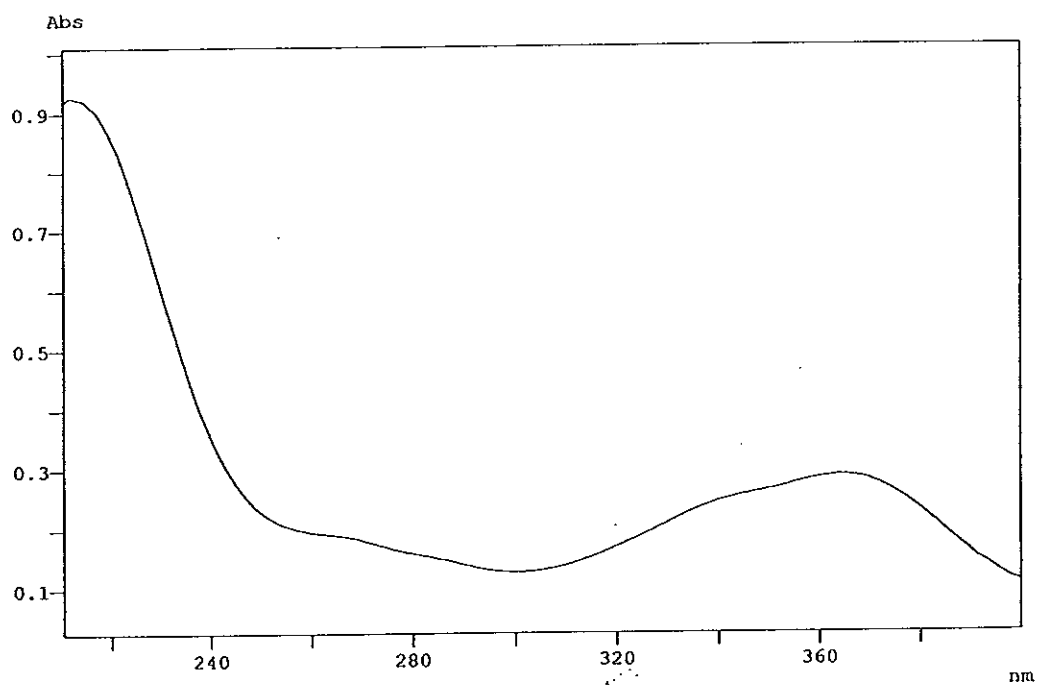


Figure 97 UV (MeOH) spectrum of PP14

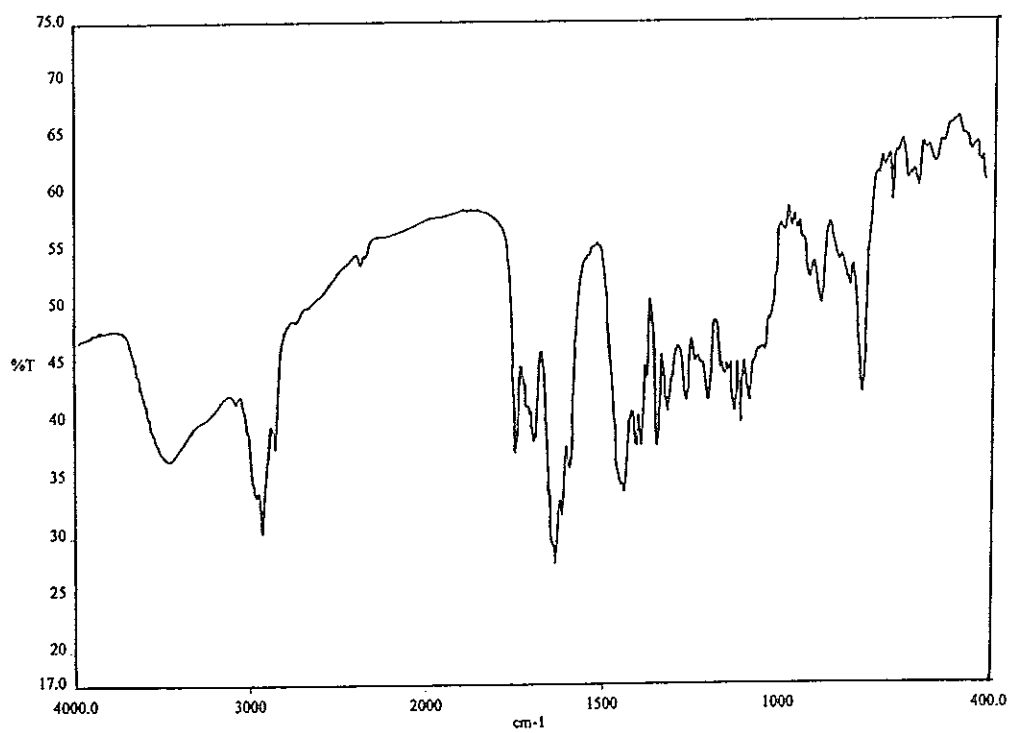


Figure 98 FT-IR (neat) spectrum of PP14

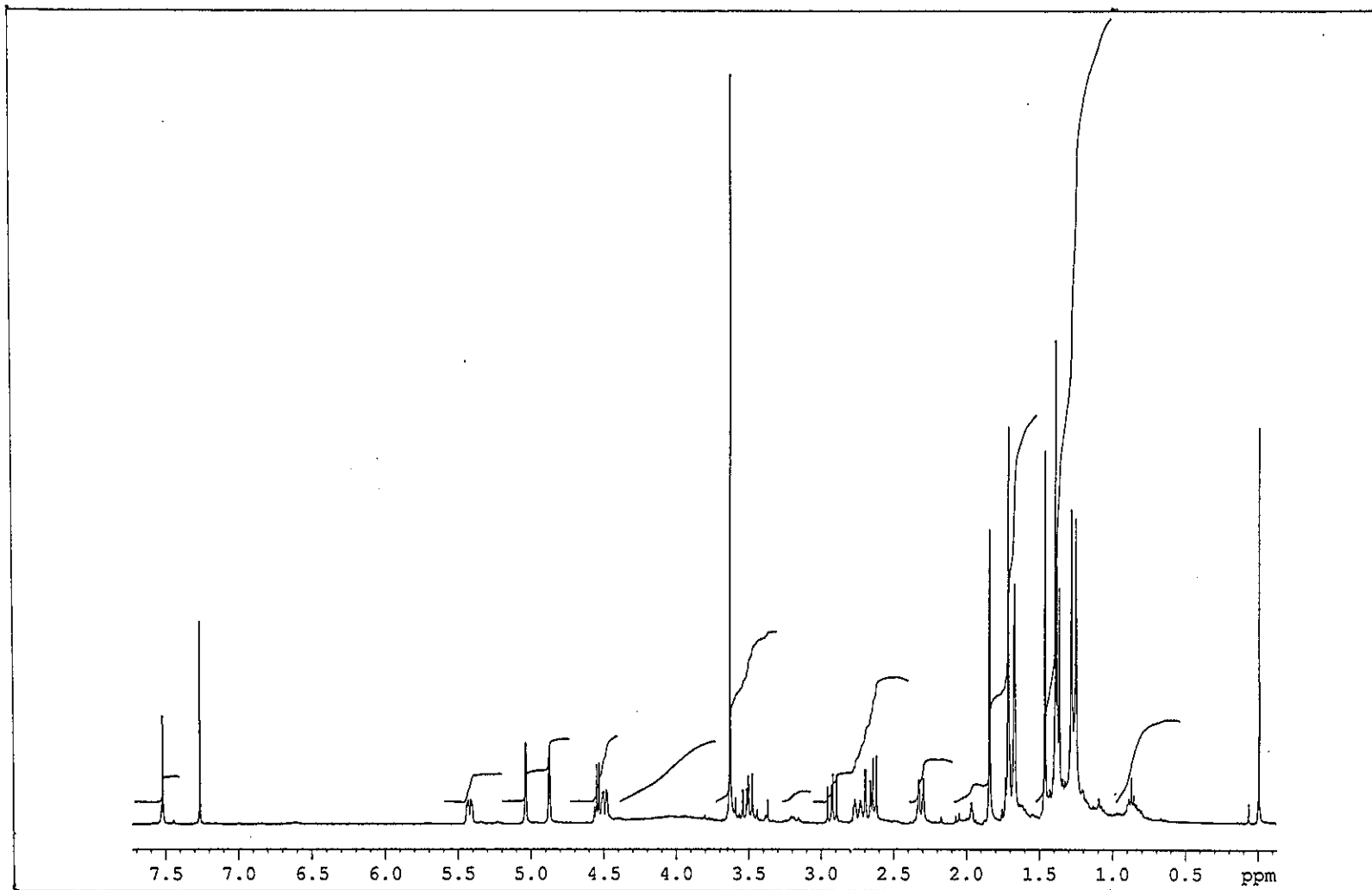


Figure 99 ^1H NMR (400 MHz) (CDCl_3) spectrum of PP14

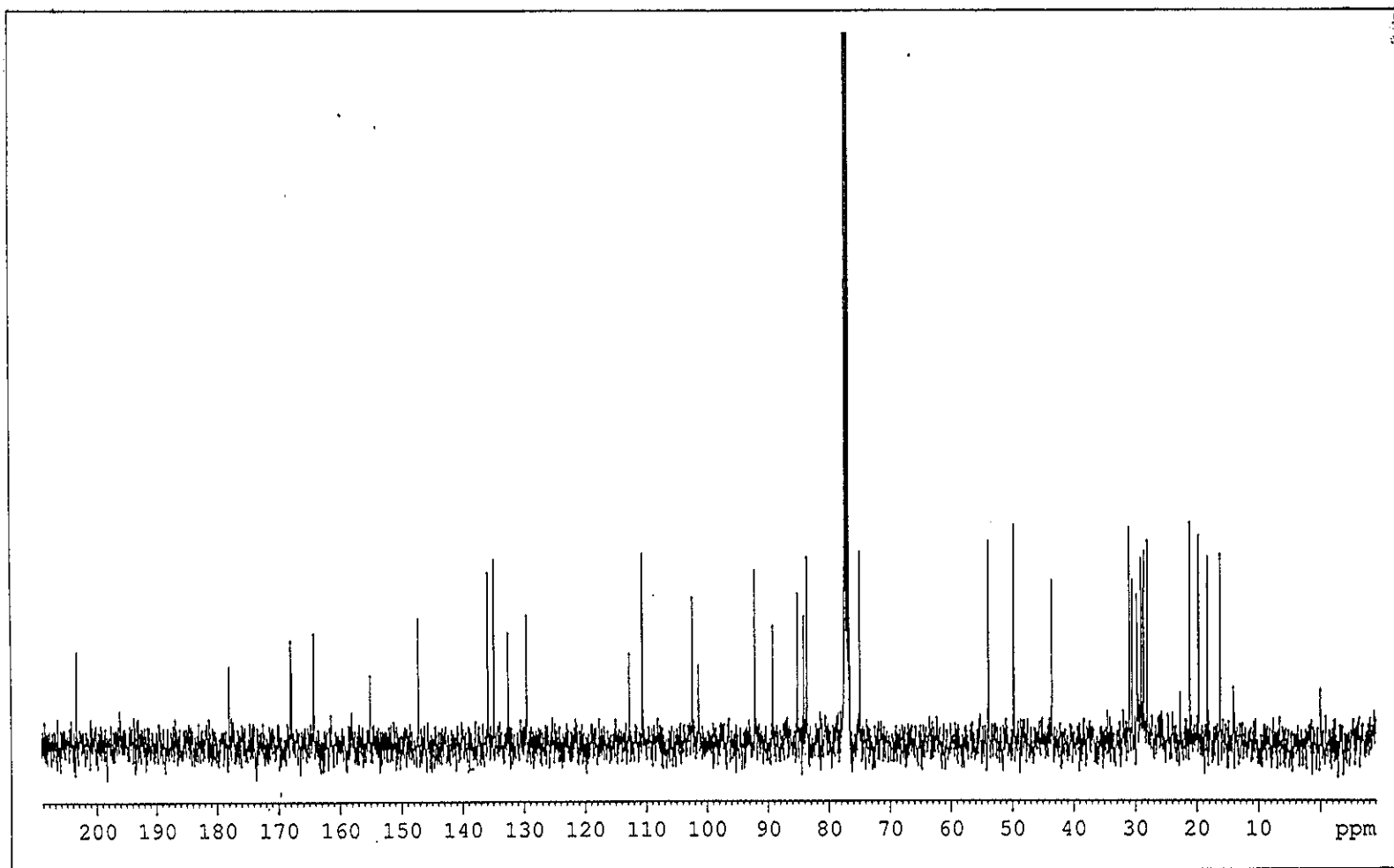


Figure 100 ^{13}C NMR (100 MHz) (CDCl_3) spectrum of PP14

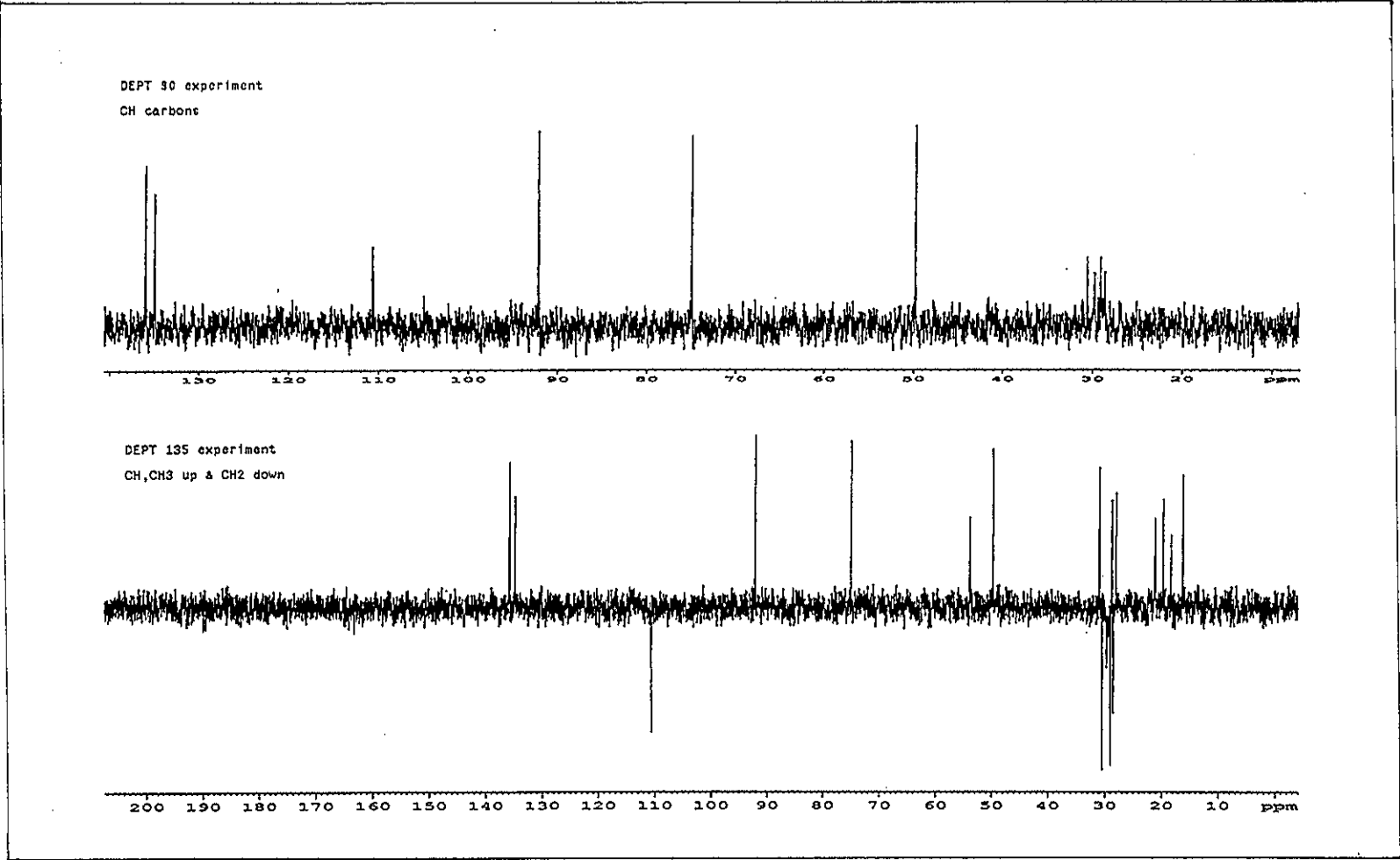


Figure 101 DEPT spectrum of PP14

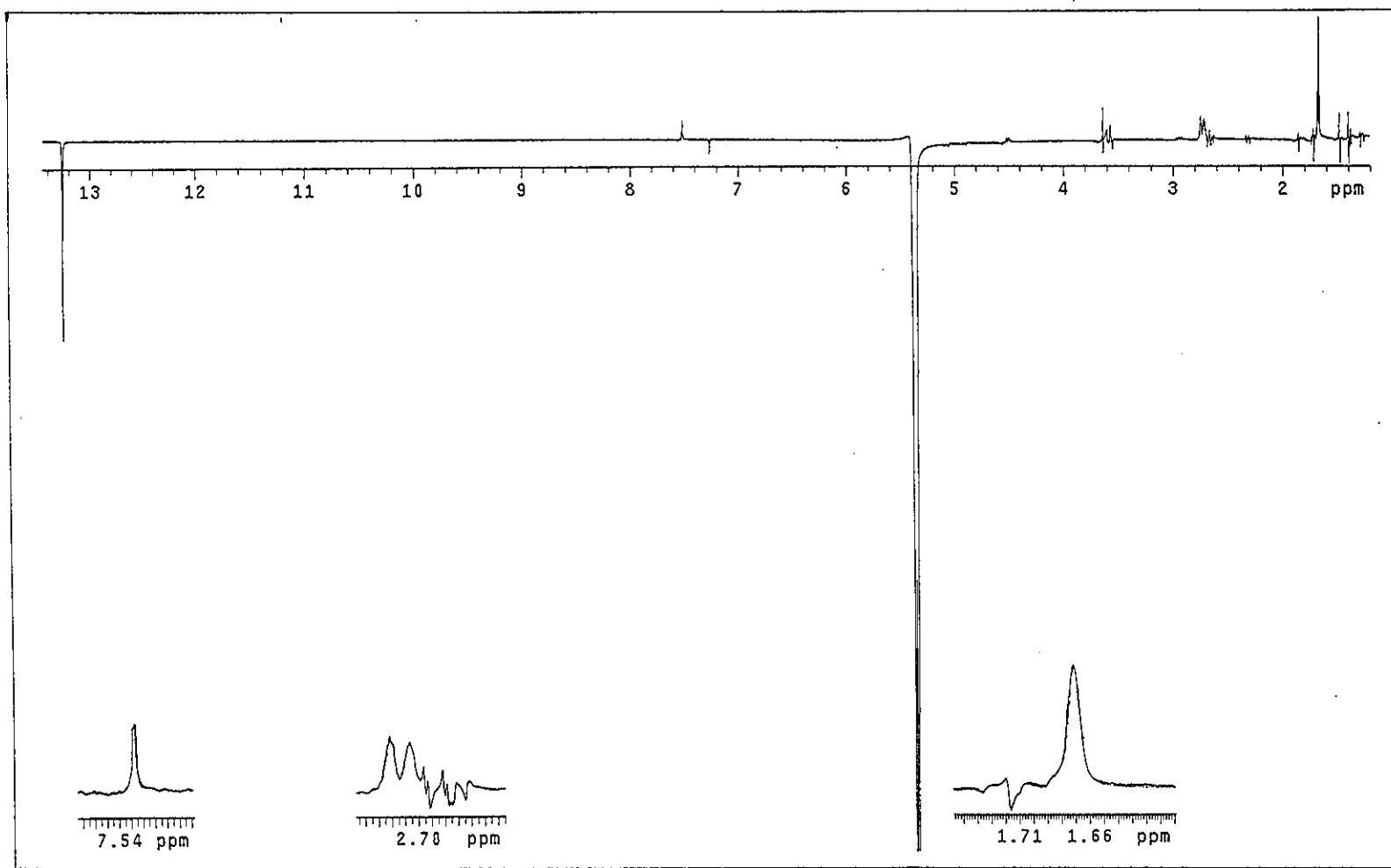


Figure 102 NOEDIFF spectrum of PP14 after irradiation at δ_H 5.43

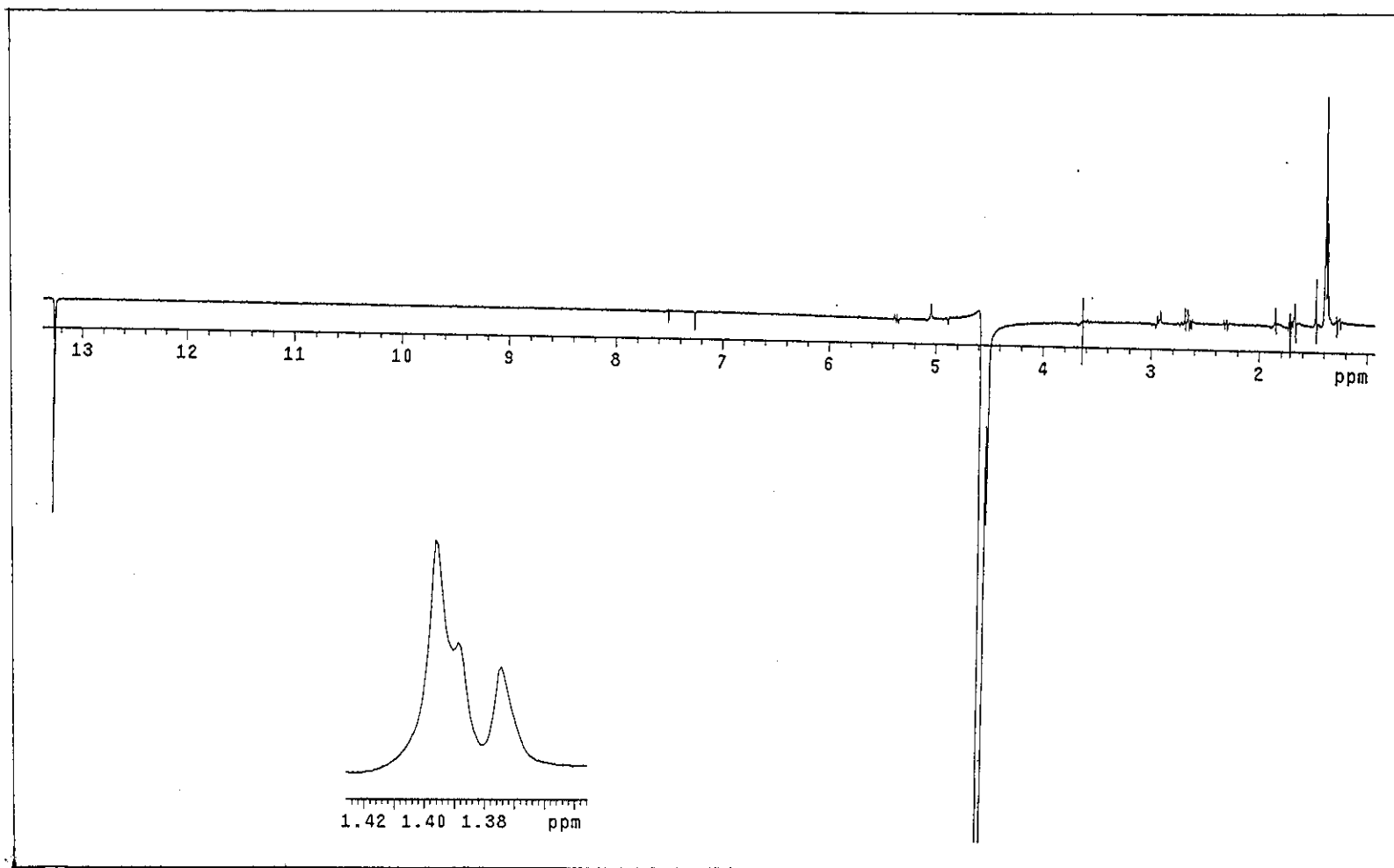


Figure 103 NOEDIFF spectrum of PP14 after irradiation at δ_H 4.55

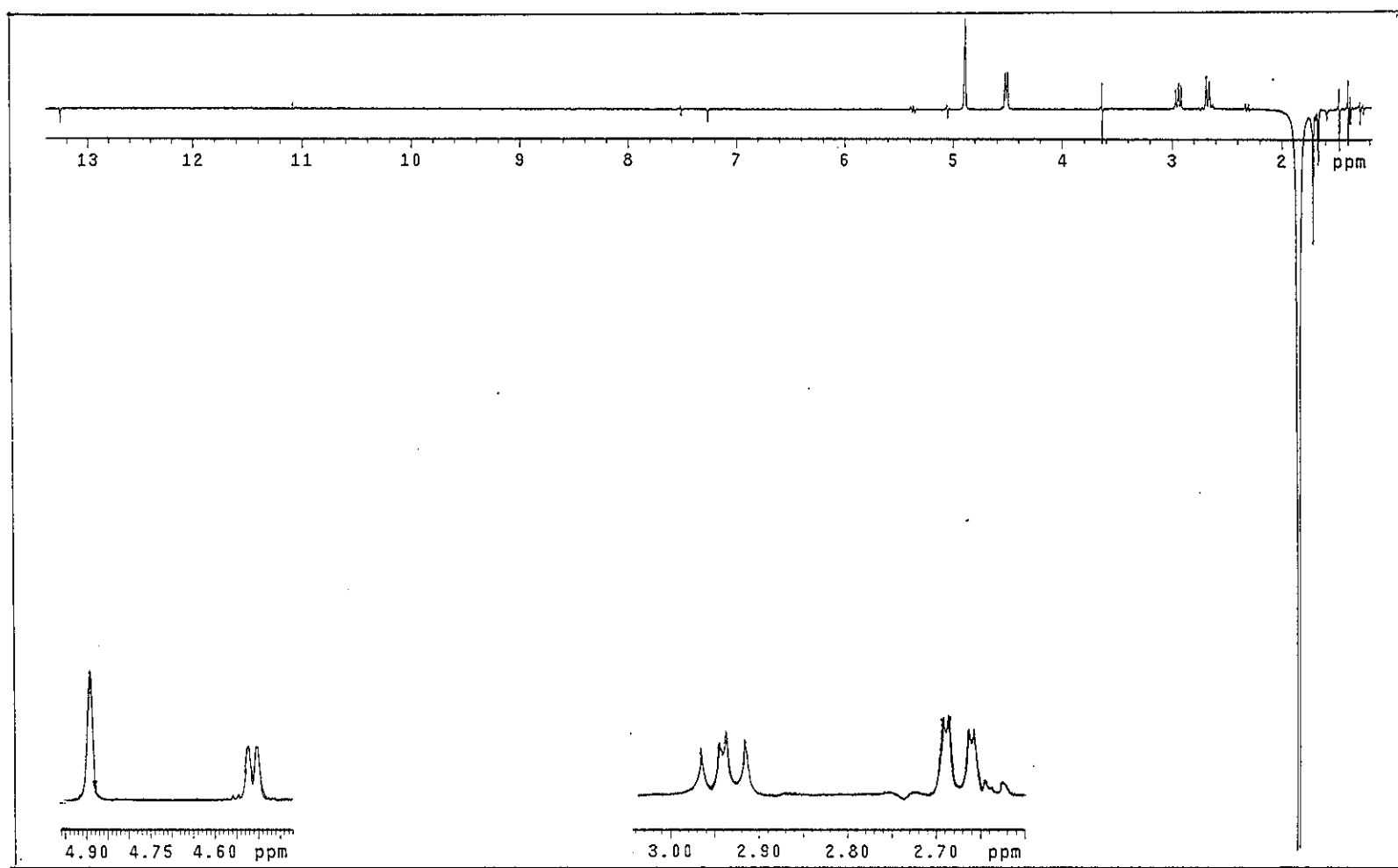


Figure 104 NOEDIFF spectrum of PP14 after irradiation at δ_H 1.84

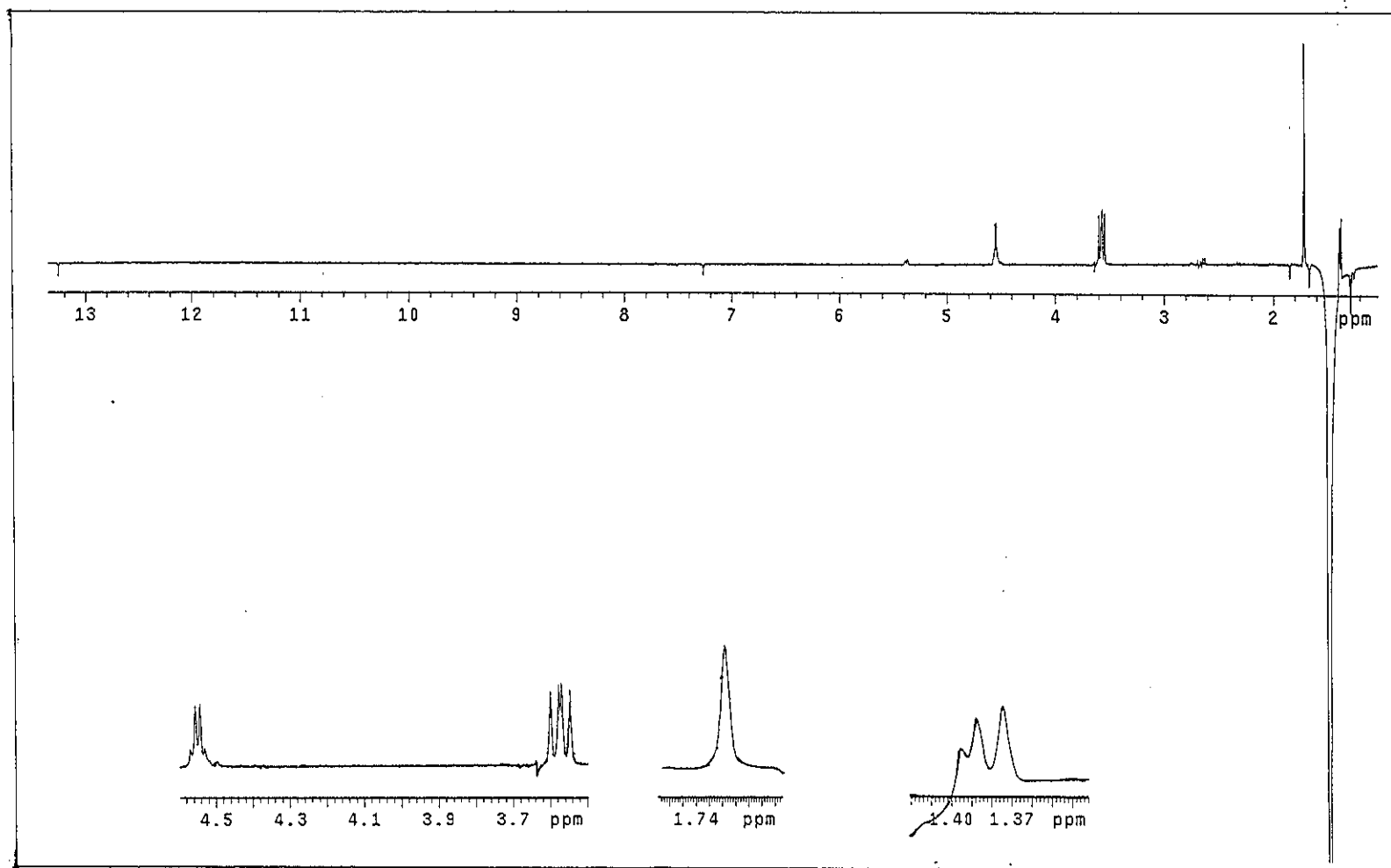


Figure 105 NOEDIFF spectrum of PP14 after irradiation at δ_H 1.46

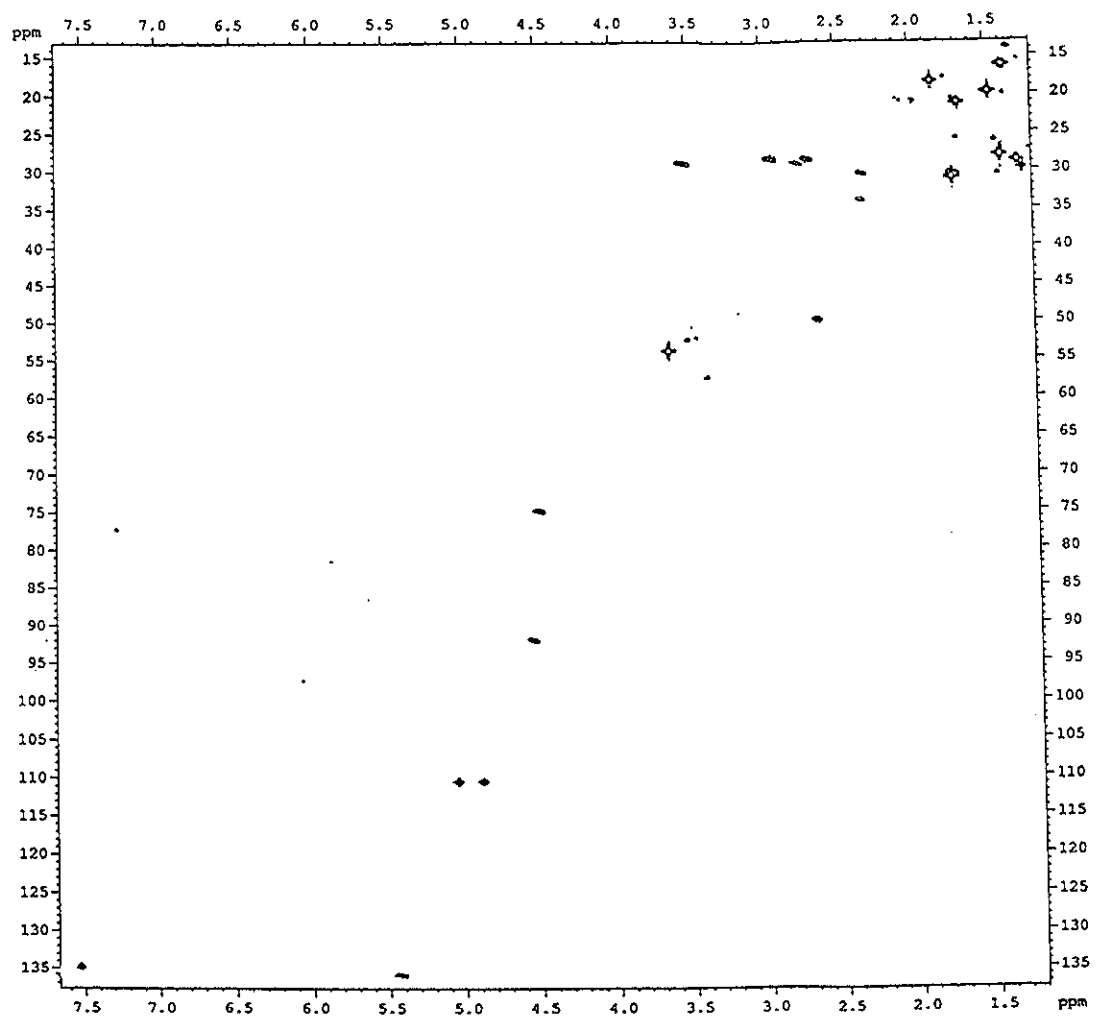


Figure 106 2D HMQC spectrum of PP14

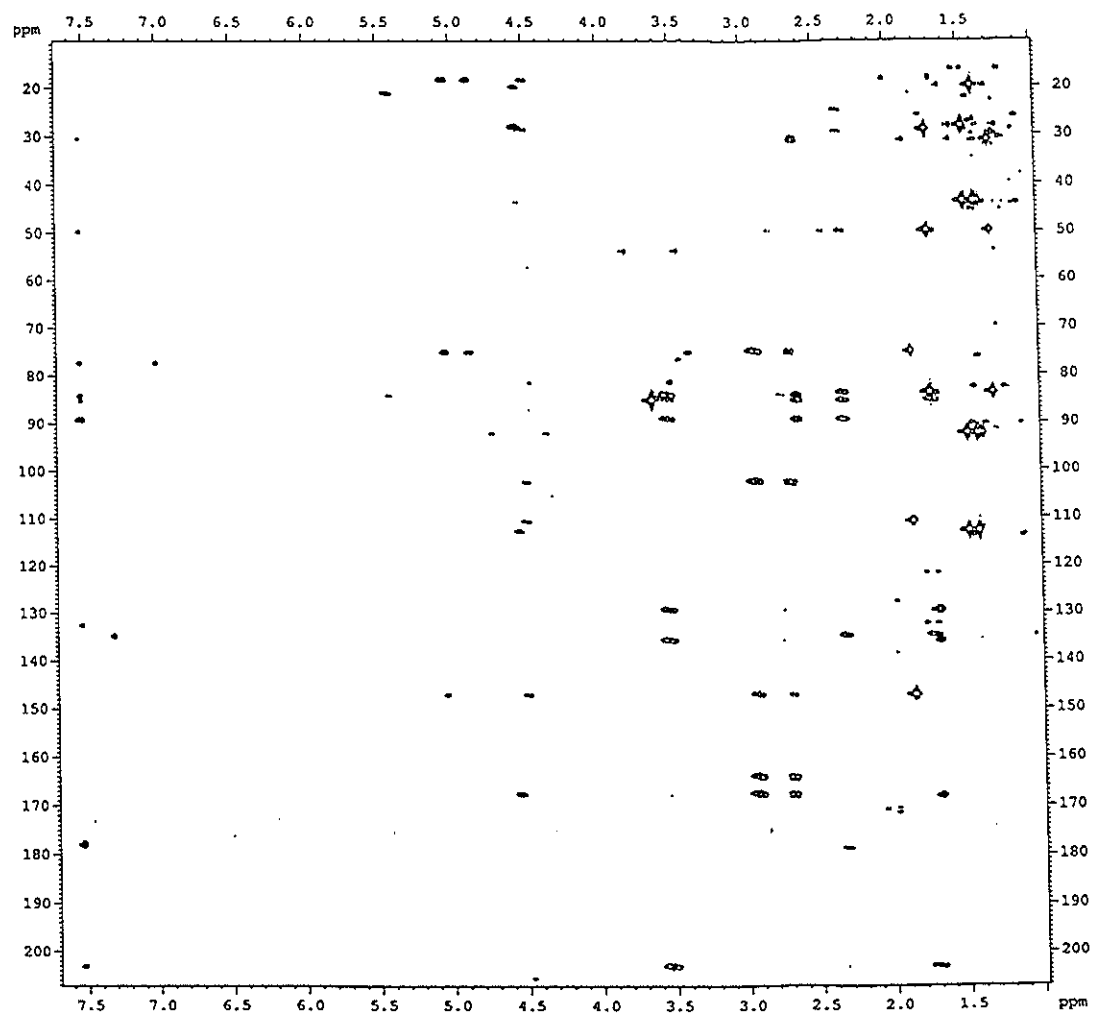


Figure 107 2D HMBC spectrum of PP14

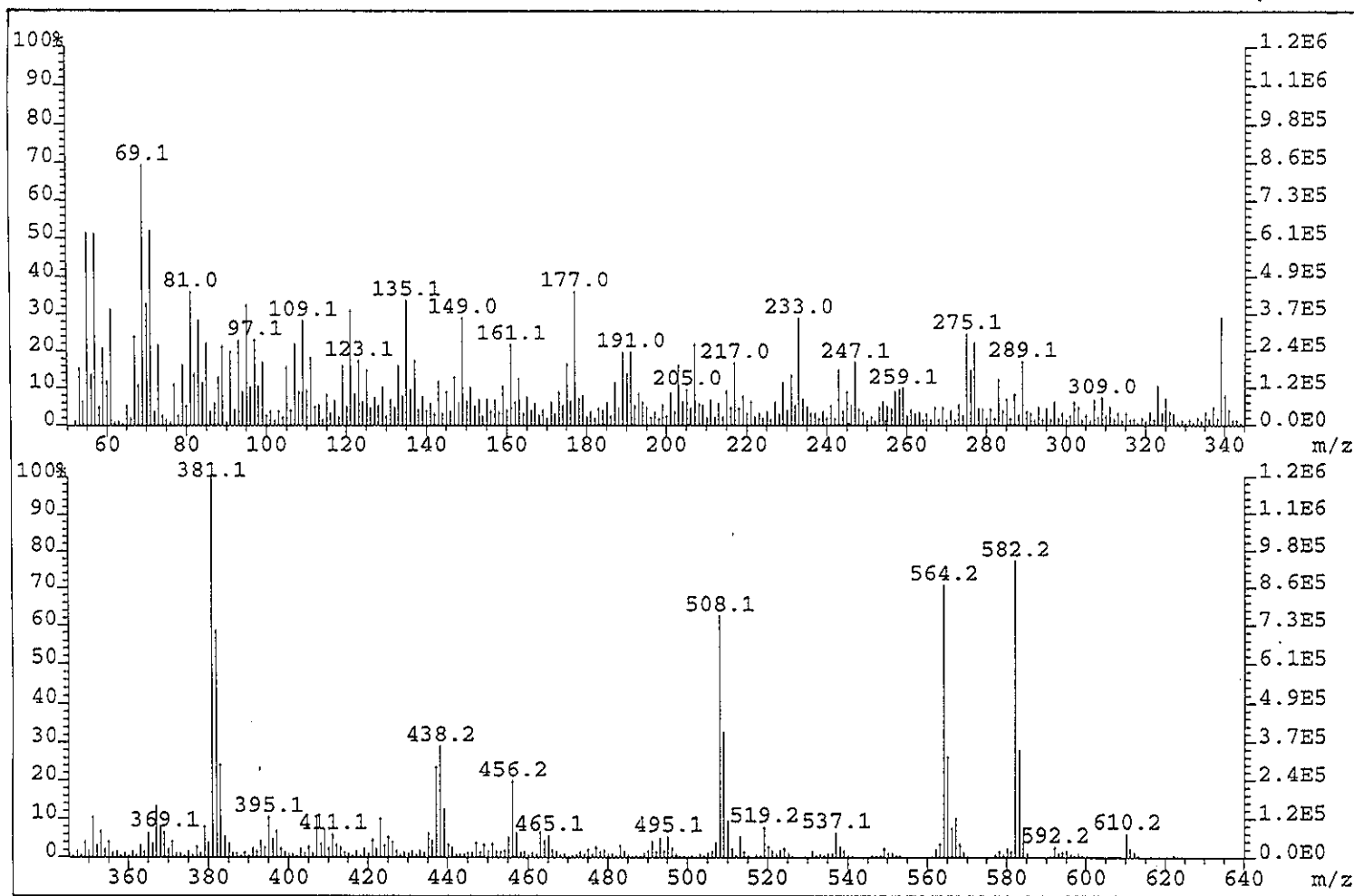


Figure 108 Mass spectrum of PP15

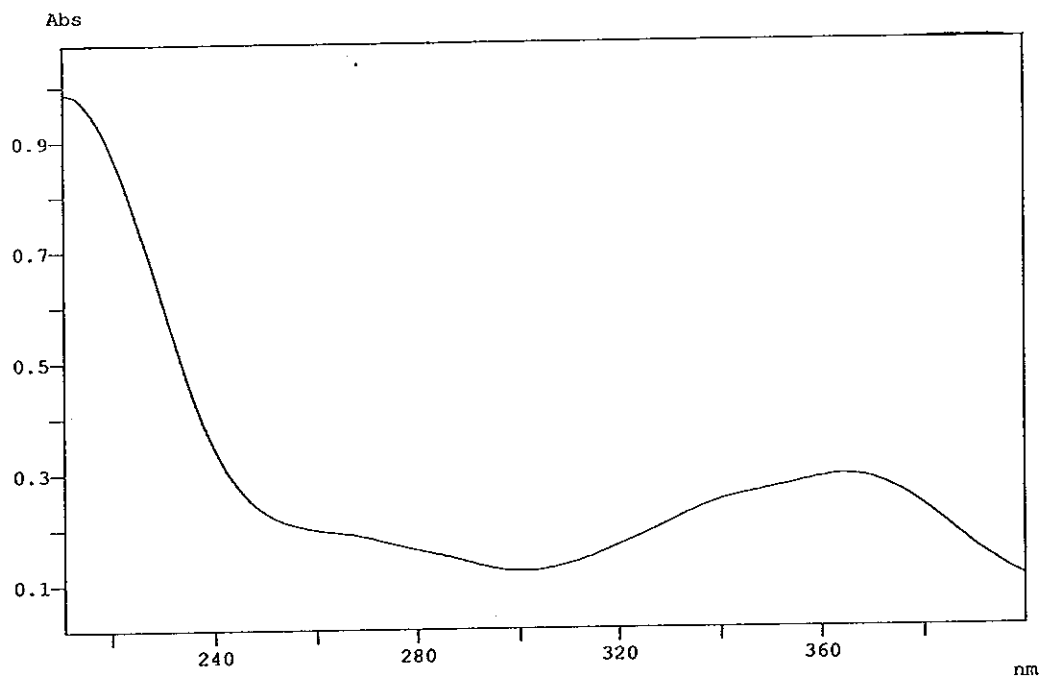


Figure 109 UV (MeOH) spectrum of PP15

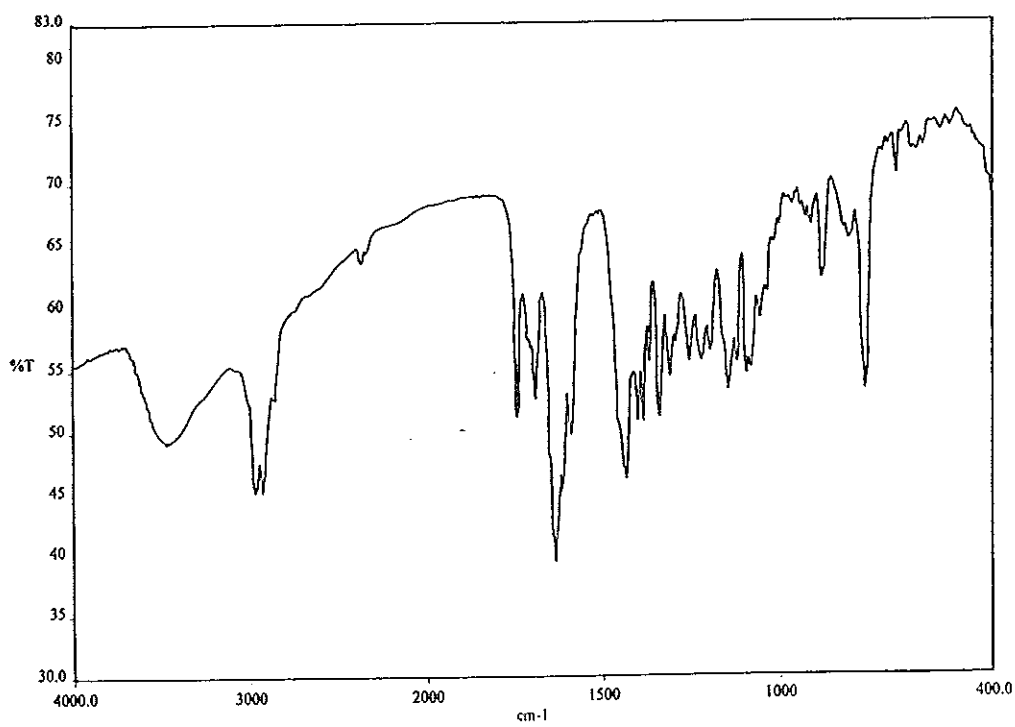


Figure 110 FT-IR (neat) spectrum of PP15

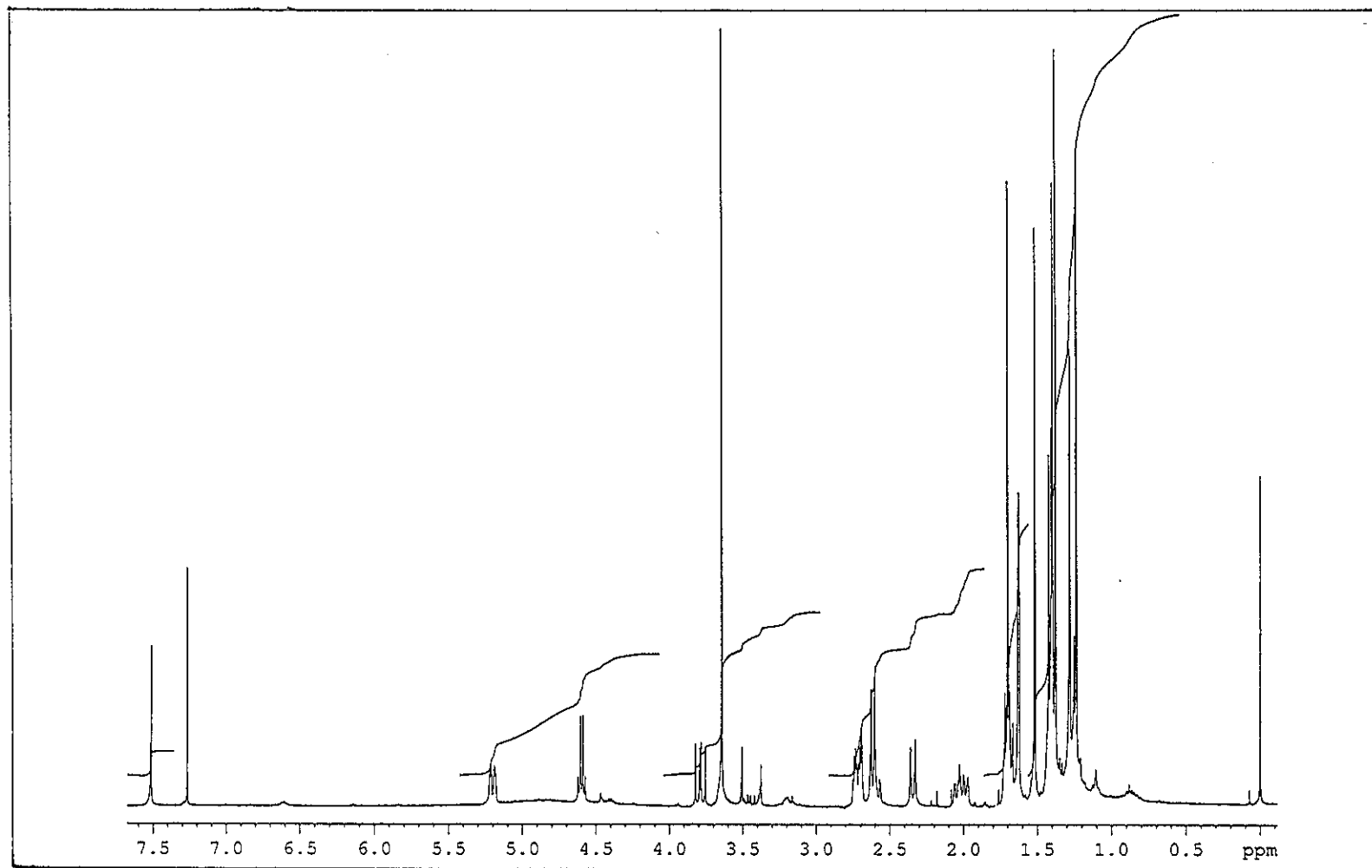


Figure 111 ^1H NMR (400 MHz) (CDCl_3) spectrum of PP15

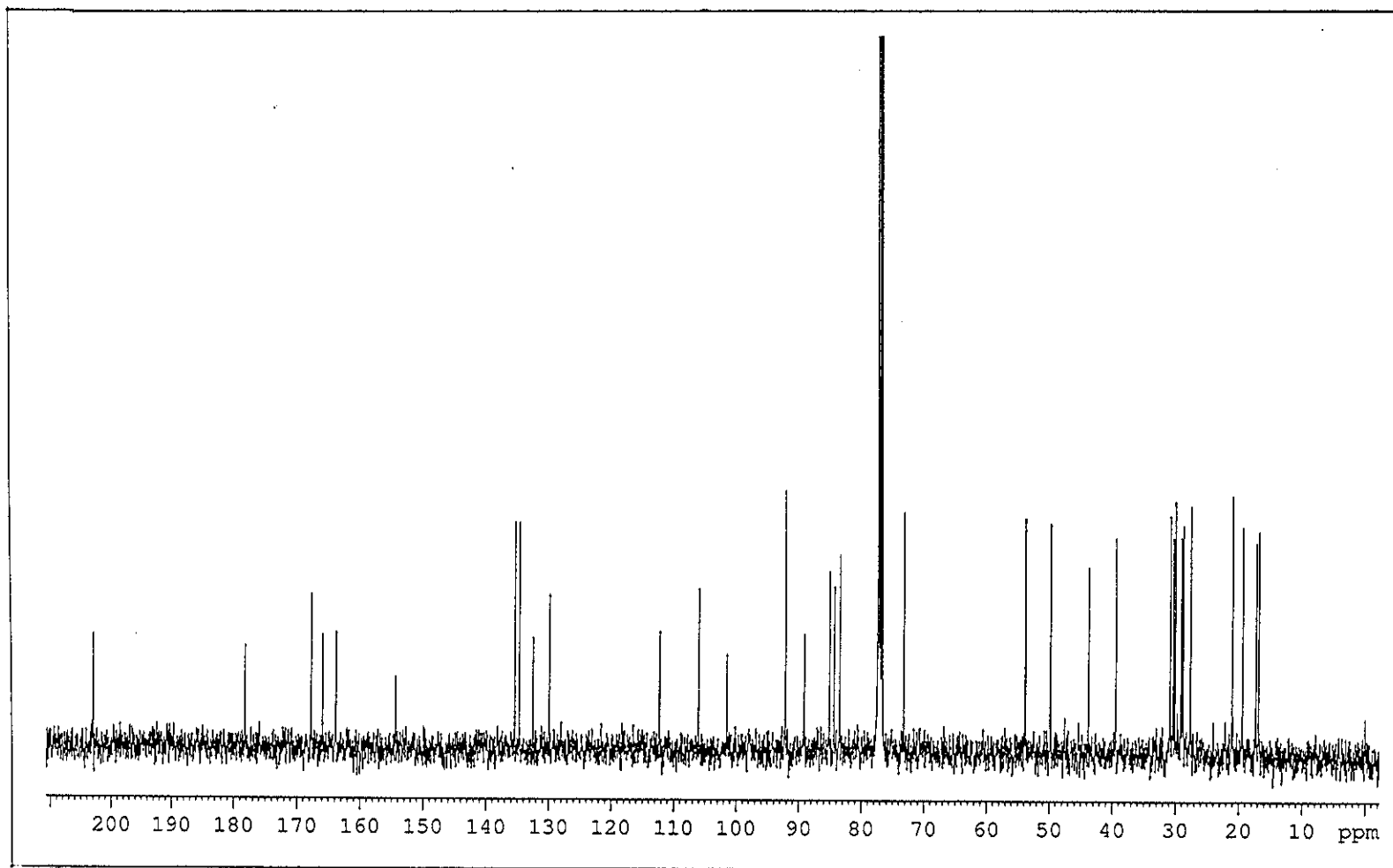


Figure 112 ^{13}C NMR (100 MHz) (CDCl_3) spectrum of PP15

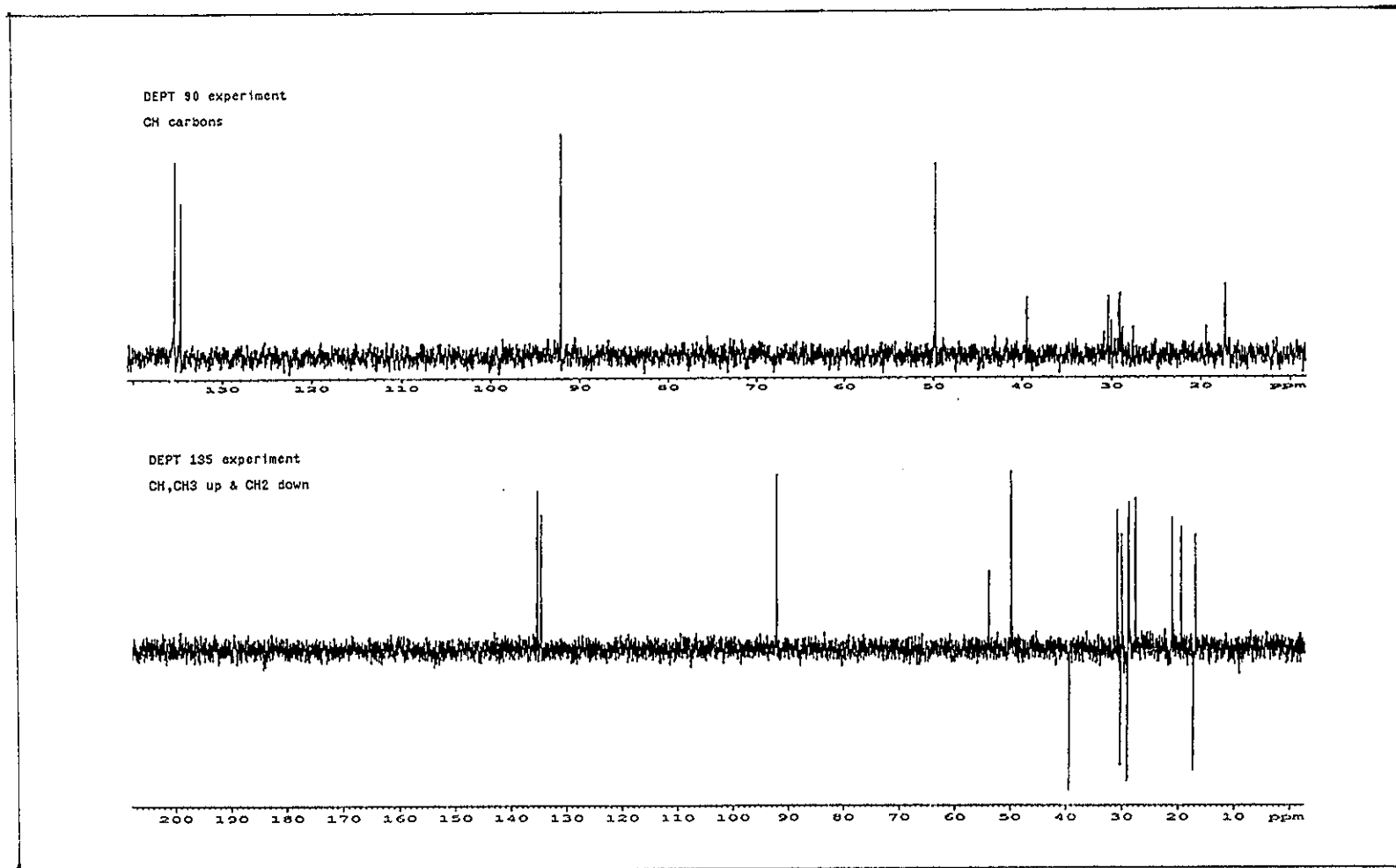


Figure 113 DEPT spectrum of PP15

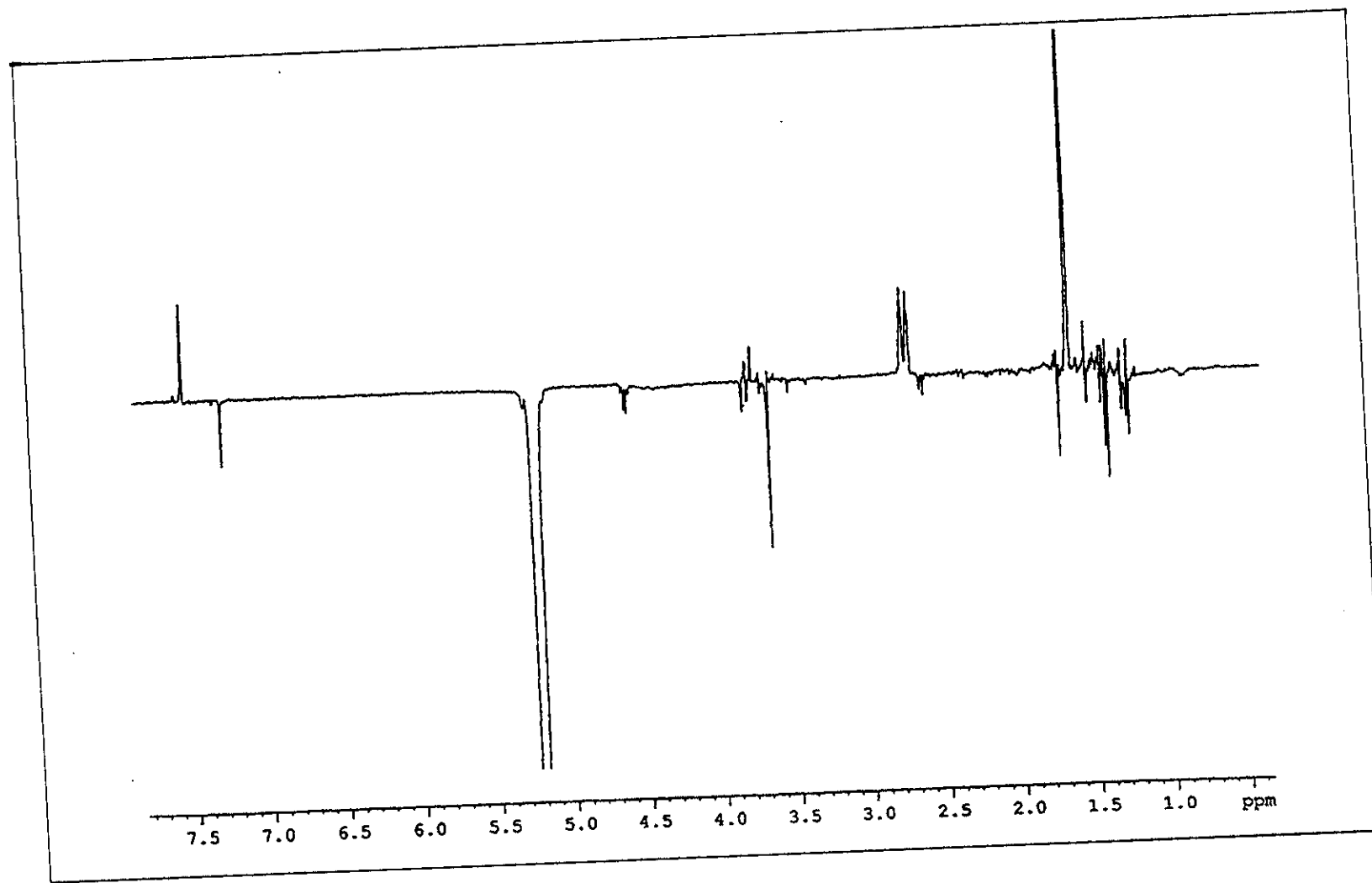


Figure 114 NOEDIFF spectrum of PP15 after irradiation at δ_H 5.20

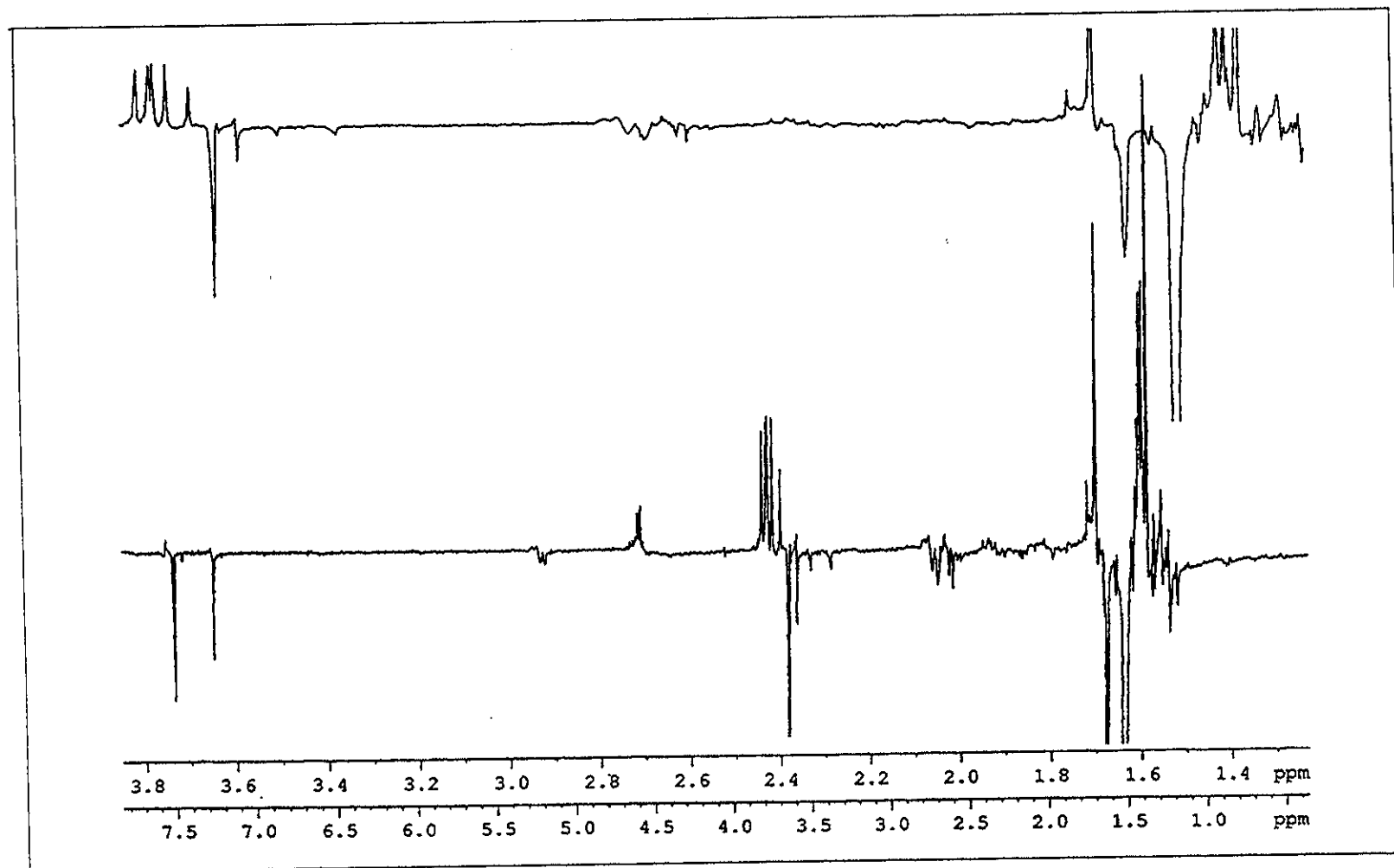


Figure 115 NOEDIFF spectrum of PP15 after irradiation at $\delta_H 1.52$

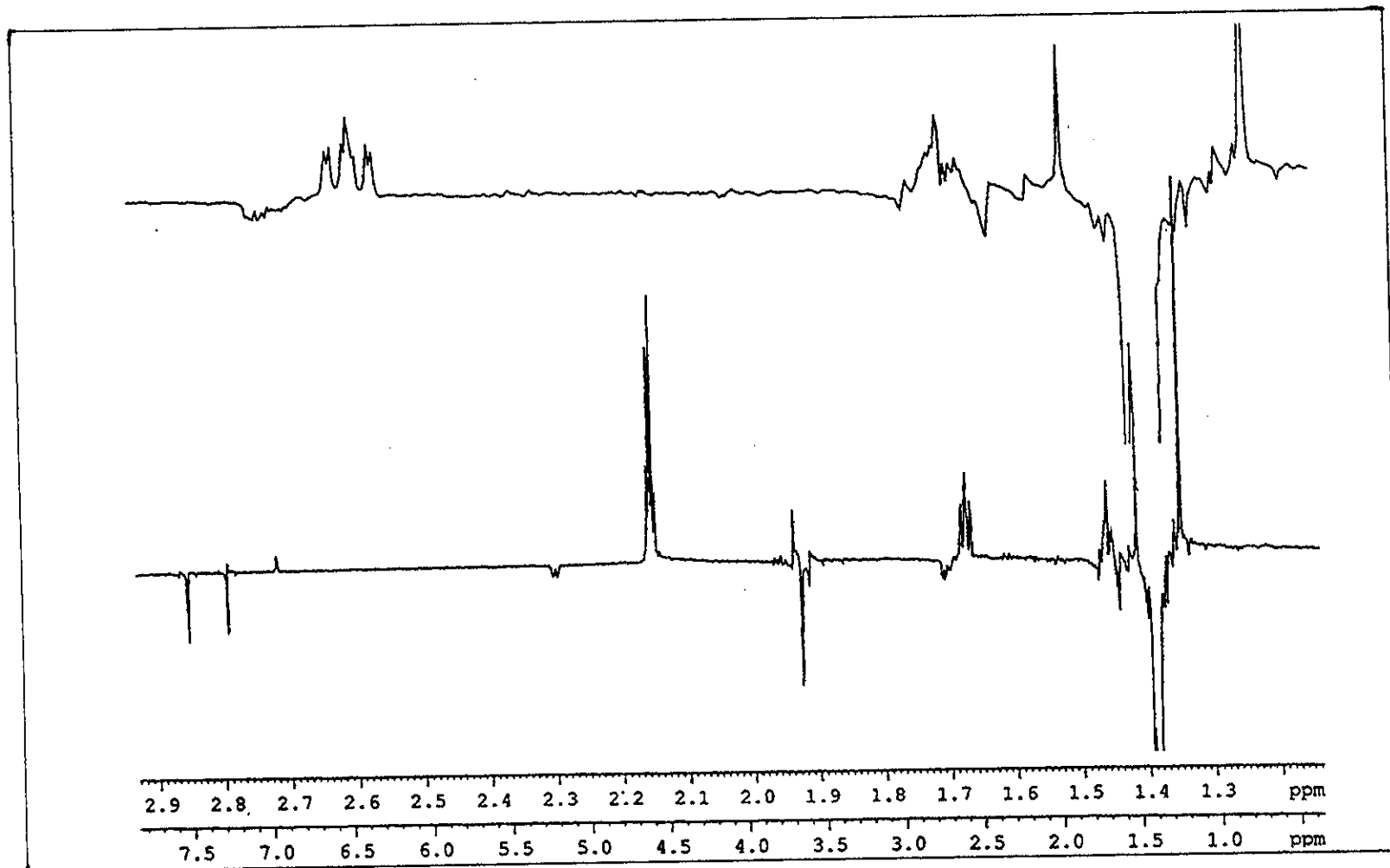


Figure 116 NOEDIFF spectrum of PP15 after irradiation at δ_H 1.42

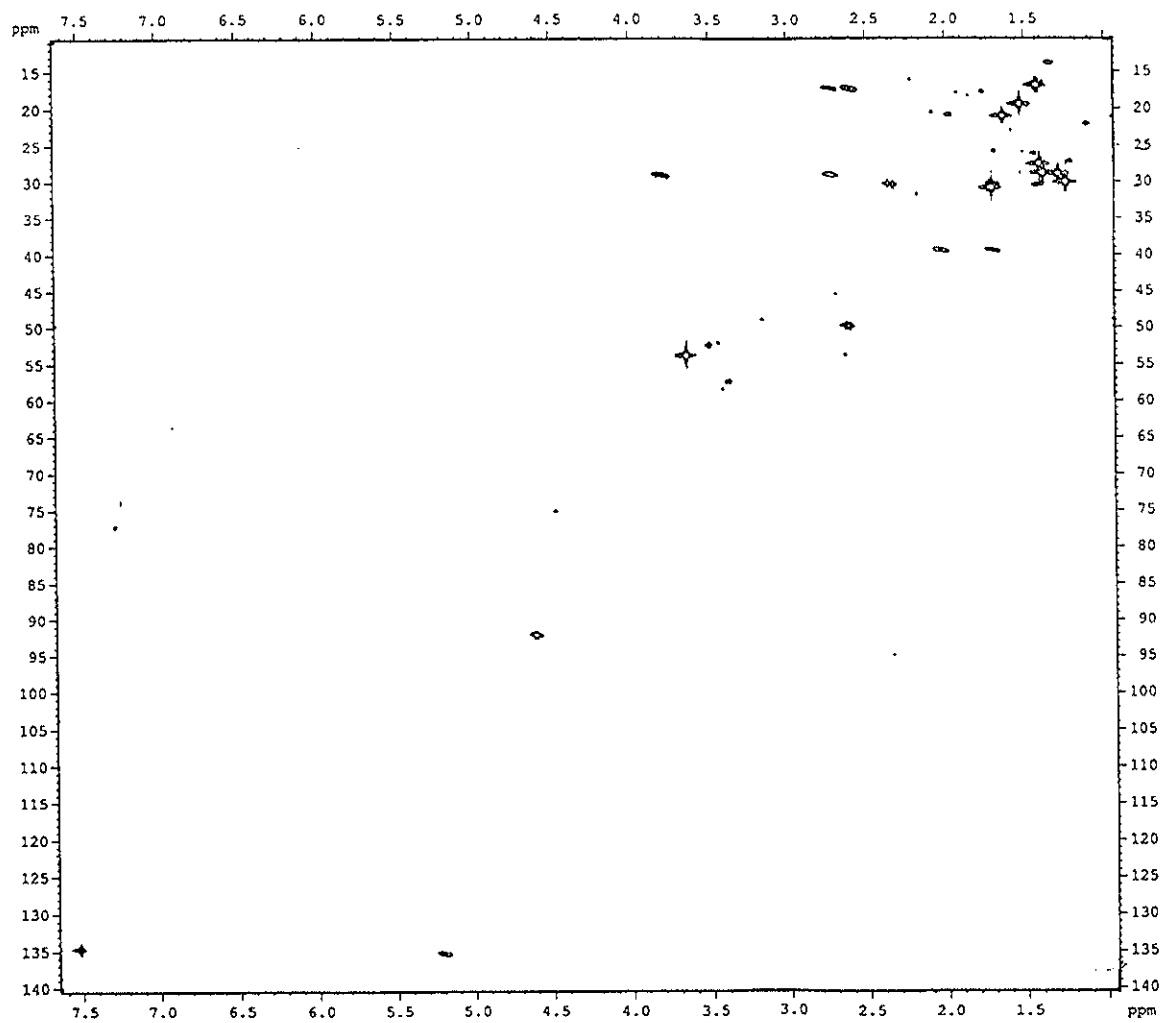


Figure 117 2D HMQC spectrum of PP15

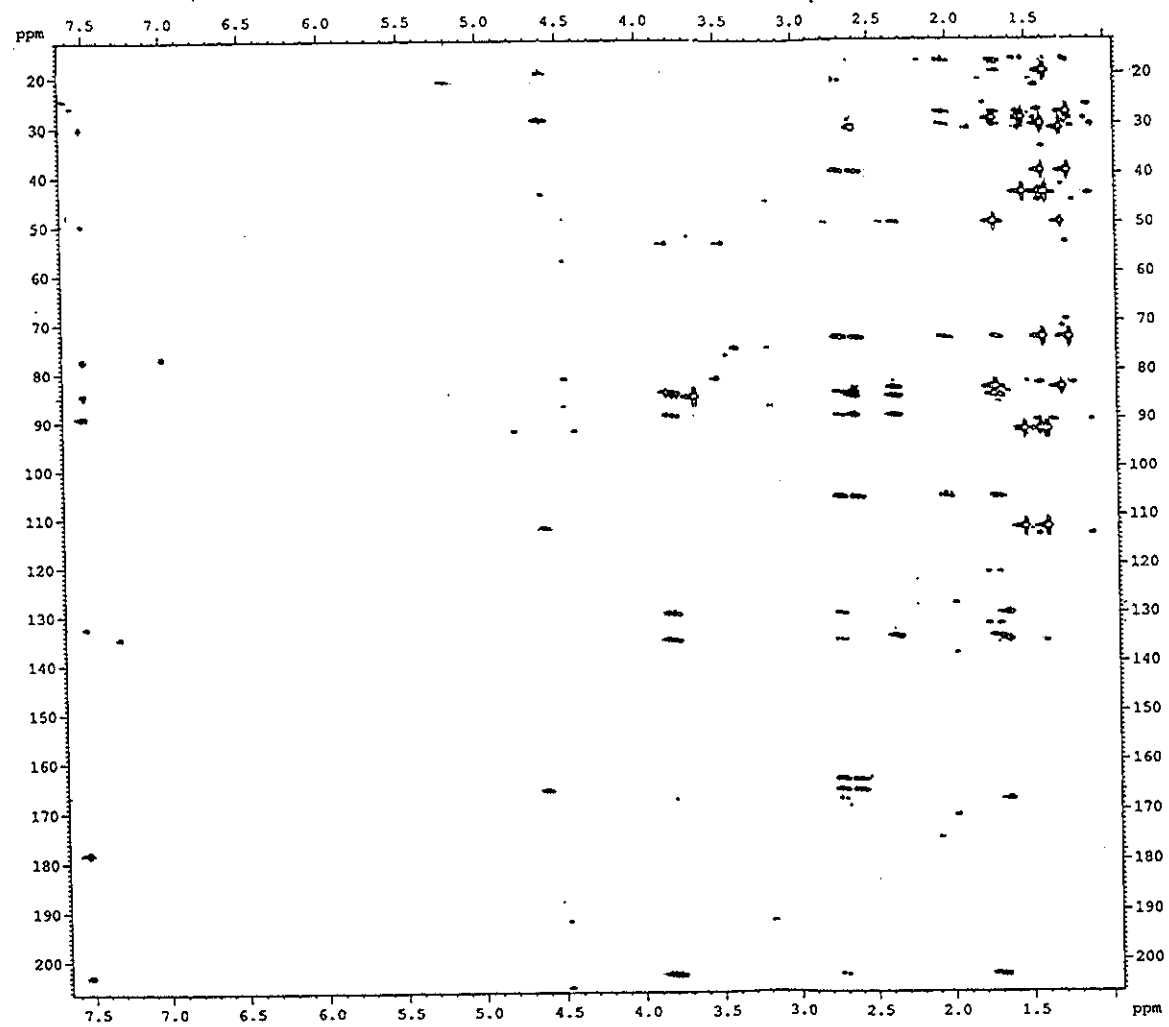


Figure 118 2D HMBC spectrum of PP15

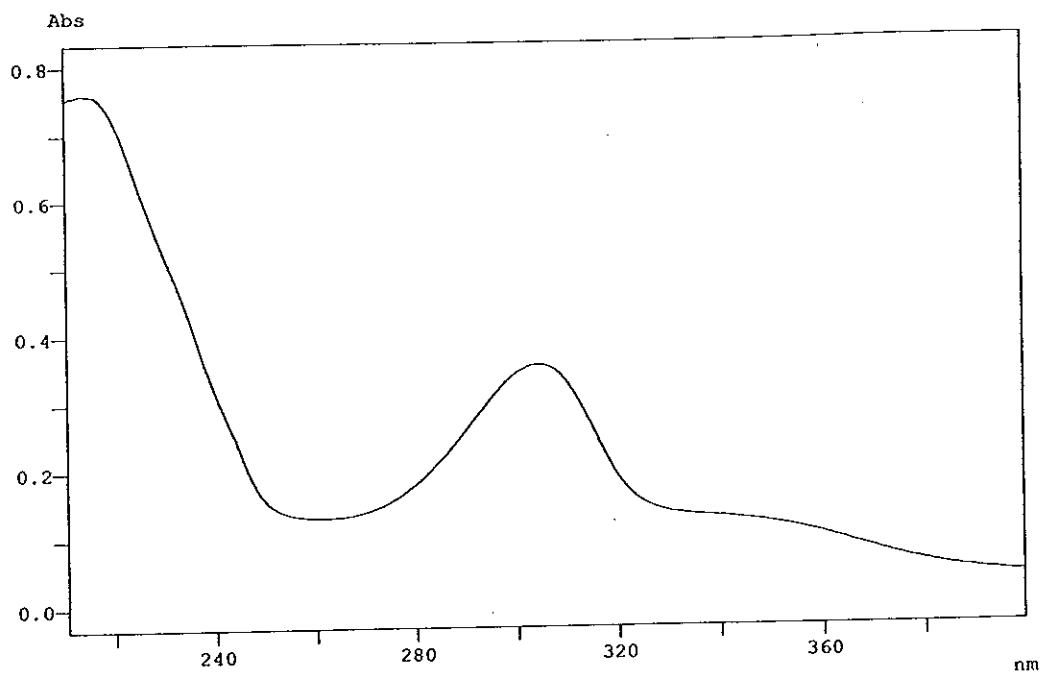


Figure 119 UV (MeOH) spectrum of PP16

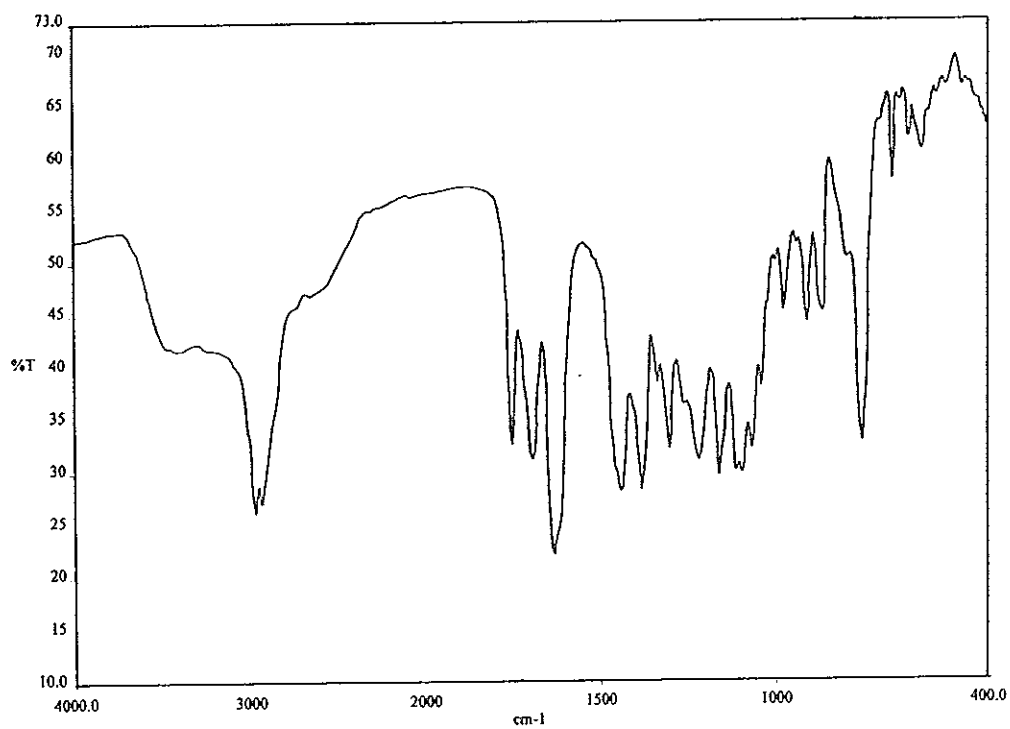


Figure 120 FT-IR (neat) spectrum of PP16

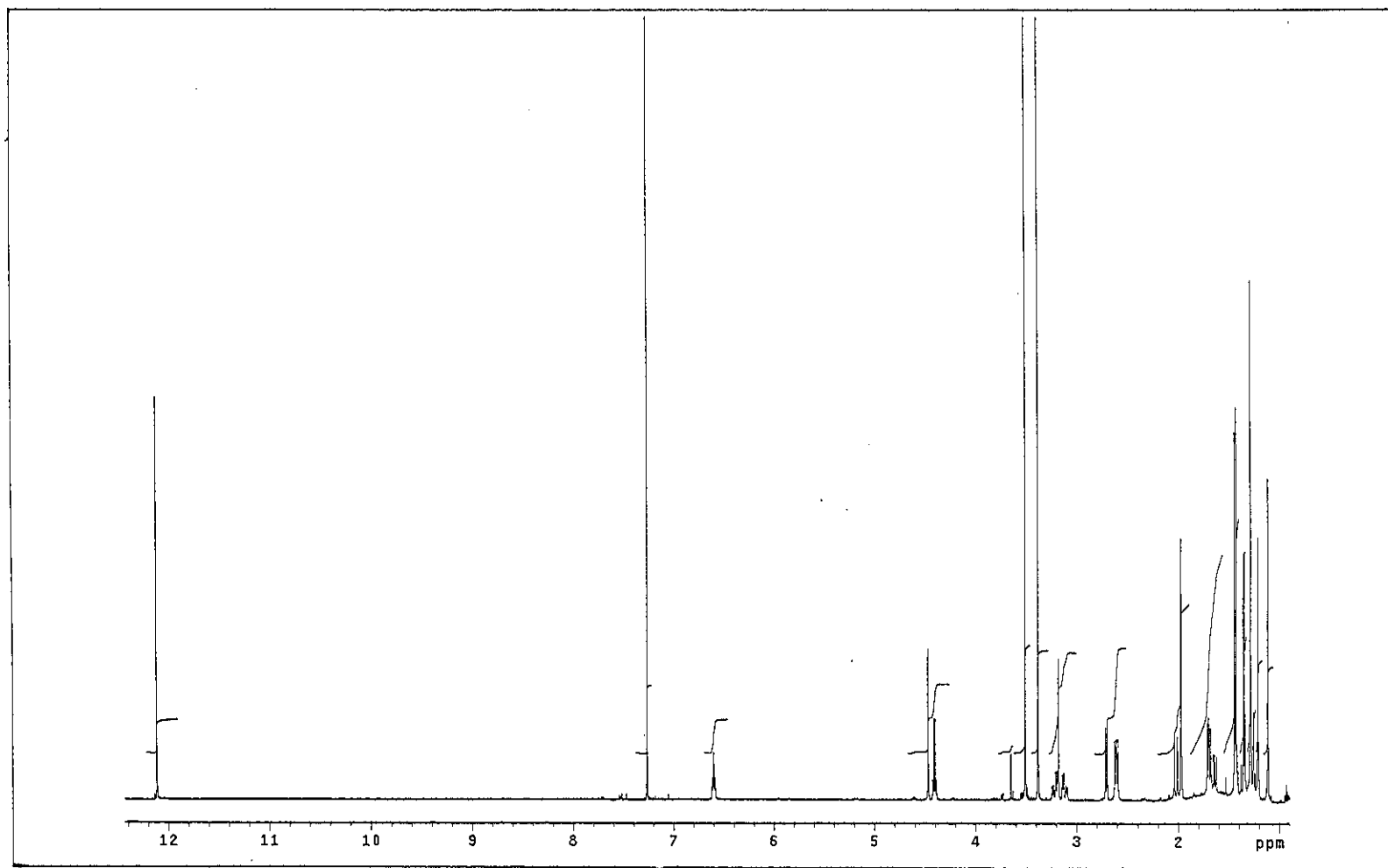


Figure 121 ^1H NMR (500 MHz) (CDCl_3) spectrum of PP16

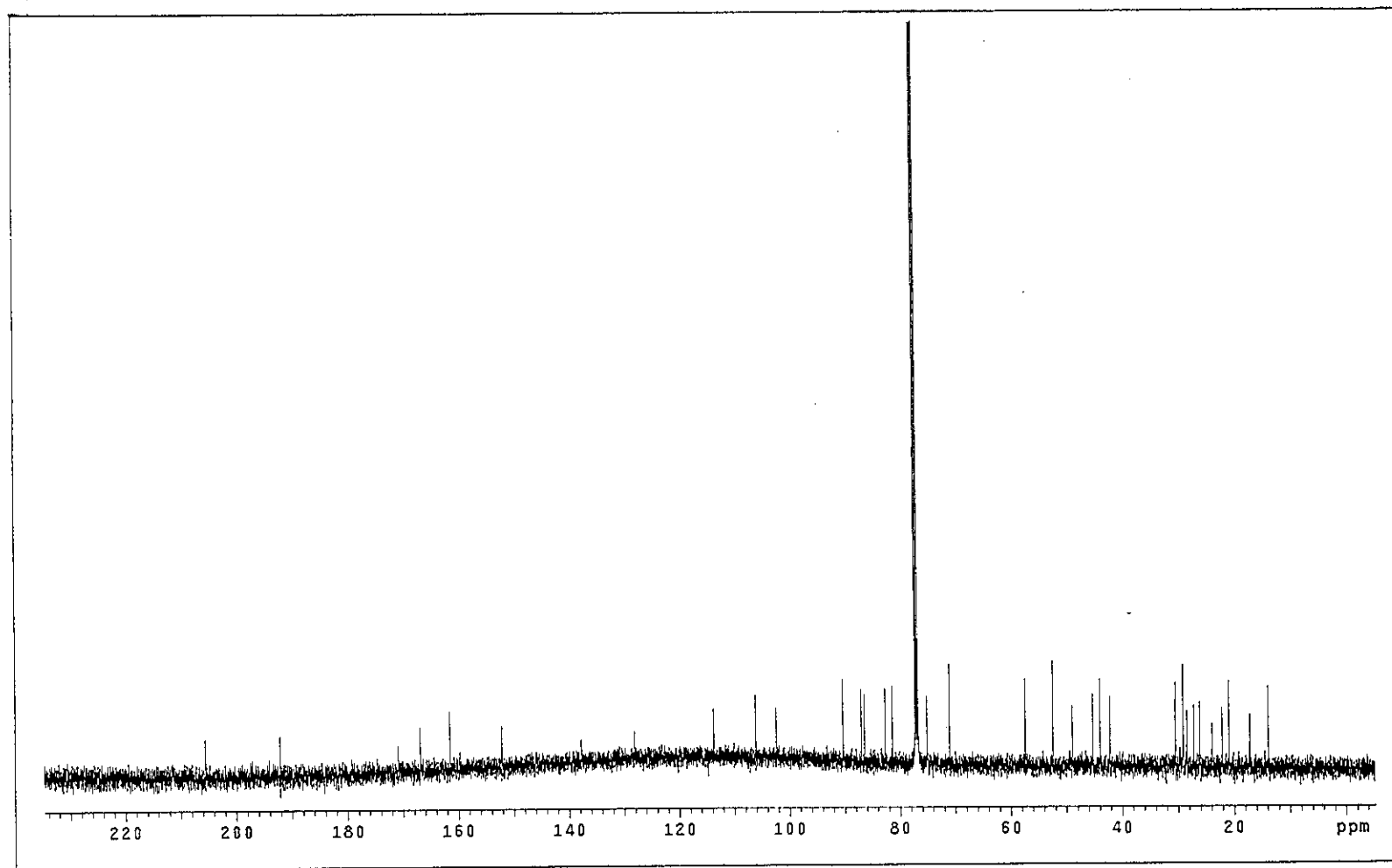


Figure 122 ^{13}C NMR (125 MHz) (CDCl_3) spectrum of PP16

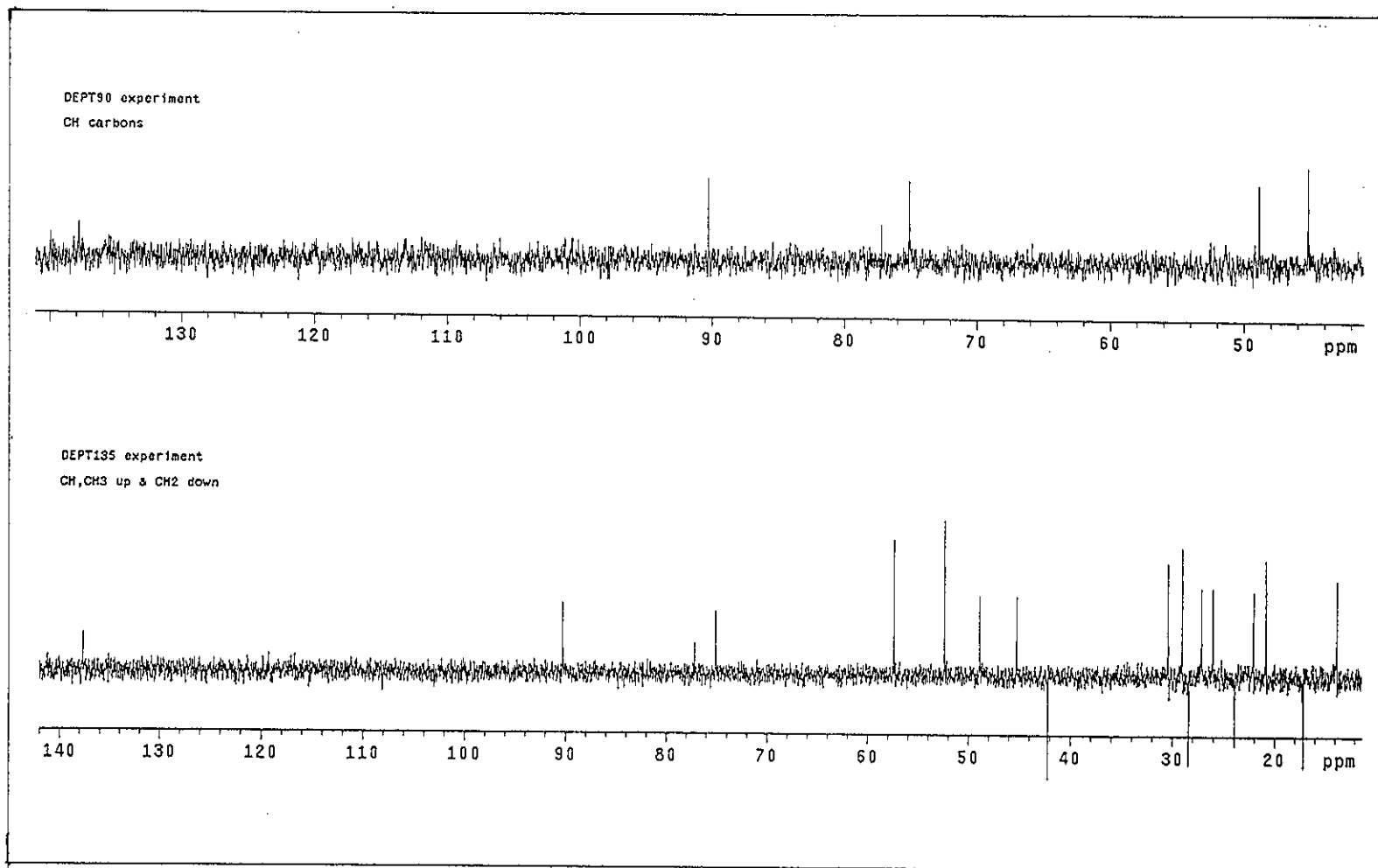


Figure 123 DEPT spectrum of PP16

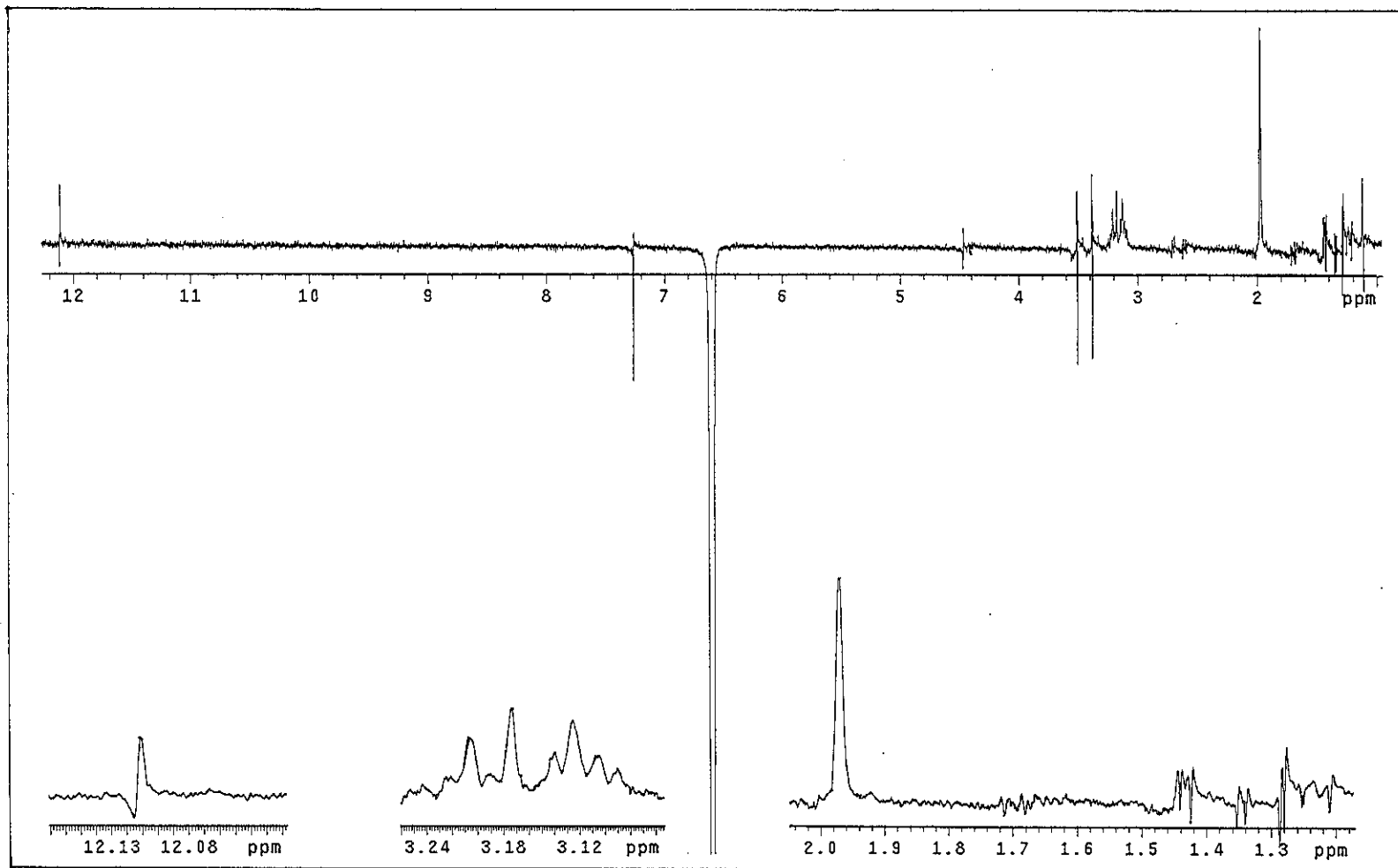


Figure 124 NOEDIFF spectrum of PP16 after irradiation at δ_H 6.60

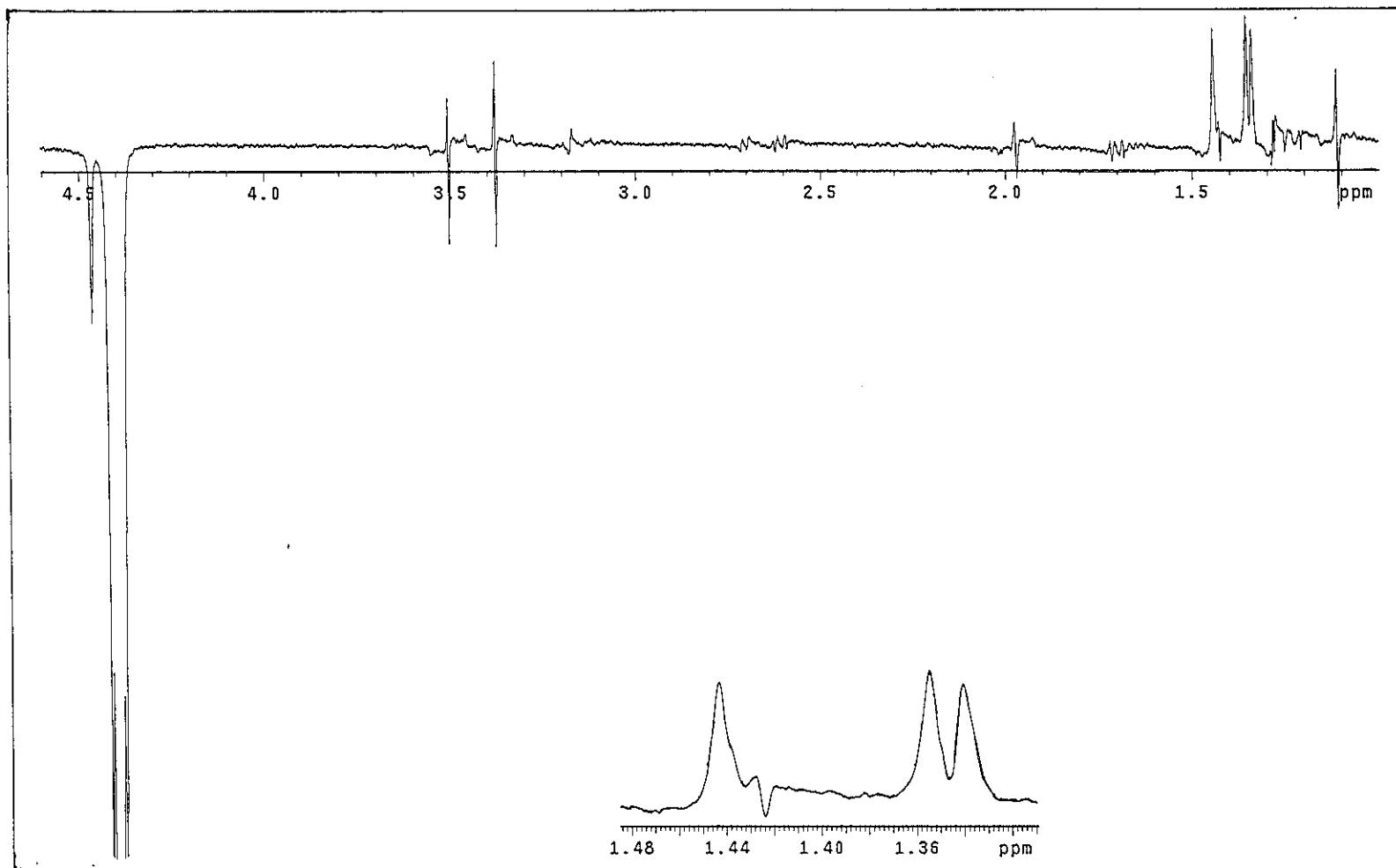


Figure 125 NOEDIFF spectrum of PP16 after irradiation at δ_H 4.40

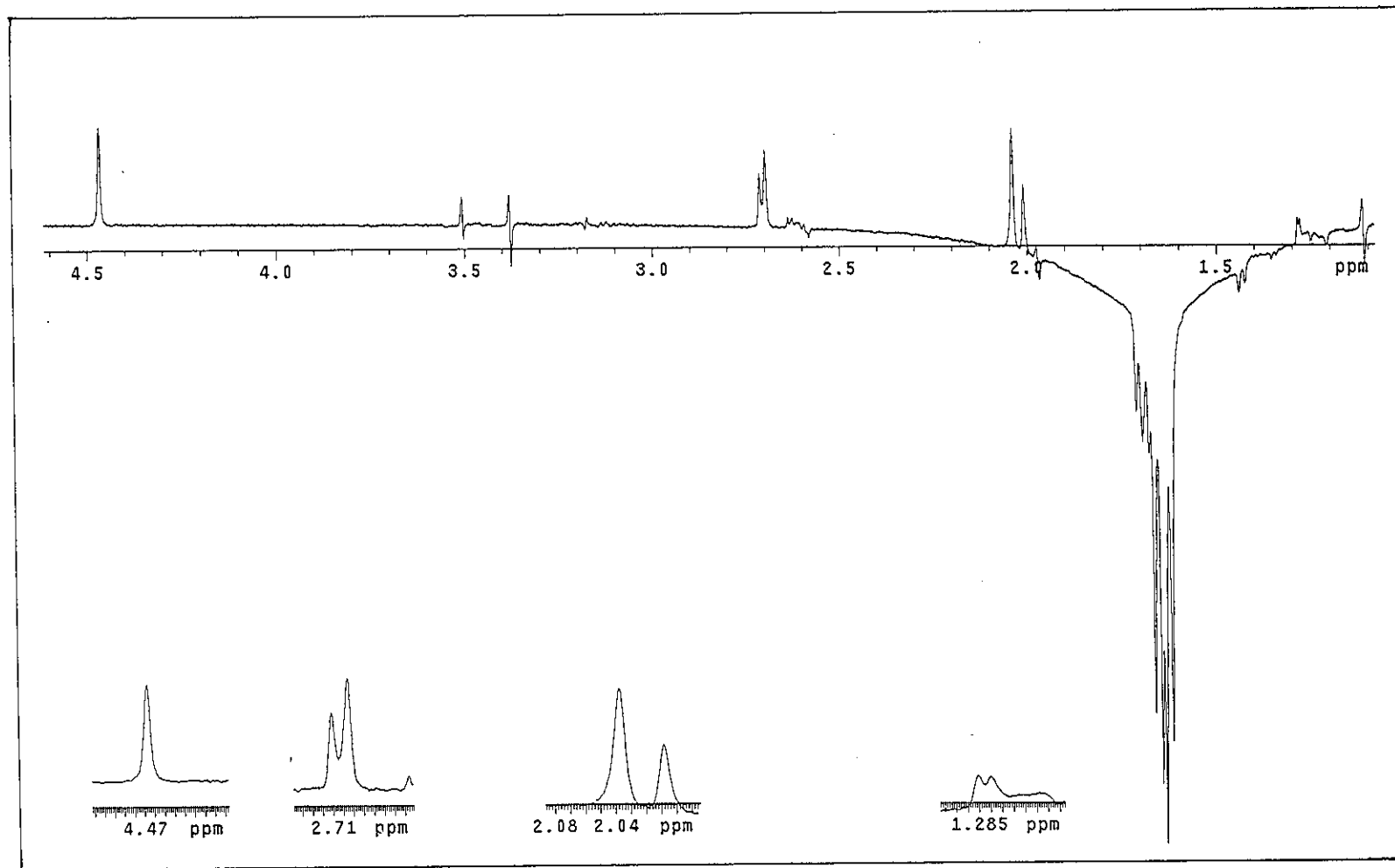


Figure 126 NOEDIFF spectrum of PP16 after irradiation at δ_H 1.65

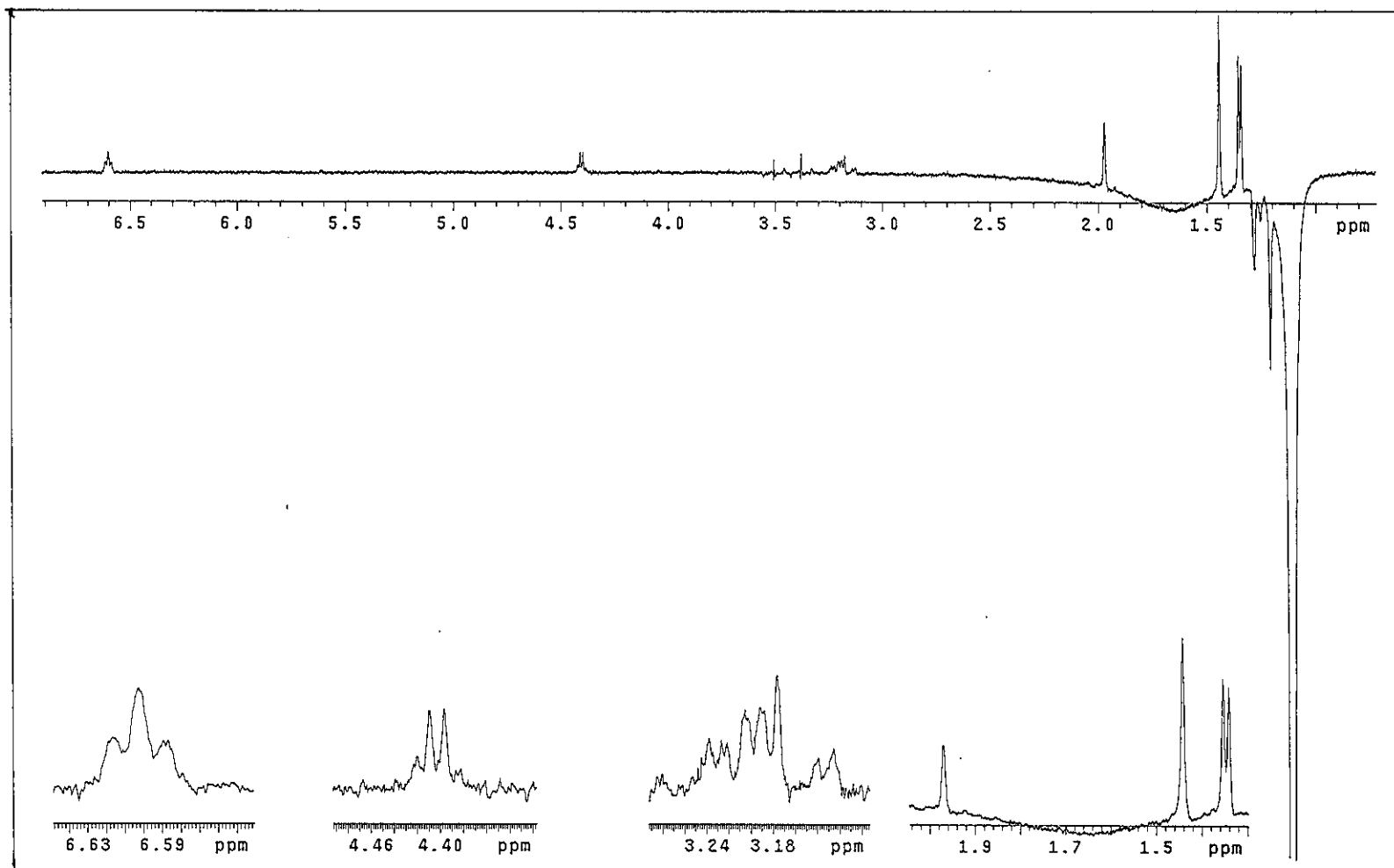


Figure 127 NOEDIFF spectrum of PP16 after irradiation at δ_H 1.11

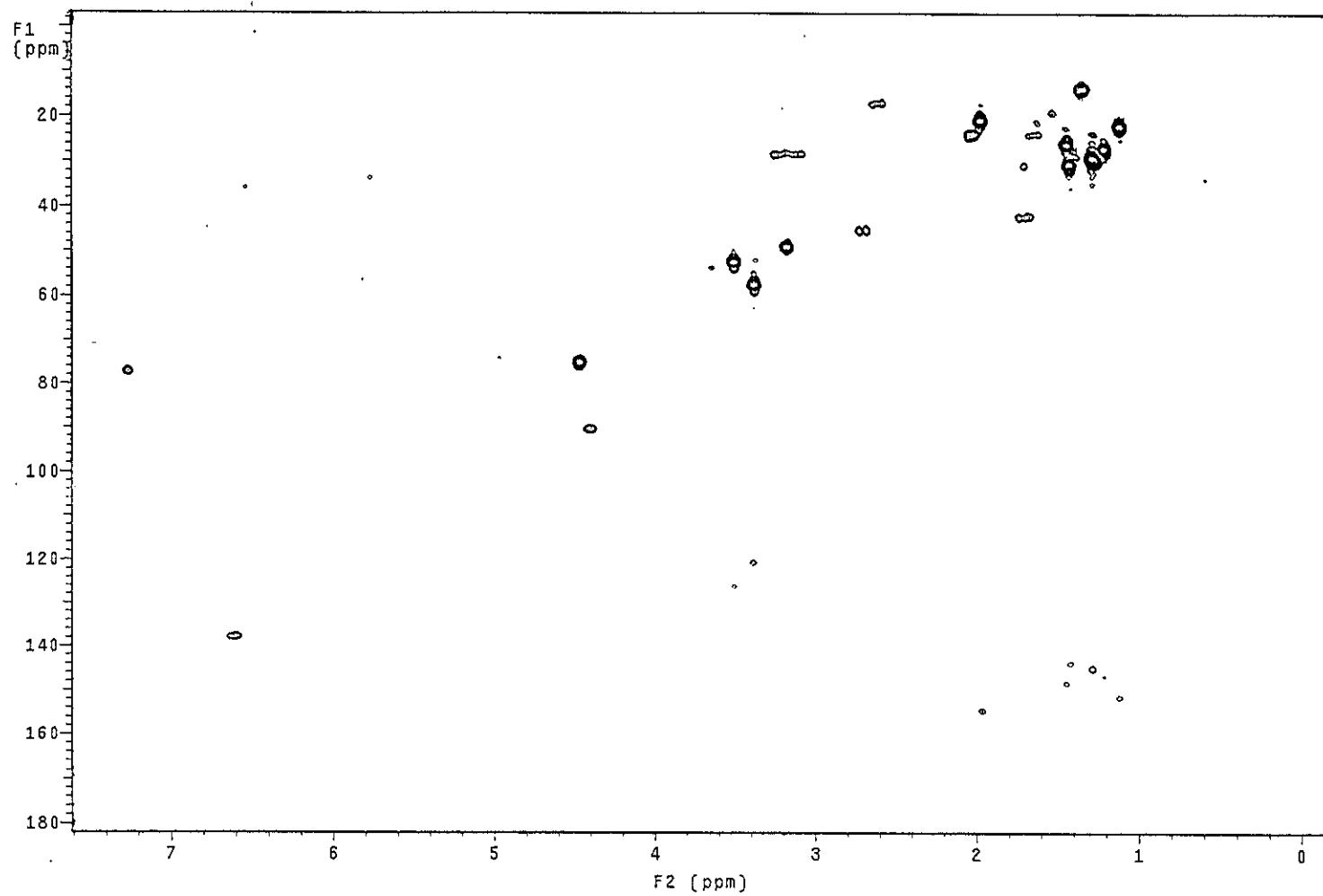


Figure 128 2D HMQC spectrum of PP16

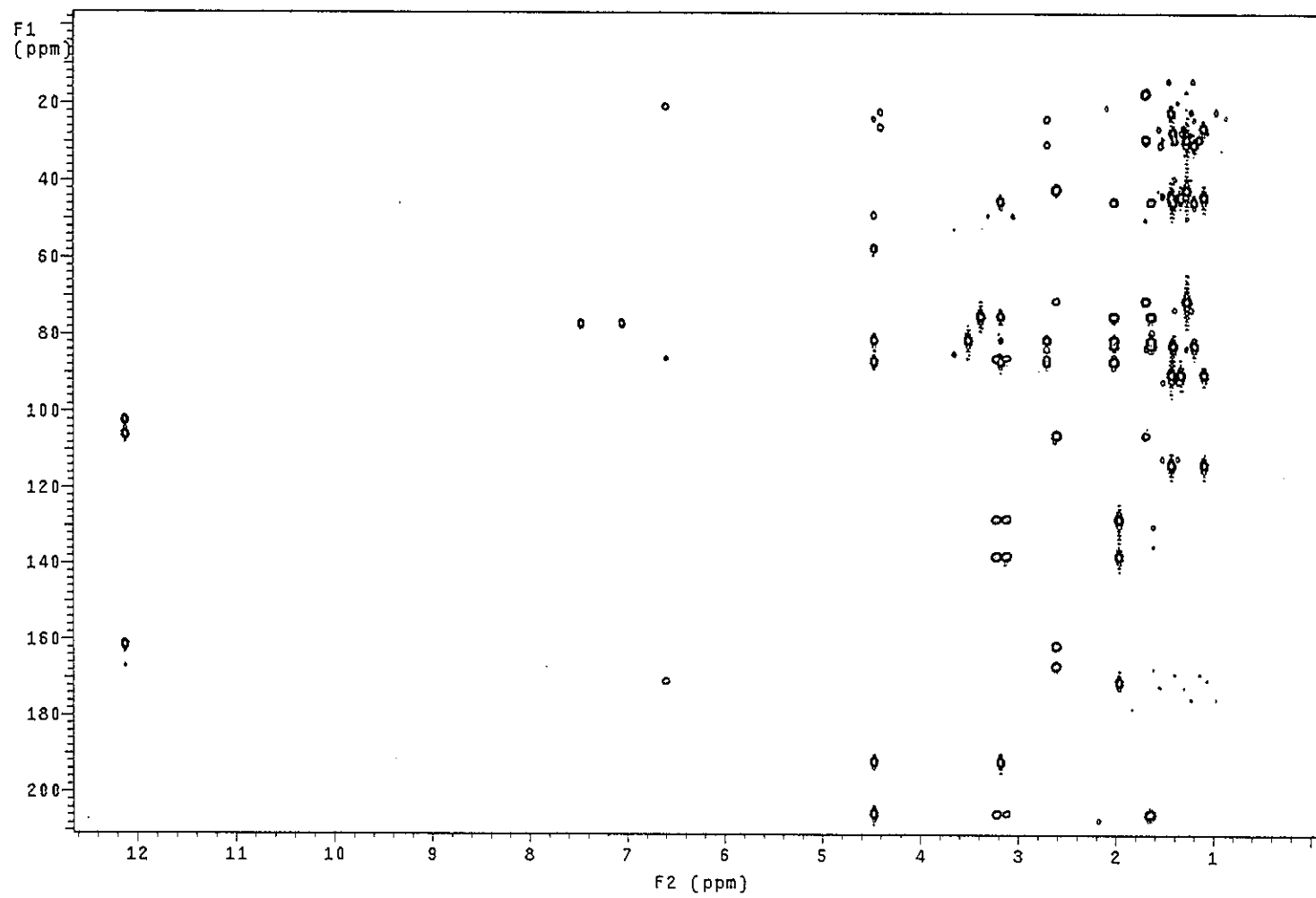


Figure 129 2D HMBC spectrum of PP16

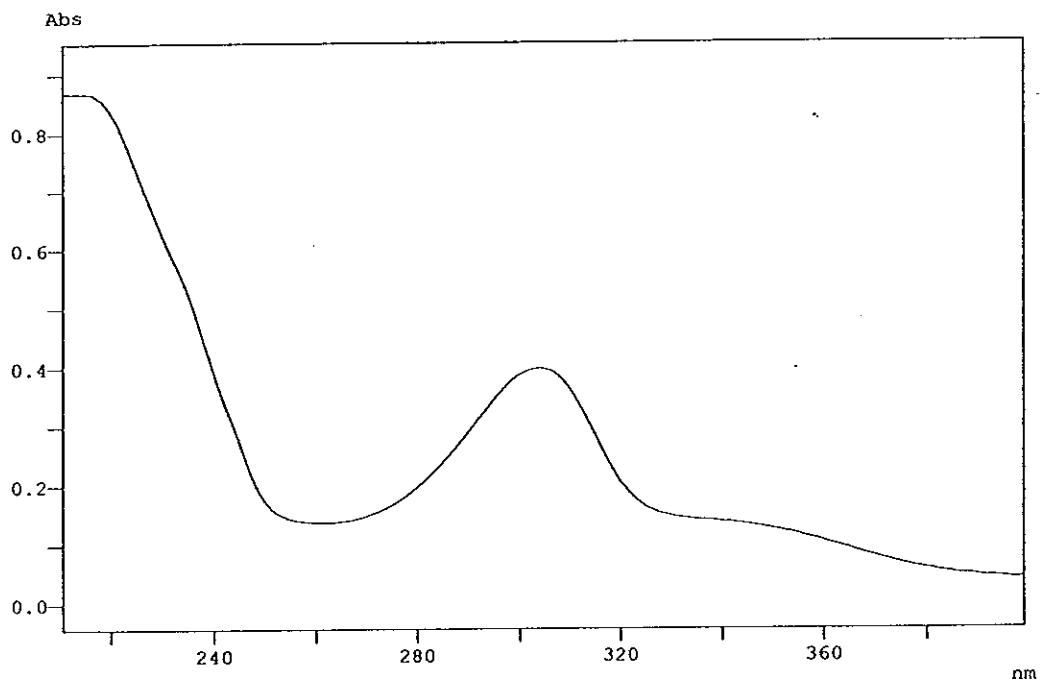


Figure 130 UV (MeOH) spectrum of PP17

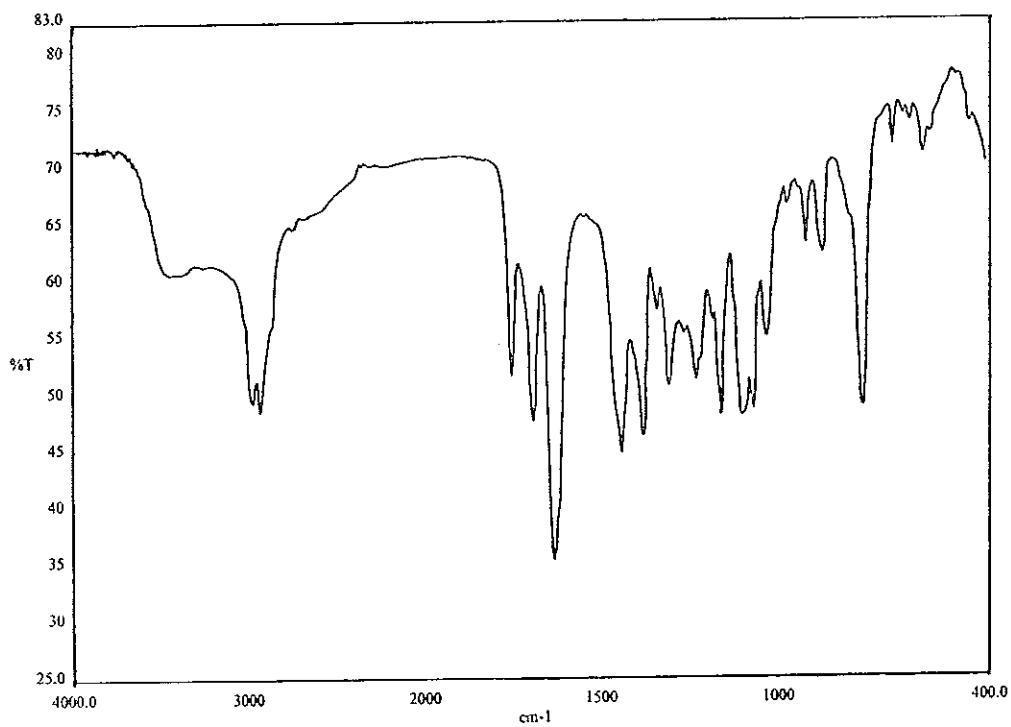


Figure 131 FT-IR (neat) spectrum of PP17

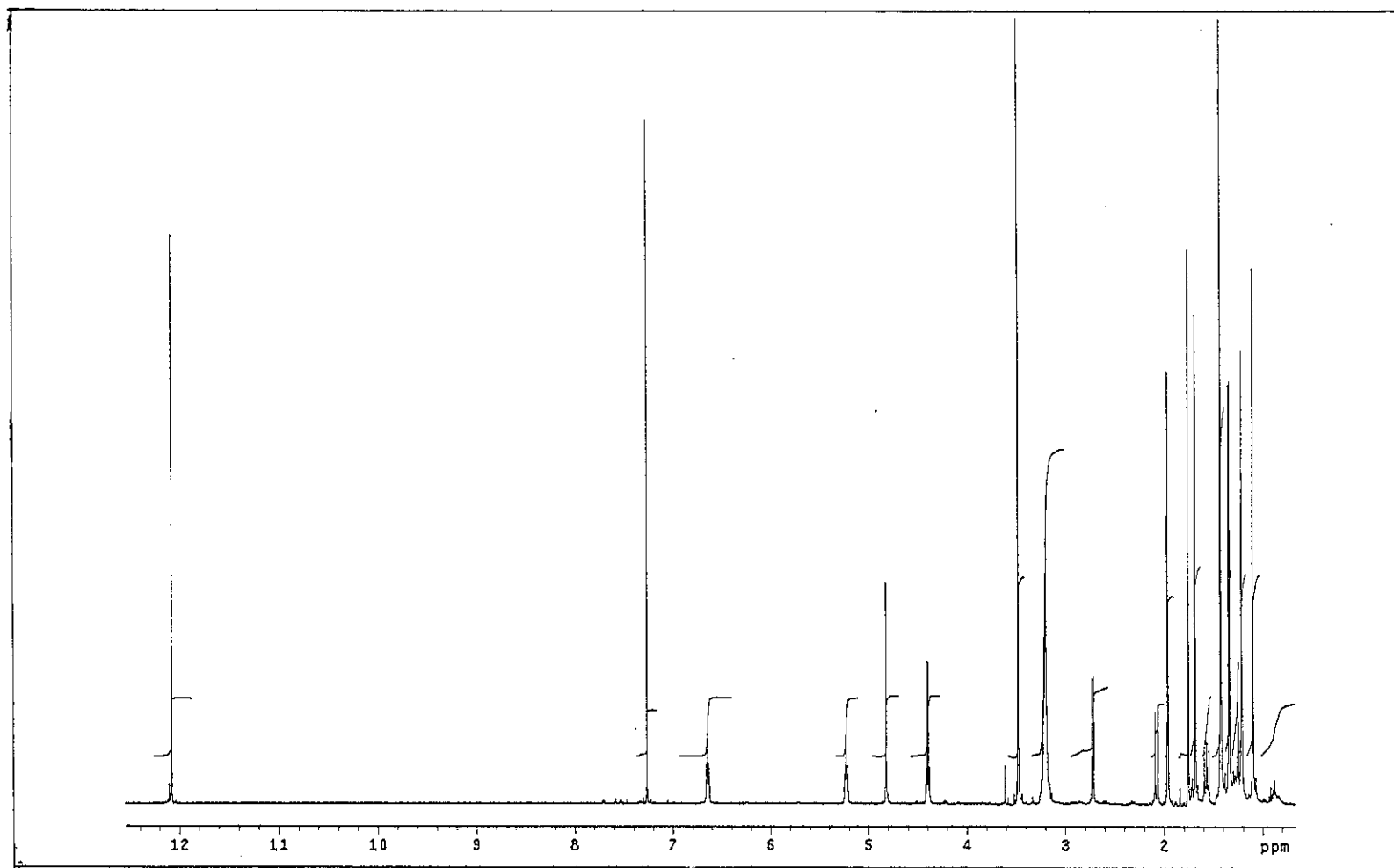


Figure 132 ^1H NMR (500 MHz) (CDCl_3) spectrum of PP17

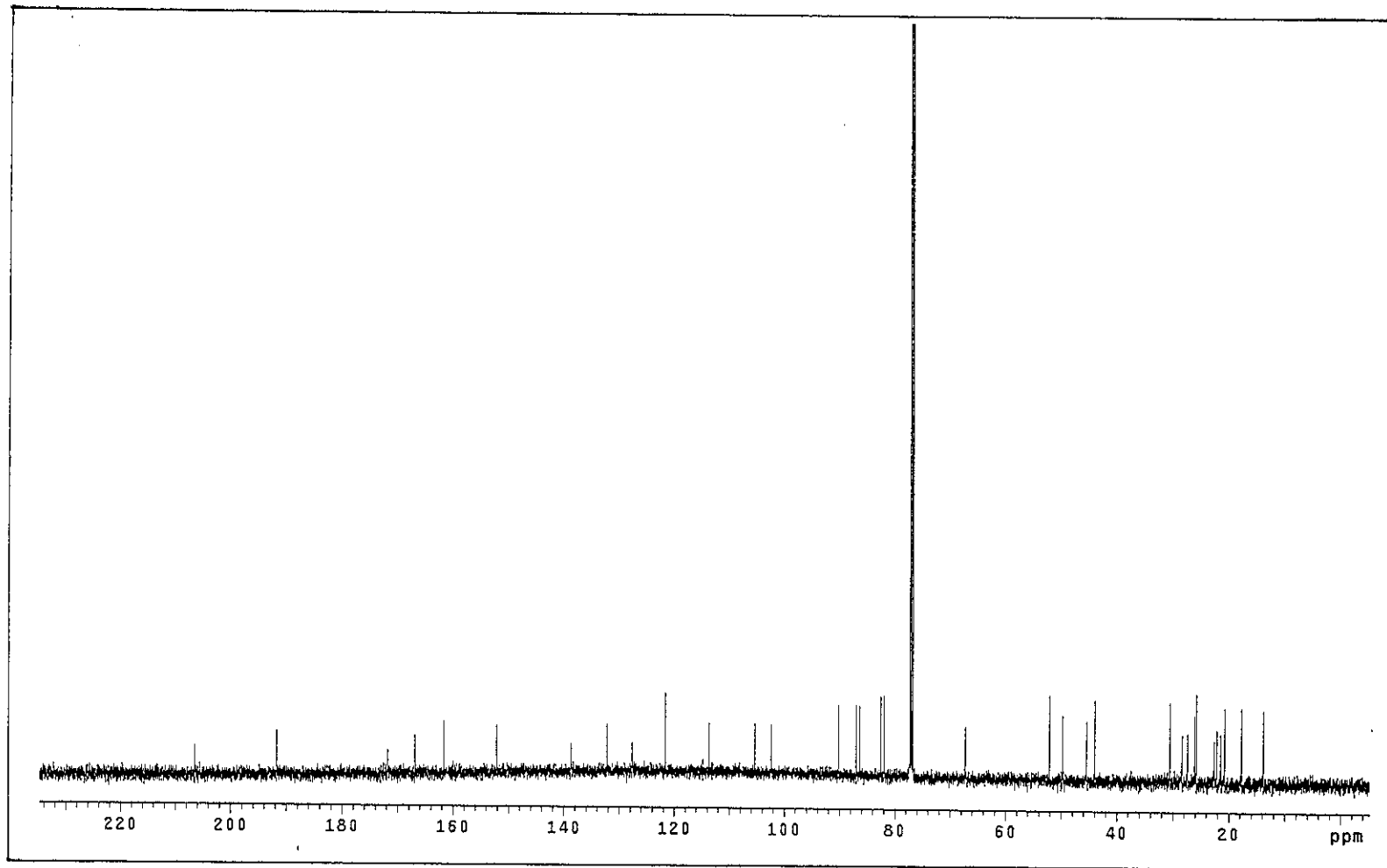


Figure 133 ^{13}C NMR (125 MHz) (CDCl_3) spectrum of PP17

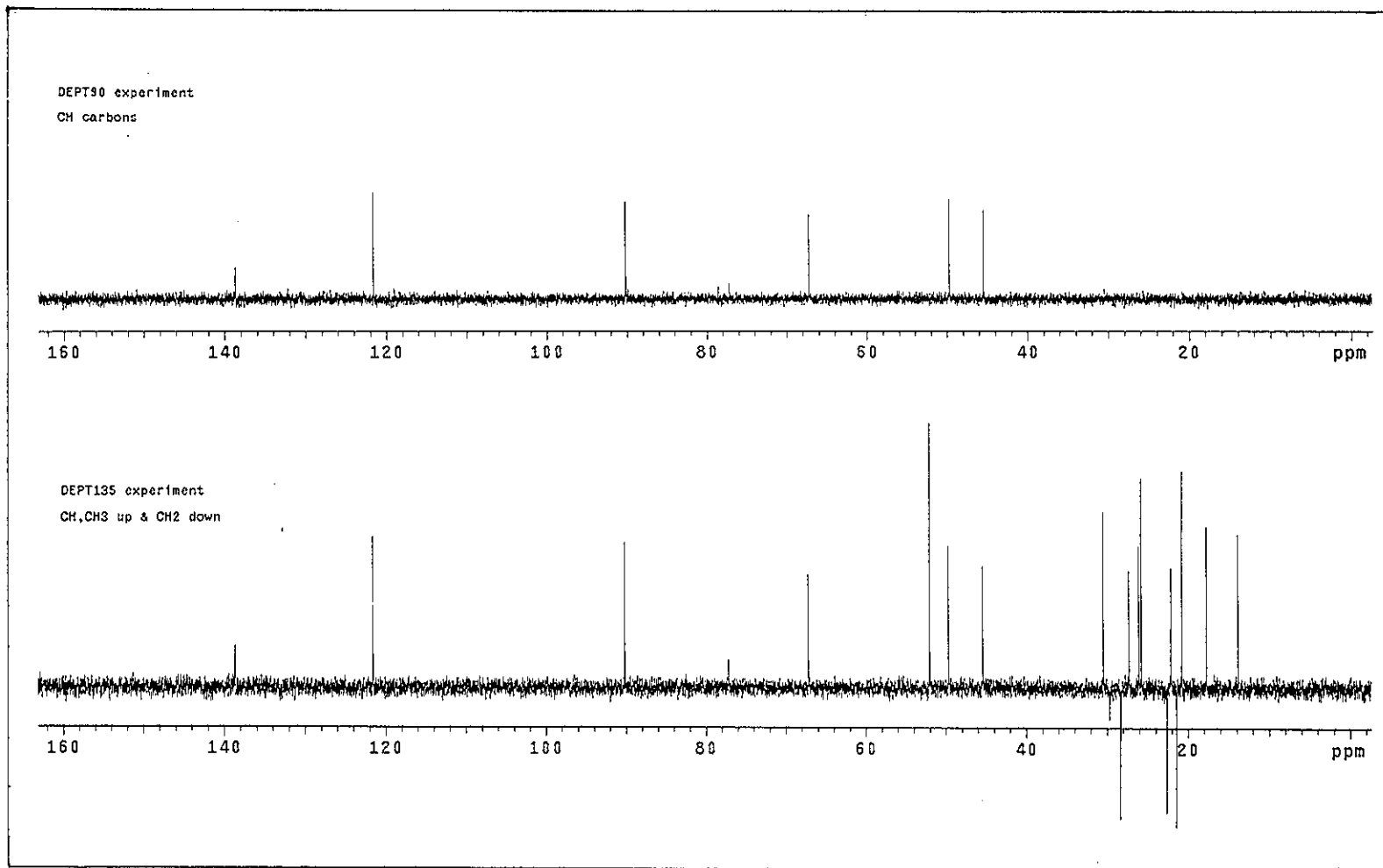


Figure 134 DEPT spectrum of PP17

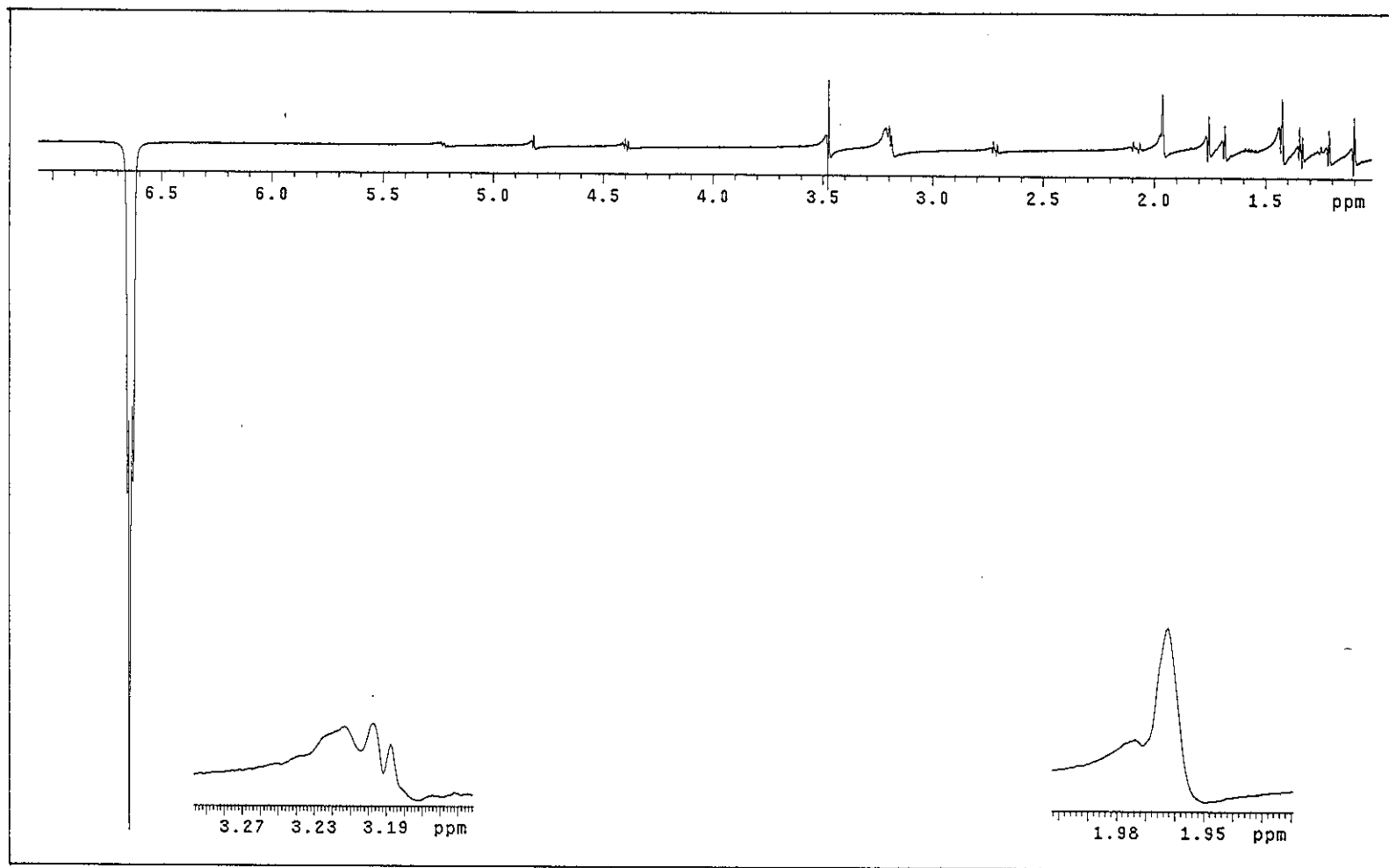


Figure 135 NOEDIFF spectrum of PP17 after irradiation at δ_H 6.64

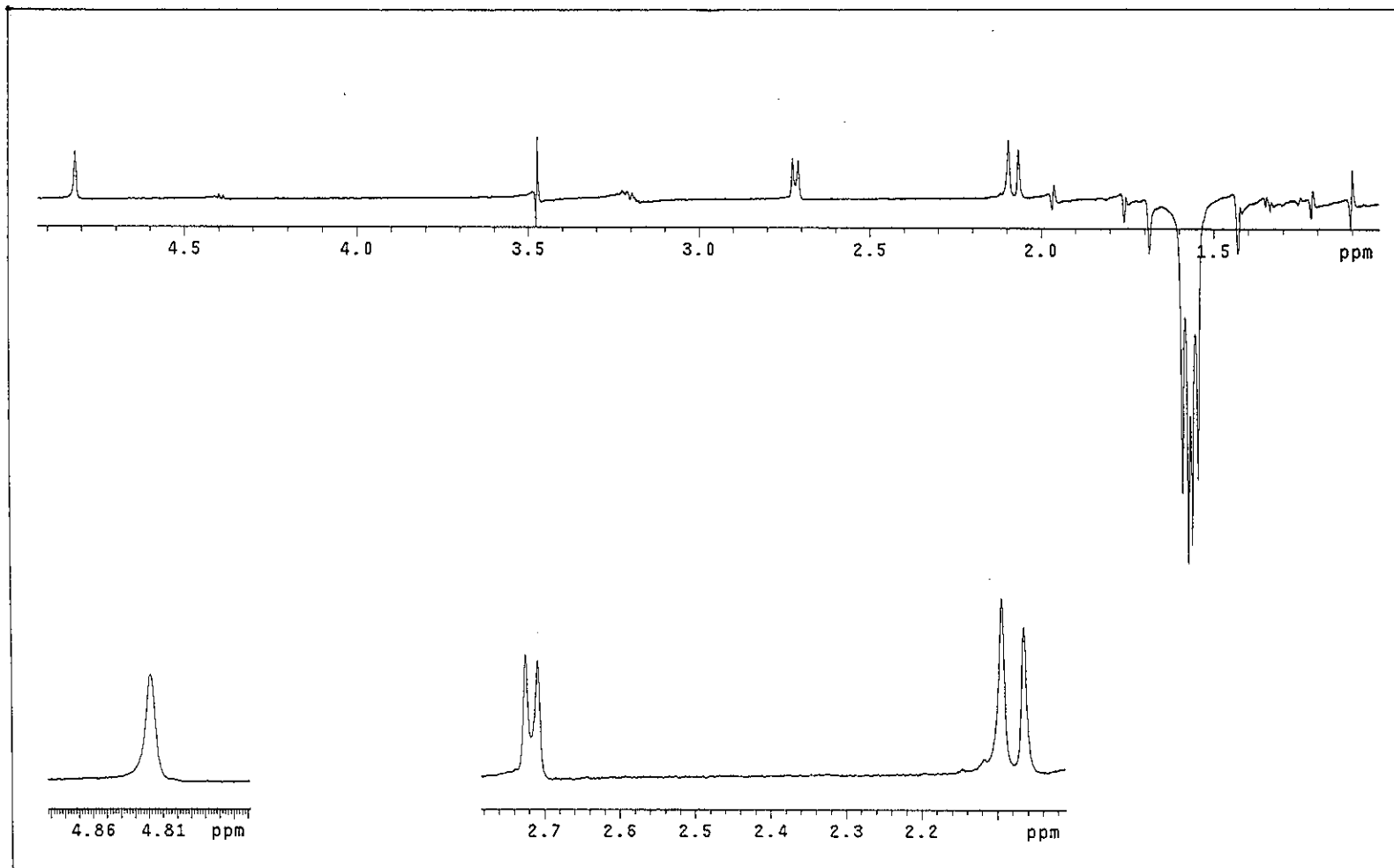


Figure 136 NOEDIFF spectrum of PP17 after irradiation at δ_H 1.57

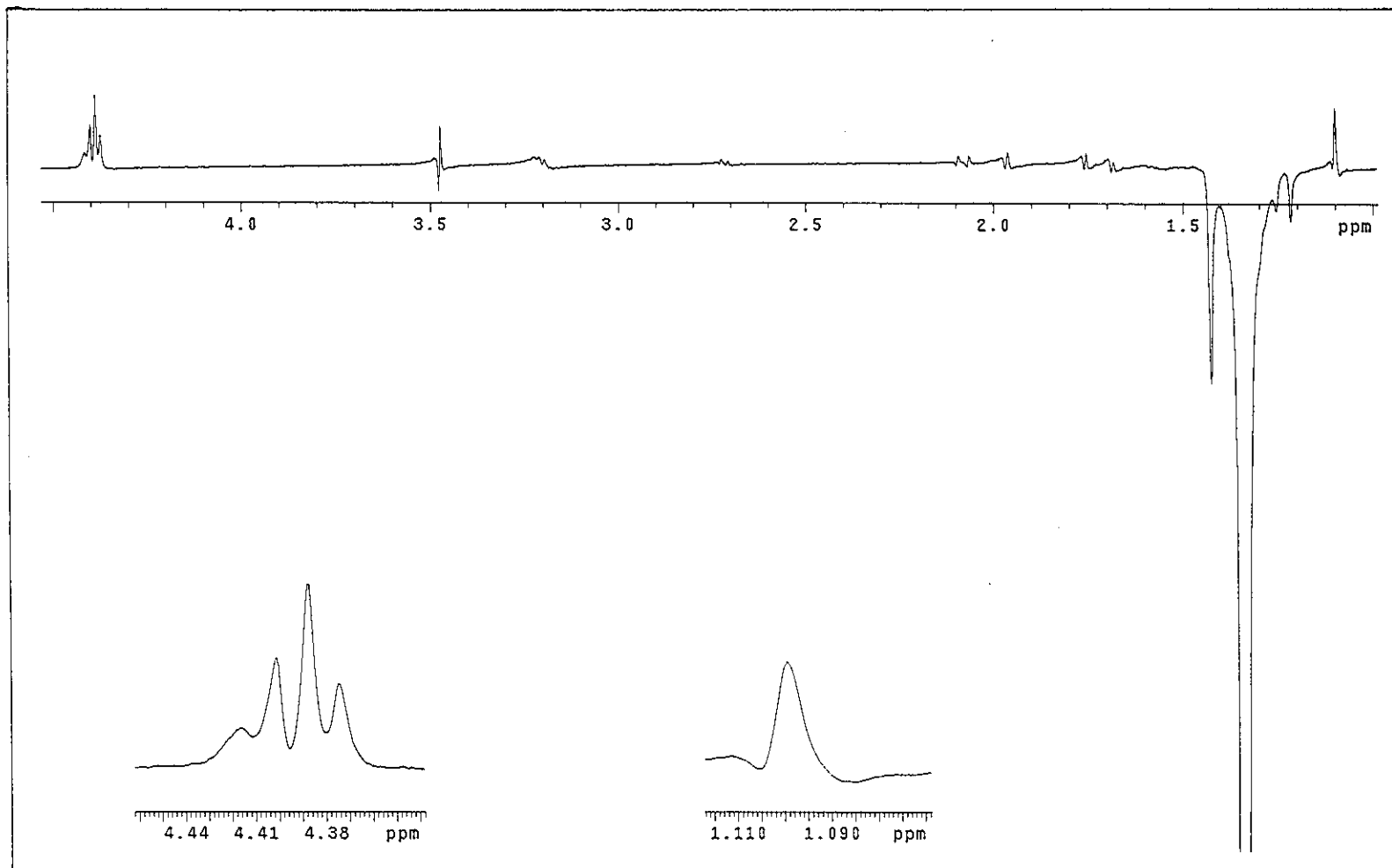


Figure 137 NOEDIFF spectrum of PP17 after irradiation at δ_H 1.34

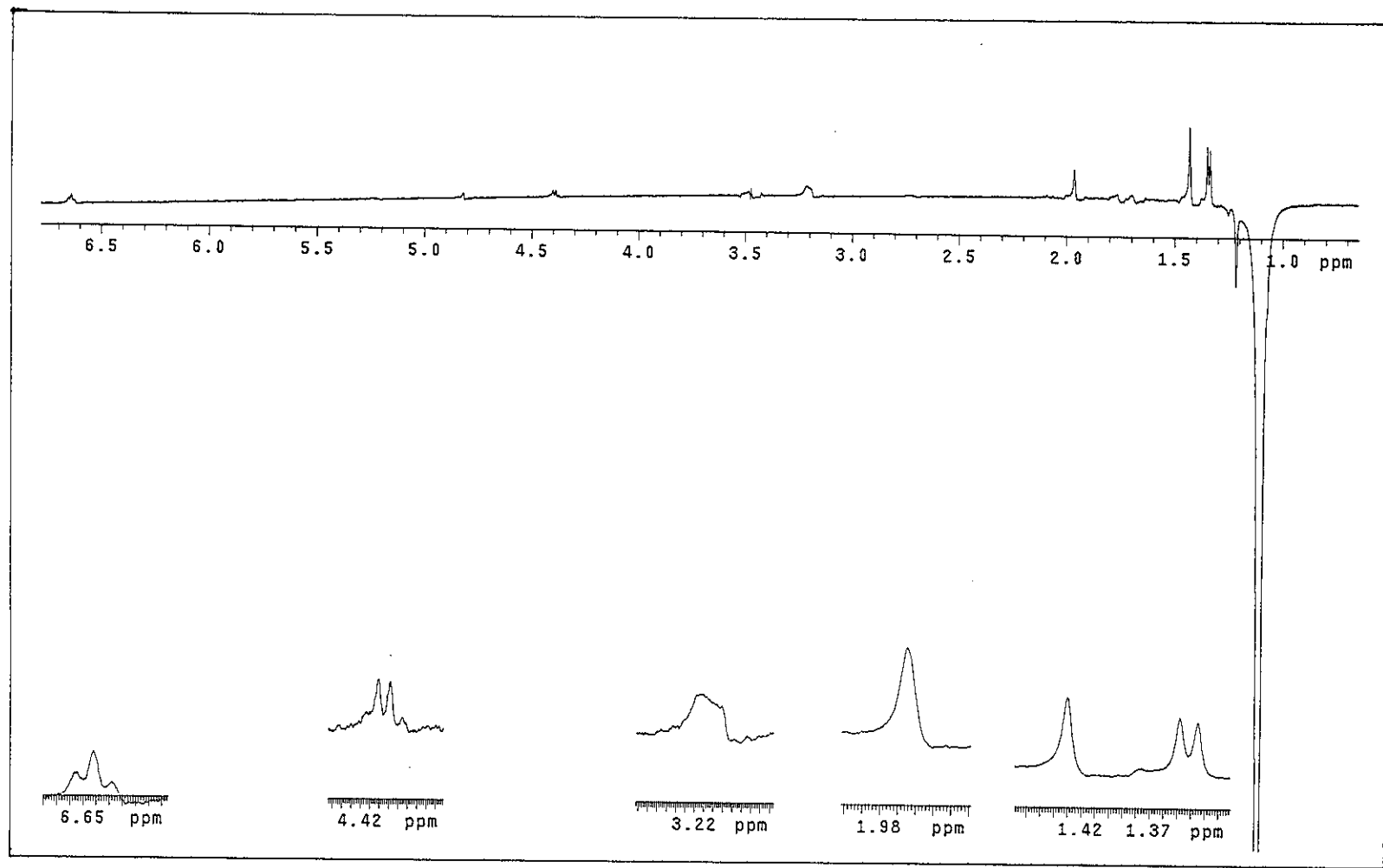
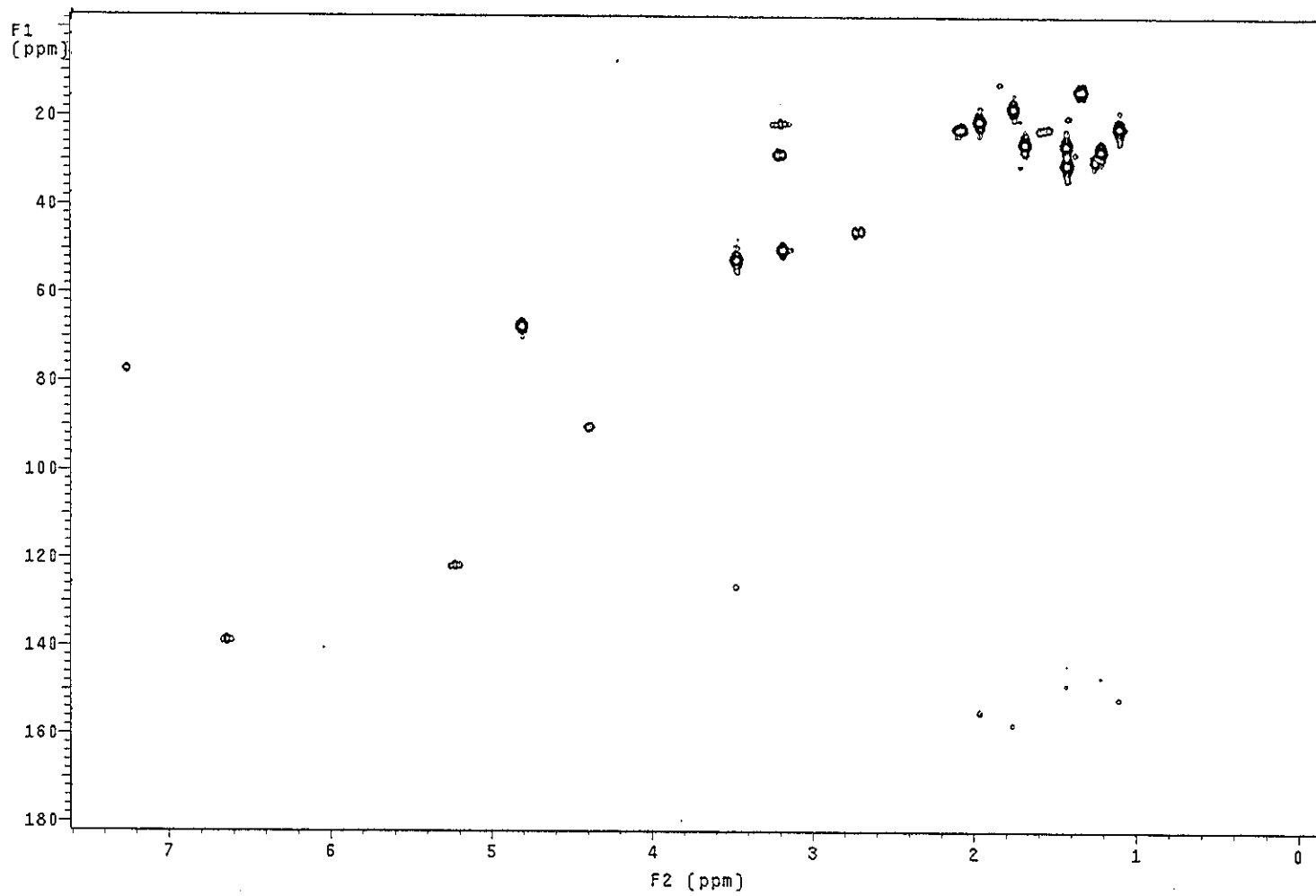


Figure 138 NOEDIFF spectrum of PP17 after irradiation at δ_H 1.10



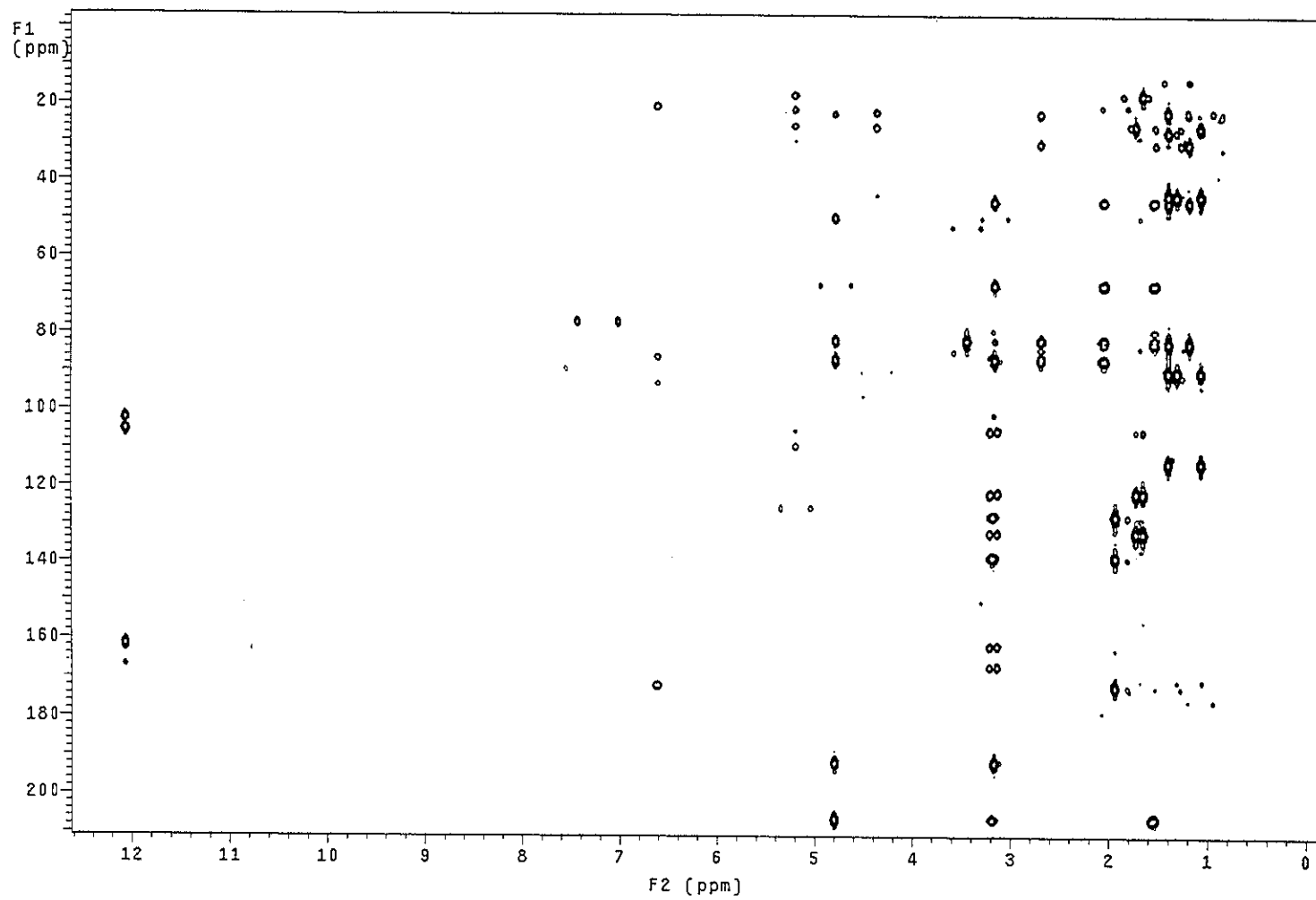


Figure 140 2D HMBC spectrum of PP17

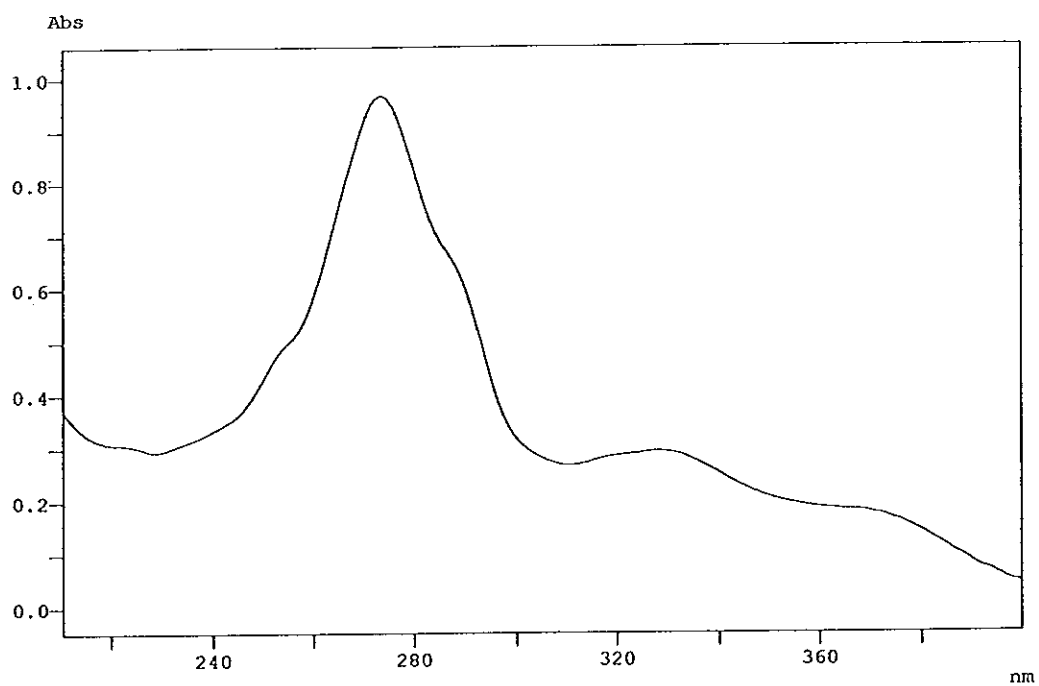


Figure 141 UV (MeOH) spectrum of PP11

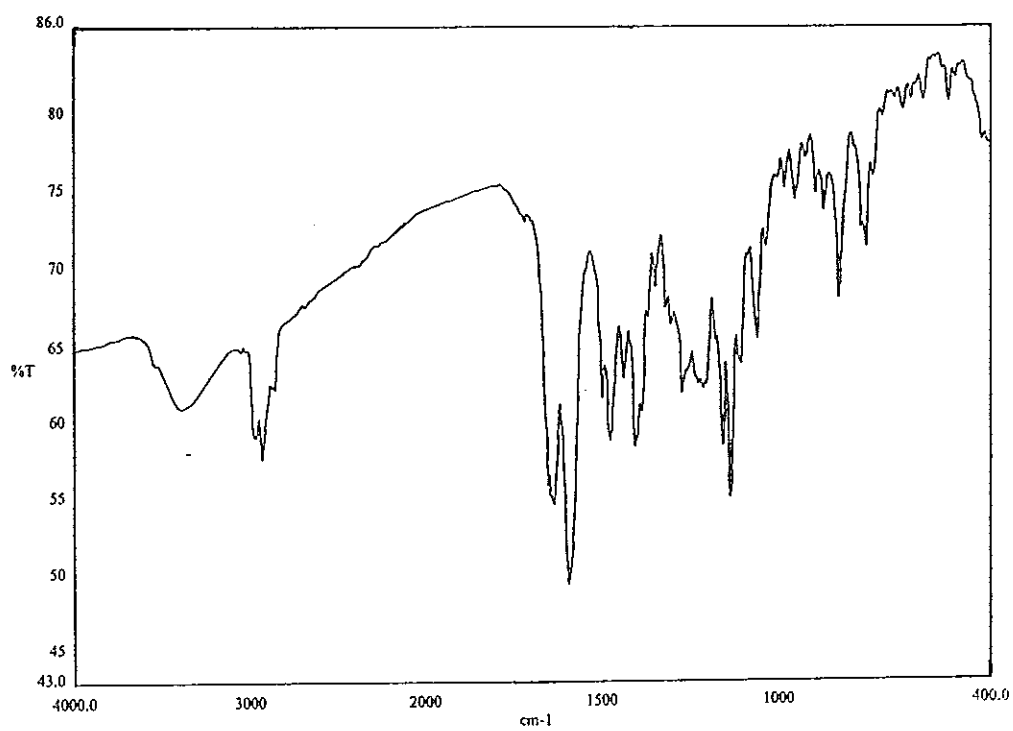


Figure 142 FT-IR (neat) spectrum of PP11

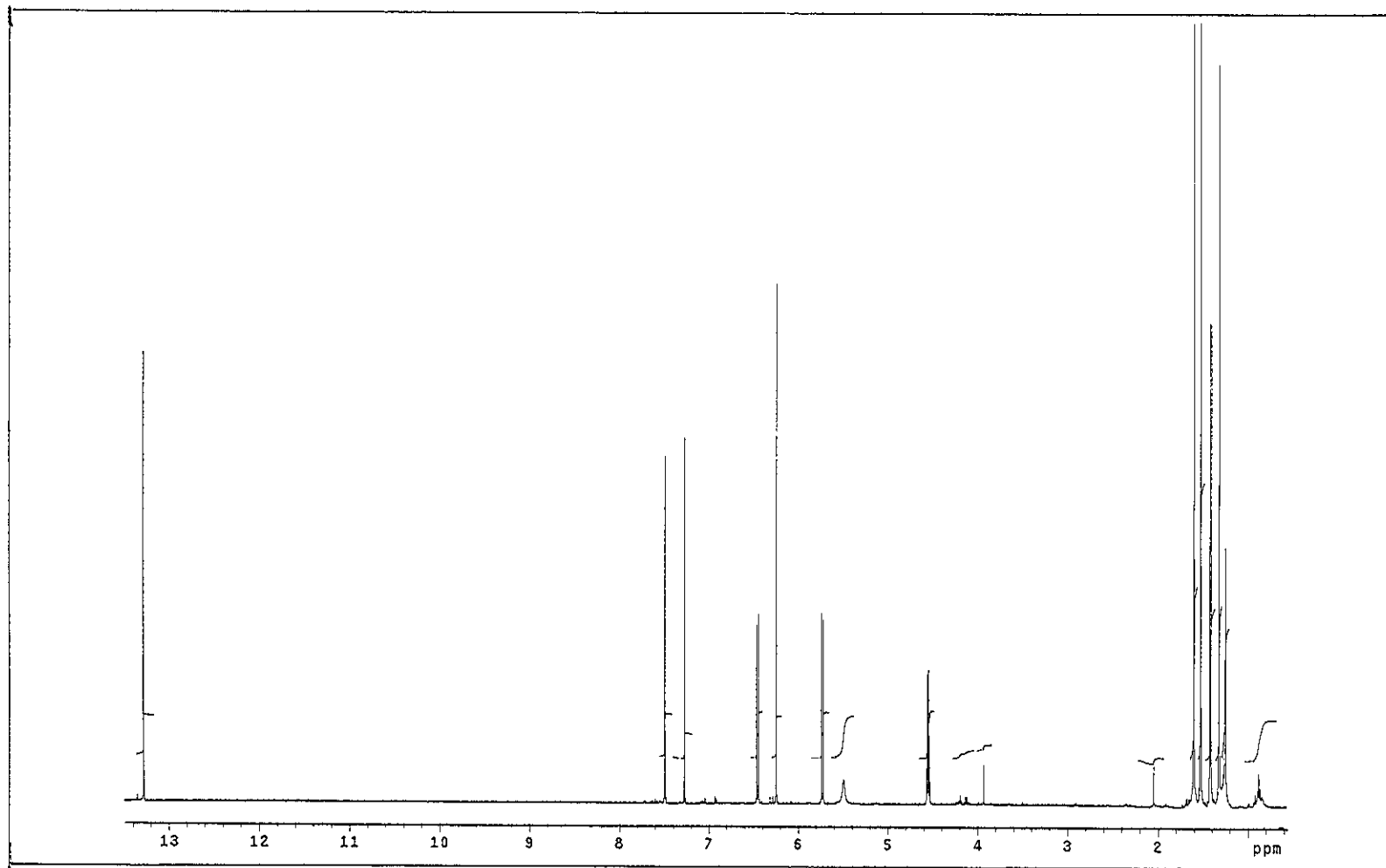


Figure 143 ^1H NMR (500 MHz) (CDCl_3) spectrum of PP11

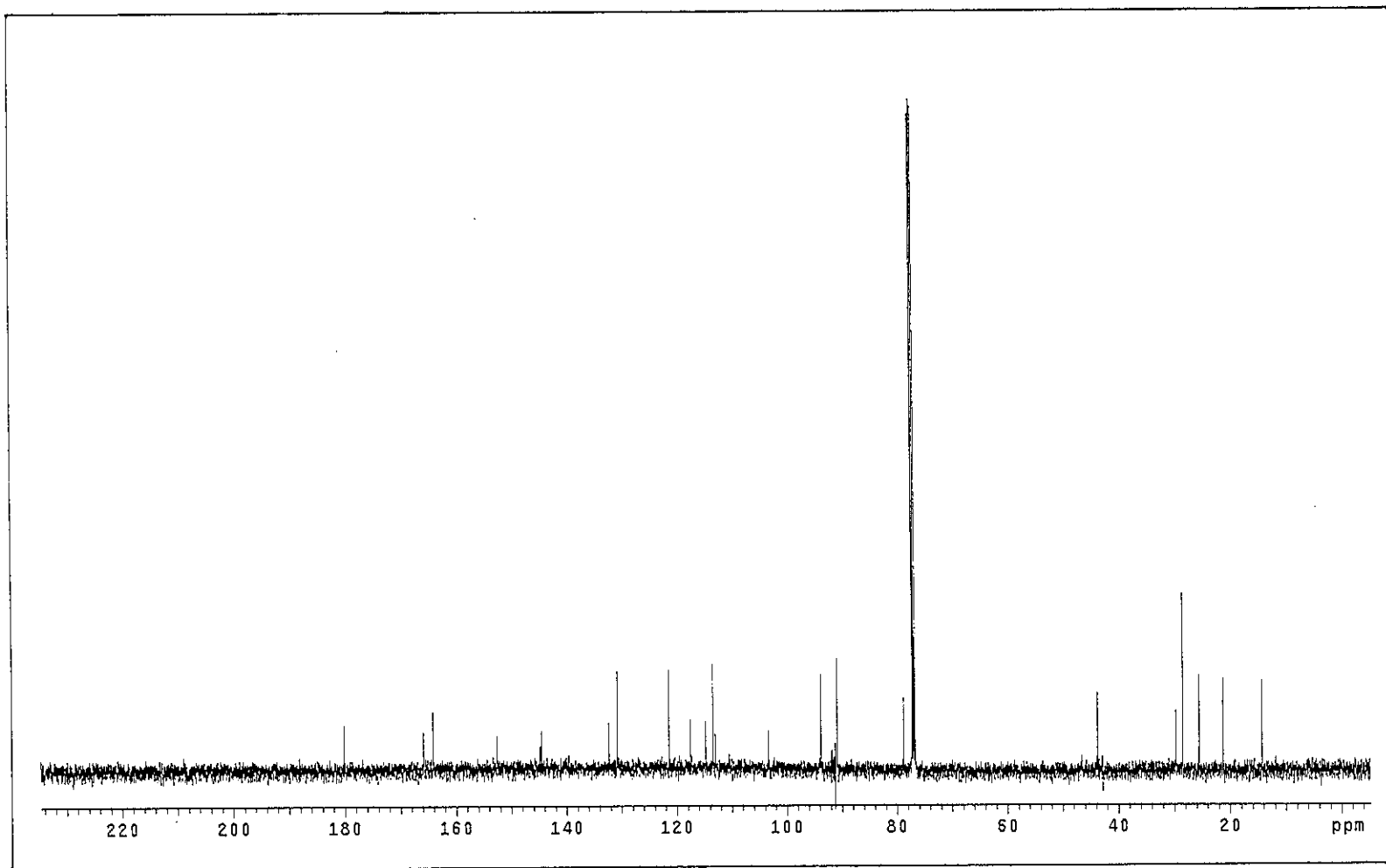


Figure 144 ^{13}C NMR (125 MHz) (CDCl_3) spectrum of PP11

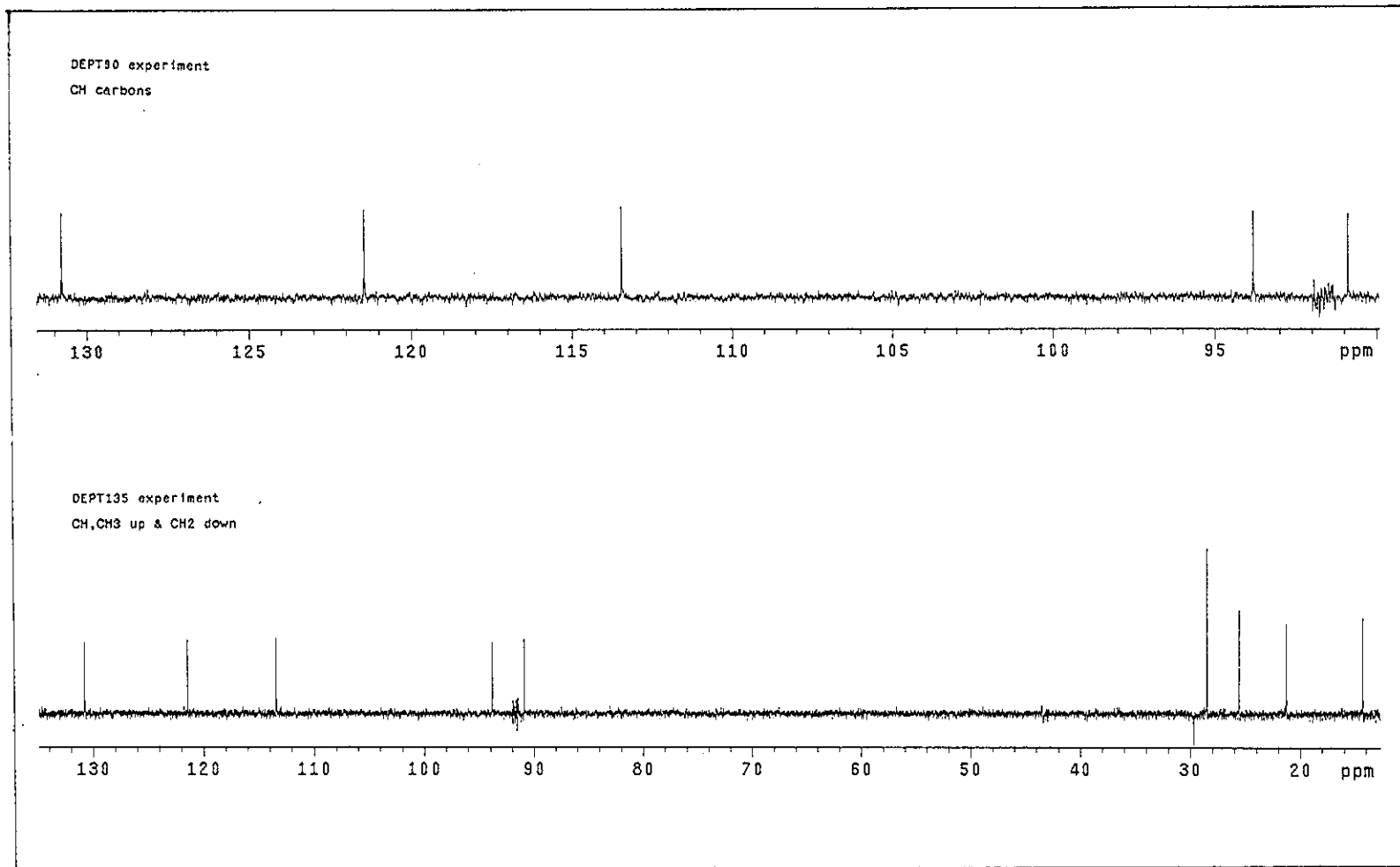


Figure 145 DEPT spectrum of PP11

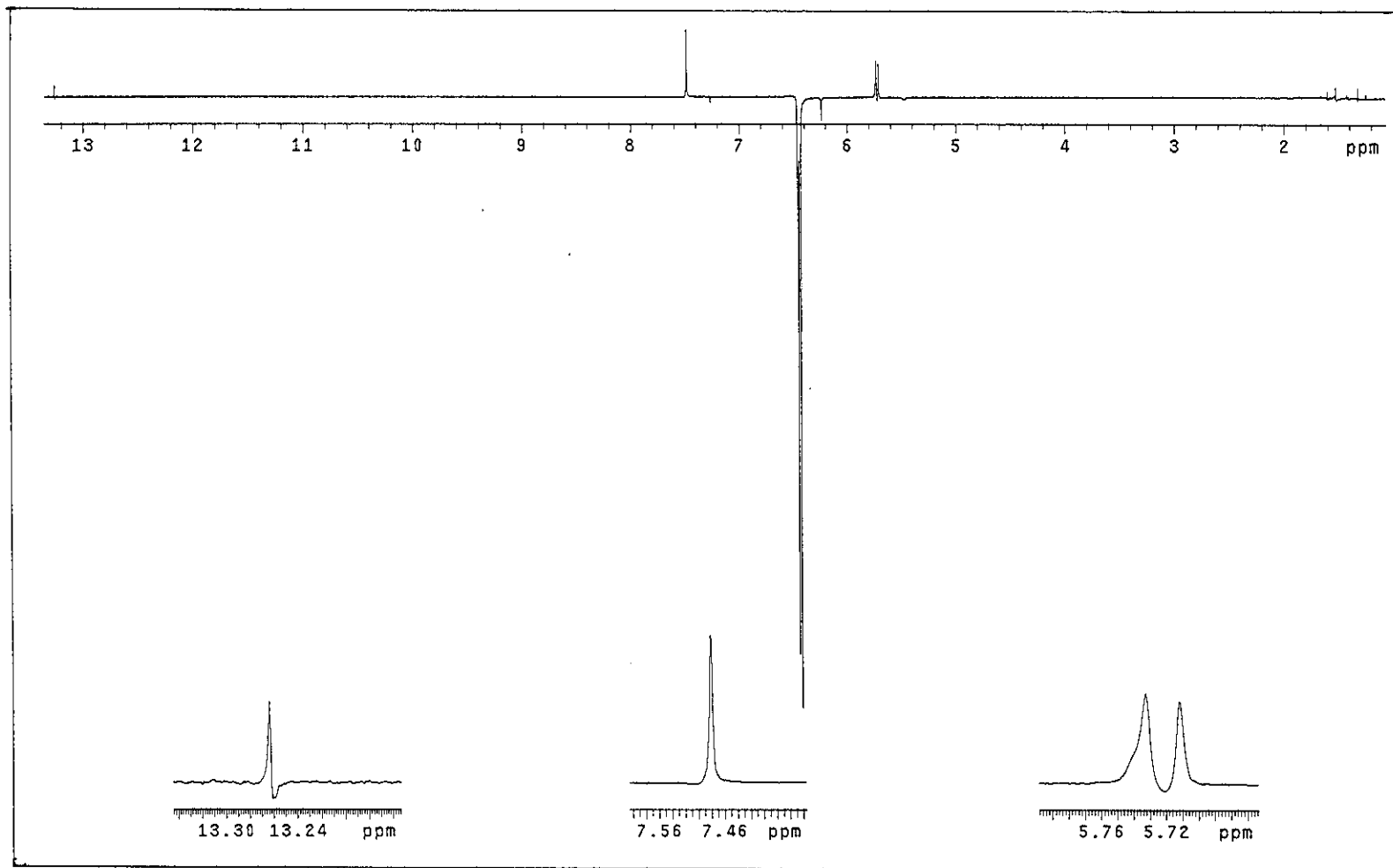


Figure 146 NOEDIFF spectrum of PP11 after irradiation at δ_H 6.45

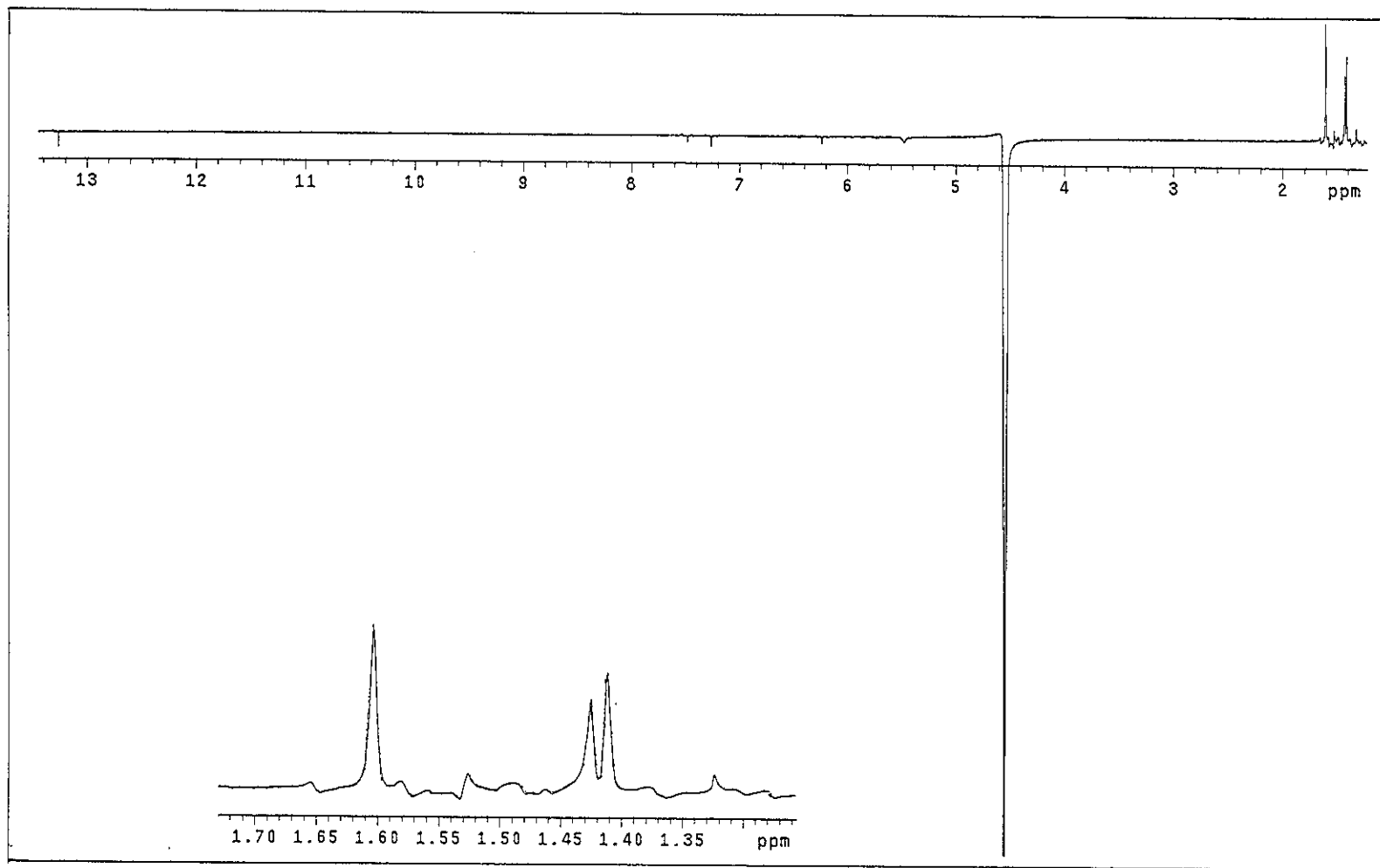


Figure 147 NOEDIFF spectrum of PP11 after irradiation at δ_H 4.55

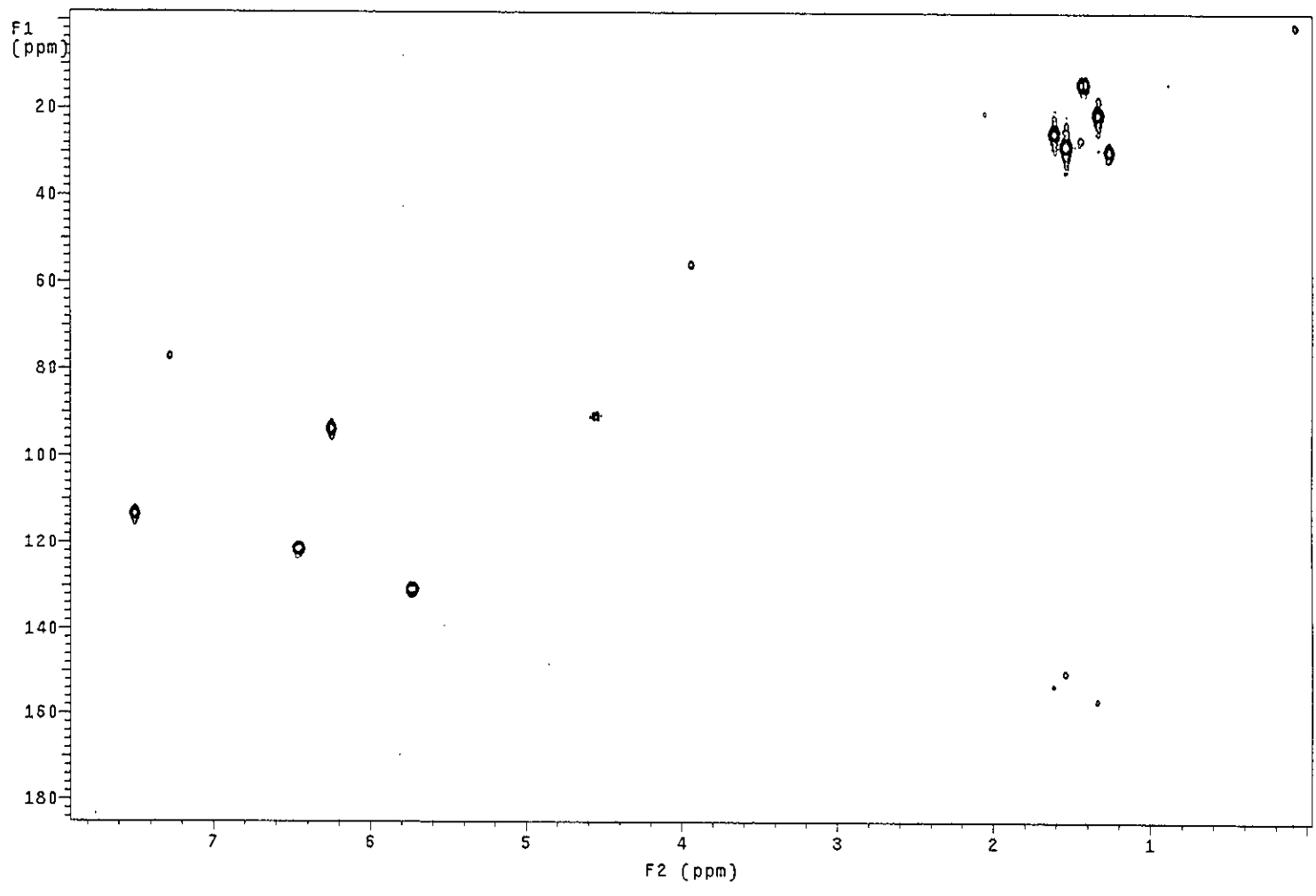


Figure 148 2D HMQC spectrum of PP11

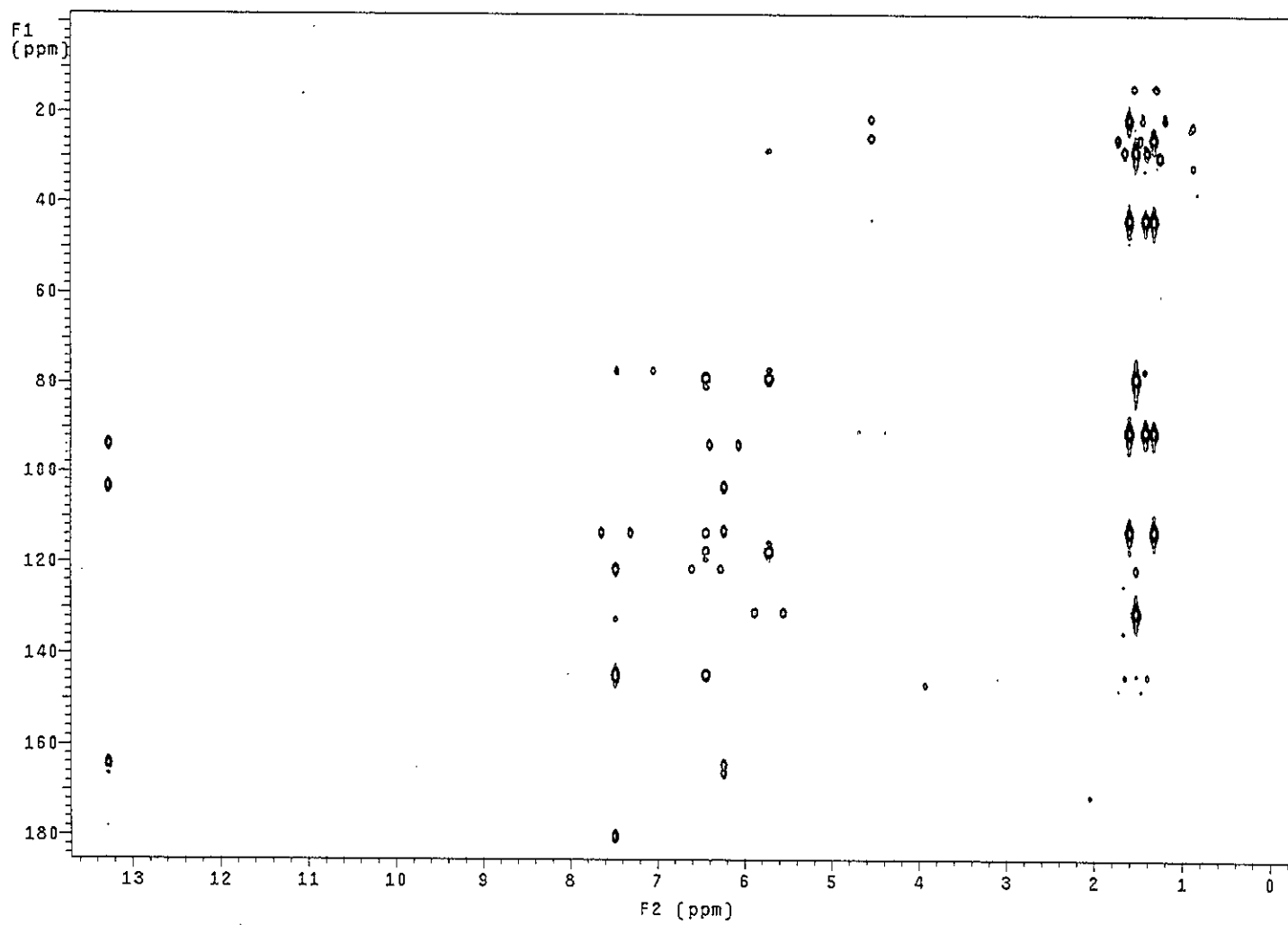


Figure 149 2D HMBC spectrum of PP11

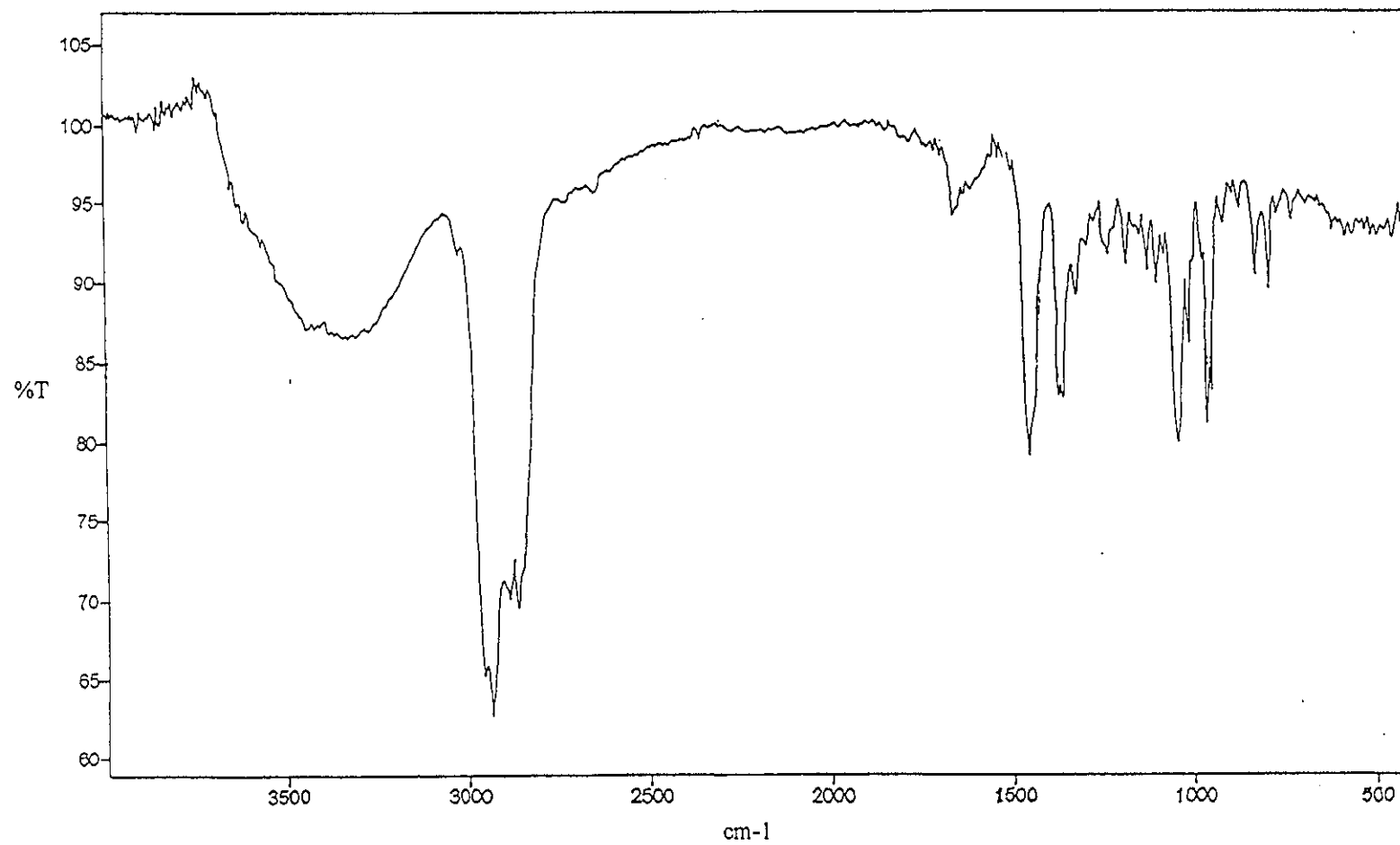


Figure 150 FT-IR (KBr) spectrum of PP12

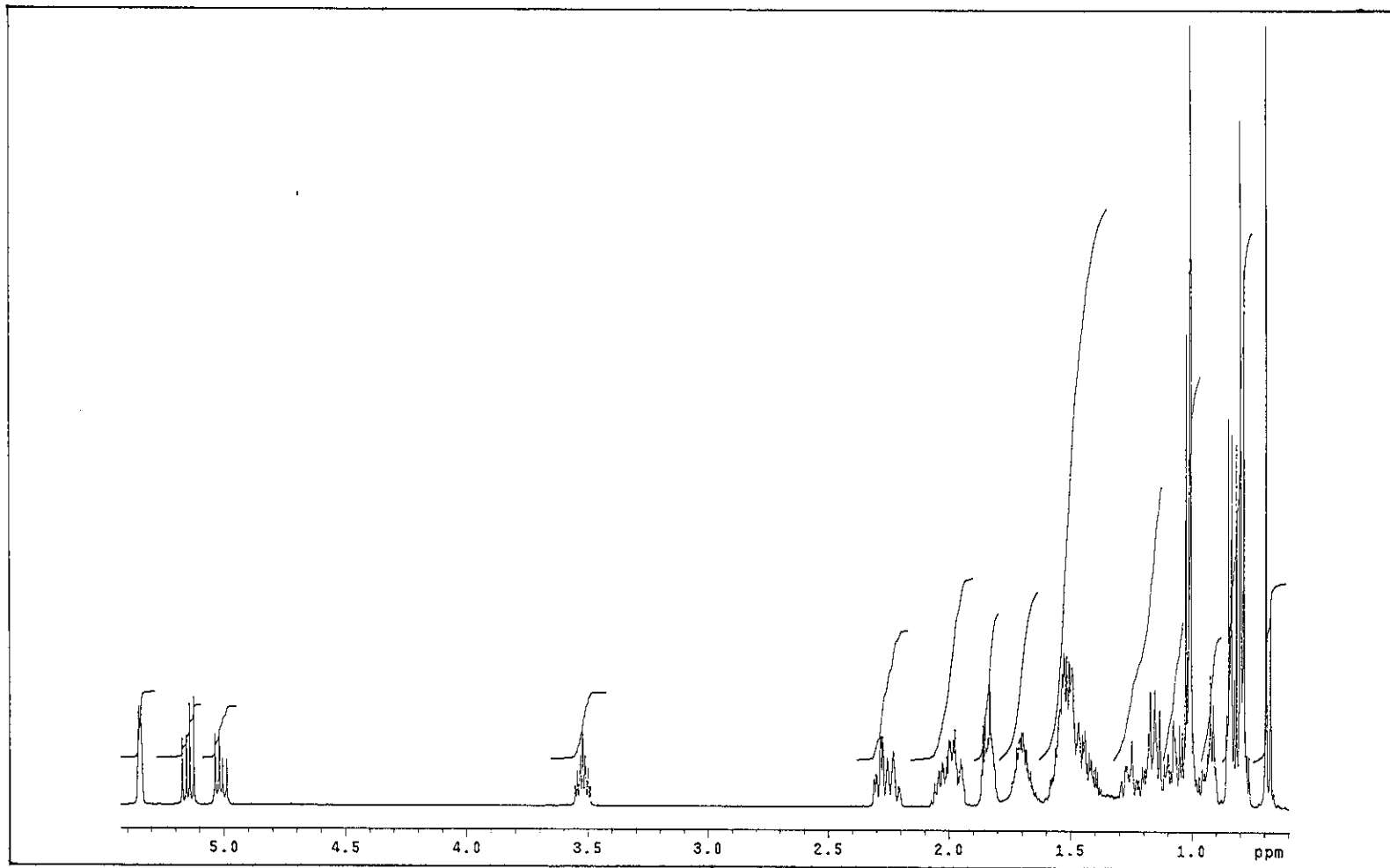


Figure 151 ^1H NMR (500 MHz) (CDCl_3) spectrum of PP12

BIBLIOGRAPHY

- Ali, S., Goundar, R., Sotheeswaran, S., Beaulieu, C. and Spino, C. 2000. "Benzophenones of *Garcinia pseudoguttifera* (Clusiaceae)", *Phytochemistry*. 53, 281-284.
- Asano, J., Chiba, K., Tada M. and Yoshii, T. 1996. "Cytotoxic xanthenes from *Garcinia hanburyi*", *Phytochemistry*. 41(3), 815-820.
- Cao, S-G., Wu, X-H., Sim, K-Y., Tan, B. K. H., Pereira, J. T., Wong, W. H., Hew, N.F. and Goh, S.H. 1998a. "Cytotoxic caged tetraprenylated xanthonoids from *Garcinia gaudichaudii* (Guttiferae)", *Tetrahedron Lett.* 39, 3353-3356.
- Cao, S-G., Sng, V. H. L., Wu, X-H., Sim, K-Y., Tan, B. K. H., Pereira, J. T., and Goh, S. H. 1998b. "Novel cytotoxic polyprenylated xanthonoids from *Garcinia gaudichaudii* (Guttiferae)", *Tetrahedron*. 54(36), 10915-10924.
- Chairungrilerd, N., Takeuchi, K., Ohizumi, Y., Nozoe, S. and Ohta, T. 1996. "Mangostanol, a prenyl xanthone from *Garcinia mangostana*", *Phytochemistry*. 43(5), 1099-1102.
- Cuesta Rubio, O., Padron, A., Velez Castro, H., Pizza, C. and Rastrelli, L. 2001. "Aristophenones A and B. A new tautomeric pair of polyisoprenylated benzophenones from *Garcinia aristata*", *J. Nat. Prod.* 64(7), 973-975.

- Delle Monache, G., Botta, B., De Mello, J. F., De Barros Coelho, J. S. and Menichini, F. 1984. "Chemical investigation of the genus *Rheedia*, VI. Three new xanthenes from *Rheedia brasiliensis*", *J. Nat. Prod.* 47(4), 620-625.
- Fukuyama, Y., Kaneshi, A., Tani, N. and Kodama, M. 1993. "Subellinone, a polyisoprenylated phloroglucinol derivative from *Garcinia subelliptica*", *Phytochemistry.* 33(2), 483-485.
- Goh, S. H., Jantan, I., Gray, A. I. and Waterman, P. G. 1992. "Prenylated xanthenes from *Garcinia opaca*", *Phytochemistry.* 31(4), 1383-1386.
- Gopalakrishnan, G., Banumathi, B. and Suresh, G. 1997. "Evaluation of the antifungal activity of natural xanthenes from *Garcinia mangostana* and their synthetic derivatives", *J. Nat. Prod.* 60(5), 519-524.
- Gottlieb, O. R. 1968. "Biogenetic proposals regarding aucuparins and xanthenes", *Phytochemistry.* 7, 411-421.
- Gunatilaka, A. A. L., Sriyani, H. T. B., Sotheeswaran, S. and Waight, E. S. 1983. "2,5-Dihydroxy-1,6-dimethoxyxanthone and biflavonoids of *Garcinia thwaitesii*", *Phytochemistry.* 22(1), 233-235.
- Gustafson, K. R., Blunt, J. W., Munro, M. H. G., Fuller, R. W., McKee, T. C., Cardellina II, J. H., McMahon, J. B., Cragg, M. C. and Boyd, M. R. 1992.

- "The guttiferones, HIV-inhibitory benzophenones from *Symphonia globulifera*, *Garcinia livingstonei*, *Garcinia ovalifolia* and *Clusia rosea*", *Tetrahedron*. 48(46), 10093-10102.
- Huang, Y-L., Chen, C-C., Chen, Y-J., Huang, R-L. and Shieh, B-J. 2001. "Three xanthenes and a benzophenone from *Garcinia mangostana*", *J. Nat. Prod.* 64 (7), 903-906.
- Ilyas, M., Kamil, M., Parveen, M. and Khan, M. S. 1994. "Isoflavones from *Garcinia nervosa*", *Phytochemistry*. 36(3), 807-809.
- Iinuma, M., Tosa, H., Ito, T., Tanaka, T. and Riswan, S. 1996a. "Three new benzophenone-xanthone dimers from the root of *Garcinia dulcis*", *Chem. Pharm. Bull.* 44(9), 1744-1747.
- Iinuma, M., Tosa, H., Ito, T., Tanaka, T. and Riswan, S. 1996b. "Garciduols A and B, new benzophenone-xanthone dimers, from *Garcinia dulcis*", *Heterocycles*. 43 (3), 535-538.
- Iinuma, M., Tosa, H., Tanaka, T. and Riswan, S. 1996c. "Three new xanthenes from the bark of *Garcinia dioica*", *Chem. Pharm. Bull.* 44(1), 232-234.
- Iinuma, M., Tosa, H., Tanaka, T., Kanamaru, S., Asai, F., Kobayashi, Y., Miyauchi, K. and Shimano, R. 1996d. "Antibacterial activity of some *Garcinia*

benzophenone derivatives against Methicillin-Resistant *Staphylococcus aureus*", *Bio. Pharm. Bull.* 19(2), 311-314.

Ito, C., Miyamoto, Y., Nakayama, M., Kawai, Y., Rao, K.S. and Furukawa, H. 1997. "A novel depsidone and some new xanthenes from *Garcinia species*", *Chem. Pharm. Bull.* 45(9), 1403-1413.

Ito, C., Itoigawa, M., Mishima, Y., Tomiyasu, H., Litaudon, M., Cosson, J. P., Mukainaka, T., Tokuda, H., Nishino, H. and Furukawa, H. 2001. "Cancer chemopreventive agents. New depsidones from *Garcinia* plant", *J. Nat. Prod.* 64(2), 147-150.

Karanjgaonkar, C. G., Nair, P. M., Venkataraman, K. 1966. "Morellic, isomorellic and gambogic acids", *Tetrahedron Lett.* 7, 687-691.

Kartha, G., Ramachandran, G. N., Bhat, H. B., Nair P. M., Raghavan V. K. V. and Venkataraman K. 1963. "The constitution of morellin", *Tetrahedron Lett.* 7, 459-472.

Kosela, S., Hu, L-H., Yip, S-C., Rachmatia, T., Sukri, T., Daulay, T. S., Tan, G-K., Vittial, J. J. and Sim, K-Y. 1999. "Dulxanthone E: a pyranoxanthone from leaves of *Garcinia dulcis*", *Phytochemistry.* 52, 1375-1377.

- Kosela, S., Hu, L-H., Rachmatia, T., Hanafi, M. and Sim, K-Y. 2000. "Dulxanthones F-H, three new pyranoxanthones from *Garcinia dulcis*", *J. Nat. Prod.* 63(3), 406-407.
- Likhitwitayawuid, K., Phadungcharoen, T. and Krungkrai, J. 1998a. "Antimalarial xanthones from *Garcinia cowa*", *Planta Medica.* 64(1), 70-72.
- Likhitwitayawuid, K., Chanmahasathien, W., Ruangrunsi, N. and Krungkrai, J. 1998b. "Xanthones with antimalarial activity from *Garcinia dulcis*", *Planta Medica.* 64(3), 281-282.
- Lin, Y-M., Anderson, H., Flavin, M. T., Pai, Y-H. S., Mata-Greenwood, E., Pengsuparp, T., Pezzuto, M. J., Schinazi, R. F., Hughes, S. H. and Chen, F-C. 1997. "In vitro anti-HIV activity of biflavonoids isolated from *Rhus succedanea* and *Garcinia multiflora*", *J. Nat. Prod.* 60(9), 884-888.
- Minami, H., Kuwayama, A., Yoshizawa, T. and Fukuyama, Y. 1996. "Novel prenylated xanthones with antioxidant property from the wood of *Garcinia subelliptica*", *Chem. Pharm. Bull.* 44(11), 2103-2106.
- Nguyen, D. L. H. and Harrison, J. L. 2000. "xanthones and triterpenoids from the bark of *Garcinia vilersiana*", *Phytochemistry.* 53, 111-114.

- Nilar and Harrison, L. J. 2002. "Xanthonenes from the heartwood of *Garcinia mangostana*", *Phytochemistry*. 60, 541-548.
- Nyemba, A-M., Mpondo, T. N., Connolly, J. D. and Rycroft, D. S. 1990. "Cycloartane derivatives from *Garcinia lucida*", *Phytochemistry*. 29(3), 994-997.
- Ollis, W. D., Ramsay, M. V. J., Sutherland, I. O. and Mongkolsuk, S. 1965. "The constitution of gambogic acid", *Tetrahedron*. 21, 1453-1470.
- Parveen, M., Khan, N. U., Achari, B. and Dutta, P. K. 1991. "A triterpene from *Garcinia mangostana*", *Phytochemistry*. 30(1), 361-362.
- Peres, V., Nagem, T. J. and Oliveira, F. F. 2000. "Tetraoxygenated naturally occurring xanthonenes", *Phytochemistry*. 55, 683-710.
- Permana, D., Lajis, N. H., Mackeen, M. M., Ali, Aimi, N., Kitajima, M. and Takayama, H. 2001. "Isolation and bioactives of constituents of the roots of *Garcinia atroviridis*", *J. Nat. Prod.* 64(7), 976-979.
- Quillinan, A. J. and Scheinmann, F. 1971. "Application of the Claisen Rearrangement to the synthesis of heterocyclic bicyclo[2,2,2]octenones: an approach to the morellins based on new biogenetic suggestions", *Chem. Commun.* 966-967.

- Ritthiwigrom, T. 2002. "Xanthenes from the Stem Bark of *Garcinia nigrolineata*", M. Sc. Thesis, Prince of Songkla University, Thailand.
- Rukachaisirikul, V., Kaewnok, W., Koysomboon, S., Phongpaichit, S. and Taylor, W. C. 2000a. "Caged-tetraprenylated xanthenes from *Garcinia scortechinii*", *Tetrahedron*. 56, 8539-8543.
- Rukachaisirikul, V., Adiar, A., Dampawan, P., Taylor, W. C. and Turner, P. C. 2000b. "Lanostanes and friedolanostanes from the pericarp of *Garcinia hombroniana*", *Phytochemistry*. 55, 183-188.
- Spino, C., Lal, J., Sotheeswaran, S. and Aalbersberg, W. 1995. "Three prenylated phenolic benzophenones from *Garcinia myrtifolia*", *Phytochemistry*. 38(1), 233-236.
- Sukpondma, Y. 2002. "Chemical constituents from the fruits of *Garcinia scortechinii*", Unpublished data, Prince of Songkla University, Thailand.
- Suksamrarn, S., Suwannapoch, N., Ratananukul, P., Aroonlerk, N. and Suksamrarn A. 2002. "Xanthenes from the green fruit hulls of *Garcinia mangostana*", *J. Nat. Prod.* 65, 761-763.
- Sultanbawa, M. U. S. 1980. "Xanthonoids of tropical plants", *Tetrahedron*. 36(11), 1465-1506.

Thoison, O., Fahy, J., Dumontet, V., Chiaroni, A., Riche, C., Tri, M. V. and Sevenet, T. 2000. "Cytotoxic prenylxanthenes from *Garcinia bracteata*", *J. Nat. Prod.* 63(4), 441-446.

Venkataraman, K. 1974. "Pigments of *Garcinia* species", *Proc. Indian Natl. Sci. Acad.* 39, 365-381.

Whitmore, M. A. 1973. "Tree Flora of Malaya", Malaysia: Forest department ministry of primary industries, Longman, 221.

Wu, J., Xu Y-J., Cheng, X-F., Harrison L. J., Sim K-Y. and Goh, S. H. 2001. "A highly rearranged tetraprenylxanthonoid from *Garcinia gaudichaudii* (Guttiferae)", *Tetrahedron Lett.* 42, 727-729.

Xu, Y-J., Lai, Y-H., Imiyabir, Z. and Goh, S-H. 2001. "Xanthenes from *Garcinia parvifolia*", *J. Nat. Prod.* 64, 1191-1195.

Yates, P., Karmarkar, S. S., Rosenthal, D., Stout, G. H., Stout, V. F. 1963. "Acetyl- α -Gambogic acid", *Tetrahedron Lett.* 24, 1623-1629.

VITAE

Name Miss Patima Phainuphong

Birth Date 19 September 1978

Place of Birth Trang, Thailand

Educational Attainment

Degree	Name of Institution	Year of Graduation
Bachelor of Science (Chemistry)	Prince of Songkla University	1996-2000
Master of Science (Organic Chemistry)	Prince of Songkla University	2000-2002

Scholarship Awards during Enrolment

1. The partail support from Higher Education Development Project : Postgraduate Education and Research Program in Chemistry, funded by The Royal Thai Government